Synthesis and Bioactivation of

Selective Estrogen Receptor Modulators (SERMs)

BY

BRADLEY THOMAS MICHALSEN
B.A., Lake Forest College, 2008

DISSERTATION

Submitted as partial fulfillment of the requirements
for the degree of Doctor of Philosophy in Medicinal Chemistry
in the Graduate College of the
University of Illinois at Chicago, 2013

Chicago, Illinois

Defense Committee:

Dr. Judy L. Bolton, Chair and Advisor
Dr. Gregory R. J. Thatcher
Dr. Pavel A. Petukhov
Dr. Karol S. Bruzik
Dr. Debra A. Tonetti, Biopharmaceutical Sciences

This dissertation is dedicated to Elissa Johnson, without whom it never would have been completed.

ACKNOWLEDGEMENTS

I wish to acknowledge and thank all those who have provided support and guidance throughout the course of my doctoral studies here at UIC. First and foremost, I would like thank my advisors Drs. Judy L. Bolton and Gregory R. J. Thatcher for giving me the opportunity to conduct research in their group. Without their mentorship and incredible wealth of scientific expertise, the writing of this dissertation could never have been accomplished. It is only through their constant support and patience that I was able to complete this work, and for their guidance I will be forever grateful. I would also like to thank Drs. Debra A. Tonetti, Karol S. Bruzik, and Pavel A. Petukhov for serving as members of my defense committee. Additionally, I thank the Department of Medicinal Chemistry & Pharmacognosy at UIC as well as NIH grant 79870 for financial support.

During my time at UIC, I have been extremely fortunate to interact with, and learn from, an exceptional group of colleagues. Among them, I would like to first thank Drs. Zhihui Qin, Isaac T. Schiefer, and Vladislav A. Litosh for teaching me the art of organic synthesis. To Drs. Yueting Wang, Sujeewa Piyankarage, and Jaewoo Choi, I thank you all for the countless hours spent training me in analytical techniques, and also for the many discussions which helped provide direction to my projects. I also reserve a very special thanks to Dr. Teshome B. Gherezghiher, as well as to Mary Ellen Molloy of the Tonetti lab. Without Dr. Gherezghiher's mentorship in conducting *in vitro* metabolism experiments, I would never have been able to complete this dissertation. Similarly, the *in vivo* experiments conducted by Ms. Molloy provided an invaluable contribution to the content of this work. To all other members of the Bolton and Thatcher research group,

ACKNOWLEDGEMENTS (continued)

past and present, I thank you all. My experience at UIC would not have been the same without the support, advice, and friendship you have all provided to me during my time here, and I could not have succeeded without you.

Additionally, I would like to acknowledge Drs. William B. Martin and Jason A. Cody from Lake Forest College. Dr. Martin played an integral role in my academic career, and it was as his student that my interest in biochemistry and medicinal chemistry was first sparked. Likewise, through conducting research in Dr. Cody's lab I first realized that I had the power to make my own contribution to science, and it was under his mentorship that I recognized my desire to further pursue academic research in graduate school.

Last but not least, I would like to express my deepest gratitude to my family and to all of my friends who have been there to support me during a challenging time in my life. The path to where I am today was not an easy one, but it was your love, encouragement, and support that gave me strength and confidence when I needed it most, and for that, I thank you.

BTM

TABLE OF CONTENTS

CHAPTER **PAGE**

TABLE OF CONTENTS (continued)

CHAPTER **PAGE**

TABLE OF CONTENTS (continued)

CHAPTER **PAGE**

LIST OF TABLES

TABLE **PAGE**

LIST OF FIGURES

FIGURE **PAGE**

LIST OF FIGURES (continued)

FIGURE **PAGE**

LIST OF FIGURES (continued)

FIGURE **PAGE**

LIST OF ABBREVIATIONS

17β-EN	17β-equilenin
4-OHEN	4-hydroxyequilenin
7-OHLAS	7-hydroxylasofoxifene; 6-phenyl-5-(4-(2-(pyrrolidin-1-yl)ethoxy)phenyl)-5,6,7,8-tetrahydronaphthalene-2,3-diol
AIBN	azobisisobutyrylnitrile
BAZ	bazedoxifene; 1-(4-(2-(azepan-1-yl)ethoxy)benzyl)-2-(4-hydroxyphenyl)-3-methyl-1H-indol-5-ol
BMD	bone mineral density
BTC	benzothiophene core; 6-hydroxy-2-(4-hydroxyphenyl)benzo[*b*]thiophene
COMT	catechol-*O*-methyl transferase
CNS	central nervous system
DCM	dichloromethane
DES	diethylstilbestrol
DHEA	dehydroepiandrosterone
DIPEA	*N,N*-diisopropylethylamine
DMA	desmethylarzoxifene
DMAP	4-dimethylaminopyridine
DMF	dimethylformamide
DMSO	dimethyl sulfoxide
EDCI	1-Ethyl-3-(3-dimethylaminopropyl)carbodiimide
E_2	17β-estradiol; estradiol
EN	equilenin

LIST OF ABBREVIATIONS (continued)

EQ	equilin
ER	estrogen receptor
EU	European Union
FDA	Food and Drug Administration
GPR30	G-protein-coupled receptor 30
GSH	glutathione
HLM	human liver microsomes
HOBt	hydroxybenzotriazole
HPLC	high-performance liquid chromatography
IC_{50}	Inhibitory concentration at 50% inhibition
LAS	lasofoxifene; 6-phenyl-5-(4-(2-(pyrrolidin-1-yl)ethoxy)phenyl)-5,6,7,8-tetrahydronaphthalen-2-ol
$LiAlH_4$	lithium aluminum hydride
LY	LY2066948; 6-(4-(methylsulfonyl)phenyl)-5-(4-(2-(piperidin-1-yl)ethoxy)phenoxy)naphthalen-2-ol
MORE	multiple outcomes of raloxifene evaluation
MPA	medroxyprogesterone acetate
MRM	multiple reaction monitoring
NADPH	Nicotinamide adenine dinucleotide phosphate
n-BuLi	*n*-butyllithium
OGD	oxygen-glucose deprivation
P450	cytochrome P450

LIST OF ABBREVIATIONS (continued)

PKCα	protein kinase C alpha
POSEM	prodrug of selective estrogen mimic
PPA	polyphosphoric acid
RAL	raloxifene
ROS	reactive oxygen species
RLM	rat liver microsomes
SAM	S-Adenosyl methionine
SEM	selective estrogen mimic
SERM	selective estrogen receptor modulator
SMART	Selective Estrogens, Menopause and Response to Therapy trials
$t_{1/2}$	half-life
TEA	triethylamine
tert-BuOH	tertiary butyl alcohol
TPP	triphenylphosphine
TSEC	tissue selective estrogen complex
TYR	tyrosinase
UDPGA	uridine 5′-diphosphoglucuronic acid
UGT	uridine triphosphate-glucuronosyltransferase
WHI	Women’s Health Initiative

SUMMARY

The metabolism of estrogens to electrophilic metabolites (bioactivation) has been postulated as a contributing factor in the initiation and/or promotion of cancer in hormone-sensitive tissues. Such metabolites have been shown to elicit toxicity both through the covalent modification of cellular proteins and DNA, and also through generation of reactive oxygen species. Bearing structural resemblance to estrogens, extensive studies have demonstrated that selective estrogen receptor modulators (SERMs) are also subject to similar bioactivation pathways. SERMs have found clinical success primarily in the treatment and prevention of breast cancer and osteoporosis; however, bioactivation of the prototypical triphenylethylene SERM tamoxifen has been associated with endometrial carcinogenesis. Conversely, while the benzothiophene SERM raloxifene may also be bioactivated to a highly reactive electrophile, this metabolic pathway has not been associated with toxicity in humans. These observations have pointed to an important need to more closely examine potential routes for toxicity resulting from the bioactivation of newer-generation SERMs. As the chemical structures of several clinical and preclinical SERMs are based upon a variety of distinct molecular scaffolds, it is crucial to elucidate which of these scaffolds may be susceptible to deleterious metabolism similar to tamoxifen, and also those which do not manifest toxicity *in vivo*, as is the case for raloxifene. Such knowledge is vital to the design of new SERMs which maintain drug efficacy while minimizing the formation of harmful metabolites.

In the present study, the oxidative metabolism of three next-generation SERMs was investigated under various *in vitro* conditions in order to determine potential routes

for drug bioactivation. LY2066948 (LY), lasofoxifene (LAS), and bazedoxifene (BAZ) possess naphthol, tetralin, and indole core moieties, respectively, and these SERMs were chosen for study as each of these core moieties has been recognized as a structural alert for bioactivation. The naphthol and tetralin cores of LY and LAS for example, are structurally analogous to those found in estradiol (E_2), and the equine estrogen, equilenin (EN), respectively. For both E_2 and EN, 4-hydroxylation to a catechol followed by oxidation to an electrophilic *o*-quinone has been established as a potentially carcinogenic pathway. Similarly, the indole core of BAZ is structurally similar to that found in clinically relevant drugs such as zafirlukast (leukotriene receptor antagonist) and indomethacin (non-steroidal anti-inflammatory drug; NSAID) for which bioactivation has been associated with hepatic and blood toxicity. Importantly, while LY is an investigational SERM in preclinical development as a potential treatment for uterine fibroids, both LAS and BAZ are currently approved in the European Union for the treatment of postmenopausal osteoporosis.

The results of this investigation demonstrate that LY, LAS, and BAZ may all be enzymatically oxidized to catechols which further oxidize to electrophilic *o*-quinones. As *o*-quinones are generally highly-reactive, transient species which are difficult to detect directly, these *o*-quinones were detected as their corresponding glutathione conjugates. For the cases of LY and BAZ, although *o*-quinone formation was observed, the primary route for P450-mediated metabolism instead involved side chain *N*-dealkylation, suggesting that bioactivation of these SERMs is not likely to account for toxicity *in vivo*. By contrast, oxidation of LAS to catechols which further oxidized to *o*-quinones

constituted the primary route of P450-mediated metabolism. Moreover, oxidation of LAS to *o*-quinones was observed even in the presence of competing Phase II detoxification pathways such as glucuronidation and methylation. These findings are analogous to what is observed for structurally similar estradiol. Furthermore, one of the major catechol metabolites of LAS was synthesized and found to form several depurinating adducts with DNA. Depurinating adducts of estrogen *o*-quinones have been shown to generate apurinic sites on DNA that are prone to improper repair, resulting in mutations that are critical for the initiation of breast, prostate, and other cancers. Collectively, these findings suggest that analogous to estradiol, bioactivation of LAS to *o*-quinones may represent a potential pathway for *in vivo* toxicity for this SERM.

The second major goal for this study was to design and synthesize novel estrogen receptor (ER) ligands based upon molecular scaffolds for which bioactivation has not been clinically associated with toxicity. As the 2-(4-hydroxyphenyl) benzo[b]thiophen-6-ol core (BTC) moiety of raloxifene best met this criterion, this scaffold was chosen as an ideal candidate. Moreover, 4'-Fluoro substitution to the BTC core has been previously demonstrated to impart resistance towards oxidative metabolism, effectively inhibiting the formation of reactive electrophiles. Structural elaboration at the 3-position of the BTC core, with and without 4'-Fluoro substitution therefore, yielded a family of SERMs and SEMs (selective estrogen mimics) which displayed a wide range of activity from potent antiestrogens (SERM-like) to potent estrogens (SEM-like). Expansion of this library led to the discovery of a novel benzothiophene SEM, HP-BTF, as a promising lead drug candidate of potential use in

the treatment of tamoxifen-resistant breast cancer. Breast tumors which exhibit resistance to tamoxifen treatment are often sensitized to the apoptotic action of estrogenic compounds such as E_2. Accordingly, the use of E_2 has been suggested as a potential treatment option for patients whose tumors display resistance. HP-BTF is a weak estrogen, and like E_2, was shown to inhibit the growth of tamoxifen-resistant tumors *in vivo*; however, unlike E_2, HP-BTF did not stimulate uterine weight gain. Furthermore, as the bioactivation of E_2 is established as a potentially carcinogenic pathway, whereas bioactivation of drugs based upon the BTC scaffold is not, HP-BTF and compounds like it may potentially offer a safer treatment alternative.

In summary, as the bioactivation of certain SERMs has been associated with carcinogenesis, while for others bioactivation represents a relatively minor or benign pathway, it is essential that the metabolic fate of any new SERM be thoroughly scrutinized. The results of this study and others like it therefore, will provide valuable information in the design of new SERMs which maintain drug efficacy while minimizing the formation of harmful metabolites.

Chapter 1: Introduction

1.1 The benefits and hazards of estrogen replacement therapy

Estrogens are the primary female sex hormones and the production of endogenous estrogen is responsible for a wide array of physiological functions in both women and men. In addition to the critical role they play in the regulation of a woman's estrous cycle, estrogens also function to maintain health in skeletal, cardiovascular, and central nervous system (CNS) tissues [1, 2]. It should not then be surprising that a marked estrogen deficiency associated with the onset of menopause in women is often accompanied by a host of physiological and/or psychological symptoms which can drastically impact quality of life. Symptoms such as vasomotor instability (hot flashes, night sweats), sleeplessness, depression, mood swings, sexual dysfunction (vaginal atrophy, vaginal dryness), and increased risk for osteopenia/osteoporosis have led millions of postmenopausal women to turn to hormone replacement therapy (HRT) options seeking symptom alleviation [3]. Although research has demonstrated that several popular forms of HRT (conjugated estrogens alone or conjugated estrogens plus a progestin; Premarin® or Prempro®, respectively) can be effective in treating many of these symptoms, and have also been associated with a decrease in risk for colon cancer [4, 5], such benefits have unfortunately not come without the potential for dangerous side effects.

While a correlation between cumulative estrogen exposure throughout the course of one's life and the incidence of hormone-dependent cancers has been well-recognized for many years [1, 6-8], the several possible mechanistic explanations for this

correlation are not entirely understood. The most widely-accepted of these is that estrogens hormonally stimulate excessive cellular proliferation through interaction with nuclear estrogen receptors (ERs). It is argued that this enhanced rate of proliferation is responsible for an increased chance for errors during DNA replication, thereby increasing the risk for genomic mutations [6]. Similar hormonal mechanisms involving rapid signaling by estrogens through extranuclear ERs have also been reported [9, 10]. Another relatively novel mechanism postulates that estrogens are carcinogenic via their metabolism to catechols which are further oxidized to electrophilic *o*-quinones. Such estrogen *o*-quinones may then act as chemical carcinogens through covalent modification of cellular proteins and/or DNA, resulting in mutations. Redox cycling through a semiquinone radical intermediate can also generate reactive oxygen species (ROS) capable of damaging DNA oxidatively, and also resulting in mutations (Figure 1) [6].

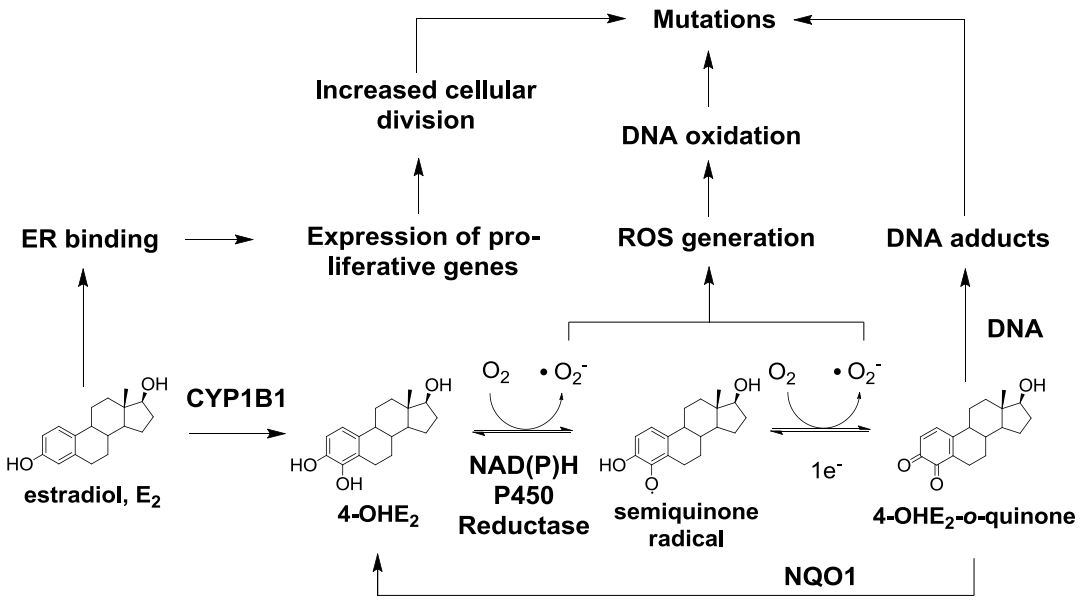

Figure 1. Hormonal and chemical mechanisms of E_2-induced carcinogenesis

At one time, the numerous benefits of HRT were generally thought to outweigh the associated risks, but findings of the large, multicenter, epidemiological Women's Health Initiative (WHI) trials seriously challenged this widely accepted belief. The WHI studies were designed to compare the effects of a variety of available HRT options on endpoints such as cardiovascular disease, osteoporosis, incidence of dementia, and incidence of gynecological cancer in postmenopausal women [6, 11]. In 2002, the estrogen plus progestin arm of the study was halted prematurely when investigators discovered significant increases in risk for breast cancer, coronary heart disease, pulmonary embolism, stroke, and vascular dementia in women taking this form of HRT [6, 11]. Similarly, the estrogen-only arm was terminated early in 2004 upon discovery of an increased risk for stroke [12]. Accordingly, the release of the WHI data coincided with a drastic decline in HRT use amongst postmenopausal women, for whom few other treatment options were available [3, 13]. Clearly, the need for a more thorough understanding of all of the potential mechanisms responsible for such toxic effects was realized, and a search for potentially safer alternatives to estrogen-based HRTs became a topic of extreme interest in women's health [1, 2, 6]. Selective estrogen receptor modulators (SERMs) were soon recognized as a drug class with the potential ability to offer just such benefits.

1.2 SERMs and the concept of an ideal SERM

SERMs are a class of compounds characterized by their ability to ligand ER, and either mimic or antagonize the function of estrogen in a manner specific to the cellular context of the target tissue [14]. Currently, FDA-approved SERMs fall into two main

structural categories: triphenylethylenes and benzothiophenes. Tamoxifen, toremifene, clomiphene, and ospemifene are triphenylethylene-based and are approved for the treatment of ER(+) breast cancer (tamoxifen and toremifene), for treatment of infertility by inducing ovulation (clomiphene), and for treatment of vulvar-vaginal atrophy (ospemifene) [15, 16]. Raloxifene is the only clinically-approved benzothiophene derivative, and is approved for the treatment of postmenopausal osteoporosis and for reducing the risk of ER(+) breast cancer [15]. SERMs are often referred to as "antiestrogens" as the prototypical SERM tamoxifen acts as an estrogen antagonist in breast tissue; however such a classification is something of a misnomer, as tamoxifen is also estrogenic in endometrial tissues [17, 18]. Interestingly, raloxifene behaves as an estrogen antagonist in both the breast and the endometrium, while all clinically approved SERMs are estrogenic in bone [1, 2, 18]. The molecular basis for such tissue-selective effects is generally believed to depend on several factors, most notably the tissue-specific expression of ERs, the conformation induced in these ERs upon ligand binding, and the availability of coactivator and/or corepressor proteins present in said target tissue. Such coregulatory proteins bind liganded ER, and are ultimately responsible for the ensuing transcription of target genes and for producing an estrogenic or antiestrogenic response in that tissue [19, 20].

In contrast to ligation of an estrogenic compound with ER, the binding of a SERM induces a markedly different receptor conformation [20]. A comparison between crystal structures of ER liganded with either estradiol (E_2) or raloxifene demonstrates this difference well. Upon binding ER, the phenolic 3-hydroxyl group of E_2 hydrogen bonds with Glu 353, Arg 394, and a water molecule, while the secondary 17β-hydroxyl group

forms a hydrogen bond with His 524 (Figure 2) [20]. These hydrogen bonds, in conjunction with several non-polar interactions between the A, B, and D rings of E_2 and hydrophobic residues within the core of the ER binding pocket, account for the subnanomolar affinity of this endogenous steroid for ER [20, 21]. Importantly, the binding of an endogenous estrogen like E_2 or a synthetic estrogen such as diethylstilbestrol (DES) yields a receptor conformation possessing competent activation function regions (AF-1 and AF-2) which are necessary for coregulator binding and the subsequent transcription of estrogen-responsive genes [20, 21]. Whereas the activity of AF-1 is regulated primarily via growth factors through the mitogen-activated protein kinase (MAP K) pathway, the activity of AF-2 is responsive to ligand binding [21, 22].

The 6- and 4'- phenolic hydroxyl groups of raloxifene are recognized by, and hydrogen bond with, the same amino acid residues as the 3- and 17-hydroxyl groups of E_2, respectively (Figure 2) [20]. However, the presence of a bulky side chain at the 3-position of raloxifene's benzothiophene core has a profound effect on the formation of a functionally active AF-2 [20]. Too large to fit inside the core binding pocket, the (4-(2-(piperidin-1-yl)ethoxy)phenyl)methanone side chain of raloxifene protrudes outward, displacing helix 12 of the ER from its agonist-bound position. In doing so, the formation of a fully active AF-2 region on the receptor is inhibited. Subsequently, the binding of coregulatory proteins responsible for facilitating the transcription of estrogen inducible genes, such as those from the SRC (steroid receptor coactivator) family, is also inhibited. Conversely, in this antagonist-bound state, recruitment of corepressor proteins such as SMRT (silencing mediator of retinoic acid and thyroid hormone receptor) and NCoR (nuclear corepressor) acts to down-regulate the transcription of estrogen

inducible genes [23]. Such molecular interactions are a general characteristic of SERMs, and are believed to account for the varying degrees of tissue selectivity observed for this structurally diverse class of compounds [19, 20].

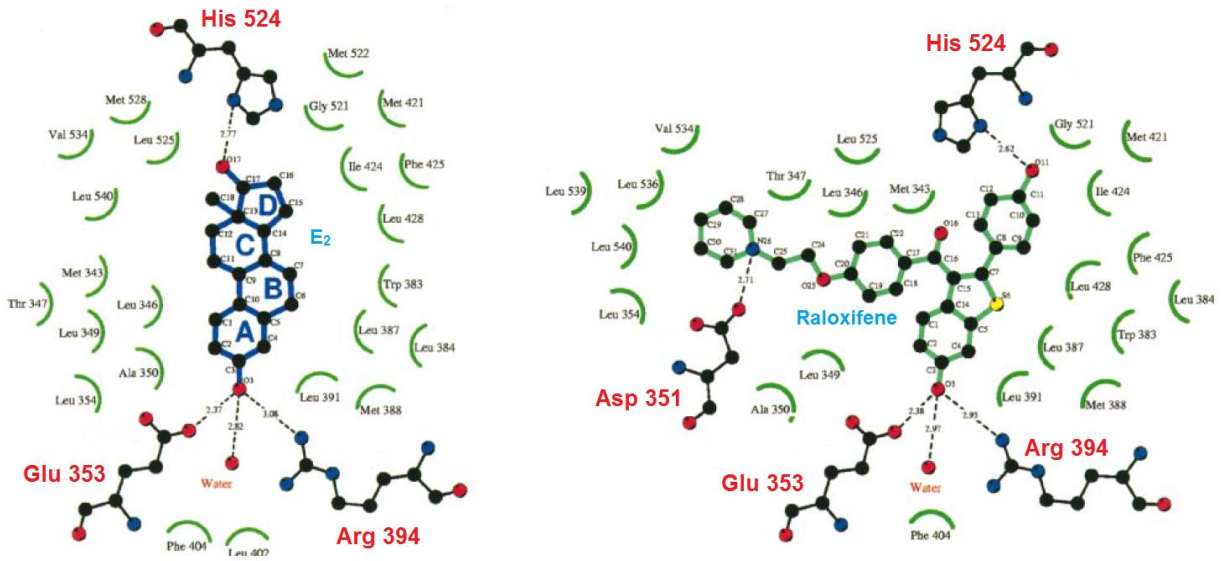

Figure 2. Interactions of E_2 and raloxifene within the LBD of ERα

While the ability of SERMs like tamoxifen and raloxifene to maintain estrogenic activity in bone whilst antagonizing the proliferative effects of estrogen in breast tissue has proven clinically useful, there remain drawbacks associated with the use of SERMs. As mentioned, tamoxifen is estrogenic in endometrial tissue, and has been shown to increase the risk of endometrial cancer [18, 24]. Accordingly, its use remains limited to short treatment durations (< 5 years) and only for the indications of breast cancer prevention and treatment [25-29]. Moreover, de novo resistance or the development of acquired resistance to tamoxifen and toremifene in the treatment of ER(+) breast cancer also represents a hurdle [30-32]. Similarly, while raloxifene has proven an effective treatment for postmenopausal osteoporosis, it has also been shown to increase the risk

for fatal stroke and thrombosis [33]. Furthermore, rather than effectively treating the vasomotor symptoms associated with menopause, SERM use frequently exacerbates them [34-36]. Such side effects certainly limit the attractiveness of currently-available SERMs as viable alternatives to traditional forms of HRT. As such, the concept of an "ideal SERM" has been a topic of immense interest in research related to women's health and drugs that target ER. Such a SERM would act as an estrogen in bone to prevent postmenopausal osteoporosis, in the CNS to prevent hot flashes and neurological disorders such as Alzheimer's disease, and in the heart to prevent cardiovascular disease. Conversely, this "ideal SERM" would antagonize the effects of estrogen in hormone sensitive tissues such as the breast and endometrium in order to prevent hormone dependent cancers.

1.3 Statement of purpose and hypothesis

A well-documented characteristic of many clinical and investigational SERMs involves the relative ease with which many are metabolized to reactive electrophiles. Analogous to the aforementioned mechanism by which estrogens are metabolized to *o*-quinone chemical carcinogens, the metabolism of SERMs has also been proposed to contribute to drug toxicity [37-39]. Tamoxifen, for example, is metabolized to at least three different types of electrophiles (refer to Section 4.2.1), including an *o*-quinone [37]. Like estrogens, hormonal, proliferative mechanisms have also been proposed to contribute to the ability of tamoxifen to initiate and/or promote endometrial cancer [17]; however, the detection of tamoxifen-DNA adducts in endometrial tissue of women taking the drug lends support to a mechanism of chemical carcinogenesis [40, 41].

Because of similarities between the metabolism of estrogens and of SERMs to potential chemical carcinogens, it is necessary to fully elucidate the metabolic fate of any novel SERM if is to realize clinical success.

LY2066948 (LY) is an investigational SERM in development by Eli Lilly for the treatment of uterine fibroids [42, 43]. The core structure of LY contains a naphthol moiety similar in structure to that of the equine estrogen, equilenin (EN, Figure 3). The primary phase I metabolism of EN involves 4-hydroxylation of the A-ring to a 3,4-catechol (4-hydroxyequilenin, 4-OHEN) which may be further oxidized to 4-OHEN-*o*-quinone. 4-OHEN has been demonstrated to behave as a complete carcinogen and tumor promoter *in vitro*, and formation of 4-OHEN has been argued to represent a major carcinogenic pathway for equine estrogens [6]. Although LY is a potent antiestrogen in breast and endometrial tissue, its potential to form reactive quinoids similar to 4-OHEN-*o*-quinone has not been thoroughly scrutinized, and formation of LY-*o*-quinone(s) could arguably result in a mechanism of toxicity similar to that of EN.

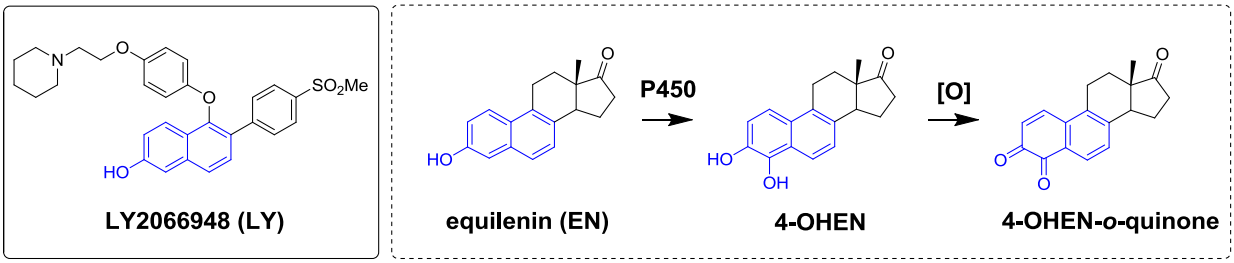

Figure 3. Structures of LY and EN; bioactivation of EN to 4-OHEN-o-quinone

Akin to the structural similarity between LY and EN, the tetralin-based SERM lasofoxifene (LAS) shares a structural motif resembling the A and B rings of E_2 (Figure 4). LAS is a third generation SERM under development by Pfizer which has completed

phase III clinical trials for the prevention and treatment of postmenopausal osteoporosis, and which is currently approved in the European Union (EU) for use in this indication [44]. It has previously been reported that, similar to E_2, two catechol regioisomers of LAS are formed as primary oxidative metabolites, accounting for roughly half of the total metabolism of LAS [45]; however, the potential for further oxidation of these catechols to electrophilic *o*-quinones has not been reported. As 4-hydroxylation of structurally similar E_2 and subsequent *o*-quinone formation has also been established as a potentially carcinogenic pathway [6], it is important to determine whether or not LAS is subject to similar bioactivation.

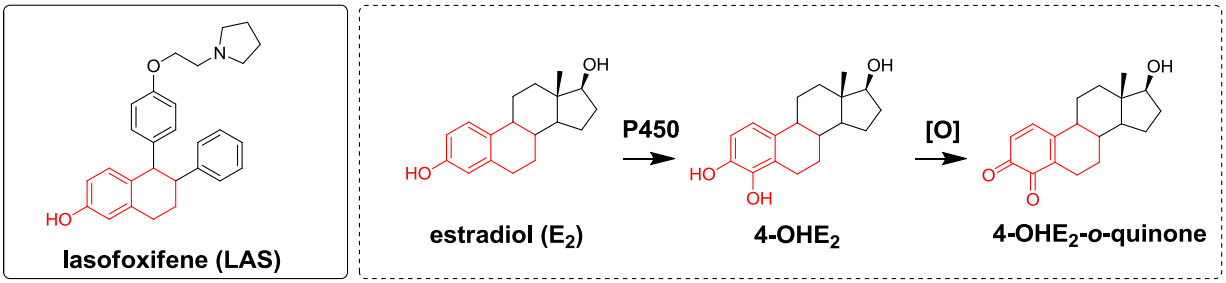

Figure 4. Structures of LAS and E_2; bioactivation of E_2 to 4-OHE$_2$-o-quinone

Bazedoxifene is an indole-based SERM which is currently under development by Pfizer, and which is also approved in the EU for the treatment of postmenopausal osteoporosis [46, 47]. Unlike LY or LAS, the 5-hydroxy-3-methylindole core of the SERM bazedoxifene (BAZ) does not bear an obvious structural similarity to endogenous or equine estrogens (Figure 5); however, the 3-methylindole moiety which BAZ possesses has been recognized as a structural alert, leading to covalent modification of proteins and DNA for a number of drugs [48-51]. 3-Methylindole itself has been shown

to cause pulmonary toxicity associated with bioactivation to both an iminium methide, and to a lesser extent, a 1,5-benzoquinone imine following 5-hydroxylation [51-53] (Figure 5). Similarly, use of the leukotriene receptor antagonist zafirlukast for treatment of asthma has resulted in idiosyncratic hepatotoxicity associated with CYP3A4 deactivation by an iminium methide metabolite [49]. Moreover, the major 5-hydroxy-3-alkylindole metabolite of the non-steroidal anti-inflammatory drug (NSAID) indomethacin has been shown to be bioactivated to a 1,5-benzoquinone imine, and formation of this reactive metabolite has been speculated to account for the high incidence of blood toxicity associated with indomethacin use [50]. Again, as is the case for LY and LAS, the potential for any such bioactivation associated with the structurally similar bazedoxifene has not been thoroughly investigated.

Interestingly, while the benzothiophene SERM raloxifene has been shown to be bioactivated to an electrophilic diquinone methide intermediate capable of labeling cellular nucleophiles [54-56] (refer to Section 4.2.2), no known toxicity has been associated with this metabolite in humans since the drug's initial approval in 1997 for the treatment of postmenopausal osteoporosis [57, 58]. It has been hypothesized that this effect could be, in part, due to the extremely short half-life (< 1 second) and transient nature of this intermediate which may preferentially react with solvent molecules over protein or DNA targets, or also due to extensive glucuronidation of the drug *in vivo* [58, 59]. Additionally, although any diquinone methide-associated toxicity remains to be observed clinically, the formation of this type of reactive intermediate can also effectively be eliminated while maintaining effective ER binding, through chemical substitution of the 2, 4'-hydroxyl group with a fluorine atom, as observed for the

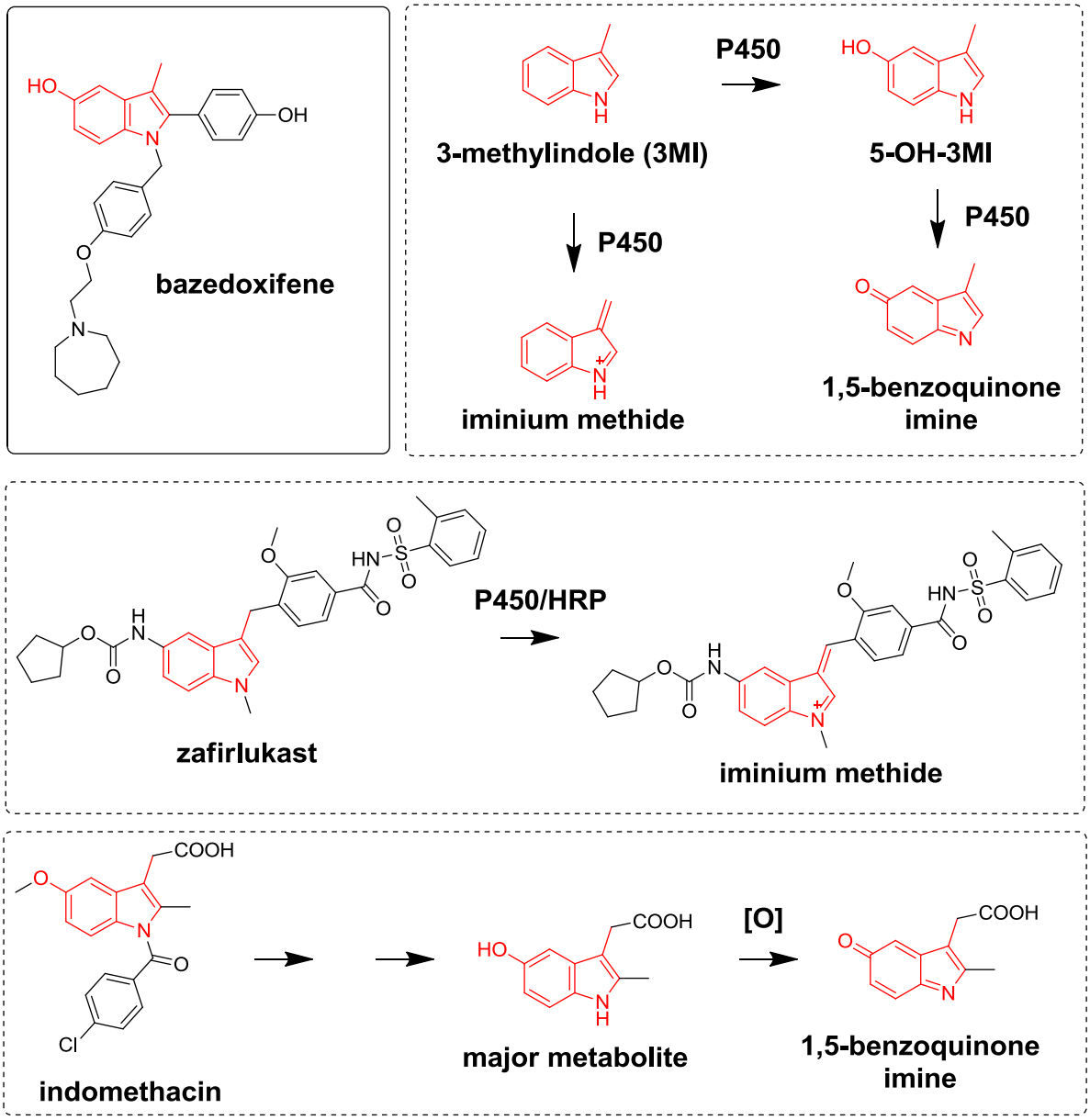

Figure 5. Structure of bazedoxifene; bioactivation of 3-methylindole, zafirlukast, and indomethacin

raloxifene analogs, desmethylarzoxifene (DMA) and 4'-fluorodesmethylarzoxifene (FDMA) [39, 60] (Figure 6). From a drug metabolism and toxicology standpoint therefore, development of novel ER ligands containing raloxifene's 2-(4-

hydroxyphenyl)benzo[b]thiophen-6-ol (BTC) core, with or without a 4'-fluoro substitution, would appear a sensible and safe approach.

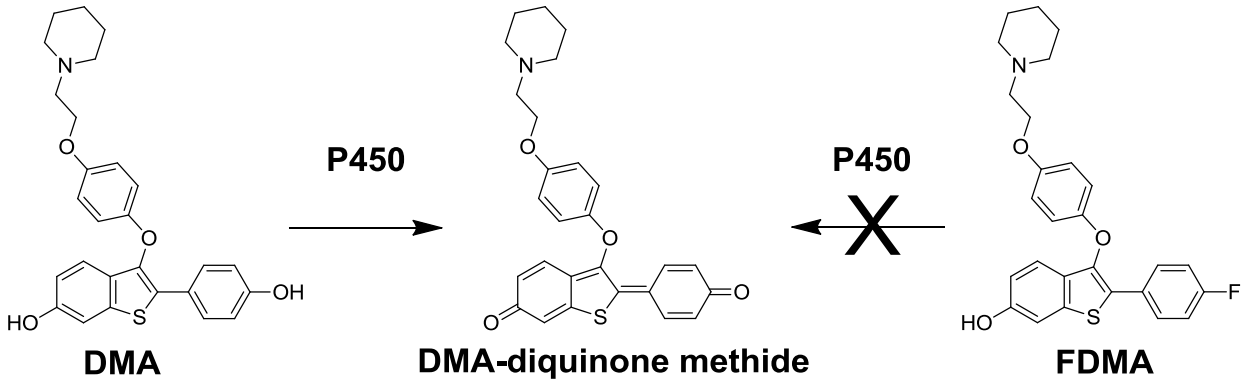

Figure 6. Bioactivation of DMA to diquinone methide; 4'-fluoro substitution blocks quinoid formation

The specific aims for the present study therefore, entail (1) determining the potential routes of bioactivation for the SERMs LY2066948 (LY), lasofoxifene (LAS), and bazedoxifene (BAZ), and (2) the design and synthesis of novel ER ligands that display a range of agonist/antagonist activity, using the BTC core (with or without 4'-Fluoro substitution) of raloxifene/DMA/FDMA as a structural template. It is hypothesized that similar to estrogens or drugs containing the 3-methylindole scaffold; LY, LAS, and BAZ will also be bioactivated to reactive quinoids which possess the potential to mediate toxicity. Finally, as bioactivation of BTC-containing drugs to a diquinone methide has yet to be shown to manifest toxic effects in humans, the development of novel SERMs, SEMs (Selective estrogen mimics), and POSEMs (Prodrugs of SEMs) which incorporate this moiety is expected to yield drugs for which mechanisms of

chemical carcinogenesis are attenuated, and which may offer potential utility in the treatment of ER-mediated pathologies.

Chapter 2: Materials and methods

2.1 Materials

Caution: SERM and estrogen-o-quinones were handled in accordance with the NIH Guidelines for the Laboratory Use of Chemical Carcinogens [61]. Solvents, chemicals, and tyrosinase (from mushroom) were purchased from Aldrich Chemical (Milwaukee, WI), Fisher Scientific (Itasca, IL), or Sigma (St. Louis, MO) unless stated otherwise. Estrogens were purchased from Steraloids Inc. (Newport, RI). Human cytochrome P450 supersomes were obtained from BD Biosciences (Woburn, MA). Human liver microsomes (pooled from 15 individuals) were purchased from In Vitro Technologies Inc. (Baltimore, MD).

2.2 Instrumentation

NMR spectra were recorded using either a Bruker Avance 400 MHz spectrometer or a Bruker DPX 400 MHz spectrometer. UV spectra were obtained using a Hewlett-Packard (Palo Alto, CA) 8452A photodiode array UV-Vis spectrophotometer. HPLC analysis was performed using an Agilent (Palo Alto, CA) 1100 instrument measuring UV absorbance at 280 nm. LC-MS/MS analyses were performed using either of two instrument configurations: (1) an Agilent 6310 ion trap mass spectrometer (Agilent Technologies, Santa Clara, CA) coupled to an Agilent 1100 HPLC (Palo Alto, CA) or (2) an API 3000 triple quadrupole mass spectrometer (Applied Biosystem, Foster City, CA) coupled to an Agilent 1200 HPLC (Palo Alto, CA).

2.3 LC methodology

For analysis of metabolites and GSH conjugates of LY2066948 using the Agilent 6310 ion trap instrument, two general methods were used: In method A, an Agilent Eclipse XDB-C18 column (4.6 mm ×150 mm, 5 µm) was used for LC-MS analysis of tyrosinase and rat liver microsomal incubations. The mobile phase consisted of solvent A, (water containing 10% methanol and 0.1% formic acid) and solvent B (acetonitrile and 0.1% formic acid). For LY2066948 analysis, the mobile phase consisted of a linear gradient from 5 to 30% B over 20 min, 10 min gradient from 30 to 60% B, and then 60 to 90% B over 5 min. In method B, a Beckman (4.6 mm×150 mm, 5 µm) Ultrasphere C_{18} column was used. The mobile phase consisted of a linear gradient from 10 to 30% B over 15 min, 10 min gradient from 30 to 60% B, and then 60 - 90% B over 5 min. A flow rate of 1.0 mL/min was used for all analyses. Reported retention times for LY 2066948 and metabolites were obtained using method A unless stated otherwise.

Analyses for metabolites and GSH conjugates of lasofoxifene were completed using the Agilent 6310 ion trap instrument equipped with an electrospray ionization source and measuring UV absorbance at 270 nm. Samples were separated using an Agilent Eclipse XDB-C_{18} column (4.6 x 150 mm, 5 µm) at a flow rate of 1.0 mL/min. The mobile phase was composed of solvent A (water containing 10% methanol and 0.1% formic acid) and solvent B (acetonitrile containing 0.1% formic acid), beginning with 5% B, increasing to 60% B over 40 min, 90% B over 5 min, and then returning to 5% B over 3 min. The system was then allowed to equilibrate for 10 min before subsequent sample injections. Ions were detected in positive mode using collision-induced dissociation (CID) ionization with a resolving power of 5000 FWHM and mass accuracy of 0.1 amu.

Analysis of depurinating adducts from 7-OHLAS incubations with CT-DNA was completed using the API 3000 triple quadrupole instrument. Samples were separated using a Phenomenex Kinetex C_{18} column (3 × 100 mm, 2.6 µm) and ADV-FFKIT filter (Analytical, Prompton Plains, NJ, USA) at a flow rate of 0.3 mL/min. The mobile phase was composed of solvent A (water containing 10% methanol and 0.1% formic acid) and solvent C (methanol containing 0.1% formic acid), beginning with 30% C, increasing to 98% C over 10 min, holding at 98% C for 10 min, and returning to 30% C over 2 min. The system was then allowed to equilibrate for 8 min before subsequent sample injections. Ions were detected in positive mode with electrospray ionization and multiple reaction (MRM) monitoring carried out at 350 ºC. Collision energies were optimized to 67 volts for 7-OHAS-Ade adducts, and 63 volts for 7-OHAS-Gua adducts. Fragmentations for the collision-induced dissociation of *m/z* 563→136, and *m/z* 579→152 were monitored for Ade and Gua adducts, respectively.

For analysis of metabolites and GSH conjugates of bazedoxifene, the 6310 ion trap setup was used. Samples were separated using an Agilent Eclipse XDB-C_{18} column (4.6 x 150 mm, 5 µm) at a flow rate of 1.0 mL/min. The mobile phase was composed of solvent A (water containing 10% methanol and 0.1% formic acid) and solvent B (acetonitrile containing 0.1% formic acid), beginning with 10% B, increasing to 50% B over 15 min, 80% B over 10 min, 90% B over 5 min, holding at 90% B for 5 min, and then returning to 10% B over 3 min. The system was then allowed to equilibrate for 10 min before subsequent sample injections. An identical instrument configuration and column were used to analyze incubations of POSEMs with human liver microsomes, except the mobile phase was composed of solvent A (water containing 10% methanol

and 0.1% formic acid) and solvent B (acetonitrile containing 0.1% formic acid), beginning with 10% B, increasing to 90% B over 10 min, holding at 90% B for 15 min, and returning to 10% B over 5 min.

2.4 Preparation of rat liver microsomes

Female Sprague−Dawley rats (200−220 g) were obtained from Sasco Inc. (Omaha, NE). To induce P450 3A isozymes, animals were pretreated with dexamethasone (100 mg/kg) in corn oil by intraperitoneal injection daily for 3 consecutive days and were sacrificed on day 4. Rat liver microsomes were prepared, and protein and P450 concentrations were determined as described previously [62].

2.5 Synthesis of SERMs; SERM metabolites; SEMs; POSEMs

2.5.1 LY2066948 (LY); lasofoxifene (LAS); 7-hydroxylasofoxifene (7-OHLAS)

LY2066948 was prepared by Dr. Teshome B. Gherezghiher according to a procedure modified from Hummel, et al [42]. Lasofoxifene and 7-OHLAS were synthesized by analogous routes according to a procedure modified from Day, et al [63] (Figure 7). For 7-OHLAS, tetralone **1b** was coupled to 1-(2-(4-bromophenoxy)ethyl)pyrrolidine using *n*-BuLi to give **2b**, which was selectively brominated using NBS to yield intermediate **3b**. Suzuki coupling with phenylboronic acid gave **4b** which was hydrogenated to give **5b**. Deprotection of **5b** using BBr_3 gave catechol 7-OHLAS.

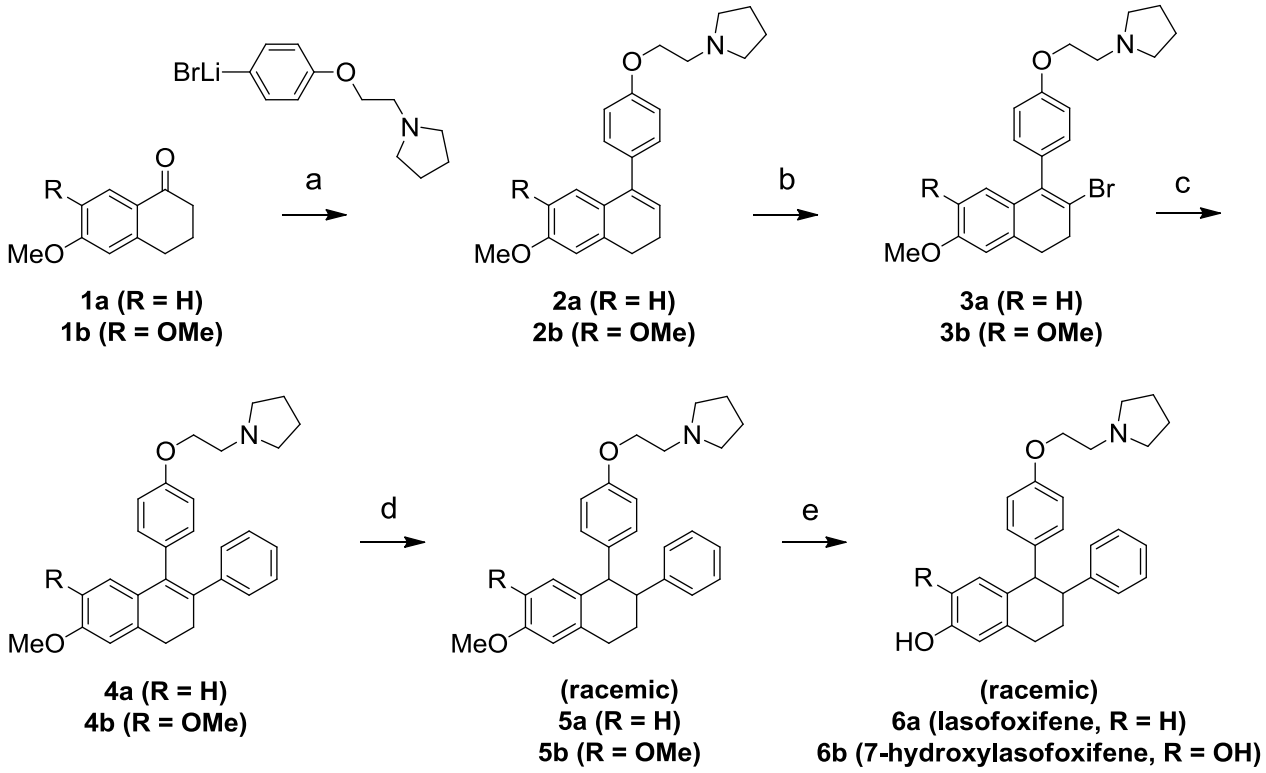

Figure 7. Synthesis of lasofoxifene; 7-hydroxylasofoxifene

Reagents and Conditions: (a) *n*-BuLi, Et_2O, -78°C; (b) NBS, DMF, AIBN, rt; (c) $PhB(OH)_2$, $Pd(Ph_3P)_4$, EtOH, reflux; (d) H_2, $Pd(OH)_2$, EtOH, 40°C; (e) *i.* HCl/EtOH; *ii.* BBr_3, DCM, 0°C.

1-(2-(4-(6,7-Dimethoxy-3,4-dihydronaphthalen-1-yl)phenoxy)ethyl)pyrrolidine **(2b)**. A solution of 1-(2-(4-bromophenoxy)ethyl)pyrrolidine (6.75g, 25.0 mmol) in Et_2O (250 mL) was cooled to -78 ºC under argon. *n*-BuLi (16.7 mL, 1.6 M) was added dropwise and the resulting solution was stirred at -78 ºC for 1h. A solution of **1b** (5.00g, 24.2 mmol) in THF (25 mL) was added dropwise over the course of 1 h and the reaction was stirred for an additional 3 h at -78 ºC. HCl (100 mL, 2N) was added, the reaction was allowed to warm to room temperature, and the pH was adjusted to 7 by addition of concentrated NaOH. The Et_2O layer was separated and the aqueous layer was extracted with ethyl acetate (2 X 100 mL). Organic layers were combined, dried over

anhydrous Na_2SO_4, and concentrated to give a crude oil which was purified by silica gel chromatography to give 3.3 g (36%) of **2b** as a colorless oil. ^{1}H NMR (400 MHz, $CDCl_3$): *δ* 1.81-1.88 (m, 4H), 2.37 (m, 2H), 2.69 (bs, 4H), 2.78 (t, *J* = 8.0 Hz, 2H), 2.96 (t, *J* = 6.0 Hz, 2H), 3.70 (s, 3H), 3.92 (s, 3H), 4.18 (t, *J* = 6.0 Hz, 2H), 5.96 (t, *J* = 4.8 Hz, 1H), 6.63 (s, 1H), 6.77 (s, 1H), 6.94 (d, *J* = 8.4 Hz, 2H), 7.29 (d, *J* = 8.8 Hz, 2H).

1-(2-(4-(2-Bromo-6,7-dimethoxy-3,4-dihydronaphthalen-1-yl)phenoxy)ethyl)pyrrolidine **(3b)**. To a solution of **2b** (848 mg, 2.23 mmol) in anhydrous DMF (20 mL) was added N-bromosuccinimide (397 mg, 2.23 mmol) dropwise at room temperature as a solution in DMF (10 mL). AIBN (15 mg, 0.09 mmol) was added and the reaction was stirred for 1 h. Most of the DMF was removed *in vacuo* and the resulting residue was partitioned between water and ethyl acetate. The ethyl acetate layer was dried over anhydrous Na_2SO_4, and evaporated to yield 864 mg (85%) of **3b** as a colorless oil which was used in the next step without further purification. ^{1}H NMR (400 MHz, $CDCl_3$): *δ* 1.85 (bs, 4H), 2.73 (bs, 4H), 2.95 (bs, 4H), 3.03 (t, *J* = 5.6 Hz, 2H), 3.59 (s, 3H), 3.89 (s, 3H), 4.21 (t, *J* = 6.0 Hz, 2H), 6.23 (s, 1H), 6.69 (s, 1H), 6.98 (d, *J* = 8.4 Hz, 2H), 7.13 (d, *J* = 8.8 Hz, 2H).

1-(2-(4-(6,7-Dimethoxy-2-phenyl-3,4-dihydronaphthalen-1-yl)phenoxy)ethyl)pyrrolidine **(4b)**. A solution of **3b** (476 mg, 1.04 mmol), phenylboronic acid (397 mg, 3.25 mmol), tetrakis (triphenylphosphine) palladium (44 mg, 0.037 mmol), and Na_2CO_3 (528 mg, 4.98 mmol) was refluxed in ethanol (25 mL) for 9 h. Ethanol was removed *in vacuo*, and the resulting residue was partitioned between ethyl acetate and water. The ethyl acetate layer was isolated, dried over anhydrous Na_2SO_4, and evaporated to give a crude oil which was purified by silica gel chromatography

(chloroform:methanol, 15:1) to give 353 mg (75%) of **4b** as a colorless oil. ^{1}H NMR (400 MHz, acetone-d_6): *δ* 1.74 (m, 4H), 2.60 (bs, 2H), 2.71 (m, 2H), 2.85 (m, 6H), 3.48 (s, 3H), 3.82 (s, 3H), 4.10 (t, 2H), 6.35 (s, 1H), 6.80-7.16 (m, 10H).

1-(2-(4-(6,7-Dimethoxy-2-phenyl-1,2,3,4-tetrahydronaphthalen-1-yl)phenoxy)ethyl)pyrrolidine **(5b)**. A solution of **4b** (353 mg, 0.775 mmol), palladium hydroxide (186 mg, 1.32 mmol), ethanol (10 mL), H_2O, (3 mL), and 2 N HCl (1 mL) was stirred at 40 ºC under H_2 (1 atm) for 12 h. The reaction was filtered through celite to remove catalyst, EtOH was removed *in vacuo*, and pH was adjusted to 8 using concentrated NaOH. The aqueous layer was extracted with ethyl acetate (3 X 25 mL) and the combined organic extracts were dried over anhydrous Na_2SO_4, and evaporated to give 287 mg (81%) of **5b** as a colorless oil which was used in the next step without further purification. ^{1}H NMR (400 MHz, acetone-d_6): *δ* 1.65 (m, 4H), 1.74 (m, 1H), 1.90 (d, 1H), 2.20 (m, 1H), 2.53 (bs, 4H), 2.63 (t, 2H), 3.00 (m, 2H), 3.53 (d, 1H), 3.60 (s, 3H), 3.80 (s, 3H), 3.93 (t, 2H), 4.20 (d, 1H), 6.35 (d, 2H), 6.45 (s, 1H), 6.53 (d, 2H), 6.68 (s, 1H), 7.10 (m, 3H).

6-Phenyl-5-(4-(2-(pyrrolidin-1-yl)ethoxy)phenyl)-5,6,7,8-tetrahydronaphthalene-2,3-diol **(6b, 7-hydroxylasofoxifene)**. A solution of **5b** (102 mg, 0.22 mmol) in ethanol (1 mL) was treated with 1.25 M HCl in ethanol (0.3 mL, 1.7 equiv) at 0 ºC and stirred at room temperature for 1 h. Solvent was removed *in vacuo*, and the sample was redissolved in anhydrous dichloromethane (1 mL). BBr_3 (0.56 mL, 1.0 M in DCM) was added at 0 ºC and the reaction was stirred for 1 h. Saturated aqueous $NaHCO_3$ (2 mL) was added and the organic layer was isolated, dried over anhydrous Na_2SO_4, and evaporated to give a white solid which was further purified using an ascorbic acid

adsorbed-silica gel column (mobile phase, chloroform:methanol, 4:1) to give 29 mg (31%) of racemic 7-hydroxylasofoxifene as a white solid. ^{1}H NMR (400 MHz, acetone-d_6): *δ* 1.65 (m, 4H), 2.20 (m, 1H), 2.50 (m, 4H), 2.80 (m, 4H), 2.95 (m, 1H), 3.50 (d, 1H), 3.95 (t, 2H), 4.05 (d, 1H), 6.33 (m, 2H), 6.60 (d, 2H), 6.66 (s, 1H), 6.84 (d, 2H), 7.10 (m, 3H), 7.55 (s, 2H). ^{13}C NMR (400 MHz, DMSO- d_6): δ 156.9, 143.3, 143.0, 138.5, 136.1, 133.6, 129.6, 128.8, 128.1, 126.0, 116.6, 115.7, 114.9, 66.8, 56.9, 56.5, 46.6, 33.9, 29.2, 23.6. Positive ion electrospray HRMS *m/z* 430.2334 $[M + H]^+$, calculated for $C_{28}H_{32}NO_3$ 430.2370.

6-Phenyl-5-(4-(2-(pyrrolidin-1-yl)ethoxy)phenyl)-5,6,7,8-tetrahydronaphthalen-2-ol **(6a, lasofoxifene, Figure 7)**. Racemic lasofoxifene was prepared using the same synthetic strategy outlined for the synthesis of 7-hydroxylasofoxifene, except that tetralone **1a** (Figure 7) was used as the starting material. ^{1}H NMR (400 MHz, $CDCl_3$): δ 1.32 (m, 2H), 1.84 (m, 2H), 2.35-2.48 (m, 5H), 2.96-3.05 (m, 4H), 3.40 (dd, *J* = 4.0, 3.0 Hz, 3H), 3.50 (m, 2H), 3.80 (m, 2H), 4.20 (m, 1H), 6.33 (d, *J* = 9.0 Hz, 2H), 6.50 (d, *J* = 9.0 Hz, 2H), 6.58 (dd, *J* = 3.0, 2.0 Hz, 1H), 6.73 (d, *J* = 2.0 1H), 6.77 (d, *J* = 8.0, 1H), 6.82 (d, *J* = 2.0, 2H), 7.1 (m, 3H). ^{13}C NMR (400 MHz, DMSO- d_6): δ 156.9, 154.3, 138.5, 137.0, 136.1, 132.2, 128.8, 128.1, 127.0, 126.0, 116.1, 114.9, 113.6, 66.8, 56.9, 56.5, 47.5, 46.3, 33.9, 29.0, 23.6. Positive ion electrospray HRMS *m/z* 414.2443 $[M + H]^+$, calculated for $C_{28}H_{32}NO_2$ 414.2421.

2.5.2 <u>Bazedoxifene (BAZ)</u>

Bazedoxifene was prepared via a procedure modified from that of Miller, et al [64] (Figure 8). Briefly, the protected propiophenone **7** was converted to **8** by Br_2 in Et_2O. The 3-methyl indole core **10** was then prepared by reaction of **8** with the protected

aniline hydrochloride **9** and Et_3N in refluxing DMF. Side chain **13** was prepared by alkylation of 4-hydroxybenzyl alcohol **11** with α-bromoethyl acetate to give **12,** followed by conversion of the alcohol to benzyl chloride **13** with $SOCl_2$ in THF. Indole **10** was coupled to side chain **13** using NaH in DMF to give ester **14**. This ester was first reduced to the primary alcohol **15** using $LiAlH_4$ in THF and then converted to the corresponding bromide **16** using triphenylphosphine and CBr_4 in THF. Substitution of this bromide with hexamethylenimine in THF yielded intermediate **17**, which was deprotected via catalytic transfer hydrogenation using 1, 4-cyclohexadiene and Pd/C in EtOH/THF to yield **18** (bazedoxifene) [64].

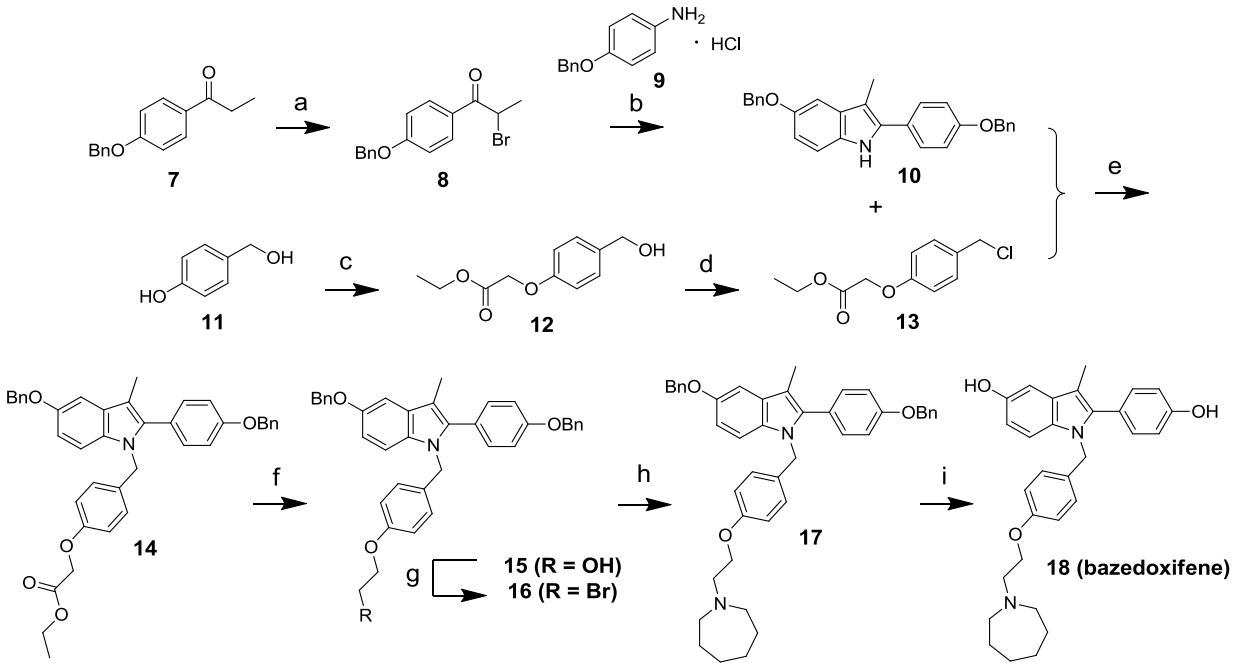

Figure 8. Synthesis of bazedoxifene

Reagents and conditions: (a) Br_2, Et_2O; (b) Et_3N, DMF, reflux; (c) K_2CO_3, ethyl 2-bromoacetate; (d) $SOCl_2$, THF; (e) NaH, DMF; (f) $LiAlH_4$, THF; (g) TPP, CBr_4, THF; (h) hexamethylenimine, THF; (i) 1,4-cyclohexadiene, Pd/C, EtOH, THF.

1-(4-(Benzyloxy)phenyl)-2-bromopropan-1-one **(8)**. To a stirred solution of 1-(4-(benzyloxy)phenyl)propan-1-one (5.00g, 20.8 mmol) in Et_2O (50 mL) was added Br_2 (1.07 mL, 20.8 mmol). The solution was stirred at room temperature for 30 min and H_2O (20mL) was added. The resulting biphasic mixture was diluted with Et_2O (50 mL) and washed carefully first with saturated aqueous $NaHCO_3$, and then saturated aqueous $Na_2S_2O_3$. The organic layer was isolated, dried over anhydrous Na_2SO_4, concentrated *in vacuo*, and purified by silica gel chromatography (hexanes:ethyl acetate, 19:1) to yield 5.05 g (76%) of **8** as a white solid. ^{1}H NMR (400 MHz, $CDCl_3$): δ 1.89 (d, *J* = 7.0 Hz, 3H), 5.15 (s, 2H), 5.26 (q, *J* = 7.0 Hz, 1H), 7.03 (d, *J* = 9.0 Hz, 2H), 7.33-7.37 (m, 1H), 7.39-7.44 (m, 4H), 8.01 (d, *J* = 9.0 Hz, 2H).

5-(Benzyloxy)-2-(4-(benzyloxy)phenyl)-3-methyl-1H-indole **(10)**. 1-(4-(benzyloxy)phenyl)-2-bromopropan-1-one (5.05g, 15.8 mmol) and 4-(benzyloxy)aniline hydrochloride **9** (5.13g, 21.8 mmol) were dissolved in anhydrous DMF (20 mL). Triethylamine (6.4 mL) was added and the reaction was stirred at 120 ºC for 2 h, after which period TLC analysis (hexanes:ethyl acetate, 4:1) verified consumption of starting material and formation of a more polar spot. The reaction was allowed to cool to room temperature and an additional 5.60g (23.7 mmol) of **9** was added. The mixture was stirred at 150 ºC for an additional 2 h, poured into H_2O (250 mL), and extracted with ethyl acetate (3 X 100 mL). The combined organic extracts were washed first with 1 M NaOH, H_2O, and then brine, and then dried over anhydrous Na_2SO_4. Removal of solvent yielded a crude tan-colored solid which was triturated first with methanol and then with Et_2O to yield 3.11 g (47%) of **10** as a white solid which was used in the next step without further purification. ^{1}H NMR (400 MHz, DMSO-d_6): δ 2.33 (s, 3H), 5.11 (s,

2H), 5.16 (s, 2H), 6.94 (dd, J = 8.8, 2.4 Hz, 1H), 7.08 (d, J = 2.2 Hz, 1H), 7.13 (d, J = 8.8 Hz, 2H), 7.21 (d, J = 7.0 Hz, 1H), 7.29-7.42 (m, 6H), 7.48 (d, J = 7.9 Hz, 4H), 7.56 (d, J = 8.8 Hz, 2H), 10.88 (s, 1H).

Ethyl 2-(4-(hydroxymethyl)phenoxy)acetate **(12)***.* To a stirred solution of 4-(hydroxymethyl)phenol **11** (5.00g, 40.3 mmol) in DMF (40 mL) was added ethyl bromoacetate (2.74 mL, 24.8 mmol) and potassium carbonate (7.34g, 53.1 mmol). The resulting suspension was stirred at 90 ºC for 2 h and solvent was removed in vacuo. The resulting residue was partitioned between 2 M aqueous potassium carbonate (100 mL) and ethyl acetate (100 mL). The organic layer was isolated, dried over anhydrous Na_2SO_4, and concentrated *in vacuo* to a yellow oil. This crude product was purified by silica gel chromatography (hexanes:ethyl acetate, 2:1) to yield 4.72 g (91%) of the desired ester **12** as a colorless oil. ^{1}H NMR (400 MHz, $CDCl_3$): δ 1.27 (t, J = 7.2 Hz, 3H), 2.05 (t, J = 5.6 Hz, 1H), 4.24 (q, J = 7.2 Hz, 2H), 4.57 (d, J = 5.6 Hz, 2H), 4.58 (s, 2H), 6.86 (d, J = 8.8 Hz, 2H), 7.25 (d, J = 8.8 Hz, 2H) [65].

Ethyl 2-(4-(chloromethyl)phenoxy)acetate **(13)**. To a solution of **12** (2.18g, 10.4 mmol) and TEA (1.6 mL, 11.4 mmol) in anhydrous dichloromethane (25 mL) was added methanesulfonyl chloride (0.8 mL, 10.4 mmol) dropwise at room temperature. The reaction was stirred at room temperature for 20 h, and then washed successively with H_2O, saturated aqueous $NaHCO_3$, and brine. The organic layer was dried over anhydrous Na_2SO_4, and removal of solvent yielded 2.34 g (99%) of **13** as a white solid which was used in the next step without further purification. ^{1}H NMR (400 MHz, $CDCl_3$): δ 1.30 (t, J = 7.0 Hz, 3H), 4.26 (q, J = 7.0 Hz, 2H), 4.56 (s, 2H), 4.60 (s, 2H), 6.88 (m, 2H), 7.30 (m, 2H) [66].

Ethyl 2-(4-((5-(benzyloxy)-2-(4-(benzyloxy)phenyl)-3-methyl-1H-indol-1-yl)methyl)phenoxy)acetate **(14)**. To a stirred solution of indole **10** (1.66g, 3.95 mmol) in DMF (40 mL) was added NaH (184 mg, 60% dispersion in mineral oil, 4.57 mmol) at 0 ºC. After stirring for 20 min, benzyl chloride **13** (1.49 g, 6.52 mmol) was added and the reaction was stirred for an additional 20 h at room temperature. The reaction mixture was poured into H_2O (500 mL), extracted with ethyl acetate (3 X 150 mL), and the combined ethyl acetate extracts were washed with brine and dried over anhydrous Na_2SO_4. Removal of solvent *in vacuo* gave a crude, tan-colored residue which was triturated with Et_2O to give 828 mg (34%) of **14** as a white solid which was used in the next step without further purification. ^{1}H NMR (400 MHz, DMSO-d_6): *δ* 1.16 (t, *J* = 7.2 Hz, 3H), 2.15 (s, 3H), 4.11 (q, *J* = 7.2 Hz, 2H), 4.66 (s, 2H), 5.11 (s, 2H), 5.13 (s, 2H), 5.16 (s, 2H), 6.73 (s, 4H), 6.80 (dd, *J* = 8.8, 2.4 Hz, 1H), 7.09-7.13 (m, 4H), 7.19 (d, *J* = 9.0 Hz, 1H), 7.29 (d, *J* = 8.8 Hz, 2H), 7.32-7.36 (m, 1H), 7.39 (q, *J* = 7.9 Hz, 4H), 7.47 (d, *J* = 7.2 Hz, 4H).

2-(4-((5-(Benzyloxy)-2-(4-(benzyloxy)phenyl)-3-methyl-1H-indol-1-yl)methyl)phenoxy)ethanol **(15)***.* To a stirred solution of ester **14** (828 mg, 1.35 mmol) in anhydrous THF (15 mL) was added $LiAl_4$ (59 mg, 1.55 mmol) at 0 ºC. After stirring for 1 h at 0 ºC the reaction was carefully quenched with water. Volatiles were removed *in vacuo* and the resulting residue was partitioned between ethyl acetate and 1 M HCl. The organic layer was isolated, dried over anhydrous Na_2SO_4, and concentrated to yield 769 mg (100%) of the desired alcohol **15** as a white foam. ^{1}H NMR (400 MHz, DMSO-d_6): *δ* 2.15 (s, 3H), 3.63 (q, J = 5.3 Hz, 2H), 3.86 (t, J = 4.8 Hz, 2H), 4.80 (t, J = 5.5 Hz,

1H), 5.11 (s, 2H), 5.13 (s, 2H), 5.15 (s, 2H), 6.73 (s, 4H), 6.80 (dd, J = 8.8, 2.4 Hz, 1H), 7.10-7.12 (m, 3H), 7.20 (d, J = 8.8 Hz, 1H), 7.27-7.42 (m, 8H), 7.46-7.48 (m, 4H).

5-(Benzyloxy)-2-(4-(benzyloxy)phenyl)-1-(4-(2-bromoethoxy)benzyl)-3-methyl-1H-indole **(16)**. To a stirred solution of 2-(4-((5-(benzyloxy)-2-(4-(benzyloxy)phenyl)-3-methyl-1H-indol-1-yl)methyl)phenoxy)ethanol **15** (769 mg, 1.35 mmol) in THF (15 mL) was added CBr_4 (673 mg, 2.03 mmol) and PPh_3 (533 mg, 2.03 mmol). The reaction was stirred at room temperature for 8 h, solvent was removed *in vacuo*, and the resulting residue was purified by silica gel chromatography (hexanes:ethyl acetate, 6:1) to give 630 mg (74%) of the desired bromide **16** as a white solid. ^{1}H NMR (400 MHz, DMSO-d_6): *δ* 2.15 (s, 3H), 3.73 (t, *J* = 5.5 Hz, 2H), 4.20 (t, *J* = 5.3 Hz, 2H), 5.11 (s, 2H), 5.13 (s, 2H), 5.16 (s, 2H), 6.73-6.77 (m, 4H), 6.80 (dd, *J* = 8.8, 2.4 Hz, 1H), 7.09-7.12 (m, 3H), 7.20 (d, *J* = 8.8 Hz, 1H), 7.29 (d, *J* = 8.8 Hz, 2H), 7.30-7.64 (m, 10H).

1-(4-(2-(Azepan-1-yl)ethoxy)benzyl)-5-(benzyloxy)-2-(4-(benzyloxy)phenyl)-3-methyl-1H-indole **(17)**. Hexamethyleneimine (461 mg, 4.65 mmol) was added to a solution of 5-(benzyloxy)-2-(4-(benzyloxy)phenyl)-1-(4-(2-bromoethoxy)benzyl)-3-methyl-1H-indole **16** (294 mg, 0.47 mmol) in THF (20 mL) and refluxed for 6 h. Solvent was removed *in vacuo* and the resulting residue was partitioned between ethyl acetate and saturated $NaHCO_3$. The organic layer was isolated, dried over anhydrous Na_2SO_4, and concentrated to give a white solid which was further purified by silica gel chromatography (ethyl acetate) to yield 185 mg (61%) of compound **17**. ^{1}H NMR (400 MHz, DMSO-d_6): *δ* 1.44-1.58 (m, 8H), 2.15 (s, 3H), 2.56-2.64 (m, 4H), 2.76 (t, *J* = 5.9 Hz, 2H), 3.90 (t, *J* = 5.9 Hz, 2H), 5.11 (s, 2H), 5.13 (s, 2H), 5.15 (s, 2H), 6.73 (s, 4H),

6.80 (dd, *J* = 8.8, 2.4 Hz, 1H), 7.10-7.14 (m, 3H), 7.19 (d, *J* = 8.8 Hz, 1H), 7.29 (d, *J* = 8.8 Hz, 2H), 7.30-7.36 (m, 2H), 7.36-7.41 (m, 4H), 7.47 (d, *J* = 8.3 Hz, 4H).

1-(4-(2-(Azepan-1-yl)ethoxy)benzyl)-2-(4-hydroxyphenyl)-3-methyl-1H-indol-5-ol **(18, bazedoxifene, Figure 8)**. A stirred suspension of 10% Pd/C (85 mg) in ethanol (5 mL) was treated with cyclohexadiene (125 µL, 1.32 mmol) and a solution of **17** (185 mg, 0.28 mmol) in THF (5 mL). The resulting suspension was stirred at room temperature for 12 h and then filtered through celite. The filtrate was concentrated to a crude oil which was purified by silica gel chromatography (dichloromethane:methanol, 19:1) to give **18** (bazedoxifene, 45 mg, 34%) as a light tan solid. ^{1}H NMR (400 MHz, DMSO-d_6): *δ* 1.47–1.63 (m, 8H), 2.10 (s, 3H), 2.63–2.81 (m, 4H), 2.86 (t, 2H, *J* = 5.6 Hz), 3.97 (t, 2H, *J* = 5.6 Hz), 5.10 (s, 2H), 6.58 (dd, 1H, *J* = 8.7 Hz, 2.3 Hz), 6.76 (s, 4H), 6.81 (d, 1H, *J* = 2.3 Hz), 6.86 (d, 2H, *J* = 8.6 Hz), 7.06 (d, 1H, *J* = 8.7 Hz), 7.16 (d, 2H, *J* = 8.7 Hz), 8.67 (s, 1H), 9.64 (s, 1H) [67]. ^{13}C NMR (400 MHz, DMSO- d_6): δ 9.9, 26.5, 46.2, 55.1, 55.2, 102.9, 107.0, 111.0, 111.8, 114.7, 115.8, 122.6, 127.9, 129.2, 131.0, 131.8, 138.2, 151.1, 157.6. Positive ion electrospray HRMS *m/z* 471.2639 $[M + H]^+$, calculated for $C_{30}H_{34}N_2O_3$ 471.2569.

2.5.3 BTC, *i*Pr-BTC,Tol-BTC, bisBTChd, PTP-BTF, HP-BTF, HP-BTC

2-(4-Hydroxyphenyl)benzo[b]thiophen-6-ol **(19, BTC, Figure 9)**. BBr_3 (4.62 mL, 1.0 M in DCM, 4.62 mmol) was added to a solution of 6-methoxy-2-(4-methoxyphenyl) benzo[b]thiophene (500 mg, 1.85 mmol) in anhydrous DCM (50 mL) at 0 ºC. The reaction was stirred at 0 ºC for 2 h and then carefully quenched by the addition of saturated $NaHCO_3$ (10 mL). DCM was removed under reduced pressure, and the residue was partitioned between water and ethyl acetate. The aqueous layer was

extracted with ethyl acetate (3 X 25 mL), and the organic extracts were combined and dried over anhydrous Na_2SO_4. Solvent was removed *in vacuo* and the crude product was purified by flash chromatography (hexanes:ethyl acetate, 4:1) to afford 394 mg (88%) of **19** as a white solid. ^{1}H NMR (400 MHz, acetone-d_6): δ 6.91-6.93 (m, 3H), 7.31 (s, 1H), 7.44 (s, 1H), 7.57 (d, J = 8.4 Hz, 2H), 7.62 (d, J = 8.8 Hz, 1H), 8.48 (s, 1H), 8.57 (s, 1H). Positive ion electrospray mass spectroscopy *m/z* 242.2 (100%) $[M+H]^+$.

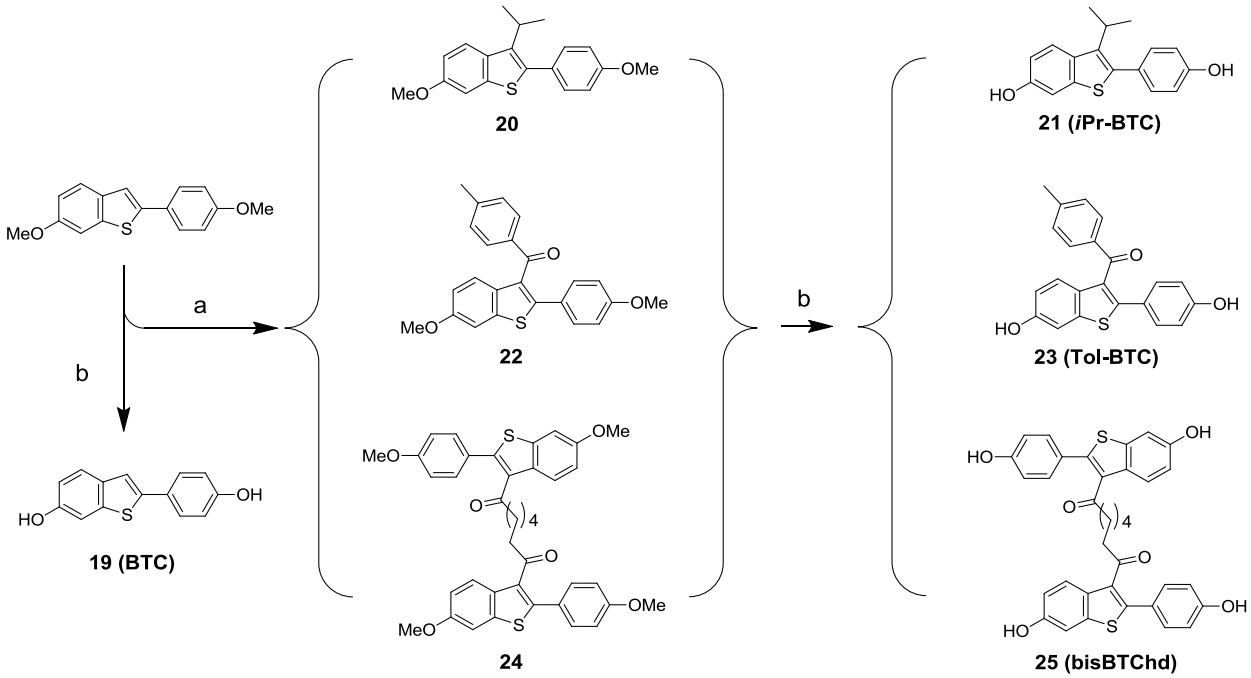

Figure 9. Synthesis of BTC; iPr-BTC; Tol-BTC; bisBTChd

Reagents and conditions: (a) 2-bromopropane, 4-methylbenzoyl chloride, or heptanedioyl dichloride; $AlCl_3$, DCM; (b) BBr_3, DCM, 0 °C.

3-Isopropyl-6-methoxy-2-(4-methoxyphenyl)benzo[b]thiophene **(20)**. Anhydrous $AlCl_3$ (617 mg, 4.63 mmol) was added in small portions to a stirred solution of 6-

methoxy-2-(4-methoxyphenyl)benzo[*b*]thiophene (500 mg, 1.85 mmol) in anhydrous DCM (60 mL) at 0 ºC. To this solution, 2-bromopropane (569 mg, 4.63 mmol) was added dropwise, and the mixture was stirred at 0 ºC for 2 h, and then at room temperature for 4 h. The reaction mixture was poured into ice water (100 mL) and extracted with DCM (3 x 50 mL). The organic layer was washed with 1 M NaOH and brine and dried over anhydrous Na_2SO_4. Solvent was removed under reduced pressure and the crude product was purified by flash chromatography (hexanes:ethyl acetate 10:1) to yield 242 mg (42%) of the desired compound. ^{1}H NMR (400 MHz, $CDCl_3$): δ 1.43 (s, 3H), 1.45 (s, 3H), 3.42 (sep, *J* = 7.2 Hz, 1H), 3.88 (s, 3H), 3.90 (s, 3H) 6.99 (d, *J* = 8.8 Hz, 2H), 7.02 (d, *J* = 2.4 Hz, 1H), 7.32 (d, *J* = 2.4 Hz, 1H), 7.40 (d, *J* = 8.8 Hz, 2H), 7.87 (d, *J* = 9.2 Hz, 1H). ^{13}C NMR (400 MHz, $CDCl_3$): δ 21.7, 27.8, 54.9, 55.2, 104.6, 113.0, 113.4, 123.8, 127.2, 130.8, 132.7, 134.3, 136.6, 140.7, 156.3, 158.9.

2-(4-Hydroxyphenyl)-3-isopropylbenzo[b]thiophen-6-ol **(21, *i*Pr-BTC, Figure 9)***.* To a stirred solution of 3-isopropyl-6-methoxy-2-(4-methoxyphenyl)benzo[b]thiophene **20** (114 mg, 0.37 mmol) in anhydrous DCM (40 mL) was added BBr_3 (1.0 M, in DCM, 1.46 mmol) at -78 ºC. The reaction was allowed to warm to room temperature over the course of 6 h, after which period it was carefully quenched by the addition of saturated $NaHCO_3$ (20 mL) at 0 ºC. DCM was removed under reduced pressure, and the residue was partitioned between water and ethyl acetate. The aqueous layer was extracted with ethyl acetate (3 X 50 mL), and the organic extracts were combined and dried over Na_2SO_4. Solvent was removed under reduced pressure and the crude product was purified by flash chromatography (hexanes:ethyl acetate, 4:1) to afford 60 mg (58%) of the desired compound. ^{1}H NMR (400 MHz, DMSO-d_6): δ 1.33 (s, 3H), 1.35 (s 3H), 3.31

(sep, J = 7.2 Hz, 1H), 6.83-6.88 (m, 3H), 7.20 (d, J = 2.4 Hz, 1H), 7.22 (d, J = 8.8 Hz, 2H), 7.78 (d, J = 8.8 Hz, 1H), 9.54 (s, 1H), 9.68 (s, 1H); ^{13}C NMR (400 MHz, DMSO- d_6): δ 21.8, 27.7, 107.3, 114.0, 115.5, 124.1, 125.1, 130.9, 131.4, 133.3, 136.1, 140.2, 154.4, 157.3. Positive ion electrospray HRMS *m/z* 285.0938 $[M + H]^+$, calculated for $C_{17}H_{17}O_2S$ 285.0905.

(6-Methoxy-2-(4-methoxyphenyl)benzo[b]thiophen-3-yl)(p-tolyl)methanone **(22)**. *p*-toluoyl chloride (343 mg, 2.22 mmol) was added to a solution of 6-methoxy-2-(4-methoxyphenyl)benzo[*b*]thiophene (BTC, 400 mg, 1.48 mmol) in anhydrous DCM (60 mL) at 0 ºC. To this mixture, $AlCl_3$ (296 mg, 2.22 mmol) was added and the reaction was stirred at 0 ºC for 2 h and at room temperature for 1 h. The reaction mixture was poured into ice water (100 mL) and extracted with DCM (3 x 50 mL). The organic layer was washed with 1 M NaOH and brine and dried over anhydrous Na_2SO_4. Solvent was removed under reduced pressure and the crude product was purified by flash chromatography (hexanes:ethyl acetate, 8:1) to yield 438 mg (76%) of the desired product. ^{1}H NMR (400 MHz, acetone-d_6): δ 2.31 (s, 3H), 3.75 (s, 3H), 3.90 (s, 3H), 6.85 (d, J = 8.8 Hz, 2H), 7.01 (dd, J = 8.8, 2.4 Hz, 1H), 7.17 (d, J = 8 Hz, 2H), 7.37 (d, J = 8.8 Hz, 2H), 7.48 (d, J = 8.8 Hz, 1H), 7.56 (d, J = 2.4 Hz, 1H), 7.67 (d, J = 8 Hz, 2H).

(6-Hydroxy-2-(4-hydroxyphenyl)benzo[b]thiophen-3-yl)(p-tolyl)methanone **(23, Tol-BTC, Figure 9)**. To a stirred solution of (6-methoxy-2-(4-methoxyphenyl)benzo[*b*]thiophen-3-yl)(*p*-tolyl)methanone **22** (200 mg, 0.52 mmol) in anhydrous DCM (20 mL) was added BBr_3 (1.0 M, in DCM, 2.06 mL, 2.06 mmol) at -78 $^{\circ}$C. The reaction was allowed to warm to room temperature over the course of 4 h, after which period it was carefully quenched by the addition of saturated $NaHCO_3$ (5 mL) at 0

ºC. DCM was removed under reduced pressure, and the residue was partitioned between water and ethyl acetate. The aqueous layer was extracted with ethyl acetate (3 X 30 mL), and the organic extracts were combined and dried over anhydrous Na_2SO_4. Solvent was removed *in vacuo* and the crude product was purified by flash chromatography (hexanes:ethyl acetate, 2:1) to afford 132 mg (66%) of the desired compound. ^{1}H NMR (400 MHz, DMSO-d_6): δ 2.29 (s, 3H), 6.66 (d, *J* = 8.4 Hz, 2H), 6.85 (dd, *J* = 8.6, 2.4 Hz, 1H), 7.16 (d, *J* = 8.4 Hz, 2H), 7.19 (d, *J* = 8 Hz, 2H), 7.27 (d, *J* = 8.8 Hz, 1H), 7.34 (d, *J* = 2 Hz, 1H), 7.59 (d, *J* = 8 Hz, 1H), 9.72 (s, 1H), 9.78 (s, 1H); ^{13}C NMR (400 MHz, DMSO-d_6): δ 21.5, 107.5, 115.6, 116.0, 123.7, 124.3, 129.8, 129.9, 130.3, 132.7, 134.6, 139.8, 141.9, 145.2, 155.4, 194.6. Positive ion electrospray HRMS *m/z* 361.0842 $[M + H]^+$, calculated for $C_{22}H_{17}O_3S$ 361.0886.

1,7-Bis(6-methoxy-2-(4-methoxyphenyl)benzo[b]thiophen-3-yl)heptane-1,7-dione **(24)**. Anhydrous $AlCl_3$ (269 mg, 2.02 mmol) was added in small portions to a stirred solution of 6-methoxy-2-(4-methoxyphenyl)benzo[*b*]thiophene (500 mg, 1.85 mmol) in anhydrous DCM (60 mL) at 0 ºC. To this solution, pimeloyl chloride (165 mg, 0.83 mmol) was added slowly, and the mixture was stirred at 0 ºC for 2 h, and then at room temperature for 2 h. The reaction mixture was poured into ice water (100 mL) and extracted with DCM (3 x 50 mL). The organic layer was washed with 1 M NaOH and brine and dried over anhydrous Na_2SO_4. Solvent was removed under reduced pressure and the crude product was purified by flash chromatography (hexanes:ethyl acetate, 6:1) to yield 264 mg (48%) of the desired compound. ^{1}H NMR (400 MHz, $CDCl_3$): δ 0.99 (quin, *J* = 2.8 Hz, 2H), 1.40 (quin, *J* = 7.6 Hz, 4H), 2.31 (t, *J* = 7.2 Hz, 4H), 3.86 (s, 6H), 3.89 (s, 6H), 6.94 (d, *J* = 8.8 Hz, 4H), 7.04 (dd, *J* = 8.8, 2.4 Hz, 2H), 7.27 (d, *J* = 2.4 Hz,

2H), 7.35 (d, *J* = 8.8 Hz, 4H), 7.90 (d, *J* = 9.2 Hz, 2H); ^{13}C NMR (400 MHz, $CDCl_3$): δ 24.0, 28.0, 42.5, 55.0, 55.2, 99.6, 103.8, 113.9, 114.7, 124.2, 125.8, 130.3, 132.2, 132.2, 139.6, 144.9, 157.3, 160.1, 201.7.

1,7-Bis(6-hydroxy-2-(4-hydroxyphenyl)benzo[b]thiophen-3-yl)heptane-1,7-dione **(25, bisBTChd, Figure 9)**. To a stirred solution of 1,7-bis(6-methoxy-2-(4-methoxyphenyl)benzo[b]thiophen-3-yl)heptane-1,7-dione **24** (72 mg, 0.11 mmol) in anhydrous DCM (30 mL) was added BBr_3 (1.0 M, in DCM, 888 µL, 0.89 mmol) at -78 ºC. The reaction was allowed to warm to room temperature over the course of 6 h, after which period it was carefully quenched by the addition of saturated $NaHCO_3$ (20 mL) at 0 ºC. DCM was removed under reduced pressure, and the residue was partitioned between water and ethyl acetate. The aqueous layer was extracted with ethyl acetate (3 X 50 mL), and the organic extracts were combined and dried over Na_2SO_4. Solvent was removed under reduced pressure and the crude product was purified by flash chromatography (hexanes:ethyl acetate, 2:1) to afford 58 mg (86%) of the desired compound. ^{1}H NMR (400 MHz, DMSO-d_6): δ 0.86 (quin, *J* = 2.8 Hz, 2H), 1.28 (quin, *J* = 7.2 Hz, 4H), 2.26 (t, *J* = 7.2 Hz, 4H), 6.84 (d, *J* = 8.8 Hz, 4H), 6.91 (dd, *J* = 8.8, 2.4 Hz, 2H), 7.19 (d, *J* = 8.8 Hz, 4H), 7.28 (d, *J* = 2 Hz, 2H), 7.66 (d, *J* = 8.8 Hz, 2H), 9.76 (s, 2H), 9.91 (s, 2H); ^{13}C NMR (400 MHz, DMSO-d_6): δ 24.3, 28.2, 42.5, 107.2, 115.8, 116.3, 124.5, 130.8, 131.3, 132.0, 139.6, 144.7, 155.9, 201.5; Positive ion electrospray HRMS *m/z* 609.1430 $[M + H]^+$, calculated for $C_{35}H_{29}O_6S_2$ 609.1361.

1-(4-Fluorophenyl)-2-((3-methoxyphenyl)thio)ethanone **(26)***.* 3-Methoxybenzenethiol (3.23 g, 23.0 mmol) was added in one portion to a freshly prepared solution of 25 mL of ethanol, 10 mL of water, and 1.53 g of KOH (27.3 mmol).

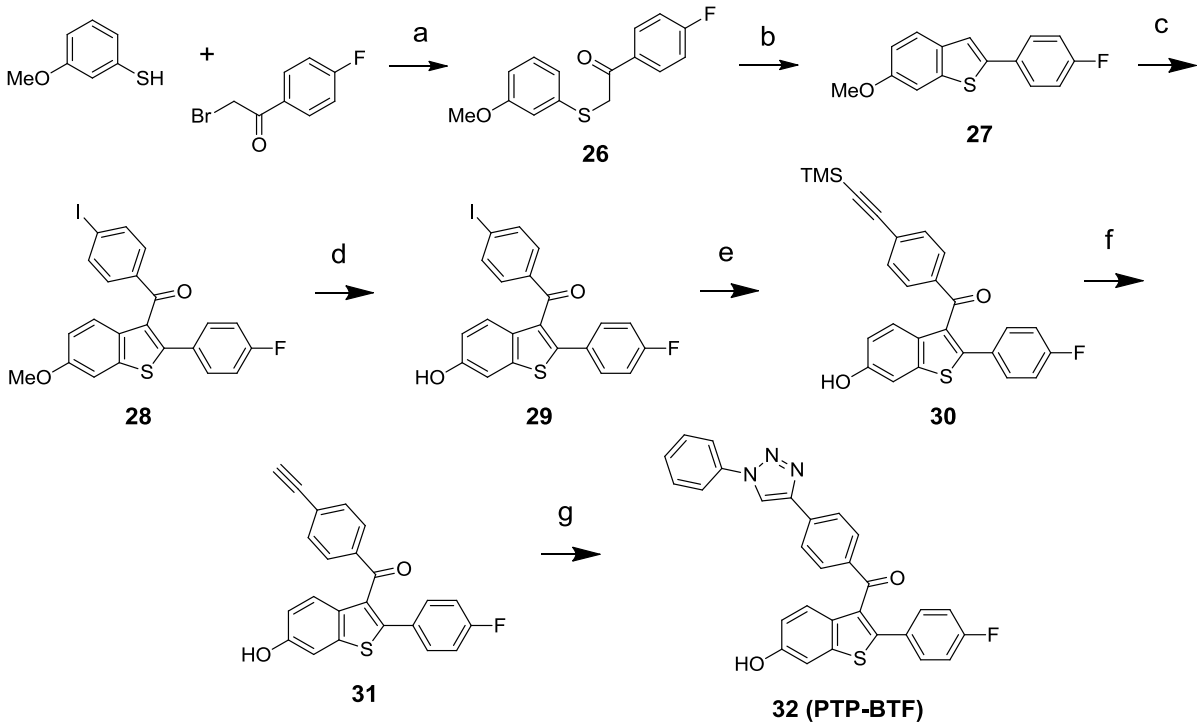

Figure 10. Synthesis of PTP-BTF

Reagents and conditions: (a) KOH, EtOH/H_2O; (b) PPA, 120 °C; (c) 4-iodobenzoyl chloride, $AlCl_3$, DCM; (d) BBr_3, DCM; (e) ethynyltrimethylsilane, $PdCl_2(PPh_3)_2$, CuI, DIPEA, toluene; (f) K_2CO_3, MeOH; (g) azidobenzene, sodium ascorbate, $CuSO_4$, *tert*-BuOH, H_2O.

The solution was cooled to 0°C. A solution of 2-bromo-1-(4-fluorophenyl)ethanone (5.00 g, 23.0 mmol) in 10 mL of ethyl acetate was added to this solution at a rate such that the temperature did not exceed 25 °C, and the reaction mixture was allowed to stir overnight at room temperature. The solvents were removed under reduced pressure, and the residue was partitioned between water and ethyl acetate. The aqueous layer was isolated and extracted several times with ethyl acetate, and the combined extracts were washed with consecutive portions of 10% HCl, water, saturated $NaHCO_3$, and water before being dried over anhydrous Na_2SO_4. After concentration in vacuo to an oil,

the crude product was purified by flash chromatography (hexanes:ethyl acetate 10:1) to give 5.81 g (91 %) of the desired compound. ^{1}H NMR (300 MHz, DMSO-d_6) δ 3.73 (s, 3H), 4.67 (s, 3H), 6.75 (m, 1H), 6.91 (m, 2H), 7.18 (t, J = 8.2 Hz, 1H), 7.34 (t, J = 8.9 Hz, 2H), 8.12 (q, J = 8.9 Hz, 2H). Positive ion electrospray mass spectroscopy *m/z* 277.2 (100%) $[M+H]^+$.

6-Methoxy-2-(4-fluorophenyl) benzo[b]thiophene **(27)***.* Polyphosphoric acid (58 g) was heated to 85 °C, with stirring. 1-(4-fluorophenyl)-2-(3- methoxyphenylsulfanyl) ethanone (5.81 g, 21.0 mmol) was added portionwise at a rate such that the temperature never exceeded 100 °C. After the addition was complete, the reaction mixture was stirred at 115 °C for 3 h, allowed to cool to 70 °C, and then slowly poured into rapidly stirring ice water. The aqueous solution was extracted several times with ethyl acetate, and the combined organic layers were washed with consecutive portions of water, saturated $NaHCO_3$, and water again before being dried over anhydrous Na_2SO_4. The organic layer was concentrated in vacuo, and the residue was purified by flash chromatography (hexane:chloroform, 6:1) to give 2.62 g (48 %) of the desired benzothiophene. ^{1}H NMR (360 MHz, DMSO-d_6) δ 3.83 (s, 3H), 7.00 (dd, J = 2.4, 8.8 Hz, 1H), 7.30 (t, J = 8.8 Hz, 2H), 7.56 (d, J = 2.2 Hz, 1H), 7.73 (m, 2H), 7.77 (q, J = 8.7 Hz, 2H). ^{13}C NMR (400 MHz, DMSO-d_6): δ 163.2, 160.5, 157.3, 140.2, 139.2, 134.3, 130.4, 127.8, 127.7, 124.4, 119.7, 116.2, 116.0, 114.7, 105.1, 55.5. Positive ion electrospray mass spectroscopy *m/z* 259.1 (100%) $[M+H]^+$.

(2-(4-Fluorophenyl)-6-methoxybenzo[b]thiophen-3-yl)(4-iodophenyl)methanone **(28)**. 4-iodobenzoyl chloride (1.06 g, 3.97 mmol) was added to a solution of 2-(4-fluorophenyl)-6-methoxybenzo[b]thiophene) **27** [39] (683 mg, 2.64 mmol) in anhydrous

DCM (60 mL) at 0 ºC. To this mixture, $AlCl_3$ (530 mg, 3.97 mmol) was added and the reaction was stirred at 0 ºC for 1 h. The reaction mixture was poured into ice water (100 mL) and extracted with DCM (3 x 50 mL). The organic layer was washed with 1 M NaOH and brine and dried over anhydrous Na_2SO_4. Solvent was removed under reduced pressure and the crude product was purified by flash chromatography (hexanes:ethyl acetate, 4:1) to yield 802 mg (62%) of the desired product. ^{1}H NMR (400 MHz, acetone-d_6): δ 3.84 (s, 3H), 7.05 (t, *J* = 8.8 Hz, 2H), 7.08 (dd, *J* = 8.8 Hz, 2.0 Hz, 1H), 7.40 (td, *J* = 5.6 Hz, 2.0 Hz, 2H), 7.41 (d, *J* = 2.0 Hz, 1H), 7.49 (d, *J* = 8.4 Hz, 2H), 7.55 (d, *J* = 8.8 Hz, 1H), 7.75 (d, *J* = 8.4 Hz, 2H). ^{13}C NMR (400 MHz, DMSO-d_6): δ 192.1, 170.3, 162.9, 159.4, 142.6, 137.7, 135.6, 132.7, 131.3, 129.3, 129.1, 126.3, 124.2, 116.0, 115.8, 110.6, 98.2, 55.8. Positive ion electrospray mass spectroscopy *m/z* 489.2 (100%) $[M+H]^+$.

(2-(4-Fluorophenyl)-6-hydroxybenzo[b]thiophen-3-yl)(4-iodophenyl)methanone **(29)**. To a stirred solution of (2-(4-fluorophenyl)-6-methoxybenzo[b]thiophen-3-yl)(4-iodophenyl)methanone **28** (802 mg, 1.64 mmol) in anhydrous DCM (50 mL) was added BBr_3 (1.0 M, in DCM, 24 mL, 24.0 mmol) at 0 ºC. The reaction was stirred for 2 h and then quenched by the addition of saturated $NaHCO_3$ (25 mL). DCM was removed under reduced pressure, and the resulting residue was partitioned between water and ethyl acetate. The aqueous layer was extracted with ethyl acetate (3 X 50 mL), and the organic extracts were combined and dried over Na_2SO_4. Solvent was removed under reduced pressure and the crude product was purified by flash chromatography (hexanes:ethyl acetate, 3:1) to afford 604 mg (78%) of the desired compound. ^{1}H NMR (400 MHz, acetone-d_6): δ 7.05 (t, *J* = 8.8 Hz, 2H), 7.11 (dd, *J* = 8.8 Hz, 2.0 Hz, 1H), 7.34

(d, *J* = 2.0 Hz, 1H), 7.40 (td, *J* = 5.6 Hz, 2.0 Hz, 2H), 7.49 (d, *J* = 8.4 Hz, 2H), 7.55 (d, *J* = 8.8 Hz, 1H), 7.75 (d, *J* = 8.4 Hz, 2H), 9.54 (s, 1H). ^{13}C NMR (400 MHz, DMSO-d_6): δ 192.1, 170.3, 162.9, 153.2, 143.0, 137.7, 131.3, 129.3, 129.1, 122.9, 124.6, 116.0, 110.9, 105.2, 98.2. Positive ion electrospray mass spectroscopy *m/z* 475.2 (100%) $[M+H]^+$.

(2-(4-Fluorophenyl)-6-hydroxybenzo[b]thiophen-3-yl)(4-((trimethylsilyl)ethynyl) phenyl)methanone **(30)***.* Ethynyltrimethylsilane (176 µL, 1.27 mmol) and (2-(4-fluorophenyl)-6-hydroxybenzo[b]thiophen-3-yl)(4-iodophenyl)methanone **29** (604 mg, 1.27 mmol) were dissolved in anhydrous toluene (100 mL). $PdCl_2(PPh_3)_2$ (27 mg, 0.038 mmol), CuI (24 mg, 0.127 mmol), and DIPEA (221 µL, 1.27 mmol) were added, and the reaction was stirred at room temperature for 24 h. Volatiles were removed *in vacuo*, and the resulting residue was purified by flash chromatography (hexanes:ethyl acetate, 5:1) to afford 512 mg (91%) of the desired compound. ^{1}H NMR (400 MHz, acetone-d_6): δ 0.22 (s, 9H), 7.05 (t, *J* = 8.8 Hz, 2H), 7.11 (dd, *J* = 8.8 Hz, 2.0 Hz, 1H), 7.34 (d, *J* = 2.0 Hz, 1H), 7.40 (td, *J* = 5.6 Hz, 2.0 Hz, 2H), 7.53 (d, *J* = 8.4 Hz, 2H), 7.56 (d, *J* = 8.8 Hz, 1H), 7.78 (d, *J* = 8.4 Hz, 2H), 9.53 (s, 1H). ^{13}C NMR (400 MHz, DMSO-d_6): δ 192.1, 170.3, 162.9, 153.2, 143.0, 135.6, 133.5, 132.4, 129.3, 129.1, 126.6, 124.6, 122.9, 116.0, 110.9, 105.2, 98.9, 53.5, 3.4. Positive ion electrospray mass spectroscopy *m/z* 445.4 (100%) $[M+H]^+$.

(4-Ethynylphenyl)(2-(4-fluorophenyl)-6-hydroxybenzo[b]thiophen-3-yl)methanone **(31)***.* K_2CO_3 (391 mg, 2.83 mmol) was added to a stirred solution of (2-(4-fluorophenyl)-6-hydroxybenzo[b]thiophen-3-yl)(4-((trimethylsilyl)ethynyl) phenyl)methanone **30** (314 mg, 0.71 mmol) in methanol (20 mL) and the reaction was stirred under argon at room

temperature for 16 h. The reaction was carefully quenched by the addition of 1N HCl, concentrated *in vacuo*, and the resulting residue partitioned between water and ethyl acetate. The organic layer was isolated, washed with brine, and removal of solvent gave 255 mg (97%) of the desired alkyne which was used in the next step without further purification. ^{1}H NMR (400 MHz, acetone-d_6): δ 4.27 (s, 1H), 7.05 (t, J = 8.8 Hz, 2H), 7.11 (dd, J = 8.8 Hz, 2.0 Hz, 1H), 7.34 (d, J = 2.0 Hz, 1H), 7.40 (td, J = 5.6 Hz, 2.0 Hz, 2H), 7.53 (d, J = 8.4 Hz, 2H), 7.56 (d, J = 8.8 Hz, 1H), 7.78 (d, J = 8.4 Hz, 2H), 9.53 (s, 1H). ^{13}C NMR (400 MHz, DMSO-d_6): δ 192.1, 170.3, 162.9, 153.2, 143.0, 135.6, 133.5, 132.4, 129.3, 129.1, 126.6, 124.6, 122.9, 116.0, 110.9, 105.2, 82.3, 81.4. Positive ion electrospray mass spectroscopy *m/z* 373.3 (100%) $[M+H]^+$.

(2-(4-Fluorophenyl)-6-hydroxybenzo[b]thiophen-3-yl)(4-(1-phenyl-1H-1,2,3-triazol-4-yl)phenyl)methanone **(32, PTP-BTF, Figure 10).** (4-ethynylphenyl)(2-(4-fluorophenyl)-6-hydroxybenzo[b]thiophen-3-yl)methanone **31** (31 mg, 0.084 mmol) was dissolved in *tert*-butanol (2 mL) and water (0.5 mL). Azidobenzene (10 mg, 0.084 mmol), sodium ascorbate (6.7 mg, 0.034 mmol), and $CuSO_4$ (2.7 mg, 0.017 mmol) were added, and the reaction was stirred at 50 ºC for 12 h. The mixture was then diluted with ethyl acetate, washed with brine, and concentrated *in vacuo* to an oil which was purified by flash chromatography (hexanes:ethyl acetate, 2:1) to afford 26 mg (63%) of the desired compound. ^{1}H NMR (400 MHz, acetone-d_6): δ 7.05 (t, J = 8.8 Hz, 2H), 7.08 (dd, J = 8.8 Hz, 2.0 Hz, 1H), 7.40 (td, J = 5.6 Hz, 2.0 Hz, 2H), 7.49 (d, J = 2.0 Hz, 1H), 7.54 (t, J = 7.2 Hz, 1H), 7.59 (d, J = 8.8 Hz, 1H), 7.65 (t, J = 8.0 Hz, 2H), 7.70 (d, J = 8.4 Hz, 2H), 7.88 (d, J = 8.4 Hz, 2H), 7.97 (d, J = 8.0 Hz, 2H), 9.06 (s, 1H). ^{13}C NMR (400 MHz, DMSO-d_6): δ 192.1, 170.3, 162.9, 153.2, 148.0, 143.0, 136.8, 135.6, 134.3, 133.8,

131.4, 130.2, 129.3, 129.1, 128.7, 127.6, 124.6, 122.9, 120.5, 116.0, 110.9, 105.2. Positive ion electrospray HRMS *m/z* 492.1132 $[M + H]^+$, calculated for $C_{29}H_{19}FN_3O_2S$ 492.1170.

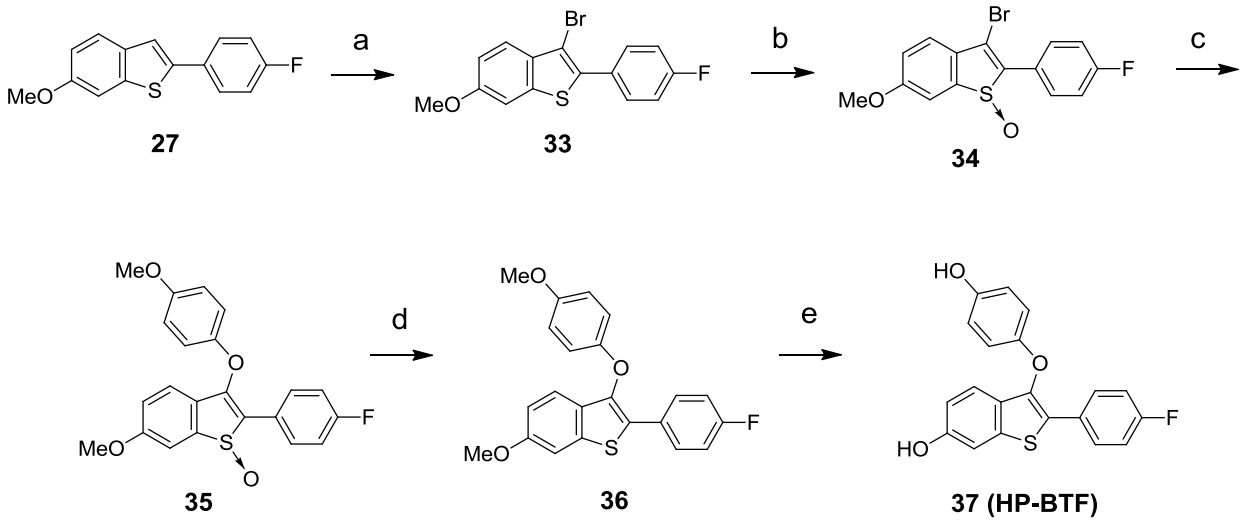

Figure 11. Synthesis of HP-BTF

Reagents and conditions: (a) N-bromoacetamide, DCM/EtOH; (b) H_2O_2, TFA, DCM; (c) 4-methoxyphenol, NaH, DMF; (d) $LiAlH_4$, THF, 0 °C; (e) BBr_3, DCM, 0 °C.

6-Methoxy-2-(4-fluorophenyl)-3-bromobenzo[b]thiophene **(33)***. N-*Bromoacetamide (443 mg, 3.21 mmol) in 5 mL of ethanol was added dropwise to a solution of 6-Methoxy-2-(4-fluorophenyl) benzo[b]thiophene **27** (790 mg, 3.06 mmol) in 100 mL of dichloromethane and 10 mL of ethanol at room temperature. After the mixture was stirred for 1 h, the solvent was removed in vacuo. The residue was then titrated with ethanol and filtered to give 938 mg (91 %) of the desired compound as a white solid. ^{1}H NMR (360 MHz, DMSO-d_6) δ 3.86 (s, 3H), 7.16 (dd, J = 2.4, 8.8 Hz, 1H),

7.30 (t, *J* = 8.8 Hz, 2H), 7.68 (m, 2H), 7.75 (q, *J* = 8.8 Hz, 2H). ^{13}C NMR (400 MHz, DMSO-d_6): δ 162.9, 159.4, 155.9, 142.6, 129.3, 129.1, 126.3, 124.2, 116.0, 115.8, 102.7, 55.8. Positive ion electrospray mass spectroscopy *m/z* 336/338 (100/97%) $[M+H]^+$.

3-Bromo-2-(4-fluorophenyl)-6-methoxybenzo[b]thiophene S-oxide **(34)**. Trifluoroacetic acid (743 µL, 4.00 mmol) was added dropwise to a solution of 6-Methoxy-2-(4-fluorophenyl)-3-bromobenzo[b]thiophene **33** (1.35 g, 4.00 mmol) in 5 mL of anhydrous dichloromethane. After the mixture was stirred for 5 min, H_2O_2 (571 µL, 4.00 mmol, 35% aqueous solution) was added dropwise, and the resulting mixture was stirred for 2 h at room temperature. Sodium bisulfite (170 mg) was added to the solution followed by 5 mL of water. The mixture was stirred vigorously for 15 min and then concentrated in vacuo. The residue was partitioned between DCM (25 mL) and saturated aqueous $NaHCO_3$ solution (25 mL). The layers were separated, and the organic layer was washed with consecutive portions of water, saturated $NaHCO_3$, and water, and then dried over anhydrous Na_2SO_4 and concentrated in vacuo. The resulting residue was purified by flash chromatography (hexane:ethyl acetate, 3:1) to give 981 mg (69%) of the desired compound as a yellow solid. ^{1}H NMR (300 MHz, DMSO-d_6) δ 3.91 (s, 3H), 7.32 (dd, *J* = 2.4, 8.5 Hz, 1H), 7.43 (t, *J* = 8.8 Hz, 2H), 7.62 (d, *J* = 8.5 Hz, 1H), 7.81 (m, 3H). ^{13}C NMR (400 MHz, DMSO-d_6): δ 162.1, 158.2, 134.6, 128.5, 128.0, 127.5, 127.4, 122.1, 115.4, 115.1, 114.3, 114.1, 55.8. Positive ion electrospray HRMS *m/z* 352.9613 $[M + H]^+$, calculated for $C_{15}H_{11}O_2FSBr$ 352.9647.

2-(4-Fluorophenyl)-6-methoxy-3-(4-methoxyphenoxy)benzo[b]thiophene S-oxide **(35)***.* NaH (167 mg, 4.17 mmol, 60% dispersion in mineral oil) was added to a solution

of 4-methoxyphenol (518 mg, 4.17 mmol) in 10 mL of anhydrous DMF at room temperature. After stirring for 15 minutes, 3-bromo-2-(4-fluorophenyl)-6-methoxybenzo[b]thiophene S-oxide **34** (981 mg, 2.78 mmol) was added in small portions, and the solution was stirred for 2 h. Ethyl acetate and water were added, and the organic layer was washed several times with water and then dried over anhydrous Na_2SO_4. The crude product was purified by flash chromatography (hexanes:ethyl acetate, 2:1) to afford 816 mg (74%) of the desired compound. ^{1}H NMR (400 MHz, acetone-d_6): δ 3.77 (s, 3H), 3.93 (s, 3H) 6.89 (d, J = 8.8 Hz, 2H), 7.12-7.18 (m, 3H), 7.28 (t, J = 8.8 Hz, 2H), 7.33 (d, J = 8.4 Hz, 1H), 7.52 (d, J = 2.4 Hz, 1H), 7.60-7.68 (m, 2H). ^{13}C NMR (400 MHz, DMSO-d_6): δ 162.1, 158.5, 154.8, 151.0, 147.2, 128.5, 128.0, 127.5, 127.4, 122.1, 118.2, 115.4, 115.0, 114.2, 114.1, 107.1, 55.8. Positive ion electrospray mass spectroscopy *m/z* 397.1 (100%) $[M+H]^+$.

2-(4-Fluorophenyl)-6-methoxy-3-(4-methoxyphenoxy)benzo[b]thiophene **(36)***.* $LiAlH_4$ (234 mg, 6.15 mmol) was added in small portions to a solution of 2-(4-fluorophenyl)-6-methoxy-3-(4-methoxyphenoxy)benzo[b]thiophene S-oxide **35** (1.44 g, 3.62 mmol) in 20 mL of anhydrous THF under N_2 at 0 °C. After the mixture was stirred for 60 min, the reaction was quenched by the slow addition of 5 mL of 2.0 M NaOH. The mixture was stirred vigorously for 30 min, and a minimal amount of 2.0 M NaOH was added to dissolve salts. THF was removed *in vacuo*, the mixture was partitioned between water and ethyl acetate, and the aqueous layer was isolated and then extracted several times with ethyl acetate. The organic layers were combined, dried over anhydrous Na_2SO_4, and then concentrated to an oil. The crude product was purified by flash chromatography (hexanes:ethyl acetate, 10:1) to afford 1.06 g (77%) of

the desired compound. ^{1}HNMR (400 MHz, acetone-d_6): δ 3.77 (s, 3H), 3.93 (s, 3H), 6.89 (d, *J* = 8.8 Hz, 2H), 7.13-7.19 (m, 3H), 7.28 (t, *J* = 8.8 Hz, 2H), 7.33 (d, *J* = 8.4 Hz, 1H), 7.52 (d, *J* = 2.4 Hz, 1H), 7.60-7.68 (m, 2H). ^{13}C NMR (400 MHz, DMSO-d_6): δ 162.9, 159.4, 156.5, 150.1, 147.5, 140.6, 129.3, 129.1, 126.3, 124.2, 123.6, 116.0, 115.8, 115.5, 115.3, 108.6, 55.9. Positive ion electrospray mass spectroscopy *m/z* 381.0 (100%) $[M+H]^+$.

2-(4-Fluorophenyl)-3-(4-hydroxyphenoxy)benzo[b]thiophen-6-ol **(37, HP-BTF, Figure 11).** To a stirred solution of 2-(4-fluorophenyl)-6-methoxy-3-(4-methoxyphenoxy)benzo[b]thiophene **36** (1.06 g, 2.79 mmol) in anhydrous DCM (30 mL) was added BBr_3 (1.0 M, in DCM, 9.75 mL, 9.75 mmol) at 0 ºC. The reaction was stirred for 2 h and then carefully quenched by the addition of saturated $NaHCO_3$ (10 mL) at 0 ºC. DCM was removed under reduced pressure, and the residue was partitioned between water and ethyl acetate. The aqueous layer was extracted with ethyl acetate several times, and the organic extracts were combined and dried over Na_2SO_4. Solvent was removed under reduced pressure and the crude product was purified by flash chromatography (hexanes:ethyl acetate, 2:1) to afford 828 mg (84%) of the desired compound. ^{1}H NMR (400 MHz, $CDCl_3$): δ 4.96 (s, 1H), 5.14 (s, 1H), 6.77 (d, *J* = 8.8 Hz, 2H), 6.90 (dd, *J* = 8.4, 2.4 Hz, 1H), 6.99 (d, *J* = 8.8 Hz, 2H), 7.14 (t, *J* = 8.8 Hz, 2H), 7.17 (d, *J* = 2.4 Hz, 1H), 7.51 (m, 3H). ^{13}C NMR (400 MHz, $CDCl_3$): δ 99.6, 107.9, 113.9, 115.1, 115.3, 115.7, 118.3, 120.1, 122.7, 130.7, 134.1, 151.7, 151.9, 152.6, 152.7, 162.9; Positive ion electrospray HRMS *m/z* 353.0638 $[M + H]^+$, calculated for $C_{20}H_{14}FO_3S$ 353.0642.

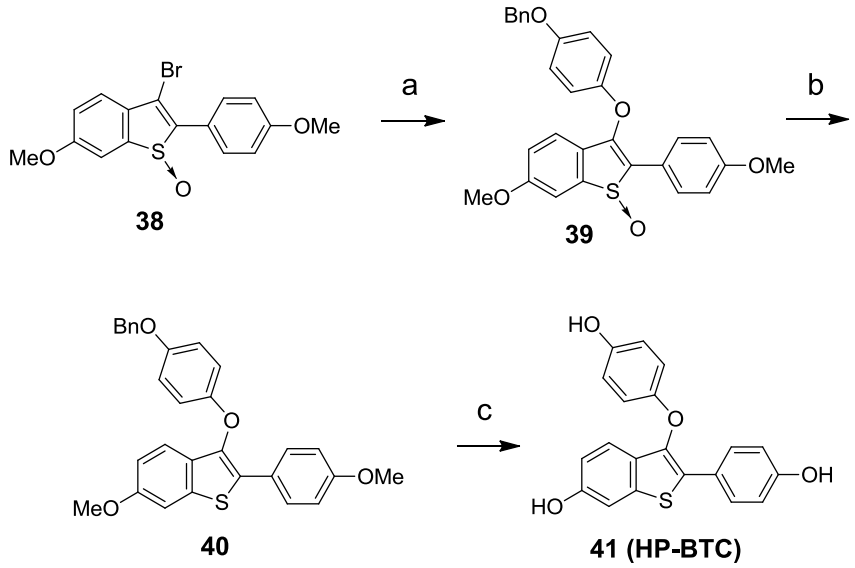

Figure 12. Synthesis of HP-BTC

Reagents and conditions: (a) 4-(benzyloxy)phenol, NaH, DMF, rt; (b) $LiAlH_4$, THF, 0 °C; (c) BBr_3, DCM, 0 °C.

3-Bromo-6-methoxy-2-(4-methoxyphenyl)benzo[b]thiophene S-oxide **(38)**. The title compound was prepared as described by Palkowitz, et al., 1997 [68]. ^{1}H NMR (DMSO-d_6, 400 MHz) δ 7.24 (d, *J* = 2.2 Hz, 1H), 7.68 (d, *J* = 8.8 Hz, 2H), 7.54 (d, *J* = 8.5 Hz, 1H), 7.26 (dd, *J* = 8.5 Hz, 2.2 Hz, 1H), 7.10 (d, *J* = 8.8 Hz, 2H), 3.86 (s, 3H), 3.80 (s, 3H). ^{13}C NMR (DMSO-d_6, 400 MHz): *δ* 159.8, 158.2, 134.6, 128.5, 127.5, 127.4, 118.8, 115.1, 114.2, 114.0, 55.8.

3-(4-(Benzyloxy)phenoxy)-6-methoxy-2-(4-methoxyphenyl)benzo[b]thiophene S-oxide **(39).** The title compound was prepared as described by Liu, et al., 2007 [55]. ^{1}H NMR (DMSO-d_6, 400 MHz): *δ* 7.65–7.72 (m, 3H), 7.34–7.43 (m, 5H), 6.96–7.09 (m, 8H), 5.03 (s, 2H), 3.86 (s, 3H), 3.77 (s, 3H). ^{13}C NMR (DMSO-d_6, 400 MHz): *δ* 160.4, 159.3, 154.6, 148.8, 147.6, 144.2, 136.9, 131.9, 129.1, 128.4, 127.8, 127.7, 125.8, 123.2, 121.7, 117.9, 117.5, 116.0, 114.5, 112.7, 69.6, 56.1, 55.2.

3-(4-(Benzyloxy)phenoxy)-6-methoxy-2-(4-methoxyphenyl)benzo[b]thiophene **(40)**. The title compound was prepared as described by Liu, et al., 2007 [55]. ^{1}H NMR (DMSO-d_6, 400 MHz): δ 7.64 (d, 2H, J = 8.8 Hz), 7.56 (d, 1H, J = 2.2 Hz), 7.31–7.42 (m, 5H), 7.19 (d, 1H, J = 8.8 Hz), 6.86–7.00 (m, 7H), 4.99 (s, 2H), 3.82 (s, 3H), 3.75 (s, 3H). ^{13}C NMR (DMSO-d_6, 400 MHz): δ 158.9, 157.7, 153.7, 151.1, 139.2, 137.0, 136.1, 128.4, 128.2, 127.8, 127.7, 127.3, 125.8, 124.1, 121.5, 116.0, 115.9, 114.7, 114.5, 106.0, 69.6, 55.5, 55.1.

3-(4-Hydroxyphenoxy)-2-(4-hydroxyphenyl)benzo[b]thiophen-6-ol **(41, HP-BTC, Figure 12)**. To a stirred solution of *3-(4-(benzyloxy)phenoxy)-6-methoxy-2-(4-methoxyphenyl) benzo[b]thiophene* **40** (200 mg, 0.43 mmol) in anhydrous DCM (10 mL) was added BBr_3 (1.0 M, in DCM, 2.15 mL, 2.15 mmol) at 0 ºC. The reaction was stirred for 2 h and then carefully quenched by the addition of saturated $NaHCO_3$ (5 mL) at 0 ºC. DCM was removed under reduced pressure, and the residue was partitioned between water and ethyl acetate. The aqueous layer was extracted with ethyl acetate several times, and the organic extracts were combined and dried over Na_2SO_4. Solvent was removed under reduced pressure and the crude product was purified by flash chromatography (hexanes:ethyl acetate, 2:1) to afford 133 mg (88%) of the desired compound. ^{1}H NMR (400 MHz, DMSO-d_6): δ 6.66 (d, J = 8.8 Hz), 6.72-6.79 (m, 5H), 7.09 (d, J = 8.8 Hz, 1H), 7.23 (d, J = 2.0 Hz, 1H), 7.49 (d, J = 8.8 Hz), 9.11 (s, 1H), 9.69 (s, 1H), 9.73 (s, 1H). ^{13}C NMR (DMSO-d_6, 400 MHz): δ 158.5, 154.4, 153.2, 150.1, 147.8, 141.0, 128.9, 126.3, 124.6, 122.9, 120.1, 116.9, 116.4, 115.5, 108.9, 105.2. Positive ion electrospray HRMS *m/z* 351.0635 $[M + H]^+$, calculated for $C_{20}H_{15}O_4S$ 351.0679.

2.5.4 <u>“Click” estrogen 3,3-TDP; G15</u>

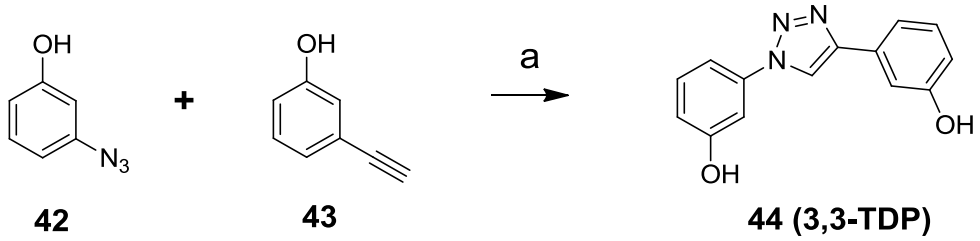

Figure 13. Synthesis of 3,3-TDP

Reagents and conditions: (a) H_2O/*tert*-BuOH (1:1), sodium ascorbate, $CuSO_4$, 60 °C.

3-Azidophenol **(42)** was prepared by diazotization of commercially available 3-aminophenol using HCl and $NaNO_2$ in water as previously described [69]. 3-ethynylphenol **(43)** was prepared by Sonogashira coupling of ethynyltrimethylsilane with 3-iodophenol and subsequent deprotection of TMS group by K_2CO_3 in MeOH, as previously described [69].

3,3'-(1H-1,2,3-Triazole-1,4-diyl)diphenol **(44, 3,3-TDP, Figure 13)**. The title compound was synthesized by a procedure analogous to that described by Pirali, et al., 2007 [69]. 3-Ethynylphenol (100 mg, 0.85 mmol) and 3-azidophenol (115 mg, 0.85 mmol) were suspended in a solution of water (5 mL) and *tert*-butanol (5 mL). Sodium ascorbate (17 mg, 0.085 mmol) and copper (II) sulfate pentahydrate (2 mg, 0.0085 mmol) were added, and the resulting reaction was stirred at 60 °C for 24 h under a nitrogen atmosphere. The reaction mixture was then diluted with water, chilled to 0 ºC, and the precipitate was collected by filtration. The crude product was further purified by flash chromatography (hexanes:ethyl acetate, 10:1) to afford 95 mg (44%) of the

desired compound as a brown solid. ^{1}H NMR (300 MHz, CD_3OD) δ 8.76 (s, 1H), 7.41-7.24 (m, 6H), 6.92 (d, *J* = 7.8 Hz, 1H), 6.81 (d, *J* = 7.7 Hz, 1H). ^{13}C NMR (400 MHz, CD_3OD): *δ* 99.6, 106.8, 110.4, 111.8, 114.8, 115.2, 116.3, 118.5, 129.3, 130.0, 130.8, 137.6, 157.3, 158.0.

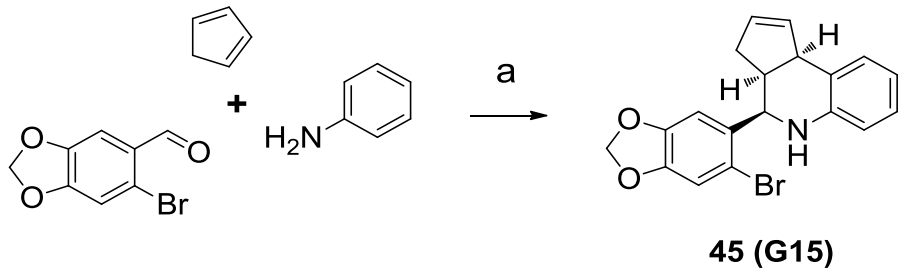

Figure 14. Synthesis of G15

Reagents and Conditions: (a) $Sc(OTf)_3$, CH_3CN.

(3aS,4R,9bR)-4-(6-bromobenzo[d][1,3]dioxol-5-yl)-3a,4,5,9b-tetrahydro-3H-cyclopenta[c]quinoline **(45, G15, Figure 14)**. The title compound was prepared according to a procedure described by Dennis, et al., 2009 [70]. To a solution of 6-bromopiperonal (0.229 g, 1.00 mmol), aniline (0.093 g, 1.00 mmol), and freshly distilled cyclopentadiene (0.33 g, 5.0 mmol) in acetonitrile (3 mL) was added a solution of $Sc(OTf)_3$ (0.049 g, 0.10 mmol) in anhydrous acetonitrile (1 mL). The reaction mixture was stirred for 3 h at room temperature and volatiles were removed *in vacuo.* The residue was dissolved in dichloromethane (10 mL) and the dropwise addition of methanol (5 mL) resulted in precipitation of the desired product (321 mg, 87%) as a white solid. ^{1}H NMR (400 MHz, (DMSO-d_6) δ 7.24 (s, 1H), 7.14 (s, 1H), 6.97 (dd, *J* = 8.0, 1.2 Hz, 1H), 6.87 (dt, *J* = 7.6, 1.2 Hz, 2H), 6.70 (dd, *J* = 8.0, 1.2 Hz, 1H), 6.61 (dt, *J* = 7.6, 1.2 Hz, 1H); 6.09 (dd, *J* = 9.2, 0.8 Hz, 2H), 5.86 (m, 1H), 5.59 (d, *J* = 4.8 Hz, 1H) ,

5.57 (s, 1H), 4.67 (d, *J* = 2.8 Hz, 1H), 4.00 (d, *J* = 8.4 Hz, 1H), 3.03 (m, 1H), 2.46 (m, 1H), 1.67 (m, 1H). Positive ion electrospray mass spectroscopy *m/z* 370.0 (100%) $[M+H]^+$.

2.5.5 POSEMs; HP-BTF analogs

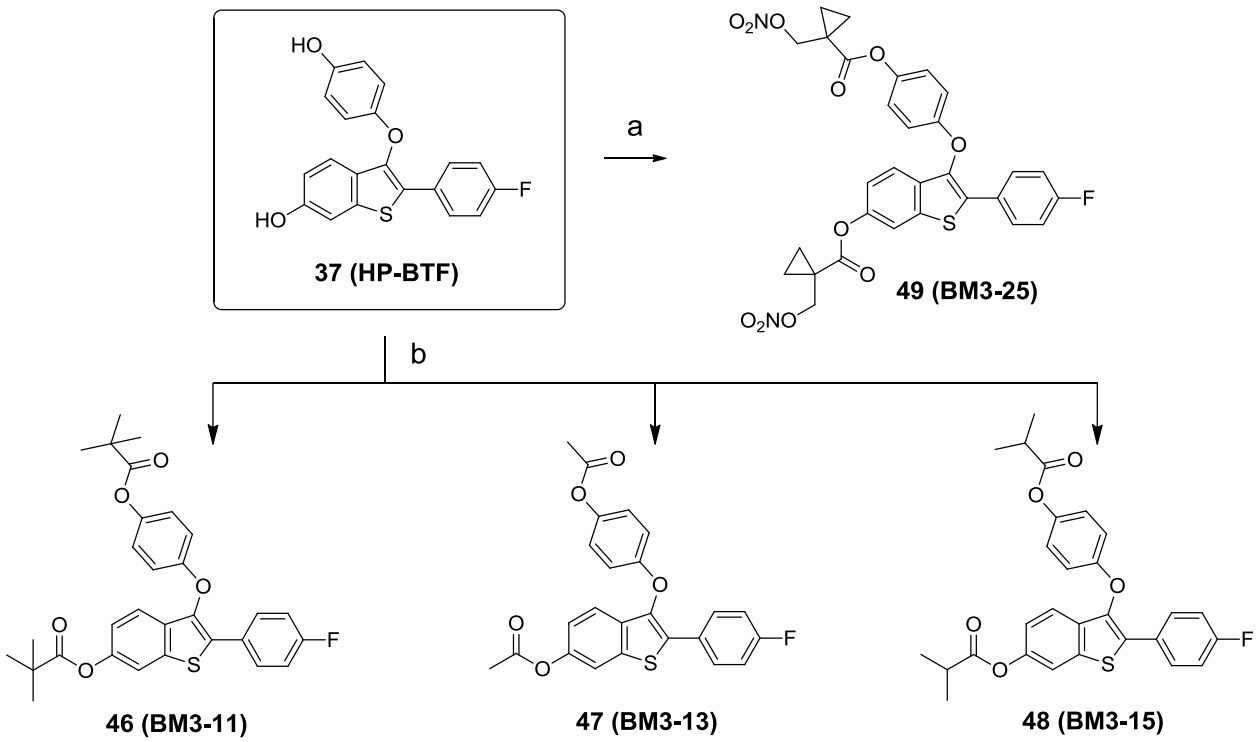

Figure 15. Synthesis of POSEMs

Reagents and conditions: (a) 1-((nitrooxy)methyl)cyclopropanecarboxylic acid, EDCI, DIPEA, DMAP, HOBt, DCM; (b) RCOCl, TEA, DCM.

2-(4-Fluorophenyl)-3-(4-(pivaloyloxy)phenoxy)benzo[b]thiophen-6-yl pivalate **(46, BM3-11, Figure 15).** To a stirred solution of 2-(4-fluorophenyl)-3-(4-hydroxyphenoxy)benzo[b]thiophen-6-ol (**37**, HP-BTF, 100 mg, 0.284 mmol) in

anhydrous DCM (2 mL) was added TEA (100 µL, 0.710 mmol) and pivaloyl chloride (77 µL 0.624 mmol). The reaction was stirred at room temperature for 1 h and then quenched with water (200 µL). DCM was removed *in vacuo*, and the resulting residue was partitioned between water and ethyl acetate. The organic layer was dried over anhydrous Na_2SO_4, and removal of solvent yielded a white solid which was further purified by flash chromatography (hexanes:ethyl acetate, 14:1) to give 136 mg (92%) of the desired diester as a white solid. ^{1}H NMR (400 MHz $CDCl_3$): δ 1.35 (s, 9H), 1.40 (s, 9H), 6.93-6.97 (m, 4H), 6.99 (dd, *J* = 8.8 Hz, 2.0 Hz, 1H), 7.08 (t, *J* = 8.8 Hz, 2H), 7.40 (d, *J* = 8.8 Hz, 1H), 7.55 (d, *J* = 1.6 Hz, 1H), 7.73 (td, *J* = 8.8 Hz, 3.2 Hz, 2H); ^{13}C NMR (400 MHz, $CDCl_3$): δ 27.0, 27.1, 27.2, 39.0, 39.1, 115.5, 115.8, 116.0, 116.1, 119.2, 122.2, 122.6, 122.7, 128.7, 129.5, 129.6, 131.4, 136.1, 145.9, 148.9, 154.8, 177.1, 177.2. Positive ion electrospray HRMS *m/z* 521.1792 $[M + H]^+$, calculated for $C_{30}H_{30}FO_5S$ 521.1792.

4-((6-Acetoxy-2-(4-fluorophenyl)benzo[b]thiophen-3-yl)oxy)phenyl acetate **(47, BM3-13, Figure 15).** To a stirred solution of 2-(4-fluorophenyl)-3-(4-hydroxyphenoxy)benzo[b]thiophen-6-ol (**37**, HP-BTF, 50 mg, 0.142 mmol) in anhydrous DCM (1 mL) was added TEA (50 µL, 0.355 mmol) and acetyl chloride (23 µL 0.312 mmol). The reaction was stirred at room temperature for 1 h and then quenched with water (100 µL). DCM was removed *in vacuo*, and the resulting residue was partitioned between water and ethyl acetate. The organic layer was dried over anhydrous Na_2SO_4, and removal of solvent yielded a white solid which was further purified by flash chromatography (hexanes:ethyl acetate, 1:1) to give 55 mg (88%) of the desired diester as a white solid. ^{1}H NMR (400 MHz $CDCl_3$): δ 2.29 (s, 3H), 2.35 (s, 3H), 6.98 (q, *J* =

14.2 Hz, 4H), 7.04 (dd, *J* = 8.8 Hz, 2.0 Hz, 1H), 7.09 (t, *J* = 8.8 Hz, 2H), 7.41 (d, *J* = 8.8 Hz, 1H), 7.57 (d, *J* = 2.0 Hz, 1H), 7.73 (td, *J* = 8.8 Hz, 3.2 Hz, 2H); ^{13}C NMR (400 MHz, $CDCl_3$): δ 21.0, 21.1, 115.6, 115.8, 116.0, 116.2, 119.3, 122.2, 122.7, 128.9, 129.5, 129.6, 131.5, 136.0, 139.8, 145.6, 148.5, 154.9, 169.5. Positive ion electrospray HRMS *m/z* 454.1135 $[M + NH_4]^+$, calculated for $C_{24}H_{21}FNO_5S$ 454.1118.

2-(4-Fluorophenyl)-3-(4-(isobutyryloxy)phenoxy)benzo[b]thiophen-6-yl isobutyrate **(48, BM3-15, Figure 15).** To a stirred solution of 2-(4-fluorophenyl)-3-(4-hydroxyphenoxy)benzo[b]thiophen-6-ol (**37**, HP-BTF, 50 mg, 0.142 mmol) in anhydrous DCM (1 mL) was added TEA (50 µL, 0.355 mmol) and isobutyryl chloride (33 µL 0.312 mmol). The reaction was stirred at room temperature for 1 h and then quenched with water (100 µL). DCM was removed *in vacuo*, and the resulting residue was partitioned between water and ethyl acetate. The organic layer was dried over anhydrous Na_2SO_4, and removal of solvent yielded a white solid which was further purified by flash chromatography (hexanes:ethyl acetate, 4:1) to give 64 mg (91%) of the desired diester as a white solid. ^{1}H NMR (400 MHz $CDCl_3$): δ 1.29-1.37 (m, 12H), 2.75-2.89 (m, 2H), 6.98 (q, *J* = 14.2 Hz, 4H), 7.04 (dd, *J* = 8.8 Hz, 2.0 Hz, 1H), 7.09 (t, *J* = 8.8 Hz, 2H), 7.41 (d, *J* = 8.8 Hz, 1H), 7.57 (d, *J* = 2.0 Hz, 1H), 7.73 (td, *J* = 8.8 Hz, 3.2 Hz, 2H); ^{13}C NMR (400 MHz, $CDCl_3$): δ 18.5, 33.7, 33.8, 115.2, 115.4, 115.6, 115.7, 118.9, 121.8, 122.3, 128.4, 129.1, 129.2, 129.3, 131.0, 135.7, 145.4, 148.3, 154.4, 175.2, 175.3. Positive ion electrospray HRMS *m/z* 493.1476 $[M + H]^+$, calculated for $C_{28}H_{25}FNO_5S$ 493.1479.

2-(4-Fluorophenyl)-3-(4-((1-((nitrooxy)methyl)cyclopropanecarbonyl)oxy) phenoxy)benzo[b]thiophen-6-yl 1-((nitrooxy)methyl)cyclopropanecarboxylate **(49, BM3-25, Figure 15).** 2-(4-fluorophenyl)-3-(4-hydroxyphenoxy)benzo[b]thiophen-6-ol (**37**, HP-

BTF, 60 mg, 0.170 mmol), 1-((nitrooxy)methyl)cyclopropanecarboxylic acid [71] (33 mg, 0.204 mmol), EDCI hydrochloride (48 mg, 0.251 mmol), DMAP (2.4 mg, 0.019 mmol), and HOBt (34 mg, 0.251 mmol) were dissolved in anhydrous DCM (1 mL). DIPEA (85 µL, 0.484 mmol) was added, and the reaction was stirred at room temperature for 12 h. DCM was removed *in vacuo*, and the resulting residue was partitioned between water and ethyl acetate. The organic layer was dried over anhydrous Na_2SO_4, and removal of solvent yielded a white solid which was further purified by flash chromatography (hexanes:ethyl acetate, 3:1) to give 56 mg (53%) of the desired diester as a white solid. ^{1}H NMR (400 MHz $CDCl_3$): δ 1.20 (q, J = 6.0 Hz, 2H), 1.25 (q, J = 6.0 Hz, 2H), 1.62 (q, J = 6.0 Hz, 2H), 1.68 (q, J = 6.0 Hz, 2H), 4.74 (s, 2H), 4.78 (s, 2H), 6.93-7.03 (m, 5H), 7.08 (t, J = 7.6 Hz, 2H), 7.39 (d, J = 8.4 Hz, 1H), 7.57 (d, J = 1.6 Hz, 1H), 7.69-7.73 (m, 2H); ^{13}C NMR (400 MHz, $CDCl_3$): δ 15.2, 15.4, 21.7, 21.9, 75.0, 75.1, 115.5, 115.9, 116.1, 116.2, 119.0, 122.2, 122.6, 129.5, 129.6, 131.7, 136.0, 145.3, 148.2, 155.1, 170.9. Positive ion electrospray HRMS *m/z* 639.1052 $[M + H]^+$, calculated for $C_{30}H_{24}FN_2O_{11}S$ 639.1079.

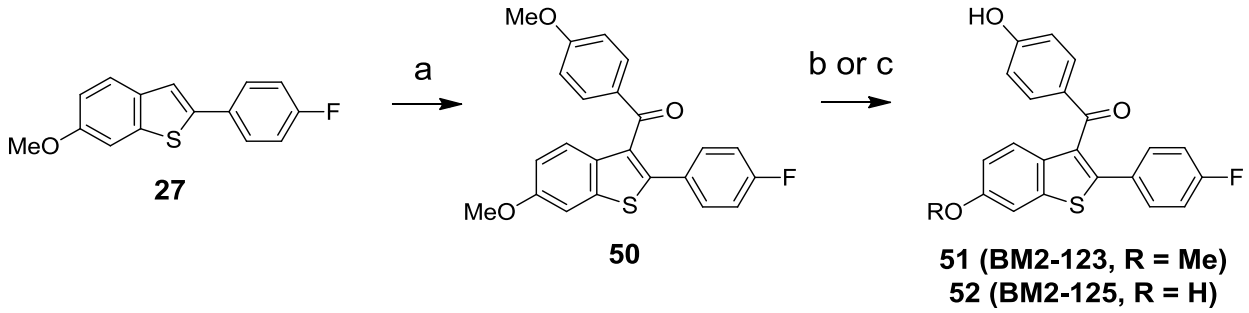

Figure 16. Synthesis of HP-BTF analogs BM2-123, BM2-125

Reagents and conditions: (a) 4-methoxybenzoyl chloride, $AlCl_3$, DCM, 0 °C; (b) NaSEt, DMF, 80 °C (c) BBr_3, DCM, 0 °C.

(2-(4-Fluorophenyl)-6-methoxybenzo[b]thiophen-3-yl)(4-methoxyphenyl)methanone **(50)***.* 4-methoxybenzoyl chloride (151 mg, 0.882 mmol) was added to a solution of 2-(4-fluorophenyl)-6-methoxybenzo[b]thiophene **27** (151 mg, 0.588 mmol) in anhydrous DCM (10 mL) at 0 ºC. To this mixture, $AlCl_3$ (118 mg, 0.882 mmol) was added and the reaction was stirred at 0 ºC for 2 h and at room temperature for 1 h. The reaction mixture was poured into ice water (20 mL) and extracted with DCM (3 x 50 mL). The organic layer was washed with 1 M NaOH and brine and dried over anhydrous Na_2SO_4. Solvent was removed under reduced pressure and the crude product was purified by flash chromatography (hexanes:ethyl acetate, 5:1) to yield 157 mg (68%) of the desired product. ^{1}H NMR (400 MHz, acetone-d_6): δ 3.80 (s, 3H), 3.95 (s, 3H), 6.79 (d, J = 8.8 Hz, 2H), 7.05-7.12 (m, 3H), 7.37 (td, J = 5.2 Hz, 2.0 Hz, 2H), 7.61 (d, J = 8.8 Hz, 4H); ^{13}C NMR (400 MHz, acetone-d_6): δ 54.6, 54.8, 104.1, 112.8, 114.6, 114.8, 115.5, 124.9, 130.0, 130.6, 131.4, 131.8, 131.9, 132.7, 138.7, 141.8, 159.2, 162.8, 188.5. Positive ion electrospray mass spectroscopy *m/z* 393.1 (100%) $[M+H]^+$.

(2-(4-Fluorophenyl)-6-methoxybenzo[b]thiophen-3-yl)(4-hydroxyphenyl)methanone **(51, BM2-123, Figure 16).** A solution of **50** (50 mg, 0.12 mmol) in dry DMF (1 mL) was added to a solution of sodium ethanethioate (16 mg, 0.19 mmol) in DMF(1 mL). The reaction mixture was heated at 80 °C for 4 h and then cooled to room temperature. Ethyl acetate (10 mL) and water (10 mL) were added to the mixture. After neutralization with 1 M HCl, the reaction mixture was extracted with ethyl acetate several times. The organic layer was removed, washed with brine, and dried over Na_2SO_4. After the solvent was removed, the crude product was purified by flash

chromatography (hexanes:ethyl acetate, 3:1) to yield 33 mg (73%) of the desired monophenol. ^{1}H NMR (400 MHz, acetone-d_6): δ 3.80 (s, 3H), 6.78 (d, J = 8.8 Hz, 2H), 7.04-7.08 (m, 3H), 7.36 (td, J = 5.6 Hz, 2.4 Hz, 2H), 7.46 (d, J = 2.0 Hz, 1H), 7.55-7.61 (m, 3H), 9.04 (bs, 1H); ^{13}C NMR (400 MHz, acetone-d_6): δ 54.8, 106.7, 112.8, 114.5, 114.7, 115.5, 125.2, 130.1, 131.4, 131.8, 131.9, 132.2, 134.7, 138.9, 141.8, 157.0, 162.7, 188.5. Positive ion electrospray HRMS *m/z* 379.0822 $[M + H]^+$, calculated for $C_{22}H_{16}FO_3S$ 379.0798.

(2-(4-Fluorophenyl)-6-hydroxybenzo[b]thiophen-3-yl)(4-hydroxyphenyl) methanone **(52, BM2-125, Figure 16).** To a stirred solution of **50** (50 mg, 0.12 mmol) in anhydrous DCM (2 mL) was added BBr_3 (1.0 M, in DCM, 360 µL, 0.36 mmol) at 0 ºC. The reaction was stirred for 2 h, and then carefully quenched by the addition of saturated $NaHCO_3$ (5 mL) at 0 ºC. DCM was removed under reduced pressure, and the residue was partitioned between water and ethyl acetate. The aqueous layer was extracted with ethyl acetate several times, and the organic extracts were combined and dried over Na_2SO_4. Solvent was removed *in vacuo* and the crude product was purified by flash chromatography (hexanes:ethyl acetate, 2:1) to afford 36 mg (82%) of the desired compound. ^{1}H NMR (400 MHz, $CDCl_3$): δ 6.69 (d, J = 8.8 Hz, 2H), 7.08 (t, J = 8.8 Hz, 3H), 7.37 (td, J = 6.4 Hz, 3.2 Hz, 2H), 7.46 (d, J = 1.6 Hz, 1H), 7.56 (t, J = 8.8 Hz, 3H), 9.04 (bs, 1H); ^{13}C NMR (400 MHz, acetone-d_6): δ 106.7, 114.2, 114.5, 114.7, 115.4, 125.1, 129.1, 131.7, 131.7, 131.8, 132.1, 156.8, 160.9, 188.5. Positive ion electrospray HRMS *m/z* 365.0630 $[M + H]^+$, calculated for $C_{21}H_{14}FO_3S$ 365.0642.

2.6 Kinetics of LAS-, LY2066948- and EN-*o*-quinone decomposition

To a solution of LAS (500 μM) in anhydrous methanol (200 μL) was added 2-iodoxybenzoic acid (0.84 mg, 30 equiv) at room temperature. After stirring for 1 min, a yellow color developed, and the reaction mixture was filtered. The LAS-*o*-quinone solution (100 μL) was immediately added to 50 mM phosphate buffer (0.9 mL, pH 7.4) at 37 °C. Disappearance of *o*-quinone was then monitored by measuring the decrease in UV absorbance at 378 nm. The half-life was subsequently determined by measuring the pseudo first-order rate of decay of the absorbance signal at 378 nm according to the equation t1/2 = ln(2)/k. An analogous procedure was utilized for measuring the decomposition of LY- and EN-*o*-quinones, measuring decreases in UV absorbances at 378 nm and 392 nm, respectively.

2.7 Incubation of SERMs or estrogens with tyrosinase

Solutions containing LAS, LY, BAZ E_2, or EN (30 μM), tyrosinase (0.1 mg/mL), and GSH (1 mM) in 50 mM phosphate buffer (pH 7.4, 0.5 mL total volume) were incubated at 37 ºC for 30 min. Reactions were terminated by chilling in an ice bath followed by the addition of perchloric acid (25 μL). Samples were then centrifuged (10,000g for 10 min at 4 ºC), and supernatants were filtered and immediately analyzed by LC-MS/MS. Controls were performed by omission of tyrosinase or GSH.

2.8 Incubation of SERMs or estrogens with liver microsomes

Solutions containing LAS, LY, BAZ E_2, or EN (30 μM), rat or human liver microsomes (1 nmol P450/mL), GSH (1 mM), and a NADPH-generating system (1 mM

$NADP^+$, 5 mM $MgCl_2$, 5 mM isocitric acid, 0.2 unit/mL isocitrate dehydrogenase) in phosphate buffer (pH 7.4, 50 mM, 0.5 mL total volume) were incubated for 30 min at 37 ºC. Reactions were quenched by chilling in ice followed by addition of perchloric acid (25 µL). Incubation mixtures were centrifuged (10,000 x g for 10 min at 4 ºC), and supernatants were filtered and analyzed by LC-MS/MS. For control incubations, either $NADP^+$ or GSH was omitted.

2.9 Microsomal incubations of LAS in presence of methylating or glucuronidating systems

In order to examine the competition between catechol LAS glucuronidation compared to catechol LAS oxidation and subsequent glutathione conjugation, solutions containing LAS (30 µM), rat liver microsomes (1 nmol P450/mL), a NADPH-generating system (1 mM $NADP^+$, 5 mM $MgCl_2$, 5 mM isocitric acid, 0.2 unit/mL isocitrate dehydrogenase), GSH (1 mM), uridine diphosphate glucuronic acid (UDPGA, 1 mM) and alamethicin (10 µg/mg protein) were incubated for 30 min at 37 ºC in 50 mM phosphate buffer (pH 7.4, 1 mL total volume). After chilling in ice, perchloric acid (50 µL) was added, and proteins were removed by centrifugation (10,000 x g for 10 min at 4 ºC). Aliquots of supernatant were then analyzed by LC-MS/MS. For control experiments, either GSH or UDPGA was omitted.

For studying the competition between catechol LAS methylation and catechol LAS oxidation followed by glutathione conjugation, solutions containing LAS (30 µM), rat liver microsomes (1 nmol P450/mL), and catechol-O-methyltransferase (COMT, 1 mM) were incubated for 30 min at 37 ºC in 50 mM phosphate buffer (pH 7.4, 1 mL total

volume). Incubations were initiated by the addition of a solution containing magnesium chloride (1 mM), *S*-adenosyl methionine (SAM, 0.3 mM), $NADP^+$ (1 mM), $MgCl_2$ (5 mM), isocitric acid (5 mM), isocitrate dehydrogenase (0.2 unit/mL), and GSH (1 mM). Reactions were quenched by chilling in ice followed by addition of perchloric acid (50 µL). Proteins were removed by centrifugation (10,000 x g for 10 min at 4 ºC), and aliquots (100 µL) of supernatant were analyzed by LC-MS/MS. For control experiments, either GSH or COMT was omitted.

2.10 Reaction of 7-OHLAS-*o*-Quinone with Deoxynucleosides

Solutions containing 7-OHLAS (30 µM), tyrosinase (0.1 mg/mL), and each of the four deoxynucleosides (dG, dA, dT, or dC, 300 µM) were incubated for 30 min at 37 ºC in 50 mM phosphate buffer (pH 7.4, 0.5 mL total volume). Reactions were quenched by chilling in ice followed by addition of cold ethanol (1 mL). Protein was removed by centrifugation (10,000 x g for 10 min at 4 ºC), the supernatant was concentrated to a volume of 0.5 mL, and aliquots of supernatant were analyzed by LC-MS/MS. For control experiments, either tyrosinase or deoxynucleoside was omitted.

2.11 Reaction of 7-OHLAS-*o*-quinone with calf thymus DNA

To a solution of 7-OHLAS (2.53 mg, 5.89 µmol) in acetonitrile (500 µL) and DMF (100 µL) was added activated MnO_2 (3.34 mg, 38.4 µmol, 6.5 equiv.) at 0 ºC. The solution was stirred at 0 ºC for 15 min and then filtered directly into a solution of CT-DNA (1 mg/mL in 50 mM phosphate buffer, pH 7.0, 5 mL total volume). The resulting mixture was incubated for 10 h at 37 ºC. Following incubation, cold ethanol (10 mL) was

added and the solution was stored at -20 ºC for 1 hr. Precipitated DNA was removed by centrifugation (3330 g for 15 min at 4 ºC) and the supernatant was concentrated to a volume of 0.5 mL, loaded onto a PrepSep C_{18} solid-phase extraction cartridge, washed with 5% methanol in water (1 mL), and eluted with 6 mL of a solution of methanol/acetonitrile/water/formic acid (8:1:1:0.1, v/v). The eluate was evaporated to dryness under a stream of nitrogen, and the residue was reconstituted in 100 µL methanol containing 0.1% formic acid. Aliquots of the resulting solution were analyzed by LC-MS/MS.

2.12 Conversion of HP-BTF POSEMs to HP-BTF in liver microsomal incubations

Solutions containing each of four POSEMs (Figure 15, 30 µM), human liver microsomes (1 nmol P450/mL), and NADPH (1 mM) in phosphate buffer (pH 7.4, 50 mM, 0.5 mL total volume) were incubated for 30 min at 37 ºC. Reactions were quenched by chilling in ice followed by addition of cold methanol (1 mL). Incubation mixtures were centrifuged (10,000 x g for 10 min at 4 ºC), and supernatants were filtered and analyzed by LC-MS/MS. For control incubations, NADPH was omitted. Generation of HP-BTF was measured by integration of relative peak areas.

Chapter 3: Synthesis of benzothiophene SERMs/SEMs, and bioactivation of the SERMs LY2066948, lasofoxifene, and bazedoxifene

3.1 Design and synthesis of benzothiophene SERMs/SEMs

The initial synthetic strategy for the present study was to develop novel ER ligands that displayed a range of antagonist (SERM-like) to agonist/estrogenic (SEM-like) activity through structural elaboration of the 3-position on the BTC or 4'-FBTC (FBTC) core moieties of raloxifene and FDMA, respectively (Figure 17). As previously mentioned (refer to Section 1.2), the antiestrogenic activity of the prototypical benzothiophene SERM raloxifene is attributable to the bulky (4-(2-(piperidin-1-yl)ethoxy)phenyl)methanone side chain (Figure 17, red) at the 3-position of its BTC scaffold, which upon ligand binding, acts to displace helix 12 of the ER and ultimately inhibit the formation of a transcriptionally competent AF-2. Similarly, for the case of FDMA, a homologous side chain (Figure 17, blue) bearing an ether, rather than a keto linkage at the 3-position, serves an identical purpose. Importantly, whereas raloxifene and FDMA are potent antiestrogens, BTC itself is estrogenic. This observation suggests that the synthesis of compounds which lack significant steric bulk at the 3-position could lead to the identification of novel, estrogenic SEMs of potential clinical use. Conversely, the introduction of larger, bulky groups at the 3-position was proposed to yield novel SERM-like antiestrogens. Synthesized compounds were assayed for estrogenic/antiestrogenic activity in Ishikawa endometrial cancer cells, and were found

to exhibit activities ranging from highly potent estrogens, to potent antiestrogens (Table 1).

Compounds bearing a 4'-OH group were synthesized using commercially available dimethoxy-BTC as a starting material. Those containing the 4'-F-substituition required 2 additional synthetic steps to first yield the key 6-methoxy, 4'-FBTC intermediate **(27)**. This was achieved via base-catalyzed coupling of 3-methoxybenzenethiol and 2-bromo-1-(4-fluorophenyl)ethanone, followed by polyphosphoric acid-catalyzed cyclization-rearrangement of the resulting ethanone **(26)**.

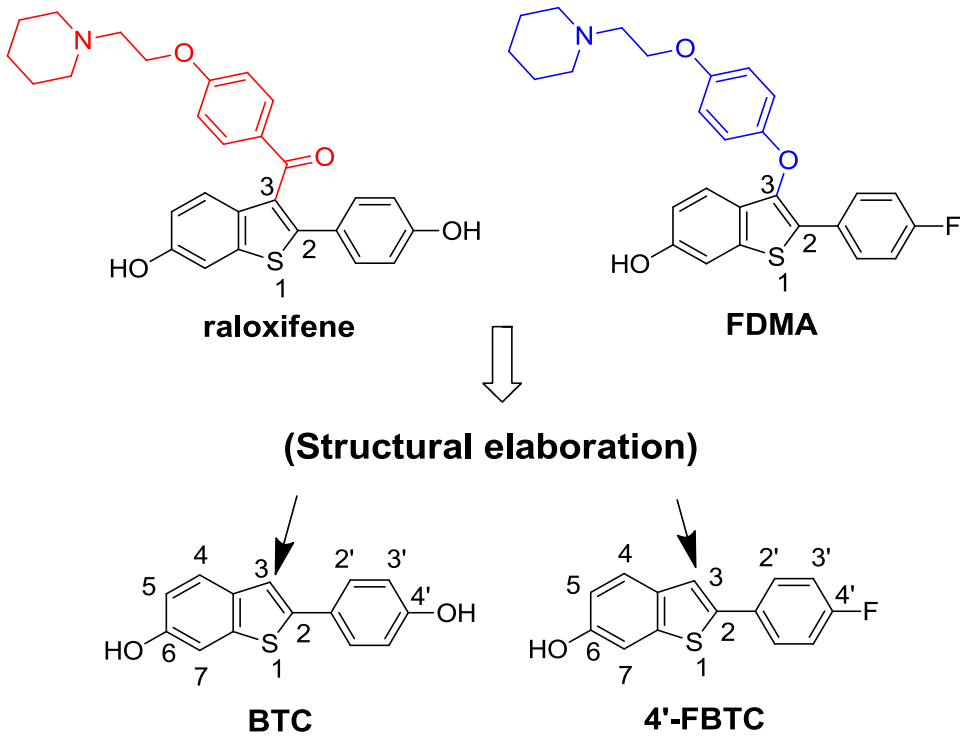

Figure 17. Structures of raloxifene, FDMA, BTC and 4'-FBTC

Introduction of a keto linkage at the 3-postion of either the BTC or FBTC core was achieved via Friedel-Crafts acylation of the respective methoxyl-protected precursors. Subsequently, such intermediates were either completely deprotected using BBr_3 to give free phenols such as Tol-BTC **(23)**, bisBTChd **(25)**, and BM2-125 **(52)**, or were selectively deprotected using NaSEt in DMF to give monophenols such as BM2-123 **(51)**. A similar strategy was employed using an initial Friedel-Crafts alkylation and subsequent demethylation to give *i*Pr-BTC **(21)**. Conversely, acylation of the 3-position on FBTC **(27)** with 4-iodobenzoyl chloride, followed by demethylation with BBr_3 gave a *p*-iodo intermediate **(29)** useful for further synthetic elaboration. Sonogashira coupling of ethynyltrimethylsilane to this intermediate, followed by removal of TMS protecting group gave a terminal alkyne **(31)** which was coupled to azidobenzene using 1,3-dipolar cycloaddition “click” chemistry conditions to give PTP-BTF **(32)**.

Introduction of an ether linkage at the 3-position of BTC or FBTC required 3 additional synthetic steps compared to 3-keto derivatives. This was accomplished via 3-bromination with *N*-bromoacetamide, followed by oxidation to the corresponding benzothiophene-*S*-oxide using H_2O_2/TFA in DCM. Resulting synthons **(34, 39)** were highly activated towards 3-substitution by phenoxide anion generated by NaH in DMF. Reduction of the resulting *S*-oxide intermediates by $LiAlH_4$, followed by demethylation using BBr_3 gave free phenols such as HP-BTC **(41)** and HP-BTF **(37)**. Finally, simple phenolic diester HP-BTF POSEMs **(46-48)** were synthesized by reaction of HP-BTF with appropriate acid chlorides in anhydrous DCM using TEA as a base, while the NO-POSEM, BM3-25 **(49)**, was prepared via standard EDCI/DMAP-catalyzed coupling to the corresponding NO-donating carboxylic acid.

Ligand	EC_{50} (nM)	IC_{50} (nM)	Classification
E_2	0.190 ± 0.05	-	Potent estrogen
Raloxifene	-	2.9 ± 1.6	Potent antiestrogen
BTC	790 ± 170	-	Weak estrogen
i-Pr-BTC	3.9 ± 0.7	-	Potent estrogen
Tol-BTC	470 ± 142	410 ± 110	Partial estrogen agonist
HP-BTC	-	18 ± 3	Potent antiestrogen
HP-BTF	202 ± 68	-	Weak estrogen
BM2-125	0.409 ± 0.157	-	Potent estrogen
bisBTChd	-	486 ± 77	Weak antiestrogen
PTP-BTF	-	5890 ± 982	Weak antiestrogen

TABLE I. ESTROGENIC ASSAY OF BT-SERMS/SEMS IN ISHIKAWA CELLS.

Ishikawa assay was performed by Ping Yao and Huali Dong. E_2 and raloxifene were included for comparison.

3.2 Metabolism of LY2066948

3.2.1 Metabolism by tyrosinase

Mushroom tyrosinase (EC 1.14.18.1) is a copper-dependent oxygenase which possesses both monophenol monooxygenase activity as well as catechol oxidase activity [72]. Tyrosinase has been demonstrated to oxidize both estrogens and SERMs to their corresponding catechols and *o*-quinones with high efficiency, thus serving as a model enzymatic system for the study of reactive metabolite formation from phenolic

compounds [37, 38, 72, 73]. Incubations of LY with tyrosinase in the presence of GSH produced mono- and di-GSH conjugates (Figure 18A) derived from trapping of LY-*o*-quinones. Mono-GSH conjugates were identified based on the detection of a strong [M + H]$^+$ peak at *m/z* 837 (Figure 19A). The base peak at *m/z* 744 corresponds to loss of water and glycine residue, and the product ions at *m/z* 819 and *m/z* 708 were formed through loss of water and loss of γ-glutamyl group, respectively. The product ion at *m/z* 564 was generated by alkyl thioether cleavage (Figure 19A). Such fragmentations are characteristic of GSH conjugates [74]. An LY-di–GSH conjugate was also observed as a

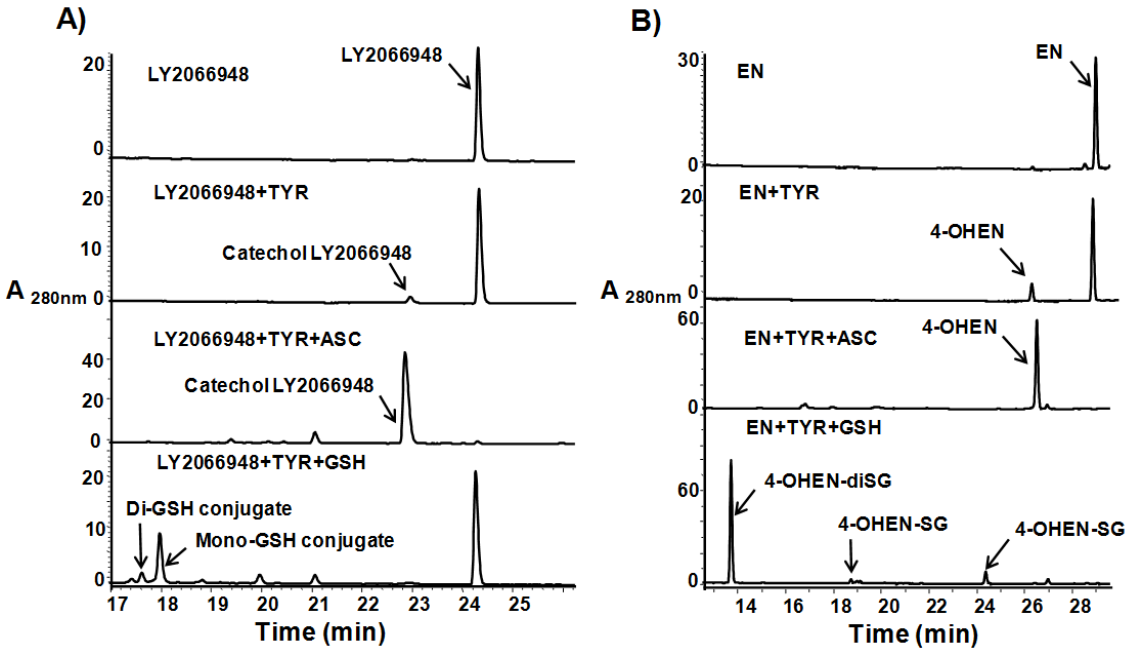

Figure 18. Metabolism of LY and EN by tyrosinase

Representative HPLC chromatograms of (A) LY (30 µM), or (B) EN (30 µM) incubated with 0.1 mg/mL tyrosinase (TYR), 1 mM ascorbic acid (ASC), and 1 mM GSH in 50 mM phosphate buffer (pH 7.4, 0.5 mL total volume) for 30 min at 37 ºC. Metabolites and GSH conjugates were detected by UV-visible absorbance (shown in arbitrary units) at 280 nm and all annotated peaks were characterized by LC-MS/MS.

doubly charged ion at *m/z* 571 $[M + 2H]^{2+}$ (data not shown). Similarly, when EN was incubated with tyrosinase in the presence of GSH, mono and di-GSH conjugates were detected (Figure 18B) as reported previously [75]. Incubation of LY with tyrosinase in the presence ascorbate as a reducing agent quantitatively converted LY to catechol (Figure 18A). Similarly, when EN was incubated with tyrosinase and ascorbate, 4-OHEN was the major product (Figure 18B) [76].

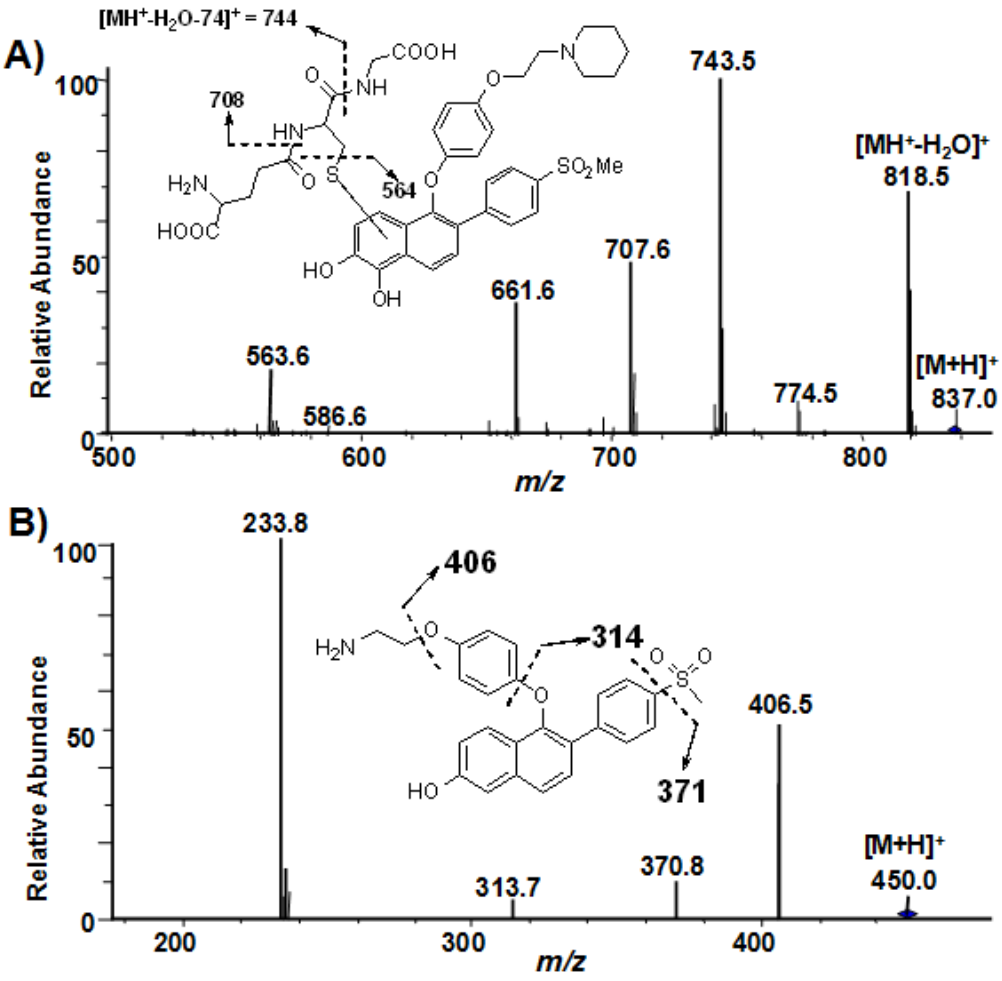

Figure 19. MS fragmentation of OH-LY-mono-GSH; N-dealkylated LY

Mass spectrometric analysis of LY metabolites. (A) MS/MS spectrum of LY-mono-GSH conjugate. (B) MS/MS spectrum of N-dealkylated LY.

3.2.2 Metabolism by liver microsomes

In the presence of rat liver microsomes, NADPH, and GSH, LY was oxidized to an *o*-quinone, which was trapped by GSH to produce one di-GSH conjugate (Figure 20A). This conjugate was identified based on the detection of $[M + 2H]^{2+}$ peak at *m/z* 571 (data not shown). In addition to the di-GSH conjugate, the *N*-dealkylated primary amine metabolite (Figure 20A) was formed as a major product, and was identified based on the detection of $[M + H]^{+}$ peak at *m/z* 450 (Figure 19B). MS/MS analysis of the molecular ion at *m/z* 450 produced fragment ions at *m/z* 406, 371, 314, and 234, corresponding to the loss of ethylamine moiety, cleavage of methyl sulfonyl moiety, loss of 2-phenoxyethylamine, and the concurrent loss of methyl sulfonyl and 2-phenoxyethylamine moieties, respectively (Figure 19B). In contrast, no GSH conjugates were obtained in the incubation of LY with human liver microsomes (data not shown). For comparison, we also investigated the metabolism of EN by rat liver microsomes in the presence of NADPH and GSH. Mono and di-GSH conjugates were detected as in the tyrosinase incubations described above resulting from trapping of 4-OHEN-*o*-quinone with GSH (Figure 20B). In addition, 17β-equilenin (17β-EN) was formed in rat liver microsomal incubations and further oxidized to *o*-quinone to give a di-GSH conjugate as a metabolite (Figure 20B). Identification of 17β-EN and its corresponding di-GSH conjugate was based on detection of the corresponding molecular ions at *m/z* 267 and 893, respectively, and also by comparison of retention times and tandem mass spectra to authentic standards [76]

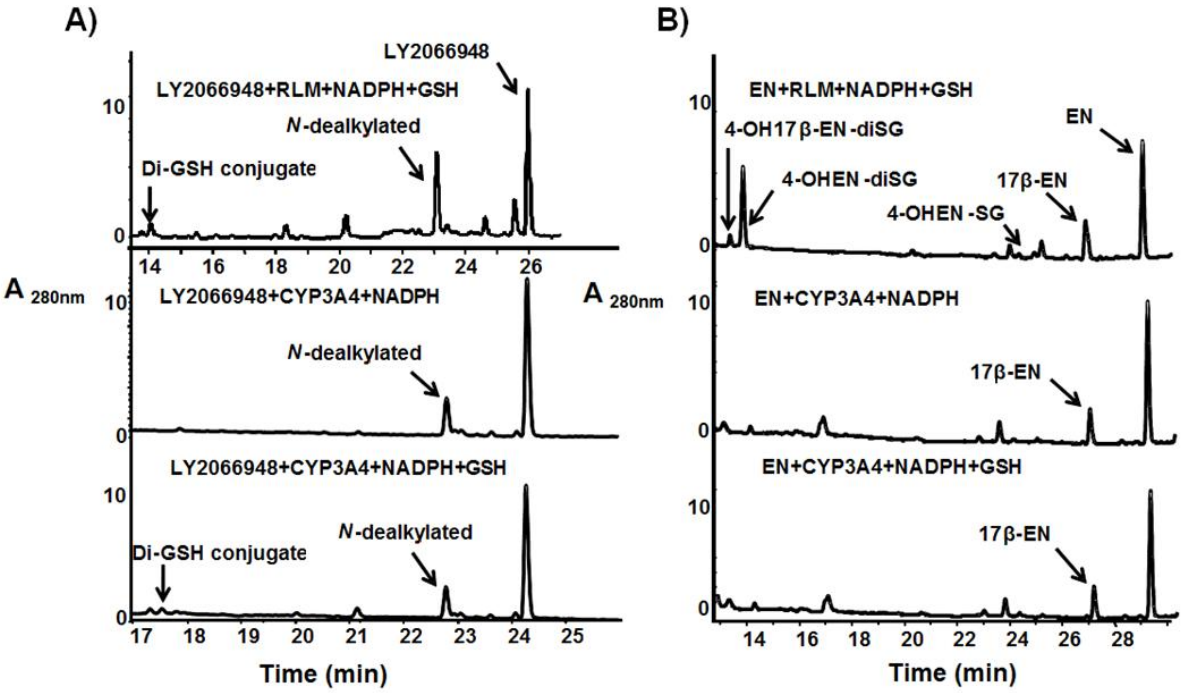

Figure 20. Metabolism of LY and EN by RLM; CYP3A4

Representative HPLC chromatograms of (A) LY (30 µM) or (B) EN (30 µM) incubated with NADPH (1 mM), GSH (1 mM), and either rat liver microsomes (RLM) (1 nmol P450/mL) or CYP3A4 (10 pmol/mL) in 50 mM phosphate buffer (pH 7.4, 0.5 mL total volume) for 30 min at 37 ºC. Metabolites and GSH conjugates were detected by UV-visible absorbance (shown in arbitrary units) at 280 nm, and all annotated peaks were characterized by LC-MS/MS analysis.

3.2.3 <u>Metabolism by P450 3A4 and 1B1 supersomes</u>

Incubation of LY with CYP3A4 supersomes also gave the LY-*o*-quinone di-GSH conjugate as a minor metabolite (4%) and the *N*-dealkylated primary amine metabolite (17%) as the major product (Figure 20A). In contrast, no GSH conjugates were observed when EN was incubated with CYP3A4 in the presence of NADPH and GSH (Figure 20B). In experiments with CYP1B1 supersomes, no LY-*o*-quinone GSH conjugates were detected (Figure 21A); however, CYP1B1 oxidized EN to an *o*-quinone

as is indicated by detection of GSH conjugates. In addition, 17β-EN was detected as a major metabolite, and its formation was NADPH independent (Figure 21B). Reduction of the 17-keto group by several human CYP isoforms has been previously reported for estrone [76, 77].

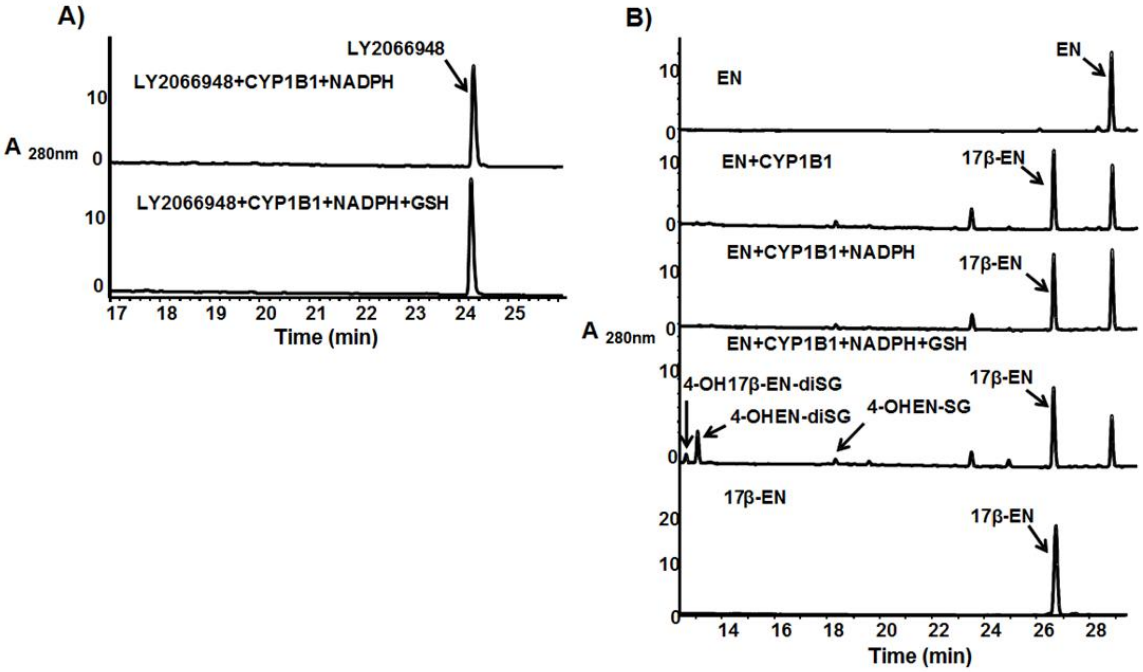

Figure 21. Metabolism of LY and EN by CYP1B1

Representative HPLC chromatograms of (A) LY (30 µM) or (B) EN (30 µM) incubated with CYP1B1 (10 pmol/mL), NADPH (1 mM), and GSH (1 mM) in 50 mM phosphate buffer (pH 7.4, 0.5 mL total volume) for 30 min at 37 ºC. Metabolites and GSH conjugates were detected by UV-visible absorbance (shown in arbitrary units) at 280 nm, and all annotated peaks were characterized by LC-MS/MS analysis.

3.2.4 <u>LY2066948-*o*-quinone decomposition kinetics</u>

LY-*o*-quinone was generated by IBX oxidation and the reactivity of the *o*-quinone was examined. Absent from the spectrum of LY itself, a strong absorbance was observed at 378 nm, which was similar to the UV spectrum of 4-OHEN-*o*-quinone [λ_{max} = 392 nm, [78]]. A protonated molecular ion at *m/z* 532 $[M+H]^+$ (data not shown) was

also observed in the positive ion electrospray mass spectrum of the LY-*o*-quinone, corresponding to two mass units less than that of catechol LY. The rate of disappearance of LY-*o*-quinone was determined and the half-life at physiological pH and temperature was approximately 3.9 ± 0.1 h. For comparison, 4-OHEN-*o*-quinone was also prepared from EN using IBX as an oxidizing agent and its rate of disappearance was determined under the same conditions. The half-life was approximately 2.5 ± 0.2 h (Figure 2B) which is consistent with the previously reported value of 2.3 h [78], within experimental error [76].

3.3 Metabolism of lasofoxifene

3.3.1 Metabolism by tyrosinase

Two mono-GSH and two di-GSH conjugates were detected in incubations of LAS with tyrosinase. The mono-GSH conjugates were arbitrarily assigned as OHLAS-SG1 and OHLAS-SG2 (Figure 22A), and were identified based upon detection of protonated molecular ions of *m/z* 735 $[M+H]^+$. CID of molecular ions *m/z* 735 produced characteristic fragments of *m/z* 717, 642, 606, and 462 corresponding to loss of water, loss of water plus glycine residue, loss of γ-glutamyl group, and cleavage of alkyl thioether bond, respectively (Figure 23A). Typical fragmentations were also observed for di-GSH conjugates, which were arbitrarily assigned as OHLAS-diSG1 and OHLAS-diSG2 and identified based upon detection of protonated molecular ions of *m/z* 1040 $[M+H]^+$. Fragment ions of *m/z* 1022, 893, 782, and 638 were observed, corresponding to loss of water, loss of γ-glutamyl group plus water, loss of two γ-glutamyl groups, and

loss of one γ-glutamyl group coupled with alkyl thioether bond cleavage, respectively (Figures 23B). Similarly, four GSH conjugates (2-OHE$_2$-diSG, 2-OHE$_2$-SG1, 2-OHE$_2$-SG2, and 4-OHE$_2$-SG) were detected when E$_2$ was incubated with tyrosinase in the presence of GSH (Figure 22B) as reported previously [79, 80].

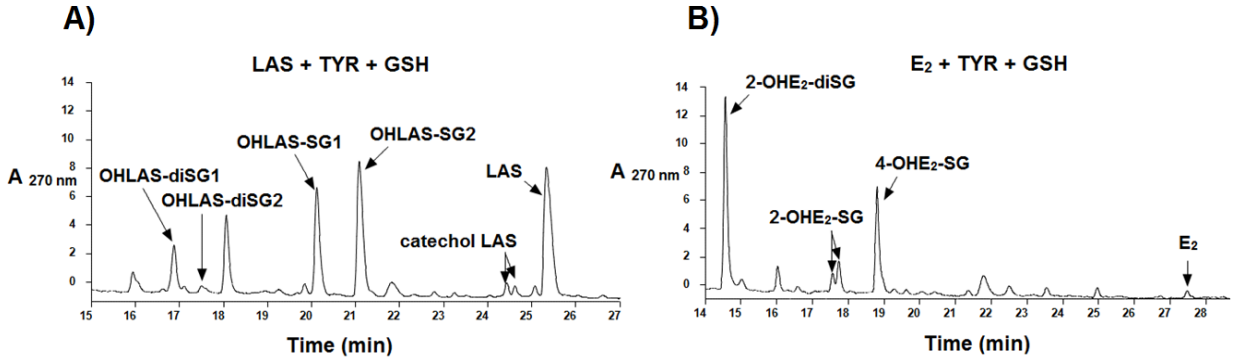

Figure 22. Metabolism of LAS and E$_2$ by tyrosinase

Representative HPLC chromatograms of (A) LAS (30 µM), or (B) E$_2$ (30 µM) incubated with 0.1 mg/mL tyrosinase (TYR) and 1 mM GSH in 50 mM phosphate buffer (pH 7.4, 0.5 mL total volume) for 30 min at 37 ºC.

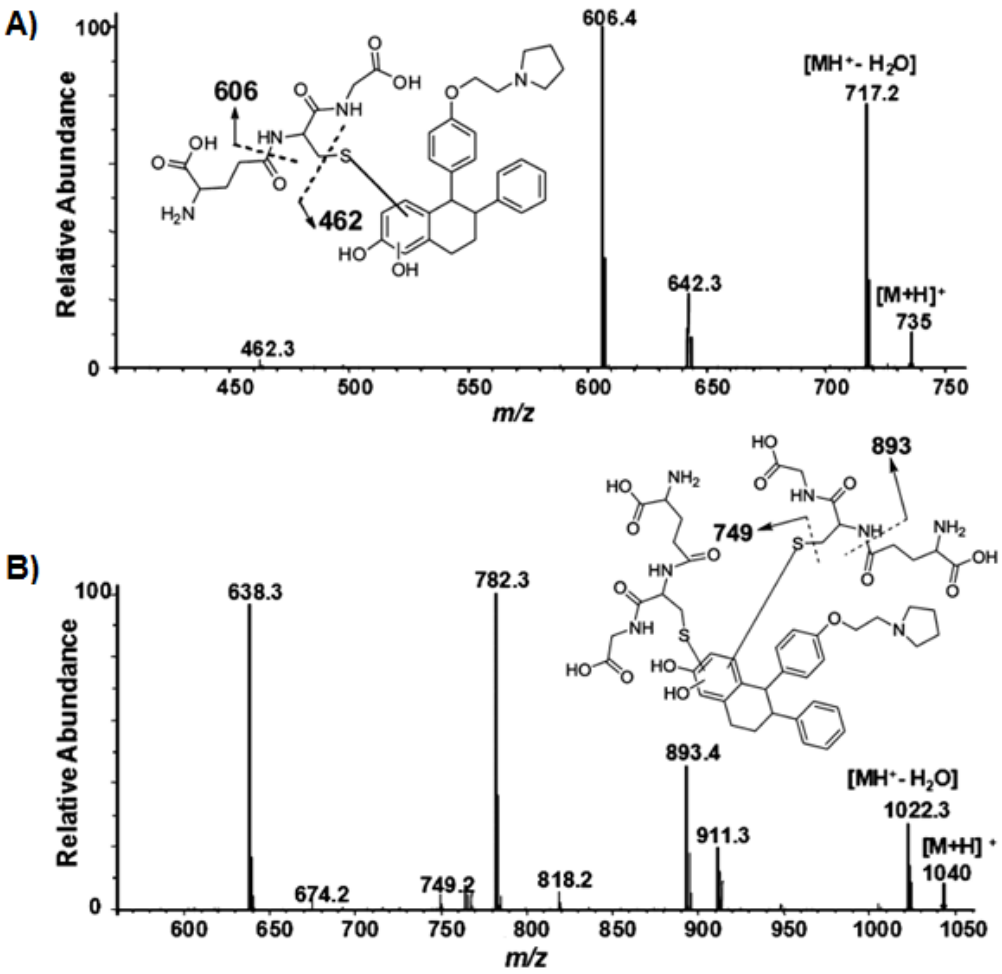

Figure 23. MS fragmentation of OH-LAS-mono-GSH; OH-LAS-di-GSH

Mass spectrometric analyses of (A) OH-LAS-mono-GSH conjugates and (B) OH-LAS-di-GSH conjugates.

3.3.2 <u>Metabolism by liver microsomes</u>

All GSH conjugates of catechol LAS identified in tyrosinase incubations (OHLAS-SG1, OHLAS-SG2, OHLAS-diSG1, and OHLAS-diSG2) were also detected in rat liver microsomal incubations (Figure 24A). Significantly less metabolism was observed in human liver microsomal incubations, although three of the four conjugates (OHLAS-

SG1, OHLAS-SG2, and OHLAS-diSG2) were detected (Figure 24B). All previously reported GSH conjugates of the E_2 catechols (2-OHE$_2$-diSG, 2-OHE$_2$-SG1, 2-OHE$_2$-SG2, and 4-OHE$_2$-SG) seen in tyrosinase incubations, were also detected in both rat and human liver microsomal incubations in similar relative amounts (Figures 24C, 24D) [80].

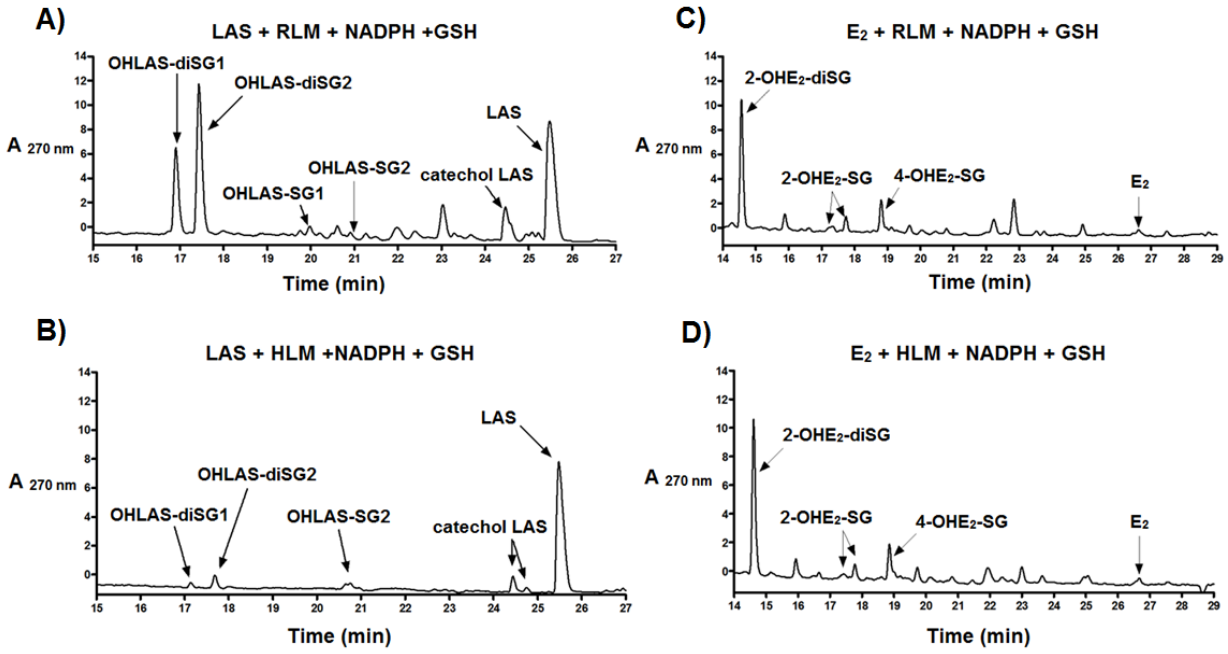

Figure 24. Metabolism of LAS and E_2 by RLM; HLM

Representative HPLC chromatograms of (A, B) LAS (30 µM), or (C, D) E_2 (30 µM) incubated with rat or human liver microsomes (1 nmol P450/mL) and GSH (1 mM) in the presence of a NADPH-generating system (1 mM $NADP^+$, 5 mM $MgCl_2$, 5 mM isocitric acid, and 0.2 unit/mL isocitrate dehydrogenase) in 50 mM phosphate buffer (pH 7.4, 0.5 mL total volume) for 30 min at 37 ºC.

3.3.3 <u>Metabolism by P450 3A4, 2D6, and 1B1 supersomes</u>

Incubations with P450 3A4 supersomes generated only di-GSH conjugates (OHLAS-diSG1, and OHLAS-diSG2) as major metabolites, whereas all four conjugates (OHLAS-SG1, OHLAS-SG2, OHLAS-diSG1, and OHLAS-diSG2) were detected in

experiments with P450 1B1 and P450 2D6 supersomes (Figures 25A-C) [80]. By comparison, 2-OHE$_2$-diSG was the major metabolite seen in incubations with E$_2$ and P450 3A4 or P450 2D6 supersomes, while 4-OHE$_2$-SG was the sole metabolite detected in experiments with P450 1B1 (Figures 25D-F), in accordance with previous studies [81].

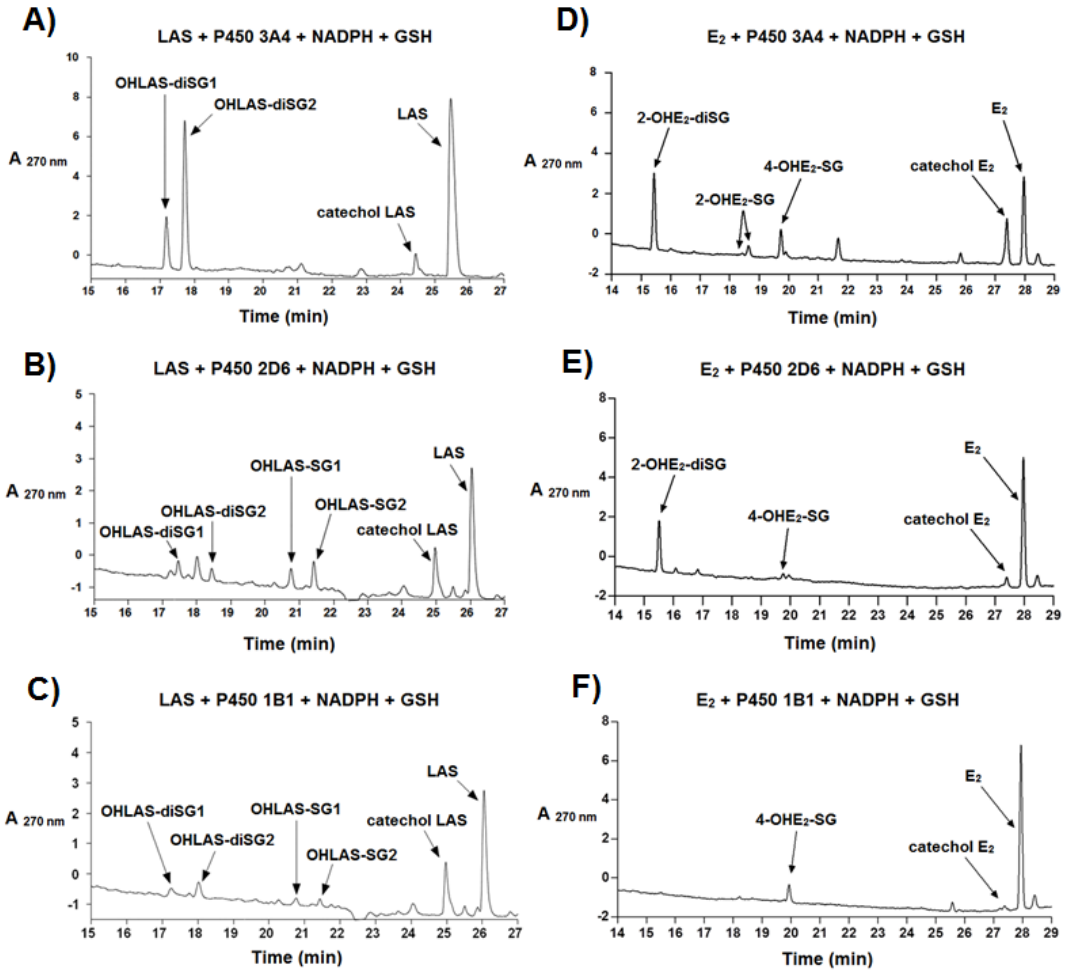

Figure 25. Metabolism of LAS and E$_2$ by P450s 3A4, 2D6, and 1B1

Representative HPLC chromatograms of (A, B, C) LAS (30 µM), or (D, E, F) E$_2$ (30 µM) incubated with P450 3A4, P450 2D6, or P450 1B1 (10 pmol/mL) supersomes, along with GSH (1 mM) and a NADPH-generating system (1 mM NADP$^+$, 5 mM MgCl$_2$, 5 mM isocitric acid, and 0.2 unit/mL isocitrate dehydrogenase) in 50 mM phosphate buffer (pH 7.4, 0.5 mL total volume) for 30 min at 37 ºC.

3.3.4 LAS-*o*-quinone decomposition kinetics

Similar to other SERM and estrogen *o*-quinones [58, 78], a strong absorbance at 378 nm was observed in the UV spectrum of the chemically generated LAS-*o*-quinone mixture which was absent from the spectrum of LAS itself. At physiological pH and temperature, the pseudo-first-order rate of decay of this signal was monitored and the half-life was calculated to be 55 ± 4 min according to the equation $t_{1/2} = \ln(2)/k$.

3.3.5 Competition of catechol LAS glucuronidation or methylation with catechol LAS oxidation and glutathione conjugation

Because glucuronide and methyl ether metabolites of LAS catechols were previously reported whereas GSH conjugates were not observed [45], we investigated the competition between these detoxification pathways. Incubations of LAS with rat liver microsomes and UDPGA in the presence of a NADPH-generating system yielded the expected glucuronide conjugate of the parent compound (LAS-Glu) as a major product, as well as glucuronidated catechol (OHLAS-Glu) as a minor metabolite (Figure 26A). LAS-Glu was identified based upon detection of a molecular ion $[M+H]^+$ at *m/z* 590 and a fragment ion of *m/z* 414 corresponding to glycosidic bond cleavage. OHLAS-Glu was detected as $[M+H]^+$ at *m/z* 606 and gave similar fragmentation to *m/z* 430 as previously reported [45]. Interestingly, with the inclusion of GSH as a trapping reagent in the above incubations, all four previously identified GSH conjugates (OHLAS-SG1, OHLAS-SG2, OHLAS-diSG1, and OHLAS-diSG2) were detected in addition to the glucuronide metabolites (Figure 26B) [80].

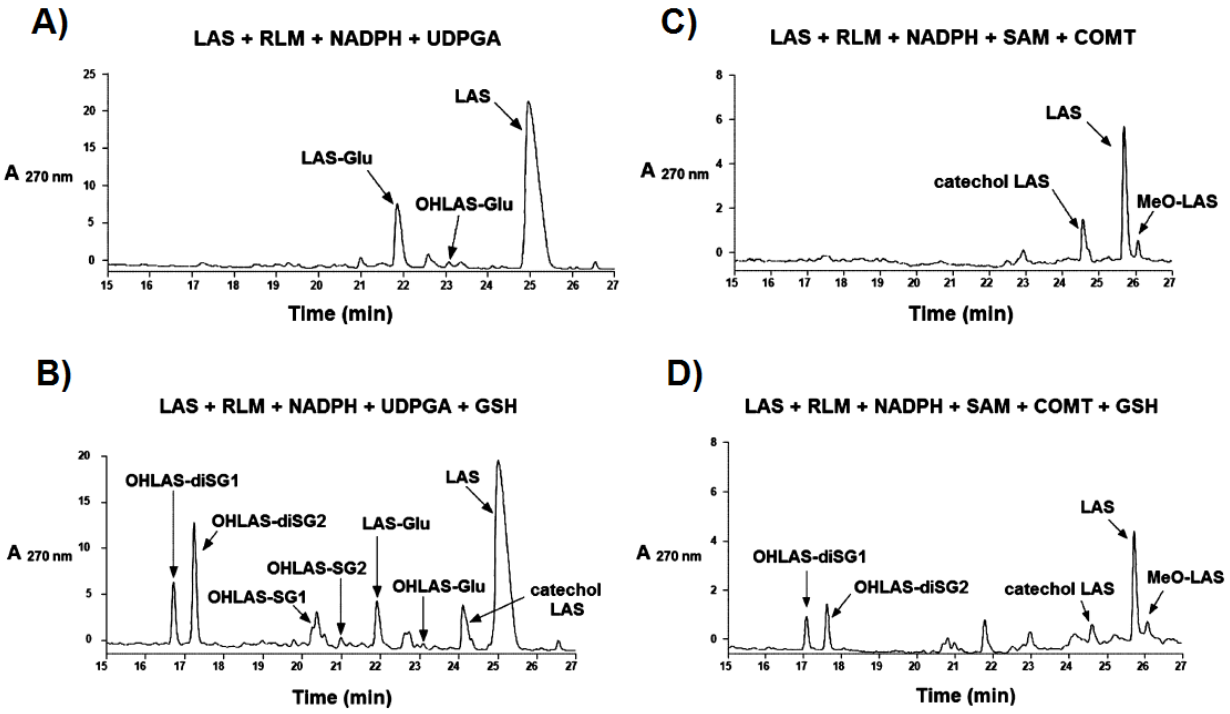

Figure 26. Formation of OH-LAS-GSH conjugates in the presence of glucuronidating or methylating systems

Representative HPLC chromatograms of LAS (30 µM), rat liver microsomes (1 nmol P450/mL), and a NADPH-generating system (1 mM $NADP^+$, 5 mM $MgCl_2$, 5 mM isocitric acid, and 0.2 unit/mL isocitrate dehydrogenase) incubated in 50 mM phosphate buffer (pH 7.4, 0.5 mL total volume) for 30 min at 37 ºC along with one of the following: (A) UDPGA (1 mM) and alamethicin (10 µg/mg protein); (B) GSH (1 mM), UDPGA (1 mM), and alamethicin (10 µg/mg protein); (C) COMT (1 mM) and SAM (0.3 mM); or (D) GSH (1 mM), COMT (1 mM), and SAM (0.3 mM).

Similarly, incubations of LAS with rat liver microsomes, COMT and appropriate cofactors (refer to Materials and Methods) generated both catechol LAS and detectable amounts of methylated LAS catechol (MeO-LAS, Figure 26C). MeO-LAS was identified based upon detection of $[M+H]^+$ at *m/z* 444 and fragment ion *m/z* 253, corresponding to loss of phenoxyethyl-pyrrolidine side chain, as previously reported [45]. Again, inclusion of GSH as a trapping reagent in these incubations resulted in GSH conjugate detection (OHLAS-diSG1 and OHLAS-diSG2, Figure 26D) [80].

3.3.6 Reaction of 7-OHLAS-*o*-quinone with deoxynucleosides; Formation of DHN-7-OHLAS

Incubation of 7-OHLAS and tyrosinase along with either of four deoxynucleosides (dG, dA, dT, or dC) resulted in detection of one depurinating adenine adduct (7-OHLAS-Ade, Figure 27A). This adduct was identified based upon detection of a molecular ion $[M+H]^+$ at *m/z* 563. Fragment ions of *m/z* 430 and *m/z* 239 were also detected, corresponding to loss of adenine and subsequent loss of phenoxyethyl-pyrrolidine side chain, respectively (Figure 27B). Although the absolute structure of 7-OHLAS-Ade was not determined due to low yield, A-ring substitution by the N3 nitrogen of adenine was deemed most probable, as similar adduction has been observed for the case of E_2 [6, 80, 82, 83].

A less polar oxidative metabolite of 7-OHLAS was also detected at *m/z* 428 as a major product in tyrosinase incubations (Figure 27A). Fragment ions of *m/z* 330 and *m/z* 237 corresponding to loss of vinylpyrrolidine and loss of phenoxyethyl-pyrrolidine side chain, respectively, suggested a loss of two mass units from the tetralin ring (data not shown). This metabolite was tentatively assigned as the 1-2 unsaturated dihydronaphthyl analog of 7-OHLAS (DHN-7-OHLAS). Formation of DHN-7-OHLAS could occur through isomerization of 7-OHLAS-*o*-quinone to a *p*-quinone methide followed by tautomerization to DHN-7-OHLAS (Figure 28). This metabolite was only observed in the absence of GSH since GSH would trap the *o*-quinones prior to the tautomerization reaction [80]. Similar pathways have previously been observed for catechol estrogens [79].

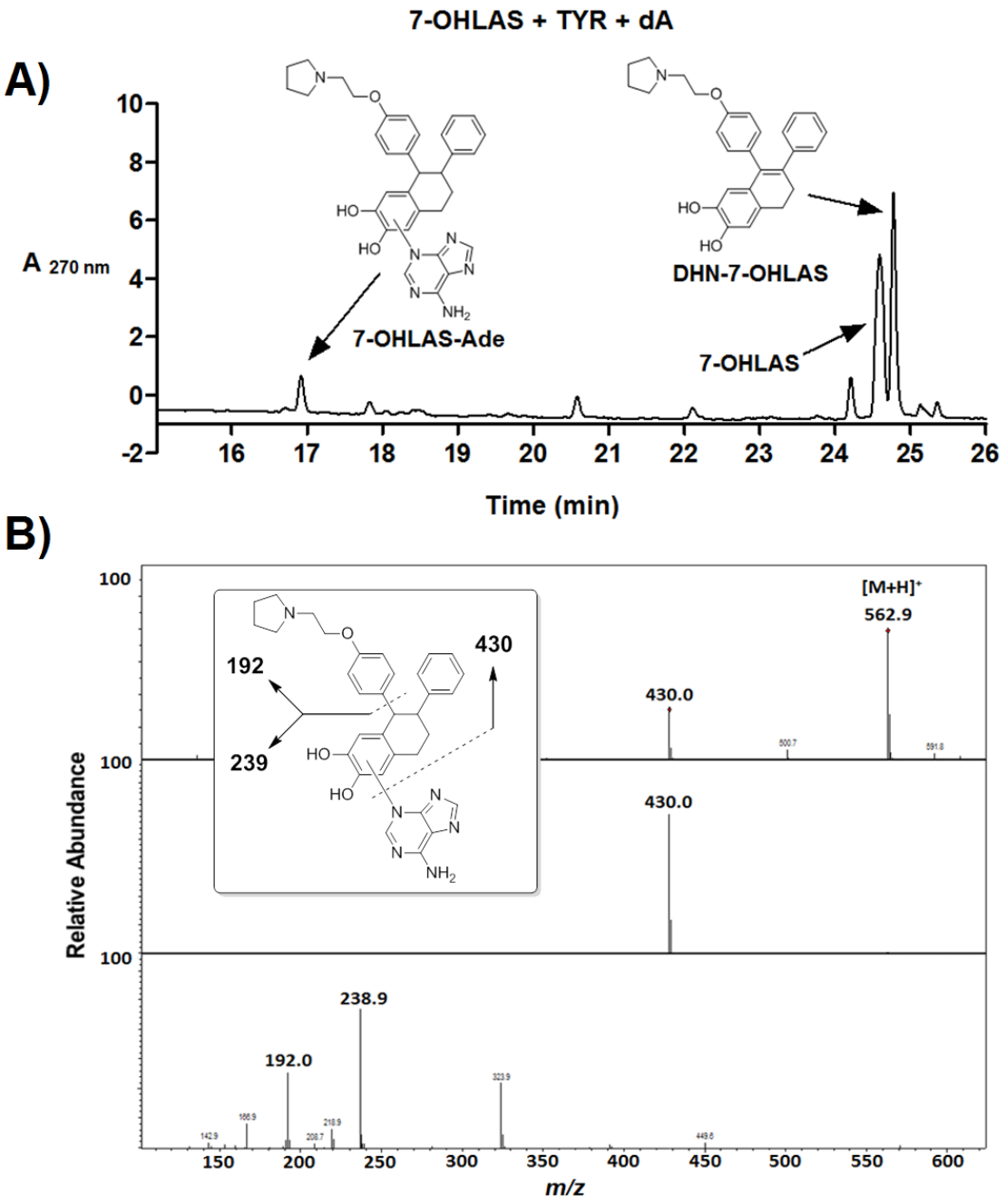

Figure 27. Formation of 7-OHLAS-Ade; DHN-7-OHLAS catalyzed by tyrosinase

Representative HPLC chromatogram of 7-OHLAS (30 µM), tyrosinase (0.1 mg/mL), and deoxyadenosine (300 µM) incubated in 50 mM phosphate buffer (pH 7.4, 0.5 mL total volume) for 30 min at 37 ºC (A) and MS-MS fragmentation of 7-OHLAS-Ade (B).

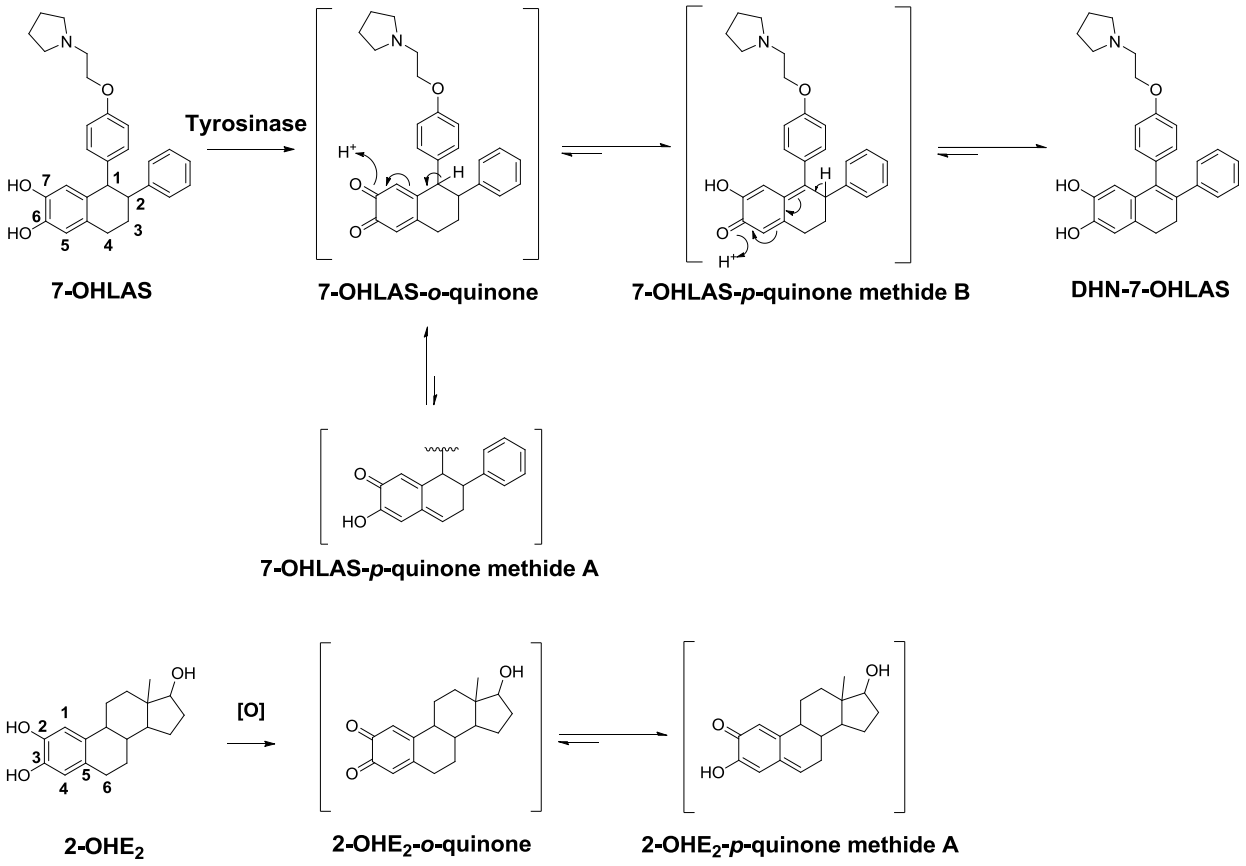

Figure 28. Proposed mechanism for formation of DHN-7-OHLAS; Formation of 2-OHE$_2$-*p*-quinone methide A

3.3.7 <u>Reaction of 7-OHLAS-*o*-quinone with calf thymus DNA</u>

Incubation of chemically-oxidized 7-OHLAS-*o*-quinone with DNA resulted in detection of 7-OHLAS-Ade (Figure 29A) as well as two depurinating guanine adducts, arbitrarily assigned as 7-OHLAS-Gua-1 and 7-OHLAS-Gua-2 (Figure 29B). While absolute structures of 7-OHLAS-Gua-1 and 7-OHLAS-Gua-2 were not determined due to low yield, A-ring substitution by the N7 nitrogen of guanine at the 5 and 8 positions of LAS was deemed most likely, again based upon similar adduction observed for depurinating guanine adducts of E_2 [6, 82, 83]. Adenine and guanine adducts were

detected with MRM and collision-induced dissociation for the fragmentation pathways of *m/z* 563→136, and *m/z* 579→152, respectively.

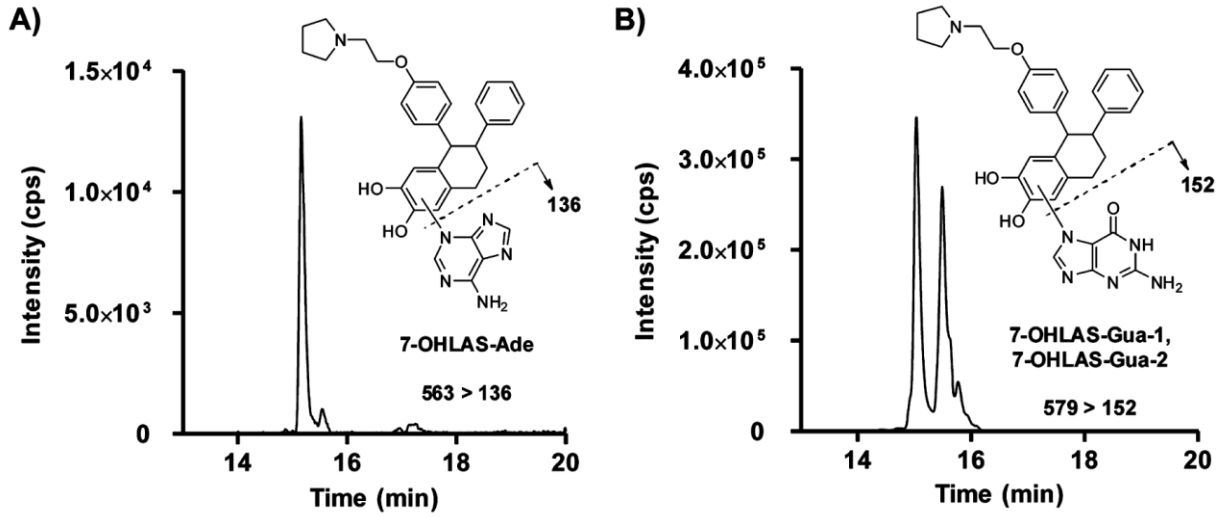

Figure 29. Detection of 7-OHLAS-Ade, 7-OHLAS-Gua-1, and 7-OHLAS-Gua-2

Detection of 7-OHLAS-Ade by MRM at *m/z* 563 > 136 (A) and 7-OHLAS-Gua-1 and 7-OHLAS-Gua-2 by MRM at *m/z* 579 > 152 (B).

3.4 Metabolism of bazedoxifene

3.4.1 Metabolism by tyrosinase

Incubations of BAZ with tyrosinase yielded a minor, but detectable amount of BAZ-catechol (data not shown). In presence of reducing ascorbate, catechol-BAZ was the major product observed (Figure 30A), and was identified based upon detection of a strong peak at *m/z* 487, and fragment ions at *m/z* 255, 268, and 361, corresponding to loss of (2-(p-tolyloxy)ethyl)azepane, (2-phenoxyethyl)azepane, and ethylazepane, respectively (Figure 31A). Four mono-GSH and two di-GSH conjugates were detected in incubations of BAZ with tyrosinase. The mono-GSH conjugates were arbitrarily

assigned as OHBAZ-SG1-4 (Figure 30B), and were identified based upon detection of protonated molecular ions of *m/z* 792 $[M+H]^+$. CID of molecular ions *m/z* 792 produced characteristic fragments of *m/z* 774, 663, and 519, corresponding to loss of water, loss of γ-glutamyl group, and cleavage of alkyl thioether bond, respectively (Figure 31B). Di-GSH conjugates (OHBAZ-diSG1-2) were also identified based upon detection of doubly charged protonated molecular ions $[M + 2H]^{2+}$ at *m/z* 549 and fragment ions of *m/z* 748 and 697, corresponding to loss of glycine plus cleavage of thioether bond, and loss of ethylazepane side chain plus cleavage of thioether bond, respectively (data not shown).

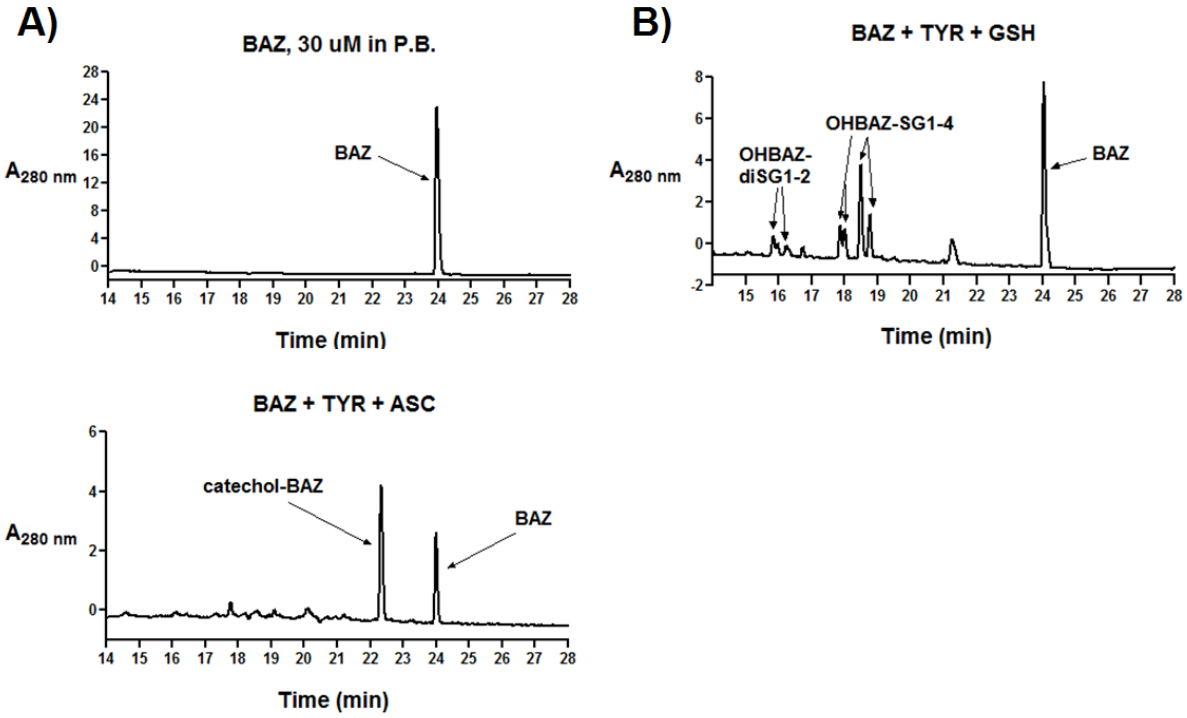

Figure 30. Metabolism of BAZ by tyrosinase

Representative HPLC chromatograms of (A) BAZ (30 µM) incubated with tyrosinase (0.1 mg/mL) and ascorbic acid (1 mM), or (B) tyrosinase (0.1 mg/mL) and GSH (1 mM) in 50 mM phosphate buffer (pH 7.4, 0.5 mL total volume) for 30 min at 37 ºC.

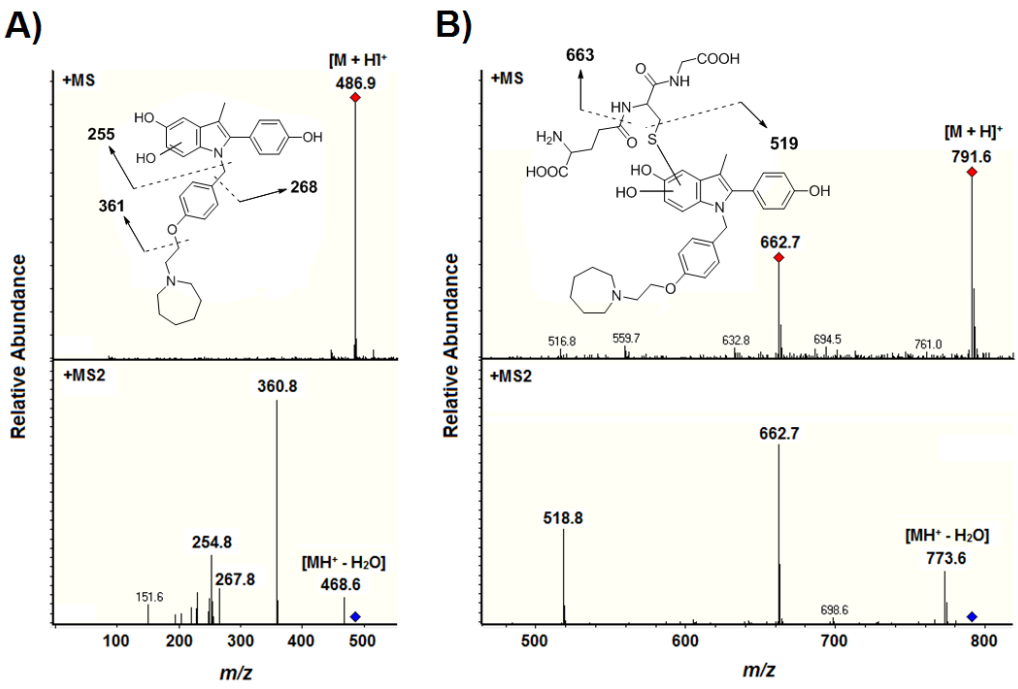

Figure 31. MS fragmentation of OHBAZ; OHBAZ-mono-GSH

Mass spectrometric analysis of (A) OHBAZ and (B) OHBAZ-SG1-4.

3.4.2 Metabolism by liver microsomes

No GSH conjugates were detected in incubations of BAZ with rat liver microsomes; however, a major product corresponding to addition of 2 oxygen atoms was observed at *m/z* 503 (Figure 32A). This metabolite was tentatively assigned as the *N*-dealkylated, hexanoic acid metabolite of BAZ (BAZ-HA, Figure 32B). Detection of fragment ions at *m/z* 264 and 158, corresponding to loss of 6-((2-(*p*-tolyloxy)ethyl)amino)hexanoic acid and 6-(ethylamino)hexanoic acid side chain fragments respectively, suggested two oxidations of the azepane side chain to give the ring-opened Ɛ-carboxylic acid derivative (Figure 32B). Such metabolism for drugs containing tertiary nitrogen heterocycles is common, and has been previously reported

[84-86]. In accordance with previous studies [87], no such metabolism was observed in experiments with human liver microsomes (Figure 32A).

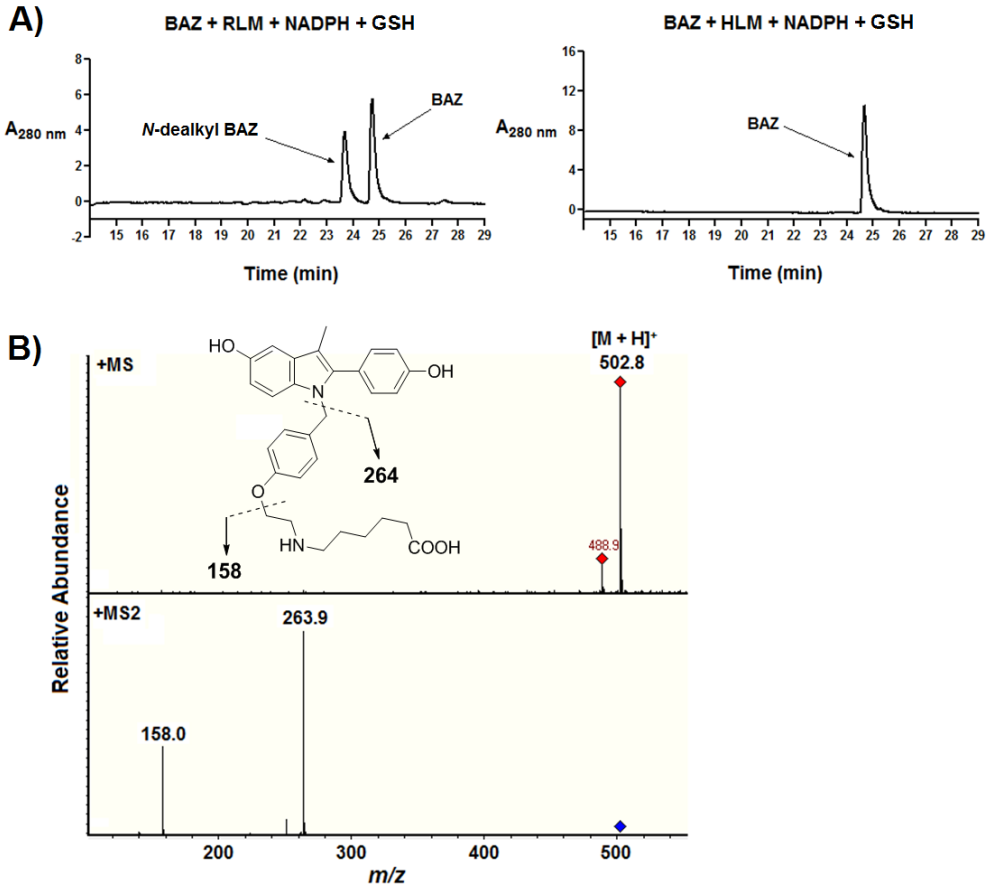

Figure 32. Metabolism of BAZ by rat liver microsomes

Representative HPLC chromatograms of (A) BAZ (30 µM) in phosphate buffer or BAZ (30 µM) incubated with rat liver microsomes (1 nmol P450/mL), NADPH (1 mM), and GSH (1 mM). (B) Mass spectrometric analysis of BAZ-HA.

3.5 Generation of HP-BTF by POSEMs in human liver microsomes

The dipivalate ester of HP-BTF (BM3-11) exhibited poor aqueous solubility, and did not generate HP-BTF in microsomal incubations (data not shown). At physiological temperature and pH, BM3-13 (diacetate ester), BM3-15 (diisobutyrate ester), and BM3-

25 (di-((nitrooxy)methyl)cyclopropanecarboxylate ester) all generated HP-BTF at 83.3%, 53.7%, and 16.0%, respectively, after 30 minutes (Figures 33A-C).

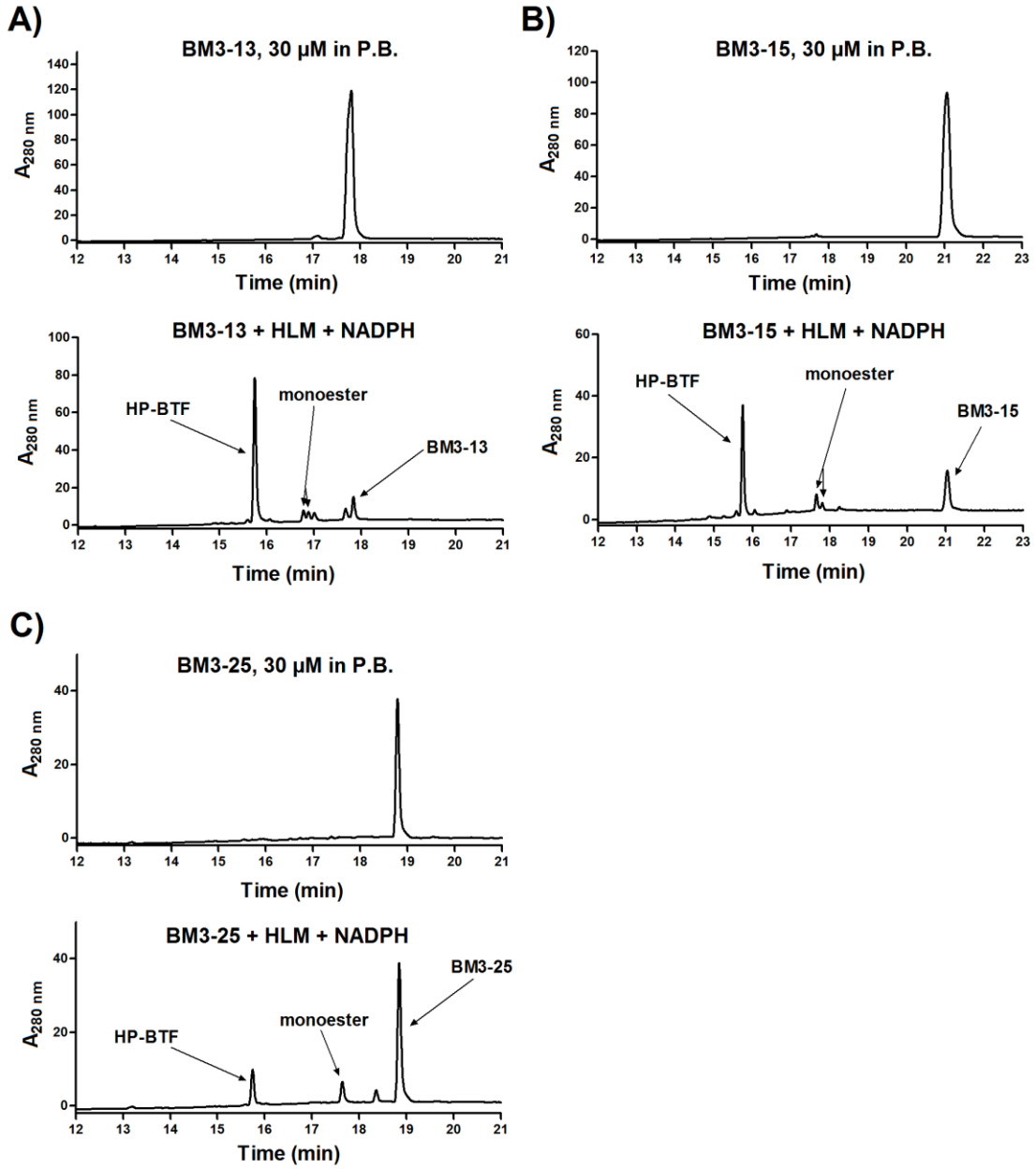

Figure 33. Generation of HP-BTF from POSEMs by HLMs

Representative HPLC chromatograms of POSEMs BM3-13, BM3-15, and BM3-25 (30 μM) incubated with human liver microsomes (1 nmol P450/mL) and NADPH (1 mM) in 50 mM phosphate buffer (pH 7.4, 0.5 mL total volume) for 30 min at 37 ºC

3.6 Summary

A family of benzothiophene SERMs and SEMs was synthesized and assayed for estrogenic activity in the Ishikawa endometrial cancer cell line. Compounds were found to range in activity from potent estrogens, to potent antiestrogens (Table 1). Preliminary data obtained by the Tonetti lab found that one of these SEMs, HP-BTF, inhibited the growth of tamoxifen-resistant breast tumors (refer to Section 4.4.3 for a more detailed discussion on HP-BTF, SEMs, and POSEMs). Subsequent verification of this growth-inhibition by the Tonetti lab in several *in vivo* models suggested HP-BTF as an ideal candidate SEM for the development of prodrugs designed to increase drug efficacy. Several POSEMs incorporating HP-BTF were therefore synthesized, and three were found to generate HP-BTF in human liver microsomal incubations.

LY, LAS, and BAZ were each oxidized to *o*-quinones by tyrosinase. These metabolites were characterized as their corresponding GSH conjugates. For LY and BAZ however, P450-mediated metabolism primarily involved side chain *N*-dealkylation rather than bioactivation to *o*-quinones. Collectively, these data suggest that bioactivation of these SERMs is unlikely to result in toxicity *in vivo*.

Conversely, for the case of LAS, bioactivation to *o*-quinones by tyrosinase or by P450s constituted the primary route of metabolism, similar to what is seen for E_2. Moreover, *o*-quinone formation by LAS was shown to occur even in the presence of UGTs and COMT suggesting that LAS catechols may oxidize to *o*-quinones and react with cellular nucleophiles prior to detoxification and clearance by these Phase II enzymes. Finally, 7-OHLAS was synthesized, and upon enzymatic or chemical oxidation, was shown to react with deoxynucleosides and DNA resulting in the detection

of several depurinating adducts. These results again are analogous to what is seen for structurally similar E_2. Depurinating adducts of estrogen *o*-quinones form through reaction with the nucleophilic N3 of adenine or N7 of guanine, which following glycosidic bond hydrolysis, results in the generation of apurinic sites on DNA. Such sites are susceptible to improper repair and have been demonstrated to result in mutations critical for carcinogenic initiation [82, 83, 88]. Similarly, depurinating adducts of 7-OHLAS-*o*-quinone were hypothesized to form via an identical mechanism (Figure 34), and confirmation of this mechanistic pathway will be a subject of future studies.

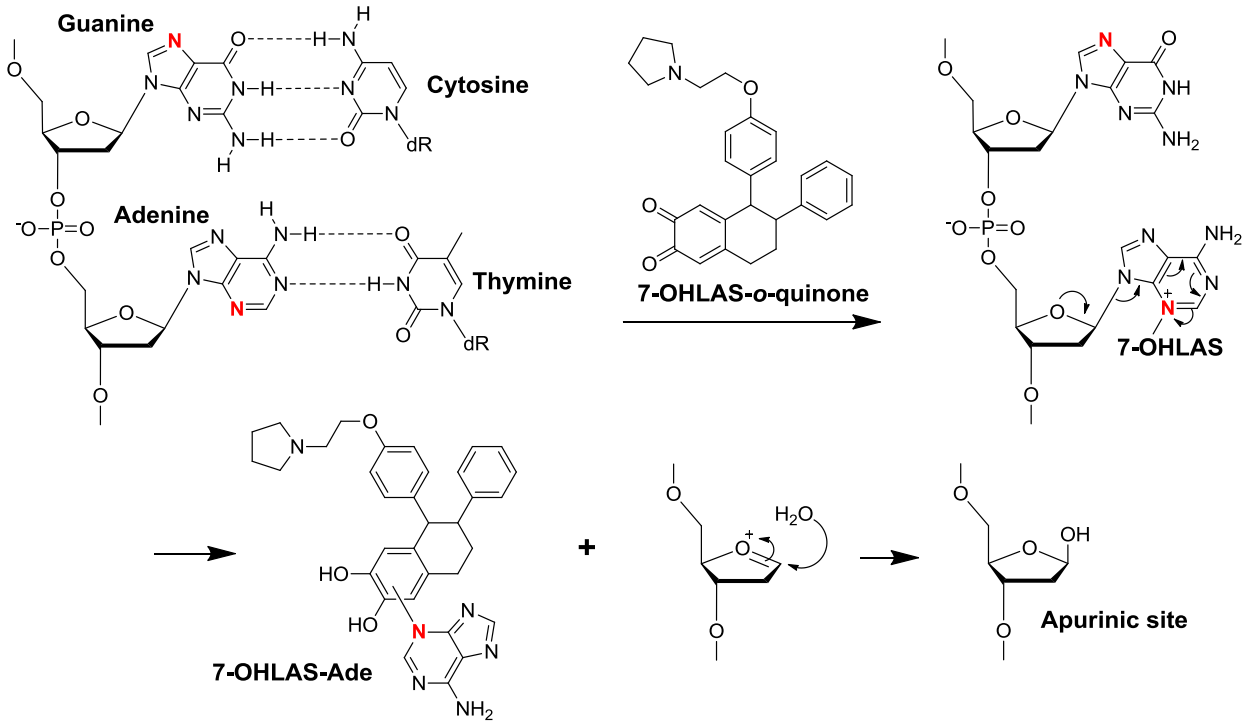

Figure 34. Proposed mechanism for formation of depurinating DNA adducts from 7-OHLAS-*o*-quinone

Proposed reaction of 7-OHLAS-*o*-quinone with DNA to generate depurinating adducts and apurinic sites. Reaction with adenine is shown as an example. The nucleophilic N3 of adenine and N7 of Guanine are shown in red.

Chapter 4: Comparative Assessment of Benzothiophene SERMs and the Classification of SERMs

4.1 Selective estrogen receptor modulators (SERMs)

4.1.1 Triphenylethylene SERMs

The prototypical triphenylethylene SERM tamoxifen (Figure 35), was initially discovered in the early 1960's as part of a program designed to develop female contraceptives; however, while effective at preventing pregnancy in animal models, tamoxifen was shown to induce ovulation in humans [14, 18]. It was later found that tamoxifen also displayed antiestrogenic action in breast tissue, leading to study of the drug in models of breast carcinoma [18, 89]. The subsequent development and successful secondary application of tamoxifen as a targeted breast cancer treatment, therefore, represents a somewhat serendipitous case of drug discovery. In 1978, tamoxifen was approved by the FDA for the treatment and prevention of ER(+) breast cancer, and to date, remains the most widely-prescribed anticancer drug in the world [28, 90]. Tamoxifen has been shown to substantially increase survival rates in women with ER(+) tumors and also to reduce the recurrence of tumors in postmenopausal women at high risk [90, 91]. Moreover, numerous studies on tamoxifen in breast cancer prevention have also demonstrated the drug's effectiveness as a chemopreventive agent [90, 92].

While tamoxifen behaves as an antiestrogen in breast tissue, it also possesses estrogenic activity in other tissues. In the cardiovascular system and in bone, these

estrogenic effects are largely beneficial. In postmenopausal women, tamoxifen use has a positive effect on lipid profiles, significantly lowering low density lipoprotein (LDL) while having minimal effects on triglyceride or high density lipoprotein (HDL) levels [93, 94]. Similarly, a number of studies have demonstrated tamoxifen to be effective in maintaining bone mineral density in the lumbar spine [95, 96]. The estrogenic action of tamoxifen in the endometrium however, represents the principle disadvantage of long-term use of the drug, as a well-documented association between duration of tamoxifen therapy, and the increased risk for developing endometrial cancer has been firmly established [18, 24]. The revelation of such a dangerous side effect is largely responsible for the further development of SERMs as a drug class in the attempt to discover new compounds which possess improved tissue selectivity and which are devoid of stimulatory action in endometrial tissues.

Other clinically relevant triphenylethylenes include toremifene, clomiphene, and ospemifene (Figure 35). Each are close structural analogs of tamoxifen, and are used for treatment of advanced metastatic breast cancer, infertility, and vulvar-vaginal atrophy, respectively [15, 16, 97]. Halogenated or hydroxylated tamoxifen analogs such as toremifene, clomiphene, idoxifene, droloxifene, and ospemifene (Figure 35) were designed as SERMs which would maintain the beneficial effects of tamoxifen while attenuating undesirable side effects associated with bioactivation to reactive metabolites (refer to Section 4.2.1). In the treatment of advanced metastatic breast cancer, toremifene shows similar efficacy to that of tamoxifen, but unfortunately, also shares a similar capacity to stimulate endometrial tissue, limiting its use to short treatment duration [98-100]. Droloxifene and idoxifene have also been examined in Phase III

clinical trials for breast cancer treatment; however, droloxifene was shown to have significantly lower efficacy than tamoxifen, and its clinical development was subsequently discontinued [101]. Similarly, development of idoxifene was halted due to inferior efficacy compared to tamoxifen, and also significant increases in both endometrial thickening and uterine prolapse [102].

Ospemifene, interestingly, is a major *N*-dealkylated, hydroxyl metabolite of toremifene which has recently completed Phase III clinical trials and received FDA approval (February, 2013) for the treatment of vulvar-vaginal atrophy [16, 97]. Data from these studies have shown ospemifene is well-tolerated, and significantly improves measures of vulvar-vaginal atrophy as well as markers for bone turnover. Moreover, recent data in several animal models have suggested a potential use for ospemifene in breast cancer chemoprevention, although human trials have yet to be conducted for this indication [97, 103].

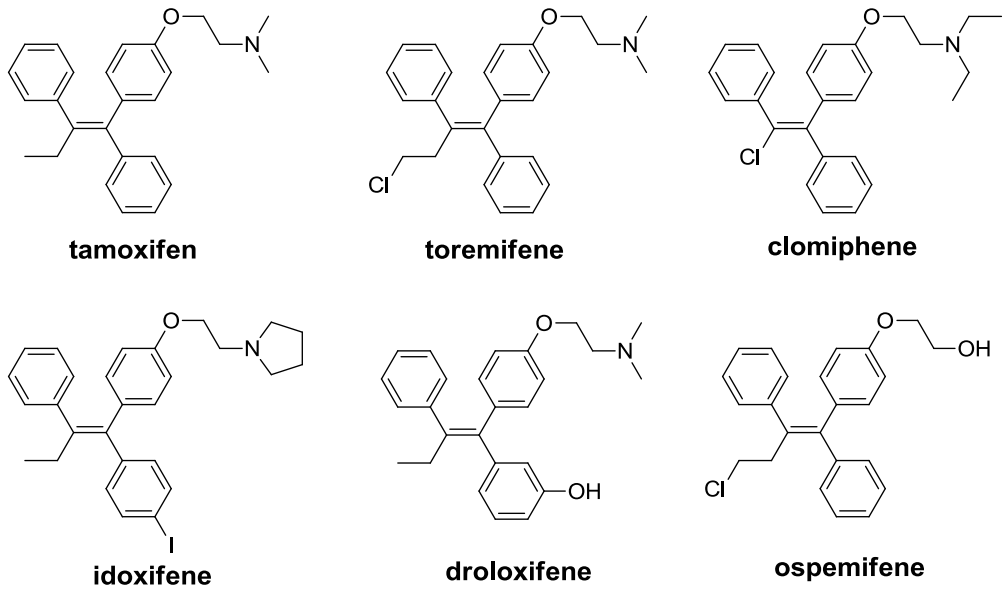

Figure 35. Structures of triphenylethylene SERMs

4.1.2 Benzothiophene SERMs

Raloxifene (Figure 36) is the only benzothiophene SERM currently approved by the FDA. It is approved both for the treatment and prevention of postmenopausal osteoporosis, and also for reducing the risk of invasive breast cancer in postmenopausal women with osteoporosis who are at an increased risk (refer to Section 4.3.4) [29, 104]. Although originally developed specifically for the treatment of ER(+) breast cancer, its efficacy for use in this indication has been demonstrated to be significantly inferior to that of tamoxifen due primarily to poor oral bioavailability [68, 105]. Raloxifene behaves as an estrogen in bone, but unlike tamoxifen, is antiestrogenic in both breast and endometrial tissues [106]. Accordingly, use of raloxifene has not been found to increase the incidence of endometrial cancer [14, 100, 106]. Although not stimulatory in endometrial tissues, studies have shown raloxifene to increase the incidence of venous thromboembolism (VTE) as well as hot flashes (refer to Section 4.3.5) [36, 107].

Arzoxifene (Figure 36) is a benzothiophene analog in which the carbonyl hinge of raloxifene is replaced by an aryl ether linkage. Additionally, arzoxifene bears a 4'-methoxyl, rather than hydroxyl group [68, 108], designed to limit the extensive first-pass glucuronidation observed with raloxifene and increase oral bioavailability [60, 108]. Arzoxifene is *O*-demethylated *in vivo* to its active metabolite, desmethylarzoxifene (DMA, Figure 36), a highly potent antiestrogen in breast and endometrial tissues [68, 108]. Arzoxifene has been investigated in Phase III clinical trials for treatment of locally advanced or metastatic breast cancer, and also for treatment of osteoporosis in postmenopausal women [14, 109]. While arzoxifene initially showed efficacy in the

treatment of locally advanced or metastatic breast cancer, its development for use in this indication was halted when interim analysis of a subsequent Phase III study revealed a significantly inferior median progression-free survival (4.0 months) to that of tamoxifen (7.5 months) [109]. Similarly, development of arzoxifene as a treatment for osteoporosis was discontinued when Phase III trials failed to meet the secondary endpoints of reducing nonvertebral fracture and cardiovascular events, while at the same time increasing incidence of VTE, hot flashes, and other gynecological disorders [14].

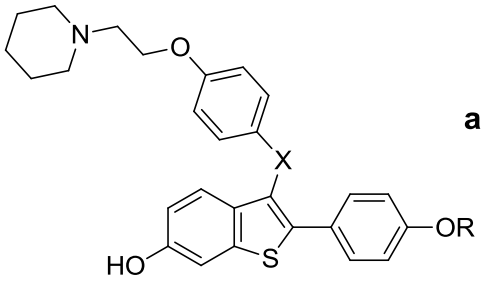

raloxifene, X = C=O
arzoxifene, X = O, R = Me
DMA, X = O, R = H

Figure 36. Structures of benzothiophene SERMs

4.1.3 <u>Benzopyran, indole, naphthol, and tetralin SERMs</u>

Acolbifene (EM-652) is a benzopyran-based SERM and is the active form of the dipivalate ester prodrug EM-800 (Figure 37) [110, 111]. Acolbifene is a potent inhibitor of cell proliferation in breast and endometrial cancer cell lines [38, 110-112]. Preclinical animal studies have demonstrated that acolbifene is an effective inhibitor of breast tumor xenograft growth while also displaying beneficial effects on bone mineral density and lipid metabolism, all without evidence of endometrial stimulation [113-115]. Promising preclinical data has led to further study of acolbifene in Phase II clinical trials for potential treatment in breast cancer chemoprevention [116] and breast cancer

treatment in women for which tamoxifen treatment has failed [117]. A larger Phase III trial [118] is also currently underway in order to examine the effects of acolbifene co-administered with dehydroepiandrosterone (DHEA) as a treatment for vasomotor symptoms.

The indole-based SERM, bazedoxifene (BAZ, Figure 37), was approved in the EU in 2009 for the treatment and prevention of postmenopausal osteoporosis [46, 47]. While this SERM has yet to receive FDA approval, Pfizer is currently developing BAZ both as a standalone therapy for the treatment and prevention of postmenopausal osteoporosis, and also in combination with conjugated estrogens (CE) as a therapy for the treatment of menopausal symptoms [119, 120]. As a monotherapy, two separate Phase III studies found that BAZ significantly reduced biomarkers for bone turnover and the risk for new vertebral fractures, while significantly increasing BMD in the hip and lumbar spine of postmenopausal women. While no significant increases in breast cancer, endometrial cancer, myocardial infarction, or stroke were observed in either study, a significant increase in VTE and hot flashes was seen, similar to raloxifene [119, 120]. As a combined therapy, BAZ plus CE represents the first clinically relevant example of a potentially new class of therapeutics in the treatment of postmenopausal symptoms, dubbed Tissue Selective Estrogen Complexes (TSECs; refer to Section 4.4.1). Evidence from several Phase III trials (SMART trials) has shown that a TSEC composed of BAZ plus CE significantly increased BMD, provided relief of hot flashes, improved measures of vulvar-vaginal atrophy, and showed no evidence of endometrial or breast stimulation in postmenopausal women (refer to Section 4.4.1) [121-128].

LY2066948 (Figure 37) is a naphthol-based SERM currently being investigated by Eli Lilly as a potential treatment for uterine fibroids [42]. Uterine fibroids are the most common type of solid tumor found in adult women and are dependent upon estrogen for growth [42]. Current standards of care for treatment of uterine fibroids are limited primarily to surgical removal, uterine artery embolization, and/or use of gonadotropin-releasing hormone (GnRH) agonists which blockade estrogen through downregulation of the hypothalamo-pituitary-ovarian (HPO) axis; however recurrence of fibroids following surgical removal or uterine artery embolization is common, and use of GnRH agonists frequently results in side effects typically associated with low estrogen levels such as hot flashes and bone loss [42, 129, 130]. Alternatively, use of an appropriate SERM for the treatment of uterine fibroids has been recognized as a potentially improved option, as SERMs may selectively antagonize estrogenic action in desired tissues while maintaining beneficial effects of estrogen in bone. While SERMs like tamoxifen, raloxifene, and clomiphene display partial ovarian stimulation which results in increased circulating estrogen and enhanced ovarian cyst formation, preclinical studies have shown that ovarian stimulation by LY2066948 is minimal at doses required for effective antiestrogenic action in the uterus. This distinct tissue-selectivity may suggest a potentially unique role for LY2066948 in the treatment of uterine fibroids [42].

Lasofoxifene (LAS, Figure 37) is a SERM with a tetralin (1,2,3,4-tetrahydronaphthalene) core structure which is currently approved in the EU for the treatment and prevention of postmenopausal osteoporosis [44]. Clinical studies have demonstrated the efficacy of LAS in decreasing bone resorption, bone loss, and LDL cholesterol in postmenopausal women [131]. The multinational Postmenopausal

Evaluation and Risk-Reduction with Lasofoxifene (PEARL) trial examined the effects of LAS (0.25 mg/day or 0.5 mg/day) in 8554 postmenopausal women over the course of 5 years [14, 132, 133]. Primary endpoints for the trial included incidence of vertebral fracture, ER(+) breast cancer, and nonvertebral fracture, while secondary endpoints included incidence of major coronary heart disease events, stroke, and vaginal atrophy [132, 133]. Results of the PEARL trial found that either 0.25 mg or 0.5 mg doses significantly reduced incidence of vertebral fracture (31% and 42%, respectively) while only the higher dose significantly reduced incidence of nonvertebral fracture (24%) [133]. Similarly, only high dose LAS reduced the incidence of ER(+) breast cancer (81%), stroke (36%), coronary heart disease (32%). LAS did not increase incidence of endometrial cancer; however, similar to other SERMs, LAS (0.5 mg) significantly increased the risk for VTE (2-fold) and pulmonary embolism (4.5-fold). Interestingly, a significant increase in all-cause mortality was also observed with low-dose, but not high-dose LAS [14, 133]. While Pfizer has attempted several times to market LAS for the treatment of postmenopausal osteoporosis (2005, 2007) and vulvar-vaginal atrophy (2006), this SERM has yet to receive FDA approval [14].

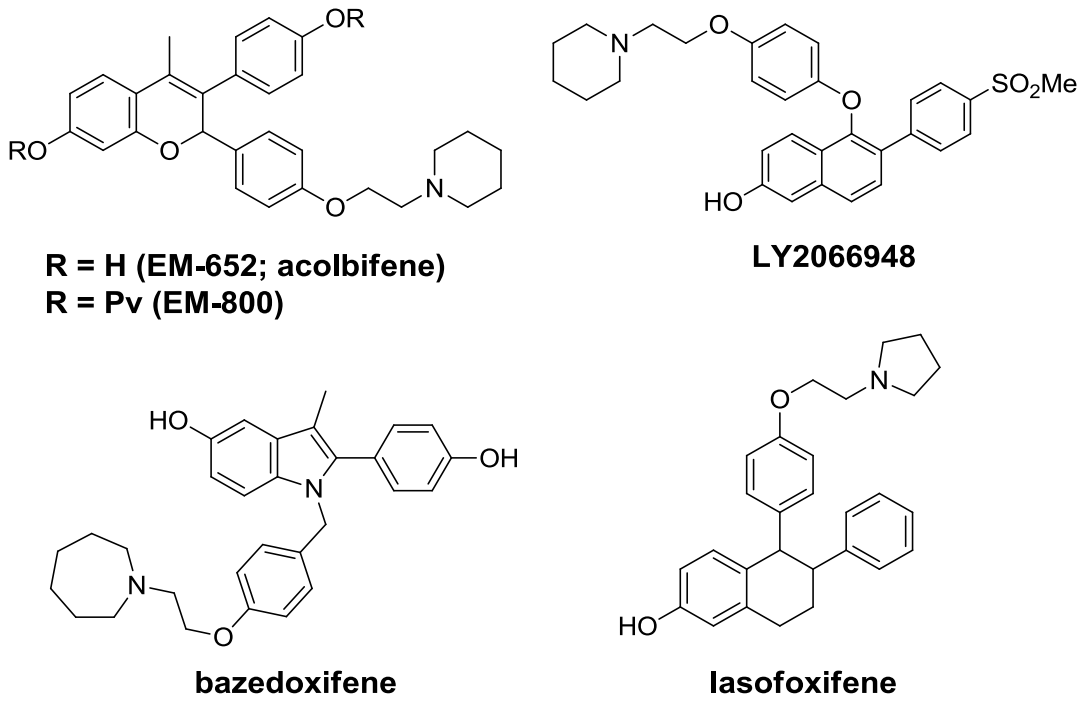

Figure 37. Structures of benzopyran, indole, naphthol, and tetralin SERMs

4.2 Bioactivation pathways for SERMs

4.2.1 Tamoxifen, toremifene

The primary Phase I metabolism of tamoxifen in humans involves oxidation of the side chain nitrogen to *N*-oxide or *N*-desmethylated metabolites, as well as aromatic hydroxylation at the 4-position, yielding active metabolites such as 4-hydroxytamoxifen (4-OHTAM) and 4-hydroxy-*N*-desmethyltamoxifen (endoxifen) which are more potent antiestrogens than tamoxifen itself. Additionally, α-hydroxylation and side chain *O*-dealkylation are observed, although in lesser amounts [134]. Further biotransformation of a number of these metabolites has been shown to produce several types of reactive

electrophiles, all of which have demonstrated the potential to modify cellular nucleophiles [37].

Aromatic hydroxylation of tamoxifen at the 4-position is catalyzed primarily by CYP2D6 (Figure 38) [135]. *o*-Hydroxylation of 4-OHTAM to give catechol 3,4-dihyroxytamoxifen is catalyzed mainly by CYP3A4 and to a lesser extent, CYP2D6 [136]. 3,4-Dihydroxytamoxifen may be further oxidized to its corresponding *o*-quinone by several oxidative enzymes; this *o*-quinone is highly electrophilic, and has been demonstrated to form conjugates with GSH and also induce single strand breaks in DNA *in vitro* [137, 138].

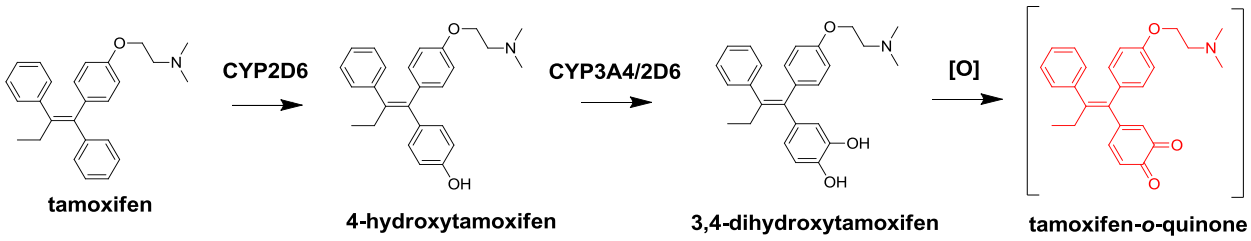

Figure 38. Bioactivation of tamoxifen to *o*-quinone

Additionally, 4-OHTAM may undergo direct P450-mediated 2-electron oxidation to form an electrophilic quinone methide. An alternative mechanism for generation of 4-OHTAM-derived quinone methide (4-OHTAM-QM) could also involve α-hydroxylation of 4-OHTAM by CYP3A4 to 4,α-dihydroxytamoxifen, with subsequent dehydration [139] (Figure 39). Simple *p*-quinone methides are transient and normally rapidly react by non-enzymatic 1,6-Michael addition in biological systems, generating benzylic adducts; however, 4-OHTAM-QM possesses extended conjugation with 2 phenyl rings and a

vinyl group and as a result is very stable ($t_{1/2}$ = 3 h) [137]. Moreover, 4-OHTAM-QM has been reported to form stable adducts with the exocyclic amine of deoxyguanosine *in vitro* via 1,8-Michael addition [139].

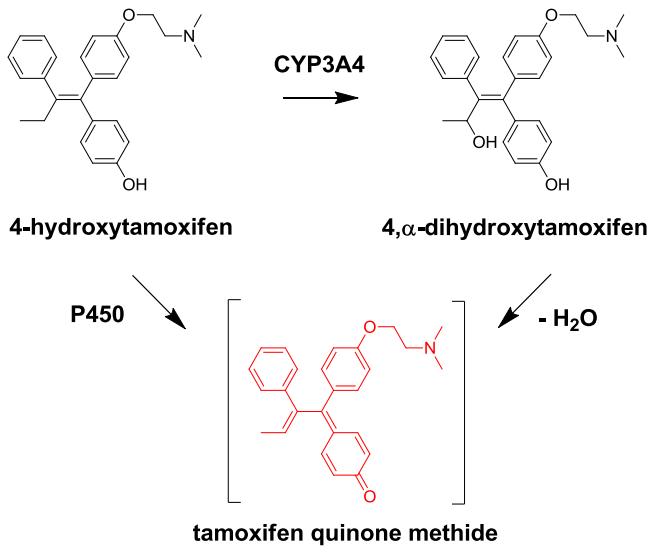

Figure 39. Bioactivation of tamoxifen to quinone methide

Metabolism of tamoxifen to α-hydroxytamoxifen is catalyzed primarily by CYP3A4 [140]. Although α-hydroxylation is a very minor metabolic pathway in humans, α-hydroxytamoxifen undergoes PAPS sulfotransferase-mediated *O*-sulfonation, and with subsequent loss of sulfate, generates a highly resonance-stabilized carbocation (Figure 40) [141]. This carbocation has been shown to generate DNA adducts through alkylation of the exocyclic amine of deoxyguanosine. Such DNA adducts have been detected in endometrial tissues of women taking tamoxifen, strongly implicating the generation of tamoxifen carbocation as a potentially carcinogenic route of metabolism [40, 41].

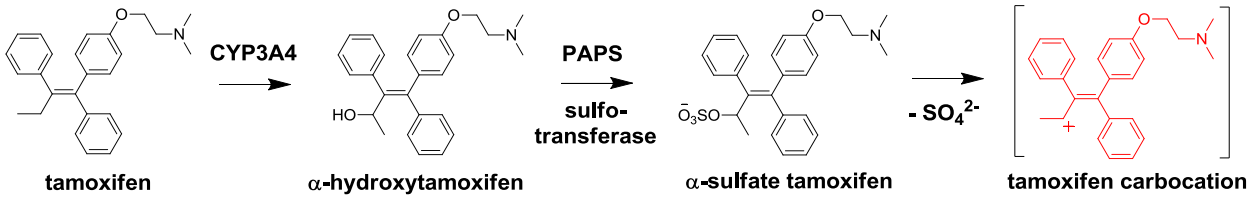

Figure 40. Bioactivation of tamoxifen to carbocation

Although structurally similar toremifene is subject to both 4- and α-hydroxylation akin to tamoxifen, formation of toremifene DNA adducts is substantially attenuated by comparison. Moreover, hepatic carcinogenicity associated with chronic high-dose tamoxifen in rats is not observed with toremifene treatment [142]. This reason for this observation is attributable to the addition of a chlorine atom at the β-position of the tamoxifen scaffold (Figure 35). A bulky, electron-withdrawing group at the β-position of toremifene not only makes this SERM a poor substrate for P450s, but also makes α-hydroxytoremifene a poor substrate for hydroxysteroid sulfotransferases. Moreover, a β-chloro substituent may act to destabilize a potential carbocation structurally similar to that formed from tamoxifen [143].

4.2.2 <u>Raloxifene, desmethylarzoxifene</u>

While raloxifene is primarily metabolized in humans through glucuronidation [58, 59], several studies have provided evidence that it may also be oxidized to both an *o*-quinone and an extended diquinone methide *in vitro* and *in vivo* (Figure 41) [54-56]. In incubations with rat or human liver microsomes, several GSH conjugates derived from each of these reactive intermediates were detected, and the corresponding *N*-acetyl

cysteine (NAC) conjugates were also detected in the urine of raloxifene-treated rats [54, 58]. The extremely short half-life ($t_{1/2}$ < 1 second) of the raloxifene diquinone methide suggests that it is likely far too reactive to alkylate DNA and cause genotoxicity, although formation of this reactive intermediate has been implicated in CYP3A4 inactivation [54, 58]. The longer-lived raloxifene 6,7-*o*-quinone ($t_{1/2}$ = 69 min) may possess a comparatively enhanced ability to selectively modify cellular nucleophiles such as DNA, although its parent catechol (7-hydroxyraloxifene) is a very minor product [54, 58], and no raloxifene-DNA adducts derived from either electrophile have been reported to date.

In vivo demethylation of arzoxifene gives desmethylarzoxifene (DMA, Figure 41) which possesses the same BTC core moiety as raloxifene. Analogously to raloxifene, DMA is extensively conjugated by Phase II enzymes (glucuronidation, sulfation), but also bioactivated to both an *o*-quinone and diquinone methide *in vitro*, characterized as their respective GSH conjugates [39, 60]. It is noteworthy that a slightly longer-lived DMA-diquinone methide ($t_{1/2}$ = 15 seconds) generated by chemical oxidation was shown to react with deoxyguanosine, albeit in amounts too low for adduct characterization [39]. Interestingly, replacement of the 4'-hydroxyl group of DMA with a fluorine atom to give the DMA analog F-DMA (refer to Section 1.3, Figure 6), was shown to prevent quinoid formation, while maintaining antiestrogenic activity comparable to that of raloxifene [39, 60, 144].

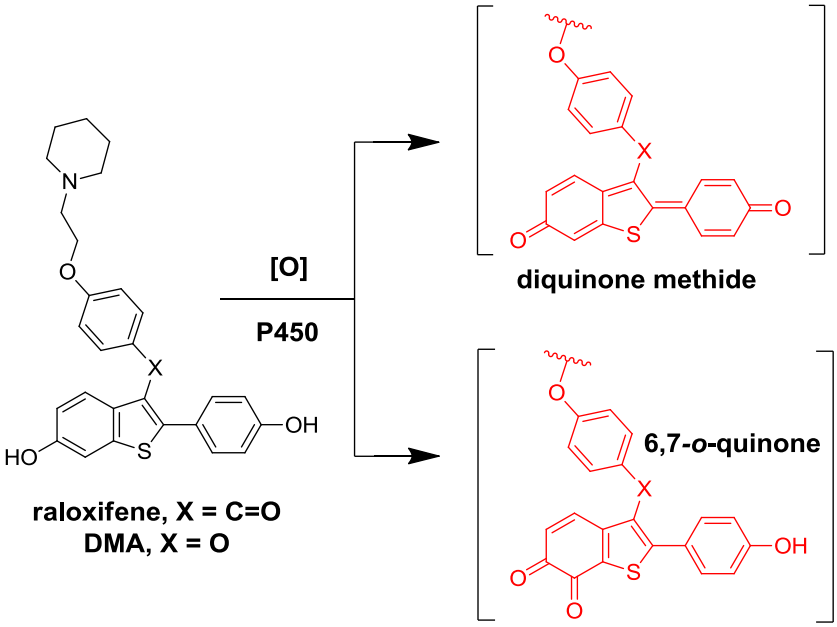

Figure 41. Bioactivation of raloxifene and DMA to quinoid metabolites

4.2.3 Acolbifene

In vitro metabolism studies have demonstrated that similar to raloxifene and DMA, acolbifene is metabolized primarily to glucuronide conjugates in human and monkey liver [145, 146]; however, *Liu, et al.* (2005) also found that acolbifene may be chemically or enzymatically oxidized to either a classical quinone methide through oxidation at the C17 methyl group, or also to an extended diquinone methide similar to raloxifene/DMA (Figure 42) [38]. In this study, each of these transient electrophilic species was found to form several conjugates with GSH or deoxynucleosides, suggesting a mechanism of potential toxicity for this SERM.

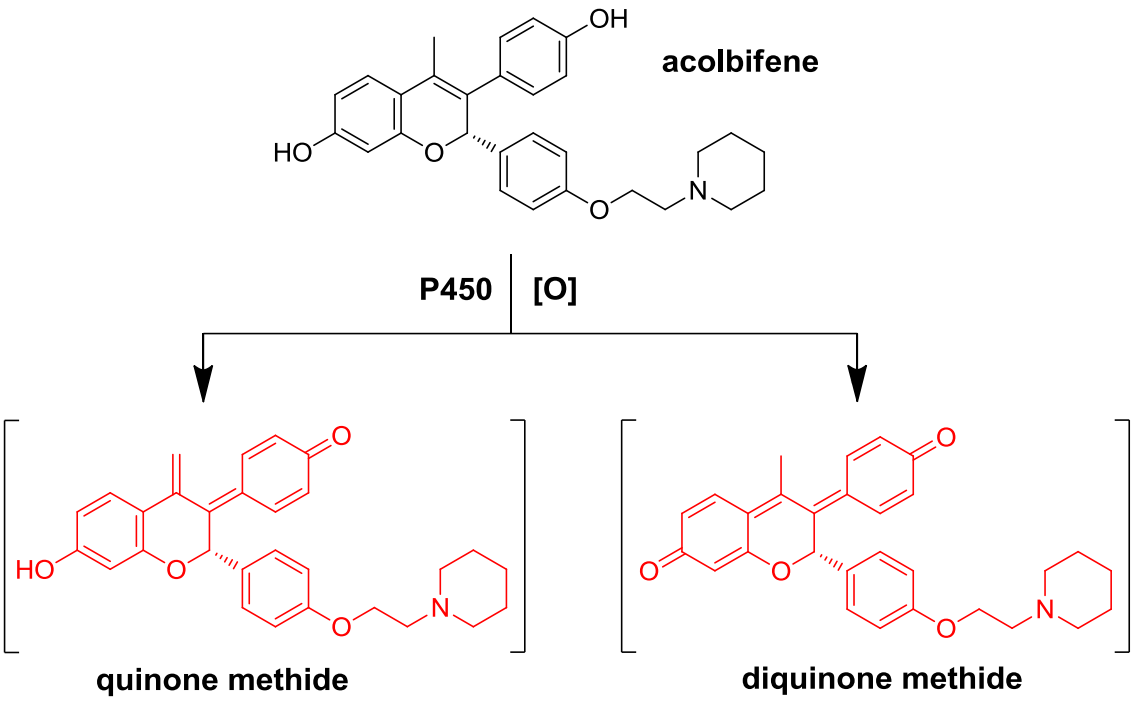

Figure 42. Bioactivation of acolbifene

4.3 Successes and limitations of SERMs in the clinic

4.3.1 Tamoxifen for treatment of ER+ breast cancer

For nearly 35 years, tamoxifen has been considered the gold standard in the treatment of hormone receptor positive breast cancer [147]. Since its introduction in the 1970's, tamoxifen has been the subject of numerous clinical trials highlighting its efficacy in breast cancer treatment and prevention. In one such study, tamoxifen was shown to increase survivorship of women with ER(+) tumors by 25% while reducing diagnosis of new tumors by 49% [90, 91]. It has been estimated that hundreds of thousands of women are alive today as a direct result of targeted long-term adjuvant tamoxifen therapy [28]. The successful secondary application of tamoxifen in the

treatment and prevention of breast cancer after its initial failure as a contraceptive represents a major milestone in women's health. Previously to its introduction, standards of care for breast cancer treatment consisted primarily of cytotoxic chemotherapy approaches, or estrogen or diethylstilbestrol treatment, all of which were associated with higher incidences of dangerous side effects [28]. Although tamoxifen would also later be demonstrated to increase incidence of endometrial cancer, its benefit to risk profile remains superior [28, 90]. Furthermore, the introduction of tamoxifen in breast cancer prevention and treatment paved the way for the use of other related antiestrogens in ER-mediated pathologies, giving rise to the development of SERMs as an important drug class [28].

4.3.2 Tamoxifen use and incidence of endometrial cancer

Although proven effective in the treatment and prevention of breast cancer, several studies conducted in the late 1980's and early 1990's began to further illuminate the increased risk of endometrial cancer associated with tamoxifen use, leading ultimately to its formal classification as a human carcinogen by the International Agency of Research on Cancer (IARC) in 1996 [24, 90, 91, 148]. In one such study of women with ER(+) tumors (n = 4914) taking tamoxifen, incidence of endometrial cancer increased 4.1-fold over the 9 year duration of the study [148]. Similarly, a separate, larger study (n = 6681) found women taking tamoxifen were at a 2.5-fold increased risk for developing endometrial cancer compared to those taking placebo [90]. Furthermore, more recent studies have observed a positive correlation between duration of tamoxifen treatment and development of higher-grade endometrial tumors, suggesting a worse

prognosis for women on long-term tamoxifen therapy [149]. While the benefits of tamoxifen for breast cancer patients certainly outweigh the associated risks, these worrisome findings warranted an in-depth investigation into the mechanisms behind tamoxifen's carcinogenic potential.

i. Proposed mechanisms of carcinogenesis

The mechanism(s) responsible for tamoxifen-induced carcinogenesis are not entirely understood; however two plausible mechanisms have been proposed. The first posits that similar to estrogens, tamoxifen acts as a mitogen in endometrial tissue. By excessively stimulating cellular proliferation in the endometrium, the risk for errors during DNA replication is increased, leading to a subsequent increase in genomic mutations and an increased chance for carcinogenic initiation/promotion [37]. The second mechanism deals with the bioactivation of tamoxifen to electrophilic or redox-active metabolites that act as chemical carcinogens. As discussed in Section 4.2.1, tamoxifen is metabolized to at least three types of reactive species, each capable of damaging DNA through adduction or oxidation [37].

In rats, tamoxifen is a potent hepatocarcinogen in both males and females [150]. The mechanism for tumor formation has been demonstrated to be directly related to P450-mediated bioactivation of the drug to reactive electrophiles which covalently modify DNA; this genotoxic mechanism is dose-dependent, but independent of ER status of the tissue [151]. While tamoxifen does not induce liver cancer in humans, there is evidence that a similar mechanism may be at least partially responsible for

carcinogenic initiation and/or promotion in the endometrium, as DNA adducts have been detected in endometrial tissues of women taking tamoxifen [40, 41].

4.3.3 Resistance to tamoxifen treatment

In addition to the increased incidence of endometrial cancer associated with tamoxifen use, drug resistance represents another major clinical obstacle. Tamoxifen therapy fails in approximately half of breast cancer patients due either to intrinsic, or acquired resistance [27, 147]. Tissue receptor status (ER; progesterone receptor, PR; Human Epidermal Growth Factor Receptor 2, Her-2) is largely predictive of whether or not a tumor will possess intrinsic resistance to tamoxifen. In general, tumors lacking expression of either ER or PR more frequently display intrinsic resistance [147, 152]. An additional mechanism for intrinsic resistance to tamoxifen involves a hindrance in metabolism of the drug to its active metabolite, endoxifen (4-hydroxy-N-desmethyltamoxifen). CYP2D6 is primarily responsible for conversion of tamoxifen to endoxifen, and it has been estimated that nearly 10% of the population express inactive variants of this isoform. Individuals lacking functional CYP2D6 are consequently less responsive to the drug [147, 152]. Finally, although the mechanisms responsible for the development of acquired resistance to tamoxifen are complex and not fully understood, it is apparent that up-regulation of other signaling pathways important for cell proliferation and survival are involved. Increased signaling through growth factor receptors such as EGFR and HER2, as well as MAPK and PI3K/Akt pathways have all been implicated in hormone resistance [152-154].

4.3.4 Raloxifene for treatment of postmenopausal osteoporosis; reduction in risk for breast cancer

Initially approved by the FDA in 1997 for the treatment and prevention of postmenopausal osteoporosis, and later in 2007 for reducing the risk for invasive breast cancer in women at high risk, raloxifene (Evista™) has been shown to significantly reduce incidence of vertebral fracture while also reducing the risk for breast cancer in several large clinical trials [29, 104-107, 155-158]. The MORE (Multiple Outcomes of Raloxifene Evaluation) trial examined the effect of raloxifene (60 mg/day or 120 mg/day) compared to placebo in 7705 postmenopausal women over a mean study duration of 40 months. Primary endpoints included incidence of vertebral and non-vertebral fracture, breast cancer, deep vein thrombosis (DVT), and pulmonary embolism [106, 107]. The CORE (Continuing Outcomes Relevant to Evista) trial enrolled 5213 (raloxifene, 60 mg/day, n = 3510; placebo, n = 1703) of the MORE trial participants who agreed to continue the study for an additional 4 years, and examined incidence of invasive breast cancer as a primary endpoint [156, 157]. Results from the MORE trial indicated that among the two treatment groups, risk for vertebral fracture was decreased 30-50%, while BMD was increased by 2% and 2.6% in the femoral neck and spine, respectively [107, 158, 159]. Results from CORE found that the incidence of invasive breast cancer was reduced by 59%. Moreover, overall reduction in breast cancer, regardless of invasiveness, was reduced by 50% [156, 157, 159]. Finally, the large (n = 19,747), multicenter STAR (Study of Tamoxifen and Raloxifene) trial demonstrated that raloxifene was as effective as tamoxifen in preventing incidence of invasive breast

cancer (incidence, 4.41 per 1,000 versus 4.30 per 1,000, respectively; RR = 1.02) [26, 29, 159].

4.3.5 Raloxifene and thrombosis; vasomotor symptoms

Unlike tamoxifen, raloxifene does not stimulate or cause cancer in endometrial tissue; however data from several clinical trials has associated raloxifene use with an increased incidence of venous thromboembolism [106, 107]. In the MORE trial, incidence of deep vein thrombosis and pulmonary embolism in raloxifene treatment groups were both increased 2.76-fold [158]. While not a life-threatening side-effect, an increased incidence of vasomotor symptoms (hot flashes) associated with raloxifene use was also observed for several sub-studies of the MORE and CORE trials (approximately 3%-6% above placebo) [106, 107, 157].

4.4 Emerging novel strategies in SERM therapies

4.4.1 Tissue selective estrogen complexes (TSECs)

While SERMs have realized clinical success in several indications such as the treatment and prevention of breast cancer and the treatment and prevention of postmenopausal osteoporosis, discovery of the conceptualized “ideal SERM” remains elusive. As previously mentioned, resistance to SERM therapies (tamoxifen, toremifene) in cancer treatment [27, 147], development of endometrial cancer (tamoxifen [18, 24]) as well as increased risk of thrombosis and exacerbation of vasomotor symptoms associated with SERM use (raloxifene [160, 161], bazedoxifene [119, 120]) are still

major hurdles in the further development of novel SERMs that would in theory exhibit desirable tissue specificity. In contrast to the idea of a singular ideal or “perfect” drug which would display an ideal blend of estrogenic/antiestrogenic activity in the desired target tissues, an alternate strategy for the treatment of postmenopausal symptoms may be employment of a Tissue Selective Estrogen Complex (TSEC) [162, 163].

TSECs, or the pairing of a SERM with conjugated estrogens (CE), have been proposed as a potentially safer alternative to combined therapies such as Prempro (CE plus medroxyprogesterone acetate, MPA) in the treatment of postmenopausal disorders such as osteoporosis, vasomotor symptoms (hot flashes), and vulvar-vaginal atrophy. [162] Progestins are added to formulations like Prempro in order to mitigate the proliferative effects of estrogens on endometrial tissue, thereby decreasing risk for endometrial cancer; however, results of the Women’s Health Initiative trial found that women taking Prempro were at a heightened risk for stroke, venous thromboembolism, and coronary heart disease [164]. Furthermore, both estrogens and progestins display proliferative activity in breast tissue, and use of these combined therapies has also been correlated to an increased risk for invasive breast cancer [6, 164]. As several SERMs (including the clinically relevant raloxifene) have been shown to behave as antiestrogens in both breast and endometrial tissues [106, 110], it is reasonable that replacement of progestin with an appropriate SERM in such a combined therapy could lead to improved treatment options for postmenopausal women. Such formulations would be expected to offer enhanced safety profiles and improved tolerability over estrogen-plus-progestin options [162].

In order to mimic the necessary criteria for an ideal SERM, the “ideal” TSEC would be composed of both CE and a SERM which would effectively antagonize the proliferative effects of CE in breast and endometrial tissue. Conversely, this SERM would minimally antagonize or have a neutral effect on the generally beneficial effects of CE on the CNS, thus preventing vasomotor symptoms [162, 165, 166]. Several studies have demonstrated the ability of various structurally diverse SERMs to significantly antagonize CE-mediated cellular proliferation in MCF-7 breast cancer cells [46, 167-169]. Importantly, gene expression profiling studies have also highlighted the ability of structurally diverse SERMs to differentially antagonize the transcription of genes induced by CE or E_2 treatment [112, 167, 169]. *Chang, et al.* (2010) for example, concluded that raloxifene, lasofoxifene, and bazedoxifene, both as singular treatments and in combination with CE as their respective TSECs, each display a unique pharmacology, and that many of the CE-transcribed genes antagonized by SERM treatments were involved in pathways such as cell cycle, growth hormone, and growth factor regulation [167]. Such observations suggest that the efficacy for a given SERM to suppress the proliferative actions of CE in target tissues is variable, and that different TSEC combinations would likely yield different clinical outcomes [167, 169, 170].

Supporting this is the preclinical observation that when compared to TSECs containing raloxifene or lasofoxifene, only bazedoxifene effectively antagonized the proliferative action of CE on uterine wet weight in ovariectomized mice [166, 171]. Similarly, human clinical trials further demonstrate that when compared to raloxifene, bazedoxifene appears to possess superior endometrial protective capabilities when concomitantly administered with estrogen. *Stovall, et al.* (2007) for example, found that

significant endometrial stimulation was observed in women transitioning from estrogen plus progestin therapy to E_2 (1 mg/day) plus raloxifene (60 mg/day) therapy over the course of a one year study [172]. Similarly, an increase in endometrial thickness was also observed over the course of a 3 month study in postmenopausal women taking raloxifene (60 mg/day) plus low-dose CE (0.312 mg/day) [173]. By contrast, large Phase III clinical trials (n = 3,397) have demonstrated that a TSEC composed of bazedoxifene (10, 20 or 40 mg) plus CE (0.45 or 0.625 mg) when administered to postmenopausal women, displayed an endometrial safety comparable to either placebo or estrogen plus progestin treatment [166, 174]. Clearly it is apparent that not all SERM + CE pairings will result in an ideal TSEC.

***i*. Bazedoxifene + conjugated estrogens (CE)**

The favorable results of several preclinical studies investigating the TSEC composed of bazedoxifene and CE [166, 171, 175] have led to extensive further trials in postmenopausal women. In one phase II clinical trial, the effects of several doses of bazedoxifene (5, 10, or 20 mg) plus CE (0.3 or 0.625 mg) on endometrial thickness, incidence of hot flashes, and incidence of amenorrhea were investigated and compared with treatments of CE alone (0.3 or 0.625 mg), CE (0.625 mg) plus MPA (2.5 mg), bazedoxifene alone (5 mg) or placebo [166, 176]. Results of this study (n = 408) indicated that BAZ plus CE treatments were associated with a significant decrease in endometrial thickness compared to unopposed CE treatments, an increased incidence of amenorrhea compared to CE plus MPA, and a decrease in incidence of hot flashes

compared to baseline [176]. Such positive results warranted further investigation in phase III trials.

The recently completed SMART (Selective estrogen Menopause And Response to Therapy) trials were composed of a series of randomized, double-blinded, Phase III clinical studies including approximately 7,500 women in total. The five separate sub studies of the SMART program each investigated the potential utility for a TSEC composed of BAZ plus CE in the treatment of various postmenopausal disorders, as compared to current standards of care [166]. SMART-1 comprised a 2 year study of postmenopausal women (n = 3397) assigned to take either BAZ (10, 20, or 40 mg) plus CE (0.45 or 0.625 mg), raloxifene (60 mg), or placebo [121, 166]. Major endpoints for SMART-1 included incidence of endometrial hyperplasia at 1 and 2 years, with secondary endpoints including effects on bone mineral density (BMD), and incidence of hot flashes, breast pain, and vaginal atrophy [121, 122, 124, 174]. The results of SMART-1 found that treatments containing BAZ (20 or 40 mg) plus CE (0.45 or 0.625 mg) correlated with a low incidence (<1%) of endometrial hyperplasia not significantly different from that of placebo groups over the 2-year duration of the study. Likewise, endometrial thickness among TSEC treatments was not statistically different from placebo [174]. BAZ plus CE treatments were also shown to significantly increase hip and lumbar spine BMD compared to raloxifene (60 mg) or placebo, and furthermore were found to have generally beneficial effects on the incidence of hot flashes, amenorrhea, breast pain, and vaginal atrophy, compared to placebo [121, 122, 124, 127, 174].

Upon establishing the lowest dose of BAZ (20 mg) necessary to effectively antagonize CE-mediated endometrial stimulation, the 12-week SMART-2 (n = 318) and SMART-3 (n = 652) trials were designed to further study the effects of two doses (20 mg BAZ plus 0.45 or 0.625 mg CE) on the primary endpoints of hot flashes and vulvar-vaginal atrophy, respectively [125, 126]. The results of SMART-2 found that incidence and severity of hot flashes in women taking either BAZ plus CE dose was decreased by 80% from baseline by week 12. Importantly, no significant difference in endometrial thickness or adverse events between treatment and placebo groups was observed [125]. Results from SMART-3 were similarly positive, finding that measures of vulvar-vaginal atrophy (measured as relative percentages of superficial cells versus parabasal cells) were significantly improved in BAZ plus CE treatment groups, as were changes in vaginal pH and sexual function, compared to placebo [126].

Lastly, SMART-4 (n = 1061) and SMART-5 (n = 1843) aimed to compare the effects of the BAZ plus CE TSEC with those of the current standard of care, CE plus MPA. Both trials utilized the dosages for BAZ plus CE (20 mg BAZ plus 0.45 or 0.625 mg CE) established in the earlier SMART trials as two treatment groups, and compared these groups to those taking CE (0.45 mg) plus MPA (1.5 mg), BAZ alone (20 mg, SMART-5 only), or placebo [123, 127, 128]. Primary endpoints for both trials were incidence of endometrial hyperplasia at 1 year, while SMART-4 also evaluated effects on BMD. Upon completion of SMART-4, no incidence of hyperplasia was observed for the BAZ, 20mg plus CE, 0.45 mg treatment group, while three cases (1.1%) were seen with the higher dose (20 mg BAZ plus 0.625 mg CE) group [128]. Hyperplasia rates in SMART-5 were similarly low (<1%) and similar among treatment groups [123].

Additionally, lumbar spine and total hip BMD were significantly increased by both BZA plus CE doses, while incidence of bleeding and breast pain were significantly lower than CE plus MPA treatment groups [123, 128].

4.4.2 Breast cancer chemoprevention: MCF-10A cells as a model system

In the development of novel ER-targeted therapies useful for cancer chemoprevention, it is important to consider not only the tissue-specific hormonal actions of a ligand, but also its effect on relative contributions to pathways of chemical carcinogenesis. The non-tumorigenic, MCF-10A human breast epithelial cell line serves a useful model for elucidation of such contributions. MCF-10A cells are formally classified as ER-negative, yet undergo transformation to a malignant phenotype upon treatment with estrogen. In the absence of ER, this observation cannot be attributed to the mitogenic action of estrogen, but is explained rather by the conversion of estrogen to its genotoxic catechol and quinoid metabolites, which in turn, induce carcinogenesis through chemical mechanisms. As such, the MCF-10A cell line serves as a useful model to study pathways of chemical carcinogenesis in the absence of confounding hormonal signaling through ER [177, 178].

Until recently, little has been known about potential chemical mechanisms which may contribute to the observed clinical efficacy of SERMs such as tamoxifen and raloxifene in the prevention of breast cancer. Data from a recent study by our lab using the MCF-10A model suggests that one important mechanism for benzothiophene (BT) SERMs like raloxifene involves a modulation in estrogen metabolism [177]. In this study, the BT SERMs raloxifene, DMA, BTC, HP-BTC, and Ac-BTC (Figure 43) were all shown

to attenuate levels of catechol estrogens detected from cultures co-treated with SERMs and E_2. It was initially suspected that this effect could be attributable to competitive inhibition of P450s responsible for metabolizing E_2 to its respective catechols, as these BT SERMs all contain the BTC core moiety capable of forming an electrophilic diquinone methide (refer to Section 4.2.2), which for the case of raloxifene, has been implicated in CYP inhibition [54, 58]. This mechanism seemed more likely with the observation that the BT SERM analogs F-DMA and HP-BTF (Figure 43), which are incapable of forming a diquinone methide, were without effect. However, concentrations of SERMs used in culture (1 uM) were below those required for effective CYP inhibition, and furthermore, expression of CYP1B1 or CYP1A1 was not effected by SERM treatment [177]. Clearly, another mechanism was at play.

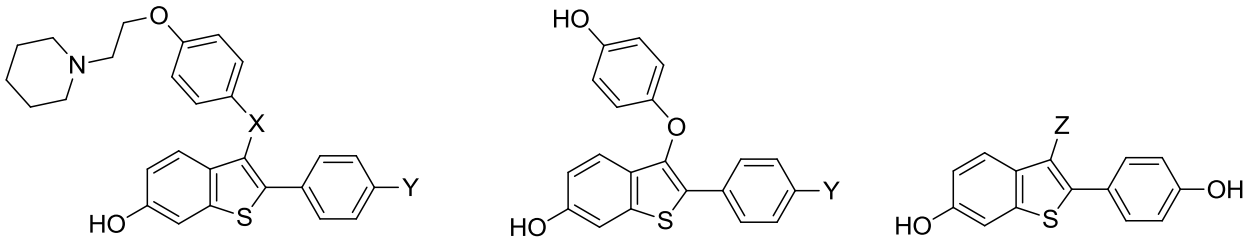

raloxifene, X = C=O; Y = OH
DMA, X = O; Y = OH
F-DMA, X = O; Y = F

HP-BTC, Y = OH
HP-BTF, Y = F

BTC, Z = H
Ac-BTC, Z = Ac

Figure 43. Structures of benzothiophene SERMs and SEMs

When modulation of Phase I metabolic pathways was disregarded as a possible explanation for the observed decrease in detection of estrogen catechols, the potential role of Phase II detoxification enzymes was investigated. Upregulation of Phase II enzymes such as glutathione-S-transferases (GSTs) have previously been implicated in

the chemopreventive effects observed for the isoflavonoid phytoestrogen, genistein, in MCF-10A cells [179]. Similarly, GSTs and other Phase II enzymes such as sulfotransferases (SULTs), UDP glucuronic acid transferases (UGTs), and catechol-*O*-methyl transferases (COMTs) have all been implicated in the detoxification of estrogen catechols. Interestingly, while expression of GST, UDP, and COMT were not perturbed by BT SERM treatments, expression of SULT1E1 was significantly enhanced, whereas analogs F-DMA and HP-BTF again had no effect. This finding suggests that BT SERMs may exert chemopreventive effects through enhanced sulfate conjugation of estrogen catechols, thereby increasing their rate of clearance, and decreasing their chance to cause genotoxicity through chemical mechanisms [177].

4.4.3 Selective estrogen mimics (SEMs)

Prior to the establishment of tamoxifen as the primary standard of care in the treatment of ER(+) breast cancer, estrogenic compounds such as E_2 or diethylstilbestrol (DES) were the preferred therapies of choice [27, 28]. While survival rates observed with E_2 or DES treatment were superior, tamoxifen use was associated with a lower incidence of serious side effects (stroke, thrombosis, uterine cancer) and was better-tolerated [27, 28, 180]. Subsequently, the clinical use of E_2 or other estrogenic compounds for the treatment of breast cancer has been largely abandoned; however, in more recent years this therapeutic strategy has reemerged as a potential option for patients with tumors displaying endocrine resistance [181-183]. Alternatively, the use of novel compounds which can selectively mimic the therapeutic action of estrogen (Selective Estrogen Mimics, SEMs) in endocrine-resistant tumors while minimizing the

known risk of cancer in other tissues associated with E_2 therapy, has been suggested as a potentially safer approach [184].

Promising data from recent *in vivo* studies performed by the Tonetti lab in ovariectomized athymic mice (Harlan-Sprague-Dawley) have demonstrated the potential utility of SEMs in the treatment of tamoxifen resistant breast cancer. Protein Kinase C alpha (PKCα) has been previously identified as a biomarker for tamoxifen resistance in breast cancer patients who may respond favorably to an "E_2-like" treatment [185-187]. Overexpression of PKCα in T47D:A18 breast cancer cells imparts a tamoxifen-resistant, hormone independent phenotype *in vitro*. T47D:A18/ PKCα tumor xenografts, interestingly, are tamoxifen-resistant and growth inhibited by E_2 *in vivo*. In xenografted animals, treatment with E_2 or raloxifene caused tumor regression; however for the case of raloxifene, tumors relapsed and continued to grow upon withdrawal of drug, whereas E_2-treated tumors continued to shrink (Figure 44). Remarkably, treatment with either of the two benzothiophene SEMs, BTC or HP-BTF (1.5 mg/day), caused tumor regression similar to the benzothiophene-based raloxifene; however, unlike raloxifene, tumors continued to shrink upon withdrawal of drug, similar to E_2 (Figure 44) [184].

BTC and HP-BTF were initially selected as they are both estrogen agonists in Ishikawa endometrial cancer cells (EC_{50} = 790 nM, 202 nM, respectively) and were each shown to inhibit T47D:A18/PKCα colony formation in 3D culture. As a novel, redox-resistant BTC analog, HP-BTF was chosen for further investigation in a second tamoxifen-resistant cell line, T47D/Tam1. T47D/Tam1 cells are derived from long-term culture of T47D cells in 4-hydroxytamoxifen, and display a phenotype similar to that of

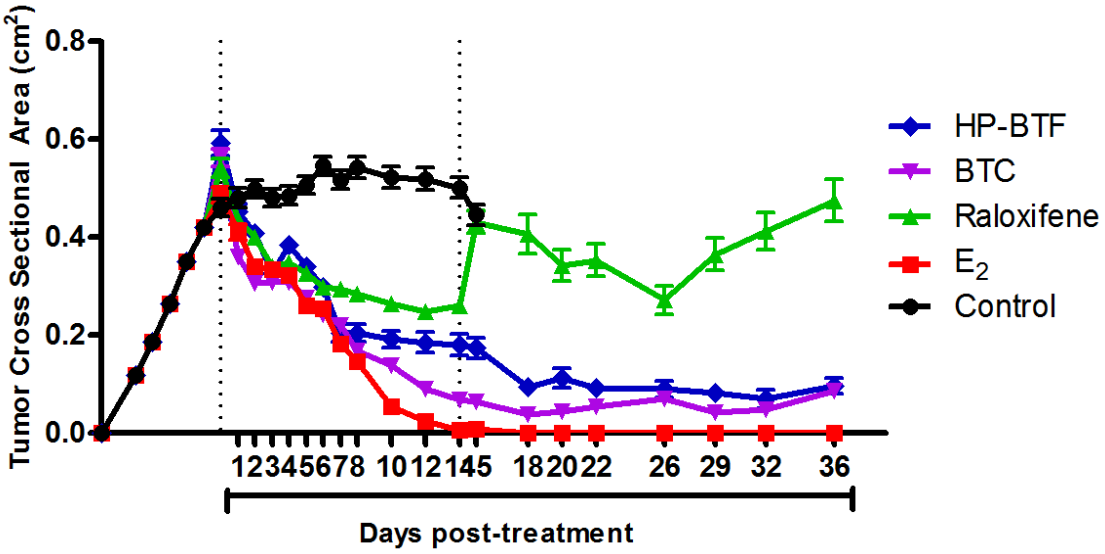

Figure 44. Effect of SEMs on T47D:A18/PKCα xenograft tumor growth

Animals with T47D:A18/PKCα xenograft tumors were treated with 1.5 mg/day HP-BTF, BTC, or raloxifene p.o. E_2 was administered by silastic capsule implantation (1 cm). Dotted lines represent initiation and termination of treatment. Data and figure were generously provided by Mary Ellen Molloy of the Tonetti lab.

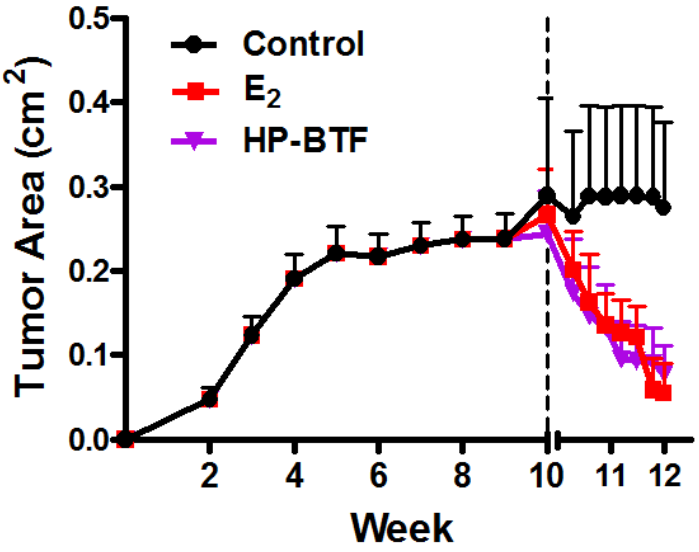

Figure 45. Effect of E_2 and HP-BTF on T47D/Tam1 tumor xenograft growth

Animals with T47D/Tam1 xenograft tumors were treated with 1.5 mg/day HP-BTF p.o. E_2 was administered by silastic capsule implantation (1 cm). Dotted line represents initiation of treatment. Data and figure were generously provided by Mary Ellen Molloy of the Tonetti lab.

T47D:A18/PKCα cells. Similar to the T47D/PKCα xenograft model, treatment with either E_2 or HP-BTF also caused regression of T47D/Tam1 tumor xenografts (Figure 45). Furthermore, while E_2 and tamoxifen expectedly caused a significant increase in the uterine weights of ovariectomized mice, neither raloxifene nor HP-BTF had a significant effect on uterine weight gain (Figure 46). These data suggest that similar to raloxifene, HP-BTF is not proliferative in endometrial tissue, and may therefore possess an improved endometrial safety profile compared to E_2 or tamoxifen. Collectively, this study suggests that HP-BTF meets the necessary criteria for an ideal SEM candidate for the potential treatment of tamoxifen-resistant breast cancer [184].

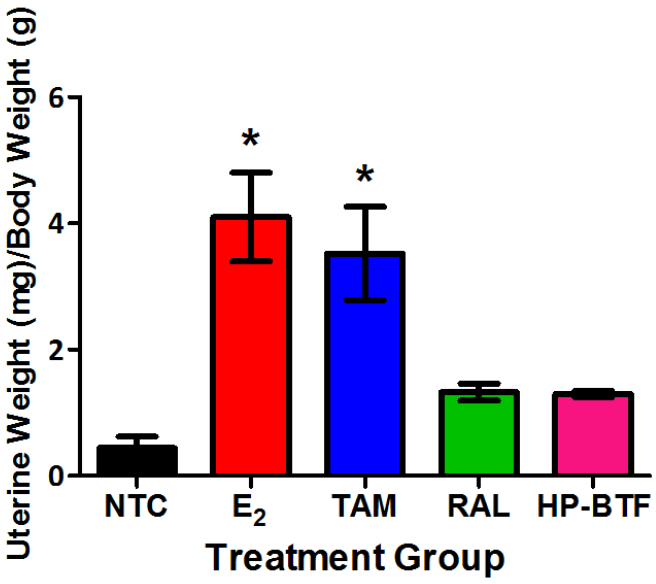

Figure 46. Effect of E_2, SERM, or SEM treatment on the uterine weight

Uterine weight of ovariectomized mice following 7 weeks of E_2/SERM/SEM treatment. Data and figure were generously provided by Mary Ellen Molloy of the Tonetti lab.

i. Neuroprotective properties of SERMs and SEMs

Evidence for the neuroprotective effects of estrogen has been documented both clinically, and in a variety of *in vitro* and *in vivo* models for brain injury [188, 189]. Initial clinical investigations reported enhanced cognition and a lower incidence of Alzheimer's Disease (AD) in postmenopausal women taking estrogen replacement therapy (ERT) [188, 189]. Initial results of the more recent Women's Health Initiative Memory Study (WHIMS) concluded just the opposite [11, 190]; however, WHIMS was terminated prior to study completion along with the several other arms of the WHI [190]. Since the advent of these contradictory findings it has become increasingly apparent that age, postmenopausal stage, as well as extent of preexisting neurodegeneration are crucial factors dictating the benefits potentially derived from beginning ERT [191, 192]. Furthermore, as increased estrogen exposure is also associated with dangerous side effects in other tissues (cancer, stroke, thrombosis) [6, 12], the therapeutic role for estrogen in the treatment of neurodegenerative disorders remains largely controversial.

Due to their tissue selective action, SERMs or SEMs which display beneficial activity in the brain but which are devoid of proliferative action in hormone-responsive tissues may represent a superior alternative for the treatment of cognitive disorders [189]. Evidence for this hypothesis has been demonstrated clinically, as raloxifene has been shown to lower the risk for cognitive impairment and enhance memory performance in both postmenopausal women and elderly men [193-196]. The mechanisms by which both estrogens and SERMs exhibit neuroprotection are complex, but have been purported to involve antioxidant effects, genomic signaling through

nuclear ERs, and most notably, non-genomic signaling through extracellular and membrane-bound ERs [189, 191, 197].

A recent study by our lab has reported the neuroprotective activity of a family of BT-SERMs and BT-SEMs (Figure 47) which elicit neuroprotection against oxygen-glucose deprivation (OGD) through activation of the membrane-bound ER, G-protein-coupled receptor 30 (GPR30) [189]. Both raloxifene and DMA were found to be neuroprotective while analogs lacking a 4'-hydroxyl group (F-DMA, Br-DMA, H-DMA, Ms-DMA, arzoxifene) were not. Similarly, BT-SEMs containing the BTC (6-hydroxy-2-(4-hydroxyphenyl)benzo[*b*]thiophene) core of raloxifene/DMA (BTC, Ac-BTC, *i*Pr-BTC, Tol-BTC, bisBTChd) all displayed neuroprotective activity unless bulky electron-withdrawing groups were present at the 7- and 3'-positions (Br_2-BTC, DNBr-BTC).

As all analogs containing the BTC core are also subject to oxidative bioactivation to an electrophilic diquinone methide while those with 4'-substitutions are not (refer to Section 4.2.2), it was of interest to elucidate whether neuroprotection resulted from the presence of a diphenolic pharmacophore, or from the potential induction of the antioxidant response element (ARE) by diquinone methide. The observation that 3,3-TDP **(44)** and HP-BTF were both neuroprotective supports the former hypothesis, as neither are capable of forming a diquinone methide, yet both may adapt conformations which separate their respective hydroxyl groups by a distance 11.8 Å, as with BTC (Figure 48). Importantly, no correlation between classical ER binding and neuroprotection was observed for this study. While raloxifene and DMA were potent antagonists in Ishikawa cells, BT-SEMs that were neuroprotective were potent agonists

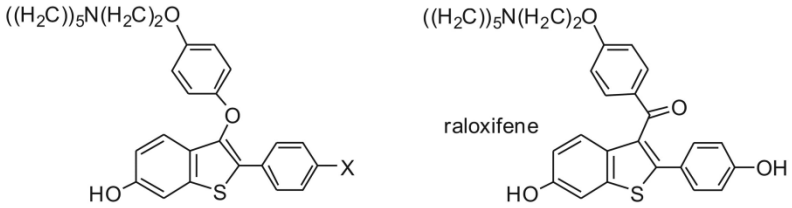

	X	ERβ, nM[a]	IC_{50} (Ishikawa), nM[b]
DMA	OH	9.6 ± 1.9	0.1 ± 0.1
F-DMA	F	28 ± 11	1.4 ± 0.4
Br-DMA	Br	67 ± 8.5	5.4 ± 1.4
H-DMA	H	16 ± 0.8	3.0 ± 0.7
Ms-DMA	$OS(O)_2\ CH_3$	1800 ± 100	4.6 ± 0.8
raloxifene	-	560 ± 150	2.9 ± 1.6
arzoxifene	OCH_3	66 ± 3.1	1.3 ± 0.3

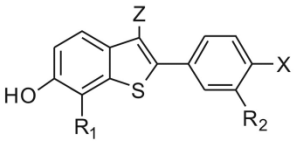

	Z	X	R_1	R_2	EC_{50} or IC_{50}, nM[b]	ERβ, nM[a]	ERβ/α[c]
BTC	H	OH	H	H	790 ± 170	14.1 ± 0.6	4.2
Ac-BTC	$C(O)CH_3$	OH	H	H	74 ± 25	27.3 ± 4.9	2.2
Br_2-BTC	Br	OH	Br	H	39 ± 5	-	-
DNBr-BTC	Br	OH	NO_2	NO_2	n.a.	-	-
iPr-BTC	$CH(CH_3)_2$	OH	H	H	3.9 ± 0.7	-	-
Tol-BTC	$C(O)C_6H_4CH_3$	OH	H	H	470 ± 142 IC_{50} = 410 ± 110	-	-
HP-BTF	OC_6H_4OH	F	H	H	202 ± 68	-	-
bisBTChd	$C(O)(CH_2)_{10}C(O)$-3-BTC	OH	H	H	IC_{50} = 486 ± 77	-	-

Figure 47. Structures and estrogenic assay of BT-SERMs/SEMs investigated for neuroprotection

[a] From radioligand binding assay using full-length ER. [b] From alkaline phosphatase reporter assays in Ishikawa cells; n.a. = not active. [c] Selectivity for ER-beta over ER-alpha from radioligand binding assay. DMA analogs were synthesized by Dr. Zhihui Qin. Br_2-BTC and DNBr-BTC were synthesized by Dr. Vladislav Litosh. SERMs and SEMs were assayed for neuroprotection by Dr. Ramy Abdelhamid and Dr. Lawren Vandevrede. Ishikawa and ER binding data were provided by Ping Yao and Huali Dong.

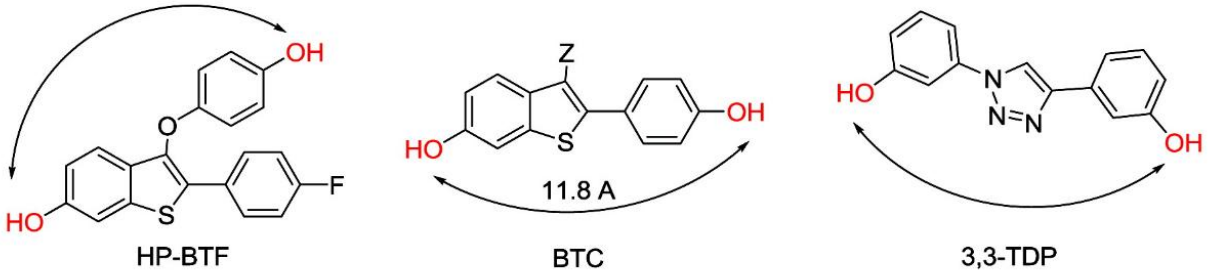

Figure 48. Proposed diphenolic pharmacophore for neuroprotection

(Ac-BTC, *i*Pr-BTC), weak agonists (BTC, HP-BTF), partial agonists (Tol-BTC), or weak antagonists (bisBTChd). Furthermore, the selective GPR30 antagonist, G15 **(45)**, abrogated neuroprotection by SERMs and SEMs while the pure antiestrogen ICI 182,780 did not, indicating neuroprotection was GPR30-coupled, but ER-independent [189]. These results suggest that BT-SERMs and BT-SEMs may confer the added benefit of neuroprotection in disease states where antiestrogenic compounds are desirable (breast cancer, osteoporosis), and also those in which estrogenic activity may be desirable (endocrine-resistant breast cancer).

***ii*. POSEMs (Prodrugs of selective estrogen mimics)**

The consideration of prodrug strategies in the development of SEMs to generate novel benzothiophene POSEMs (Prodrugs of selective estrogen mimics) has the potential to offer several benefits over simple compositions containing only the active drug moiety. The benzothiophene SERM raloxifene, for example, suffers from poor oral bioavailability due to extensive intestinal glucuronidation [59]. The raloxifene analog, arzoxifene, was designed as a mono-methoxy ether prodrug which is metabolized in vivo to its active metabolite DMA, which limits first-pass glucuronidation and increases

oral bioavailability [68, 108]. Also, a common structural distinction between SEMs and SERMs is the presence of a basic tertiary nitrogen atom on the side chain of the latter. As most clinical or preclinical SERMs are formulated as their respective amine-hydrochloride, -citrate, or -acetate salts, water solubility and absorption are not significant issues. The lack of a basic nitrogen on a prototypical SEM such as HP-BTF however, points to a potential need to introduce polar substituents at one or both free phenol groups in order to increase water solubility and oral bioavailability, as HP-BTF is rather lipophilic (CLogP = 5.78). Furthermore, although perhaps less important in breast cancer therapy, the enhanced metabolic stability prodrugs frequently display over their active metabolites often acts to improve a compound's safety profile, which would be necessary for extended SEM treatment durations in other potential indications such as neurodegenerative disorders.

Additionally, the most serious side effect still associated with use of clinical SERMs, including raloxifene, is the increased risk for thrombosis [106, 107]. A recent study by our lab has highlighted a nitric oxide (NO) -donating prodrug strategy of potential use not only in counteracting the prothrombotic side effects associated with SERMs, but also potentiating their procognitive activity [198]. NO is an important signaling molecule known to inhibit thrombosis through inhibition of platelet recruitment, adhesion and aggregation [199]. Although raloxifene has been shown to increase NO signaling through activation of endothelial nitric oxide synthase (eNOS), postmenopausal women often express eNOS at lower levels which contributes to increased thromboembolisms [200, 201]. This observation suggests that activation of eNOS accompanied by delivery of an exogenous source of NO may act to attenuate or

reverse thromboembolic side effects. In accord with this hypothesis, a novel NO-donating DMA analog (NO-DMA, Figure 49) was compared to DMA in several *in vitro* and *in vivo* models for thrombosis and cognition. Compared to parent DMA, NO-DMA

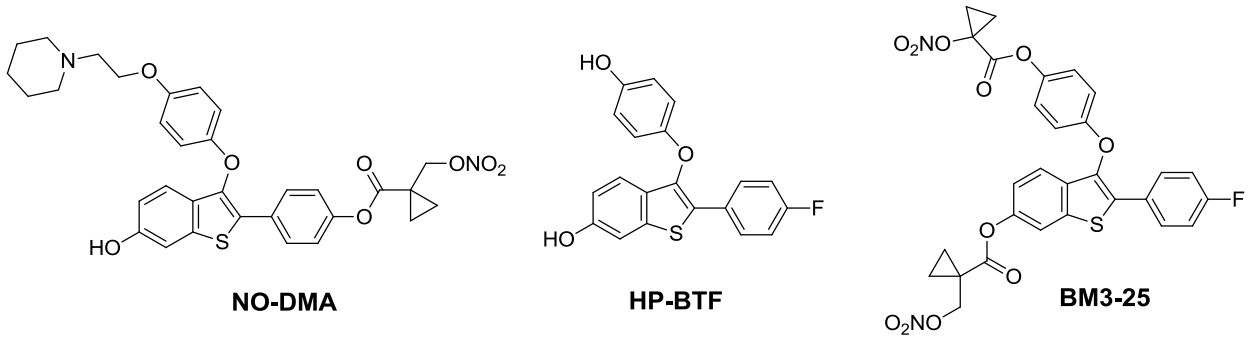

Figure 49. Structures of NO-DMA, HP-BTF, and BM3-25

showed increased antithrombotic potency when eNOS activity was inhibited pharmacologically or abrogated completely. Moreover, NO-DMA but not DMA, was shown to reverse scopolamine-induced cognitive deficits in behavioral studies with eNOS knockout mice [198]. Collectively, these data suggest a potential utility for both NO-SERMs and NO-SEMs for the treatment of cognitive disorders in individuals with attenuated eNOS activity such as postmenopausal women.

Finally, the synthesis of POSEMs designed to modulate the physiochemical properties of parent SEMs has been initiated by the preparation of simple carboxylate diesters of HP-BTF (refer to Sections 2.5.6). Three of the synthesized POSEMs were converted to active HP-BTF in microsomal incubations (refer to Section 3.5), one of which (BM3-25, Figure 49) is designed to release NO akin to NO-DMA. In addition, the synthesis of phosphate, sulfate, and mono-carboxylate esters is currently underway and the *in vivo* effects of these and related POSEMs will be a subject of further studies.

4.5 Conclusion and future directions

Whether endogenous or exogenous, the bioactivation of organic compounds to reactive metabolites is well-recognized as a mechanism for potential toxicity. For the case of estrogens and SERMs, bioactivation to reactive metabolites has been associated with mechanisms of carcinogenesis. In the present study, the oxidative metabolism of the SERMs LY2066948 (LY), lasofoxifene (LAS), and bazedoxifene (BAZ) was investigated *in vitro* under various conditions in order to determine potential routes for bioactivation.

In the presence of tyrosinase, all three SERMs were oxidized to *o*-quinone metabolites which were trapped as their corresponding GSH conjugates. For LY, P450-mediated bioactivation to *o*-quinones was detected, but *N*-dealkylation was the primary route of metabolism. For BAZ, P450-mediated bioactivation to *o*-quinones was not observed. While *N*-dealkylation of BAZ was seen in rat liver microsomal incubations, this SERM was remarkably stable in corresponding incubations with human liver microsomes, in accordance with studies performed by other groups. For the case of LAS, bioactivation to *o*-quinones was the primary route of P450-mediated metabolism. *o*-Quinone formation was catalyzed by P450s 3A4, 2D6, and to a lesser extent, 1B1. Furthermore, catechol LAS was shown to oxidize to *o*-quinones even in the presence of Phase II detoxification enzymes. Perhaps most importantly, synthesized 7-OHLAS was also shown to form depurinating adducts with DNA, suggesting a potential mechanism of carcinogenesis for LAS very similar to that of E_2.

The second major aim for this study was to develop novel SERMs and SEMs based on the BTC core of raloxifene, as bioactivation of this moiety has not been

clinically associated with toxicity. One initial strategy to generate novel antiestrogen BT-SERMs using 1,3-dipolar cycloaddition “click” chemistry was modeled after the synthesis of the click estrogen, 3,3-TDP; however the model click antiestrogen, PTP-BTF, showed only modest activity (IC_{50} ~ 6 µM) in Ishikawa cells and this synthetic strategy was not further pursued. Structural elaboration of the 3- and 4’-positions on the BTC scaffold yielded BT derivatives ranging from potent estrogen agonists to potent antagonists in Ishikawa endometrial cancer cells. Along with raloxifene and DMA, BTC (weak estrogen), Ac-BTC (potent estrogen), and HP-BTC (potent antiestrogen, IC_{50} = 18 ± 3 nM) were all shown to inhibit estrogen metabolism in MCF-10A cells. Interestingly, a similar non-dependence on classical ER binding was observed for neuroprotection elicited by *i*Pr-BTC, HP-BTF, Tol-BTC, and bisBTChd. Excitingly, the efficacy of the SEM, HP-BTF, in the regression of tamoxifen-resistant tumors *in vivo* coupled with a lack of uterine stimulation, represents an extremely promising milestone in the development of SEMs for the treatment of endocrine-resistant cancer. The synthesis of POSEMs designed to liberate HP-BTF or other candidate SEMs is expected to further increase drug efficacy.

As related to the bioactivation of SERMs to reactive metabolites, future studies should investigate the oxidative metabolism of the triphenylethylene SERM, ospemifene, as well as the LAS metabolite, 5-hydroxylasofoxifene (5-OHLAS). Ospemifene is a structural analog of tamoxifen and toremifene (Figure 50) which has recently received FDA-approval (February, 2013) for the treatment of vulvar-vaginal atrophy [16, 97, 202]. Both tamoxifen and toremifene have been shown to be metabolized to reactive quinoids, but similar studies for ospemifene have not been

done. Moreover, 4-hydroxyospemifene has been identified as a major metabolite of this SERM [16, 203]. This may suggest that metabolism to a 3,4-ospemifene catechol and respective *o*-quinone is highly probable, similar to what is observed for tamoxifen and toremifene. Lastly, the second catechol regioisomer, 5-OHLAS (refer to Section 3.3), should be synthesized and assayed for its ability to form thiol and DNA adducts similar to those formed from 7-hydroxylasofoxifene.

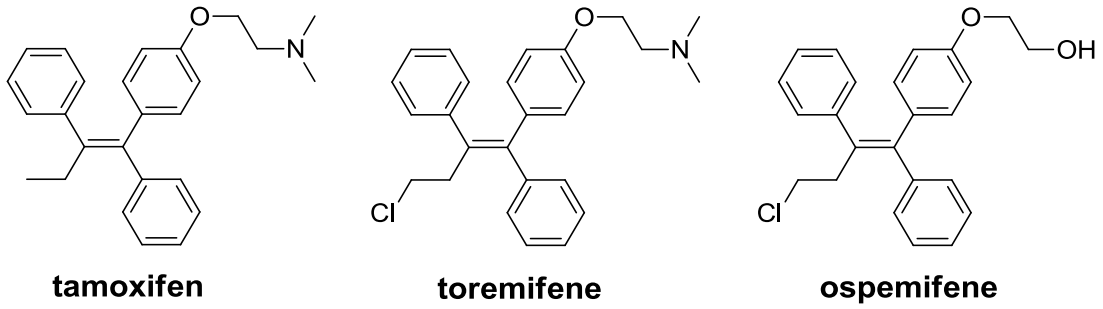

Figure 50. Structures of tamoxifen, toremifene, and ospemifene

Pertaining to SEMs and POSEMs, future studies should focus on establishing pharmacokinetic parameters for HP-BTF, including measurement of drug bioavailability in plasma. Additionally, although synthetically facile, the masking of both phenolic hydroxyl groups of HP-BTF to generate diesters may represent a potential limitation in terms of aqueous drug solubility and overall absorption. As such, further efforts should focus upon the development of HP-BTF monocarboxylate, monosulfate, and monophosphate esters, as well as monoethers. Such prodrugs would be predicted to benefit from enhanced aqueous solubility, potentially improved physiochemical properties, and for the case of monocarboxylate esters, a likely enhanced rate of HP-

BTF formation when compared to structurally similar diesters. Preliminary data also indicate that the SEM, BM2-125 (3-keto analog of HP-BTF, refer to Section 2.5.5) is an extremely potent estrogen in Ishikawa cells (EC_{50} = 409 ± 157 pM). Moreover, similar to E_2, BTC, and HP-BTF, BM2-125 was also observed to stimulate the growth of T47D/neo cells (data not shown). As E_2, BTC and HP-BTF also stimulate T47/neo cell growth, and as each also inhibit the growth of T47D/PKCα and T47D/Tam1 tumors in both 3D culture and xenograft models, future studies should similarly examine the effect of BM2-125 on growth inhibition in these systems. Finally, as the results of the current study have found the 2-(4-hydroxyphenyl)-3-methyl-1H-indol-5-ol core of bazedoxifene to be largely inert towards P450-mediated bioactivation, development of novel SEMs and POSEMs which elaborate upon this scaffold should be investigated.

Cited Literature

1. Cosman, F. and Lindsay, R. (1999) Selective estrogen receptor modulators: clinical spectrum. *Endocrine Reviews 20*, 418-434.

2. Mitlak, B.H. and Cohen, F.J. (1997) In search of optimal long-term female hormone replacement: the potential of selective estrogen receptor modulators. *Hormone Research 48*, 155-163.

3. Hersh, A.L., Stefanick, M.L., and Stafford, R.S. (2004) National Use of Postmenopausal Hormone Therapy; Annual Trends and Response to Recent Evidence. *Journal of the American Medical Association 291*, 47-53.

4. Hays, J., Ockene, J.K., Brunner, R.L., Kotchen, J.M., Manson, J.E., Patterson, R.E., Aragaki, A.K., Shumaker, S.A., Brzyski, R.G., LaCroix, A.Z., Granek, I.A., and Valanis, B.G. (2003) Effects of Estrogen plus Progestin on Health-Related Quality of Life. *New England Journal of Medicine 348*, 1839-1854.

5. Rossouw, J., Anderson, G., Prentice, R., LaCroix, A., Kooperberg, C., Stefanick, M., Jackson, R., Beresford, S., Howard, B., Johnson, K., Kotchen, J., and Ockene, J. (2002) Risks and benefits of estrogen plus progestin in healthy postmenopausal women: principal results From the Women's Health Initiative randomized controlled trial. *Journal of the American Medical Association 288*, 321-333.

6. Bolton, J.L. and Thatcher, G.R. (2008) Potential mechanisms of estrogen quinone carcinogenesis. *Chem. Res. Toxicol. 21*, 93-101.

7. Service, R.F. (1998) New role for estrogen in cancer? *Science 279*, 1631-1633.

8. Zumoff, B. (1998) Does postmenopausal estrogen administration increase the risk of breast cancer? Contributions of animal, biochemical, and clinical investigative studies to a resolution of the controversy. *Proc. Soc. Exp. Biol. Med. 217*, 30-37.

9. Levin, E.R. (2005) Integration of the extranuclear and nuclear actions of estrogen. *Molecular Endocrinology 19*, 1951-1959.

10. Madak-Erdogan, Z., Kieser, K.J., Kim, S.H., Komm, B., Katzenellenbogen, J.A., and Katzenellenbogen, B.S. (2008) Nuclear and extranuclear pathway inputs in the regulation of global gene expression by estrogen receptors. *Molecular Endocrinology 22*, 2116-2127.

11. Shumaker, S.A., Legault, C., Rapp, S.R., Thal, L., Wallace, R.B., Ockene, J.K., Hendrix, S.L., Jones, B.N., Assaf, A.R., Jackson, R.D., Kotchen, J.M., Wassertheil-Smoller, S., and Wactawski-Wende, J. (2003) Estrogen plus progestin and the incidence of dementia and mild cognitive impairment in postmenopausal women. The Women's Health Initiative Memory Study: A randomized controlled trial. *Journal of the American Medical Association 289*, 2651-2662.

12. Brass, L.M. (2004) Hormone replacement therapy and stroke: Clinical trials review. *Stroke 35*, 2644-2647.

13. Ravdin, P.M., Cronin, K.A., Howlader, N., Berg, C.D., Chlebowski, R.T., Feuer, E.J., Edwards, B.K., and Berry, D.A. (2007) The decrease in breast-cancer incidence in 2003 in the United States. *New England Journal of Medicine 356*, 1670-1674.

14. Pickar, J.H., MacNeil, T., and Ohleth, K. (2010) SERMs: progress and future perspectives. *Maturitas 67*, 129-138.

15. Shelly, W., Draper, M.W., Krishnan, V., Wong, M., and Jaffe, R.B. (2008) Selective estrogen receptor modulators: an update on recent clinical findings. *Obstet. Gynecol. Surv. 63*, 163-181.

16. Elkinson, S. and Yang, L.P.H. (2013) Ospemifene: First Global Approval. *Drugs 73*, 605-612.

17. Shang, Y. (2006) Molecular mechanisms of oestrogen and SERMs in endometrial carcinogenesis. *Nat. Rev. Cancer 6*, 360-368.

18. Jordan, V. (2003) Tamoxifen: a most unlikely pioneering medicine. *Nature Reviews Drug Discovery 2*, 205-213.

19. McKenna, N.J., Lanz, R.B., and O'Malley, B.W. (1999) Nuclear receptor coregulators: cellular and molecular biology. *Endocrine Reviews 20*, 321-344.

20. Brzozowski, A.M., Pike, A.C.W., Dauter, Z., Hubbard, R.E., Bonn, T., Engstrom, O., Ohman, L., Greene, G.L., Gustafsson, J.-A., and Carlquist, M. (1997) Molecular basis of agonism and antagonism in the oestrogen receptor. *Nature 389*, 753-758.

21. Shiau, A.K., Barstad, D., Loria, P.M., Cheng, L., Kushner, P.J., Agard, D.A., and Greene, G.L. (1998) The Structural Basis of Estrogen Receptor/Coactivator Recognition and the Antagonism of This Interaction by Tamoxifen. *Cell 95*, 927-937.

22. Kato, S., Endoh, H., Masuhiro, Y., Kitamoto, T., Uchiyama, S., Sasaki, H., Masushige, S., Gotoh, Y., Nishida, E., Kawashima, H., Metzger, D., and Chambon, P. (1995) Activation of the estrogen receptor through phosphorylation by mitogen-activated protein kinase. *Science 270*, 1491-1494.

23. Smith, C.L. and O'Malley, B.W. (2004) Coregulator Function: A Key to Understanding Tissue Specificity of Selective Receptor Modulators. *Endocrine Reviews 25*, 45-71.

24. Fisher, B., Costantino, J., Redmond, C., Fisher, E., Wickerham, D., and Cronin, W. (1994) Endometrial cancer in tamoxifen-treated breast cancer patients: findings from the National Surgical Adjuvant Breast and Bowel Project. *Journal of the National Cancer Institute 86*, 527-537.

25. Delozier, T., Spielmann, M., Macé-Lesec'h, J., Janvier, M., Hill, C., Asselain, B., Julien, J., Weber, B., Mauriac, L., Petit, J., Kerbrat, P., Malhaire, J., Vennin, P., Leduc, B., and Namer, M. (2000) Tamoxifen Adjuvant Treatment Duration in Early Breast Cancer: Initial Results of a Randomized Study Comparing Short-Term Treatment With Long-Term Treatment. *Journal of Clinical Oncology 18*, 3507-3512.

26. Vogel, V., Costantino, J., Wickerham, D., Cronin, W., Cecchini, R., Atkins, J., Bevers, T., Fehrenbacher, L., Pajon, E.J., Wade, J.r., Robidoux, A., Margolese, R., Lippman, J.J., Runowicz, C., Ganz, P., Reis, S., McCaskill-Stevens, W., Ford, L., Jordan, V., and Wolmark, N. (2006) Effects of tamoxifen vs raloxifene on the risk of developing invasive breast cancer and other disease outcomes: the NSABP Study of Tamoxifen and Raloxifene (STAR) P-2 trial. *Journal of the American Medical Association 295*, 2727-2741.

27. Jordan, V.C., Obiorah, I., Fan, P., Kim, H.R., Ariazi, E., Cunliffe, H., and Brauchd, H. (2011) The St. Gallen Prize Lecture 2011: Evolution of long-term adjuvant anti-hormone therapy: consequences and opportunities. *The Breast 20*, S1-S11.

28. Jordan, V.C. (2008) Tamoxifen: catalyst for the change to targeted therapy. *Eur J Cancer 44*, 30-38.

29. Waters, E.A., McNeel, T.S., Stevens, W.M., and Freedman, A.N. (2012) Use of tamoxifen and raloxifene for breast cancer chemoprevention in 2010. *Breast Cancer Res Treat 134*, 875-880.

30. Johnston, S. (1997) Acquired tamoxifen resistance in human breast cancer--potential mechanisms and clinical implications. *Anticancer Drugs 8*, 911-930.

31. Pyrrhonen, S., Valavaara, R., Vuorinen, J., and Hajba, A. (1994) High dose toremifene in advanced breast cancer resistant to or relapsed during tamoxifen treatment. *Breast Cancer Res Treat 29*, 223-228.

32. Vogel, C., Shemano, I., Schoenfelder, J., Gams, R., and Green, M. (1993) Multicenter phsase II efficacy trial of toremifene in tamoxifen refractory patients with advanced breast cancer. *Journal of Clinical Oncology 11*, 345-350.

33. Barret-Connor, E., Mosca, L., Collins, P., Geiger, M., Grady, G., Kornitzer, M., McNabb, M., and Wenger, N. (2006) Effects of raloxifene on cardiovascular events and breast cancer in postmenopausal women. *New England Journal of Medicine 355*, 125-237.

34. Anthony, M., Williams, J., and Dunn, B. (2001) What would be the properties of an ideal SERM? *Annals New York Academy of Sciences 949*, 261-278.

35. Love, R.R., Cameron, L., Connell, B.L., and Leventhal, H. (1991) Symptoms associated with tamoxifen treatment in postmenopausal women. *Arch Intern Med 151*, 1842-1847.

36. Davies, G., Huster, W., Lu, Y., Plouffe, L., and Lakshmanan, M. (1999) Adverse events reported by postmenopausal women in controlled trials with raloxifene. *Obstet Gynecol 93*, 558-565.

37. Dowers, T.S., Qin, Z.-H., Thatcher, G.R.J., and Bolton, J.L. (2006) Bioactivation of Selective Estrogen Receptor Modulators (SERMs). *Chem. Res. Toxicol. 19*, 1125-1137.

38. Liu, J., Liu, H., van Breemen, R.B., Thatcher, G.R., and Bolton, J.L. (2005) Bioactivation of the selective estrogen receptor modulator acolbifene to quinone methides. *Chemical Research in Toxicology 18*, 174-182.

39. Liu, H., Liu, J., van Breemen, R.B., Thatcher, G.R., and Bolton, J.L. (2005) Bioactivation of the selective estrogen receptor modulator desmethylated arzoxifene to quinoids: 4'-fluoro substitution prevents quinoid formation. *Chem. Res. Toxicol. 18*, 162-173.

40. Shibutani, S., Ravindernath, A., Suzuki, N., Terashima, I., Sugarman, S.M., Grollman, A.P., and Pearl, M.L. (2000) Identification of tamoxifen-DNA adducts in the endometrium of women treated with tamoxifen. *Carcinogenesis 21*, 1461-1467.

41. Shibutani, S., Suzuki, N., Terashima, I., Sugarman, S., Grollman, A., and Pearl, M. (1999) Tamoxifen-DNA adducts detected in the endometrium of women treated with tamoxifen. *Chem. Res. Toxicol. 12*, 646-653.

42. Hummel, C.W., Geiser, A.G., Bryant, H.U., Cohen, I.R., Dally, R.D., Fong, K.C., Frank, S.A., Hinklin, R., Jones, S.A., Lewis, G., McCann, D.J., Rudmann, D.G., Shepherd, T.A., Tian, H., Wallace, O.B., Wang, M., Wang, Y., and Dodge, J.A. (2005) A selective estrogen receptor modulator designed for the treatment of uterine leiomyoma with unique tissue specificity for uterus and ovaries in rats. *J. Med. Chem. 48*, 6772-5.

43. Geiser, A., Hummel, C., Draper, M., Henck, J., Cohen, I., Rudmann, D., Donnelly, K., Adrian, M., Shepherd, T., Wallace, O., McCann, D., Oldham, S., Bryant, H., Sato, M., and Dodge, J. (2005) A new selective estrogen receptor modulator with potent uterine antagonist activity, agonist activity in bone, and minimal ovarian stimulation. *Endocrinology 146*, 4524-4535.

44. Gennari, L., Merlotti, D., De Paola, V., and Nuti, R. (2010) Lasofoxifene: Evidence of its therapeutic value in osteoporosis. *Core Evid 4*, 113-129.

45. Prakash, C., Johnson, K.A., and Gardner, M.J. (2008) Disposition of lasofoxifene, a next-generation selective estrogen receptor modulator, in healthy male subjects. *Drug Metab. Dispos. 36*, 1218-1226.

46. Komm, B.S., Kharode, Y., and Bodine, P.V.N. (2005) Bazedoxifene acetate: a selective estrogen receptor modulator with improved selectivity. *Endocrinology 146*, 3999-4008.

47. Taylor, H.S. (2010) Approaching the ideal selective estrogen receptor modulator for prevention and treatment of postmenopausal osteoporosis. *Formulary 45*, 52-61.

48. Lévesque, J.-F., Day, S.H., Chauret, N., Seto, C., Trimble, L., Bateman, K.P., Silva, J.M., Berthelette, C., Lachance, N., Boyd, M., Li, L., Sturino, C.F., Wang, Z., Zamboni, R., Young, R.N., and Nicoll-Griffith, D.A. (2007) Metabolic activation of indole-containing prostaglandin D2 receptor 1 antagonists: Impacts of glutathione trapping and glucuronide conjugation on covalent binding. *Bioorganic & Medicinal Chemistry Letters 17*, 3038-3043.

49. Kassahun, K., Skordos, K., McIntosh, I., Slaughter, D., Doss, G.A., Baillie, T.A., and Yost, G.S. (2005) Zafirlukast Metabolism by Cytochrome P450 3A4 Produces an Electrophilic alpha, beta-Unsaturated Iminium Species That Results in the Selective Mechanism-Based Inactivation of the Enzyme. *Chem. Res. Toxicol. 18*, 1427-1437.

50. Ju, C. and Uetrecht, J.P. (1998) Oxidation of a metabolite of indomethacin (Desmethyldeschlorobenzoylindomethacin) to reactive intermediates by activated neutrophils, hypochlorous acid, and the myeloperoxidase system. *Drug Metab Dispos 7*, 676-680.

51. Regal, K.A., Laws, G.M., Yuan, C., Yost, G.S., and Skiles, G.L. (2001) Detection and Characterization of DNA Adducts of 3-Methylindole. *Chem. Res. Toxicol. 14*, 1014-1024.

52. Formosa, P.J., Bray, T.M., and Kubow, S. (1988) Metabolism of 3-methylindole by prostaglandin H synthase in ram seminal vesicles. *Canadian Journal of Physiology and Pharmacology 66*, 1524-1530.

53. Yan, Z., Easterwood, L.M., Maher, N., Torres, R., Huebert, N., and Yost, G.S. (2007) Metabolism and Bioactivation of 3-Methylindole by Human Liver Microsomes. *Chem. Res. Toxicol. 20*, 140-148.

54. Chen, Q., Ngui, J.S., Doss, G.A., Wang, R.W., Cai, X., DiNinno, F.P., Blizzard, T.A., Hammond, M.L., Stearns, R.A., Evans, D.C., Baillie, T.A., and Tang, W.

(2002) Cytochrome P450 3A4-Mediated Bioactivation of Raloxifene: Irreversible Enzyme Inhibition and Thiol Adduct Formation. *Chem. Res. Toxicol. 15*, 907-914.

55. Liu, H., QIn, Z., Thatcher, G.R., and Bolton, J.L. (2007) Uterine peroxidase-catalyzed formation of diquinone methides from the selective estrogen receptor modulators raloxifene and desmethylated arzoxifene. *Chem. Res. Toxicol. 20*, 1676-1684.

56. VandenBrink, B.M., Davis, J.A., Pearson, J.T., Foti, R.S., Wienkers, L.C., and Rock, D.A. (2012) Cytochrome P450 Architecture and Cysteine Nucleophile Placement Impact Raloxifene-Mediated Mechanism-Based Inactivation. *Molecular Pharmacology 82*, 835-842.

57. Sun, L.A. and Chines, A. (2005) Prevention and treatment of postmenopausal osteoporosis. *Current Topics in Osteoporosis* 261-290.

58. Yu, L., Liu, H., Li, W., Zhang, F., Luckie, C., van Breemen, R.B., Thatcher, G.R., and Bolton, J.L. (2004) Oxidation of raloxifene to quinoids: potential toxic pathways via a diquinone methide and *o*-quinones. *Chemical Research in Toxicology 17*, 879-888.

59. Morello, K.C., Wurz, G.T., and DeGregorio, M.W. (2003) Pharmacokinetics of Selective Estrogen Receptor Modulators. *Clinical Pharmacokinetics 42*, 361-372.

60. Qin, Z., Kastrati, I., Ashgodom, R., Lantvit, D., Overk, C., Choi, Y., van Breemen, R., Bolton, J., and Thatcher, G. (2009) Structural Modulation of Oxidative Metabolism in Design of Improved Benzothiophene Selective Estrogen Receptor Modulators. *Drug Metab Dispos 37*, 161-169.

61. NIH (1981) *NIH Guidelines for the Laboratory Use of ChemicalCarcinogens, U.G.P.O., 2381-2385*. *NIH, Washington, DC.*

62. Thompson, J.A., Malkinson, A.M., Wand, M.D., Mastovich, S.L., Mead, E.W., Schullek, K.M., and Laudenschlager, W.G. (1987) Oxidative metabolism of butylated hydroxytoluene by hepatic and pulmonary microsomes from rats and mice. *Drug Metab Dispos 15*, 833-40.

63. Day, W.W., Johnson, K.A., Prakash, C.A., and Eggler, J.F. (2001) Preparation of estrogen agonist/antagonist metabolites. PCT Int. Appl. WO 2001077093.

64. Miller, C., Collini, M., Tran, B., Harris, H., Kharode, Y., Marzolf, J., Moran, R., Henderson, R., Bender, R., Unwalla, R., Greenberger, L., Yardley, J., Abou-Gharbia, M., Lyttle, C., and Komm, B. (2001) Design, Synthesis, and Preclinical Characterization of Novel, Highly Selective Indole Estrogens. *J. Med. Chem. 44*, 1654-1657.

65. Li, X., Abell, C., Warrington, B.H., and Ladlow, M. (2003) Polymer-assisted solution phase synthesis of the antihyperglycemic agent Rosiglitazone (Avandia™). *Org. Biomol. Chem. 1*, 4392-4395.

66. Sato, M., Kawashima, Y., Goto, J., Yamane, Y., Chiba, Y., Jinno, S., Satake, M., and Iwata, C. (1994) Synthesis and evaluation of novel sulfonamide derivatives as thromboxane A_2 receptor antagonists I. *Eur. J. Med. Chem. 29*, 185-190.

67. Lušin, T., Tomašić, T., Trontelj, J., Mrhar, A., and Peterlin-Mašič, L. (2012) In vitro bioactivation of bazedoxifene and 2-(4-hydroxyphenyl)-3-methyl-1H-indol-5-ol in human liver microsomes. *Chemico-biological interactions 197*, 8-15.

68. Palkowitz, A.D., Glasebrook, A.L., Thrasher, K.J., Hauser, K.L., Short, L.L., Phillips, D.L., Muehl, B.S., Sato, M., Shetler, P.K., Cullinan, G.J., Pell, T.R., and Bryant, H.U. (1997) Discovery and Synthesis of [6-Hydroxy-3-[4-[2-(1-piperidinyl)ethoxy]phenoxy]-2-(4-hydroxyphenyl)]benzo[b]thiophene: A Novel, Highly Potent, Selective Estrogen Receptor Modulator. *J. Med. Chem. 40*, 1407-1416.

69. Pirali, T., Gatti, S., Di Brisco, R., Tacchi, S., Zaninetti, R., Brunelli, E., Massaroti, A., Sorba, G., Canonico, L.P., Moro, L., Genazzani, A.A., Tron, G.C., and Billington, R.A. (2007) Estrogenic Analogues Synthesized by Click Chemistry. *ChemMedChem 2*, 437-440.

70. Dennis, M.K., Burai, R., Ramesh, C., Petrie, W.K., Alcon, S.N., Nayak, T.K., Bologa, C.G., Leitao, A., Brailoiu, E., Deliu, E., Dun, N.J., Sklar, L.A., Hathaway, H.J., Arterburn, J.B., Oprea, T.I., and Prossnitz, E.R. (2009) *In vivo* effects of a GPR30 antagonist. *Nature Chemical Biology 5*, 421-427.

71. Qin, Z., Luo, J., VandeVrede, L., Tavassoli, E., Fa, M., Teich, A.F., Arancio, O., and Thatcher, G.R.J. (2012) Design and Synthesis of Neuroprotective Methylthiazoles and Modification as NO-Chimeras for Neurodegenerative Therapy. *J. Med. Chem. 55*, 6784-6801.

72. Pezzella, A., Lista, L., Napolitano, A., and d'Ischia, M. (2005) Tyrosinase-Catalyzed Oxidation of 17β-Estradiol: Structure Elucidation of the Products Formed beyond Catechol Estrogen Quinones. *Chem Res Toxicol 18*, 1413-1419.

73. Moridani, M., Scobie, H., Salehi, P., and O'Brien, P. (2001) Catechin Metabolism: Glutathione Conjugate Formation Catalyzed by Tyrosinase, Peroxidase, and Cytochrome P450. *Chem Res Toxicol 14*, 841-848.

74. Dieckhaus, C.M., Fernandez-Metzler, C.L., King, R., Krolikowski, P.H., and Baillie, T.A. (2005) Negative ion tandem mass spectrometry for the detection of glutathione conjugates. *Chem. Res. Toxicol. 18*, 630-8.

75. Chang, M., Zhang, F., Shen, L., Pauss, N., Alam, I., van Breemen, R.B., Blond, S.Y., and Bolton, J.L. (1998) Inhibition of glutathione S-transferase activity by the quinoid metabolites of equine estrogens. *Chem. Res. Toxicol. 11*, 758-65.

76. Gherezghiher, T., Michalsen, B., Chandrasena, R.E.P., Qin, Z., Sohn, J., Thatcher, G.R.J., and Bolton, J.L. (2012) The naphthol selective estrogen receptor modulator (SERM), LY2066948, is oxidized to an *o*-quinone analogous to the naphthol equine estrogen, equilenin. *Chemico-biological interactions 196*, 1-10.

77. Lee, A.J., Cai, M.X., Thomas, P.E., Conney, A.H., and Zhu, B.T. (2003) Characterization of the oxidative metabolites of 17beta-estradiol and estrone formed by 15 selectively expressed human cytochrome p450 isoforms. *Endocrinology 144*, 3382-98.

78. Shen, L., Pisha, E., Huang, Z., Pezzuto, J.M., Krol, E., Alam, Z., van Breemen, R.B., and Bolton, J.L. (1997) Bioreductive activation of catechol estrogen-ortho-quinones: aromatization of the B ring in 4-hydroxyequilenin markedly alters quinoid formation and reactivity. *Carcinogenesis 18*, 1093-101.

79. Iverson, S.L., Shen, L., Anlar, N., and Bolton, J.L. (1996) Bioactivation of estrone and its catechol metabolites to quinoid-glutathione conjugates in rat liver microsomes. *Chem. Res. Toxicol. 9*, 492-499.

80. Michalsen, B., Gherezghiher, T., Choi, J., Chandrasena, R.E.P., Qin, Z., Thatcher, G.R., and Bolton, J.L. (2012) Selective estrogen receptor modulator (SERM) lasofoxifene forms reactive quinoids similar to estradiol. *Chemical Research in Toxicology 25*, 1472-1483.

81. Spink, D.C., Zhang, F., Hussain, M.M., Katz, B.H., Liu, X., Hilker, D.R., and Bolton, J.L. (2001) Metabolism of equilenin in MCF-7 and MDA-MB-231 human breast cancer cells. *Chem. Res. Toxicol. 14*, 572-581.

82. Zhang, Y., Gaikwad, N.W., K., O., Zahid, M., Cavalieri, E., and Rogan, E. (2007) Cytochrome P450 isoforms catalyze formation of catechol estrogen quinones that react with DNA. *Metabolism 56*, 887-894.

83. Zahid, M., Kohli, E., Saeed, M., Rogan, E., and Cavalieri, E. (2006) The greater reactivity of estradiol-3,4-quinone vs estradiol-2,3-quinone with DNA in the formation of depurinating adducts: implications for tumor-initiating activity. *Chem. Res. Toxicol. 19*, 164-172.

84. Kaiser, C., Swagzdis, J.E., Flanagan, T.L., Lester, B.M., Burghard, G.L., Green, H., and Zirkle, C.L. (1972) Metabolism of Diphenidol. Urinary Products in Humans and Dogs. *Journal of Medicinal Chemistry 15*, 1146-1150.

85. Slatter, J.G., Schaaf, L.J., Sams, J.P., Feenstra, K.L., Johnson, M.G., Bombardt, P.A., Cathcart, K.S., Verburg, M.T., Pearson, L.K., Compton, L.D., Miller, L.L., Baker, D.S., Pesheck, C.V., and Lord III, R.S. (2000) Pharmacokinetics, Metabolism, and Excretion of Irinotecan (CPT-11) Following I.V. Infusion of [14C]CPT-11 in Cancer Patients. *Drug Metab Dispos 28*, 423-433.

86. McManus, K.T. and deBethizy, D.J. (1990) A new quantitative thermospray LC-MS method for nicotine and its metabolites in biological fluids. *Journal of Chromatographic Science 28*, 510-516.

87. Shen, L., Ahmad, S., Park, S., DeMaio, W., Oganesian, A., Hultin, T., Scatina, J., Bungay, P., and Chandrasekaran, A. (2010) In Vitro Metabolism, Permeability, and Efflux of Bazedoxifene in Humans. *Drug Metab Dispos 38*, 1471-1479.

88. Cavalieri, E. and Rogan, E. (2012) The etiology and prevention of breast cancer. *Drug Discovery Today: Disease Mechanisms 9*, e55-e69.

89. Richardson, D. (1988) The history of Nolvadex. *Drug Des Deliv 3*, 1-14.

90. Fisher, B., Costantino, J.P., Wickerham, D.L., Redmond, C.K., Kavanah, M., Cronin, W.M., Vogel, V., Robidoux, A., Dimitrov, N., Atkins, J., Daly, M., Wieand, S., Tan-Chiu, E., Ford, L., and Wolmark, N. (1998) Tamoxifen for prevention of

breast cancer: report of the National Surgical Adjuvant Breast and Bowel Project. *J. Natl. Cancer Inst. 90*, 1371-1388.

91. EBCTCG, e.a. (1998) Tamoxifen for early breast cancer: an overview of the randomised trials. Early Breast Cancer Trialists' Collaborative Group. *Lancet 351*, 1451-1467.

92. Smigel, K. (1998) Breast cancer prevention trial shows major benefit, some risk. *J. Natl. Cancer Inst. 6*, 647-648.

93. Chang, J., Powles, T., Ashley, S., Gregory, R., Tidy, V., Treleaven, J., and Singh, R. (1996) The effect of tamoxifen and hormone replacement therapy on serum cholesterol, bone mineral density and coagulation factors in healthy postmenopausal women participating in a randomised, controlled tamoxifen prevention study. *Ann Oncol. 7*, 671-675.

94. Jordan, V.C., Gapstur, S., and Morrow, M. (2001) Selective estrogen receptor modulation and reduction in risk of breast cancer, osteoporosis, and coronary heart disease. *J. Natl. Cancer Inst. 93*, 1449-1457.

95. Grey, A., Stapleton, J., Evans, M., Tatnell, M., Ames, R., and Reid, I. (1995) The effect of the antiestrogen tamoxifen on bone mineral density in normal late postmenopausal women. *Am. J. Med. 99*, 636-641.

96. Love, R.R., Mazess, R.B., Barden, H.S., Epstein, S., Newcomb, P.A., Jordan, V.C., Carbone, P.P., and DeMets, D.L. (1992) Effects of Tamoxifen on Bone Mineral Density in Postmenopausal Women with Breast Cancer. *New England Journal of Medicine 326*, 852-856.

97. Wurz, G.T., Soe, L.H., and DeGregorio, M.W. (2013) Ospemifene, vulvovaginal atrophy, and breast cancer. *Maturitas 74*, 220-225.

98. Pyrhönen, S., Ellmén, J., Vuorinen, J., Gershanovich, M., Tominaga, T., Kaufmann, M., and Hayes, D.F. (1999) Meta-analysis of trials comparing toremifene with tamoxifen and factors predicting outcome of antiestrogen therapy in postmenopausal women with breast cancer. *Breast Cancer Res Treat 56*, 131-141.

99. Tomás, E., Kauppila, A., Blanco, G., Apaja-Sarkkinen, M., and Laatikainen, T. (1995) Comparison between the effects of tamoxifen and toremifene on the uterus in postmenopausal breast cancer patients. *Gynecol. Oncol. 59*, 261-266.

100. Goldstein, S.R. (2001) The effect of SERMs on the endometrium. *Annals New York Academy of Sciences 949*, 237-242.

101. Buzdar, A., Hayes, D., El-Khoudary, A., Yan, S., Lønning, P., Lichinitser, M., Gopal, R., Falkson, G., Pritchard, K., Lipton, A., Wolter, K., Lee, A., Fly, K., Chew, R., Alderdice, M., Burke, K., and Eisenberg, P. (2002) Phase III Randomized Trial of Droloxifene and Tamoxifen As First-Line Endocrine Treatment of ER/PgR-Positive Advanced Breast Cancer. *Breast Cancer Res Treat 73*, 161-175.

102. Hendrix, S.L. and McNeeley, S.G. (2001) Effect of Selective Estrogen Receptor Modulators on Reproductive Tissues Other Than Endometrium. *Annals New York Academy of Sciences 949*, 243-250.

103. Komm, B.S. and Chines, A.A. (2012) An update on selective estrogen receptor modulators for the prevention and treatment of osteoporosis. *Maturitas 71*, 221-226.

104. Vogel, V.G. (2011) Update on Estrogen Receptor-Positive Breast Cancer Risk Reduction. *Current Breast Cancer Reports 3*, 156-164.

105. Gradishar, W., Glusman, J., Lu, Y., Vogel, C., Cohen, F., and Sledge, G.J. (2000) Effects of high dose raloxifene in selected patients with advanced breast carcinoma. *Cancer 88*, 2047-2053.

106. Cummings, S., Eckert, S., Krueger, K., Grady, D., Powles, T., Cauley, J., Norton, L., Nickelsen, T., Bjarnason, N., Morrow, M., Lippman, M., Black, D., Glusman, J., Costa, A., and Jordan, V. (1999) The effect of raloxifene on risk of breast cancer in postmenopausal women: results from the MORE randomized trial. Multiple Outcomes of Raloxifene Evaluation. *Journal of the American Medical Association 281*, 2189-97.

107. Ettinger, B., Black, D.M., Mitlak, B.H., Knickerbocker, R.K., Nickelsen, T., Genant, H.K., Christiansen, C., Delmas, P.D., Zanchetta, J.R., Stakkestad, J., Gluer, C.C., Krueger, K., Cohen, F.J., Eckert, S., Ensrud, K.E., Avioli, L.V., Lips, P., and Cummings, S.R. (1999) Reduction of vertebral fractrue risk in

postmenopausal women with osteoporosis treated with raloxifene. *Journal of the American Medical Association 282*, 637-645.

108. Sato, M., Turner, C.H., Wang, T., Adrian, M.D., Rowley, E., and Bryant, H.U. (1998) LY353381.HCl: A Novel Raloxifene Analog with Improved SERM Potency and Efficacy In Vivo. *J. Pharmacol. Exp. Ther. 287*, 1-7.

109. Deshmane, V., Krishnamurthy, S., Melemed, A., Peterson, P., and Buzdar, A. (2007) Phase III Double-Blind Trial of Arzoxifene Compared With Tamoxifen for Locally Advanced or Metastatic Breast Cancer. *Journal of Clinical Oncology 25*, 4967-4973.

110. Labrie, F., Labrie, C., Bélanger, A., Simard, J., Gauthier, S., Luu-The, V., Mérand, Y., Giguere, V., Candas, B., Luo, S., Martel, C., Singh, S.M., Fournier, M., Coquet, A., Richard, V., Charbonneau, R., Charpenet, G., Tremblay, A., Tremblay, G., Cusan, L., and Veilleux, R. (1999) EM-652 (SCH 57068), a third generation SERM acting as pure antiestrogen in the mammary gland and endometrium. *The Journal of Steroid Biochemistry and Molecular Biology 69*, 51-84.

111. Gauthier, S., Caron, B., Cloutier, J., Dory, Y.L., Favre, A., Larouche, D., Mailhot, J., Ouellet, C., Schwerdtfeger, A., Leblanc, G., Martel, C., Simard, J., Merand, Y., Belanger, A., Labrie, C., and Labrie, F. (1997) (S)-(+)-4-[7-(2,2-Dimethyl-1-oxopropoxy)-4-methyl-2-[4-[2-(1-piperidinyl)-ethoxy]phenyl]-2H-1-benzopyran-3-yl]-phenyl 2,2-Dimethylpropanoate (EM-800): A Highly Potent, Specific, and Orally Active Nonsteroidal Antiestrogen. *Journal of Medicinal Chemistry 40*, 2117-2122.

112. Calvo, E., Luu-The, V., Belleau, P., Martel, C., and Labrie, F. (2012) Specific transcriptional response of four blockers of estrogen receptors on estradiol-modulated genes in the mouse mammary gland. *Breast Cancer Res Treat 134*, 625-647.

113. Luo, S., Sourla, A., Labrie, C., Belanger, A., and Labrie, F. (1997) Combined Effects of Dehydroepiandrosterone and EM-800 on Bone Mass, Serum Lipids, and the Development of Dimethylbenz(A)Anthracene-Induced Mammary Carcinoma in the Rat. *Endocrinology 138*, 4435-4444.

114. Couillard, S., Gutman, M., Labrie, C., Belanger, A., Candas, B., and Labile, F. (1998) Comparison of the Effects of the Antiestrogens EM-800 and Tamoxifen on

the Growth of Human Breast ZR-75-1 Cancer Xenografts in Nude Mice. *Cancer Research 58*, 60-64.

115. Lemieux, C., Gelinas, Y., Lalonde, J., Labile, F., Richard, D., and Deshaies, Y. (2006) Hypocholesterolemic action of the selective estrogen receptor modulator acolbifene in intact and ovariectomized rats with diet-induced hypercholesterolemia. *Metabolism Clinical and Experimental 55*, 605-613.

116. Fabian, C. (2012) Phase II Study of Acolbifene in Pre-Menopausal Women at High Risk for Breast Cancer. *www.ClinicalTrials.gov* NCT00853996.

117. Labrie, F., Champagne, P., Labrie, C., Roy, J., Laverdiere, J., Provencher, L., Potvin, M., Drolet, Y., Pollak, M., Panasci, L., L'Esperance, B., Dufresne, J., Latreille, J., Robert, J., Samson, B., Jolivet, J., Yelle, L., Cusan, L., Diamond, P., and Candas, B. (2004) Activity and Safety of the Antiestrogen EM-800, the Orally Active Precursor of Acolbifene, in Tamoxifen-Resistant Breast Cancer. *Journal of Clinical Oncology 22*, 864-871.

118. Cusan, L. (2012) Dehydroepiandrosterone (DHEA) + Acolbifene Against Vasomotor Symptoms (Hot Flushes) in Postmenopausal Women. *www.ClinicalTrials.gov* NCT01452373.

119. Silverman, S., Christiansen, C., Genant, H., Vukicevic, S., Zanchetta, J., de Villiers, T., Constantine, G., and Chines, A. (2008) Efficacy of bazedoxifene in reducing new vertebral fracture risk in postmenopausal women with osteoporosis: results from a 3-year, randomized, placebo-, and active-controlled clinical trial. *Journal of Bone and Mineral Research 12*, 1923-1934.

120. Miller, P., Chines, A., Christiansen, C., Hoeck, H., Kendler, D., Lewiecki, E., Woodson, G., Levine, A., Constantine, G., and Delmas, P. (2008) Effects of bazedoxifene on BMD and bone turnover in postmenopausal women: 2-yr results of a randomized, double-blind, placebo-, and active-controlled study. *Journal of Bone and Mineral Research 23*, 525-535.

121. Lindsay, R., Gallagher, J.C., Kagan, R., Pickar, J.H., and Constantine, G. (2009) Efficacy of tissue-selective estrogen complex of bazedoxifene/conjugated estrogens for osteoporosis prevention in at-risk postmenopausal women. *Fertility and Sterility 92*, 1045-1052.

122. Lobo, R.A. (2009) Evaluation of bazedoxifene/conjugated estrogens for the treatment of menopausal symptoms and effects on metabolic parameters and overall safety profile. *Fertility and Sterility 92*, 1025-1038.

123. Boucher, M., Archer, D.F., Lobo, R.A., Pan, K., Ryan, K.A., Chines, A.A., and Mirkin, S. (2012) Safety and Tolerability of Bazedoxifene/Conjugated Estrogens in Postmenopausal Women: Findings From a 1-Year, Randomized, Placebo- and Active-controlled, Phase 3 Trial. *Poster, 68th Annual Meeting of the Society of Obstetricians and Gynaecologists of Canada*

124. Archer, D.F., Lewis, V., Carr, B.R., Olivier, S., and Pickar, J.H. (2009) Bazedoxifene/conjugated estrogens (BZA/CE): incidence of uterine bleeding in postmenopausal women. *Fertility and Sterility 92*, 1039-1044.

125. Pinkerton, J.V., Utian, W., Constantine, G., Olivier, S., and Pickar, J.H. (2007) SMART-2: A phase III study of the efficacy and safety of bazedoxifene/conjugated estrogens for the treatment of menopausal vasomotor symptoms. *Menopause 14*, 1081.

126. Kagan, R., Williams, R.S., Pan, K., Mirkin, S., and Pickar, J.H. (2010) A randomized, placebo- and active-controlled trial of bazedoxifene/conjugated estrogens for treatment of moderate to severe vulvar/vaginal atrophy in postmenopausal women. *Menopause 17*, 281-289.

127. Gallagher, J.C., Lindsay, R., Dietrich, J., Constantine, G., and Pickar, J.H. (2007) Smart trials: effects of a tissue selective estrogen complex (TSEC) comprised of bazedoxifene (BZA) and conjugated estrogens (CEs) on bone mineral density (BMD) in postmenopausal women. *Fertility and Sterility 88*, S241.

128. Mirkin, S., Komm, B.S., Pan, K., and Chines, A.A. (2012) Effects of bazedoxifene/conjugated estrogens on endometrial safety and bone in postmenopausal women. *Climacteric*

129. Friedman, A., Hoffman, D., Comite, F., Browneller, R., and Miller, J. (1991) Treatment of leiomyomata uteri with leuprolide acetate depot: a double-blind, placebo-controlled, multicenter study. The Leuprolide Study Group. *Obstet Gynecol 77*, 720-725.

130. Gupta, J., Sinha, A., Lumsden, M., and Hickey, M. (2012) Uterine artery embolization for symptomatic uterine fibroids. *Cochrane Database of Systematic Reviews doi:10.1002/14651858.CD005073.pub3*,

131. McClung, M.R., Siris, E., Cummings, S., Bolognese, M., Ettinger, M., Moffett, A., Emkey, R., Day, W., Somayaji, V., and Lee, A.M. (2006) Prevention of bone loss in postmenopausal women treated with lasofoxifene compared with raloxifene. *Menopause 13*, 377-386.

132. Taylor, H.S. (2009) Designing the ideal selective estrogen receptor modulator-an achievable goal? *Menopause 16*, 609-615.

133. Cummings, S.R., Ensrud, K., Delmas, P.D., LaCroix, A.Z., Vukicevic, S., Reid, D.M., Goldstein, S., Sriram, U., Lee, A., Thompson, J., Armstrong, R.A., Thompson, D.D., Powles, T., Zanchetta, J., Kendler, D., Neven, P., and Eastell, R. (2010) Lasofoxifene in Postmenopausal Women with Osteoporosis. *New England Journal of Medicine 362*, 686-696.

134. Desta, Z., Ward, B.A., Soukhova, N.V., and Flockhart, D.A. (2004) Comprehensive evaluation of tamoxifen sequential biotransformation by the human cytochrome P450 system in vitro: prominent roles for CYP3A and CYP2D6. *J. Pharmacol. Exp. Ther. 310*, 1062-1075.

135. Furr, B.a.J., VC (1984) The phamacology and clinical uses of tamoxifen. *Pharmacol. Ther. 25*, 127-205.

136. Dehal, S.S. and Kupfer, D. (1999) Cytochrome P-450 3A and 2D6 catalyze ortho hydroxylation of 4-hydroxytamoxifen and 3-hydroxytamoxifen (droloxifene) yielding tamoxifen catechol: involvement of catechols in covalent binding to hepatic proteins. *Drug Metab Dispos 27*, 681-688.

137. Zhang, F., Fan, P.W., Liu, X., Shen, L., van Breeman, R.B., and Bolton, J.L. (2000) Synthesis and reactivity of a potential carcinogenic metabolite of tamoxifen: 3,4-dihydroxytamoxifen-o-quinone. *Chem Res Toxicol 13*, 53-62.

138. Liu, X., Pisha, E., Tonetti, D.A., Yao, D., Li, Y., Yao, J., Burdette, J.E., and Bolton, J.L. (2003) Antiestrogenic and DNA Damaging Effects Induced by Tamoxifen and Toremifene Metabolites. *Chem. Res. Toxicol. 16*, 832-837.

139. Marques, M.M.a.B., F. A. (1997) Identification of tamoxifen-DNA adducts formed by 4-hydroxytamoxifen quinone methide. *Carcinogenesis 18*, 1949-1954.

140. Boocock, D., Brown, K., Gibbs, A., Sanchez, E., Turteltaub, K., and White, I. (2002) Identification of human CYP forms involved in the activation of tamoxifen and irreversible binding to DNA. *Carcinogenesis 11*, 1897-1901.

141. Shibutani, S., Shaw, P., Suzuki, N., Dasaradhi, L., Duffel, M., and Terashima, I. (1998) Sulfation of alpha-hydroxytamoxifen catalyzed by human hydroxysteroid sulfotransferase results in tamoxifen-DNA adducts. *Carcinogenesis 11*, 2007-2011.

142. Hard, G., Iatropoulos, M., Jordan, K., Radi, L., Kaltenberg, O., Imondi, A., and Williams, G. (1993) Major difference in the hepatocarcinogenicity and DNA adduct forming ability between toremifene and tamoxifen in female Crl:CD(BR) rats. *Cancer Research 53*, 4534-4541.

143. Shibutani, S., Ravindernath, A., Terashima, I., Suzuki, N., Laxmi, Y., Kanno, Y., Suzuki, M., Apak, T., Sheng, J., and Duffel, M. (2001) Mechanism of lower genotoxicity of toremifene compared with tamoxifen. *Cancer Research 61*, 3925-3931.

144. Liu, H., Bolton, J.L., and Thatcher, G.R. (2006) Chemical modification modulates estrogenic activity, oxidative reactivity, and metabolic stability in 4'F-DMA, a new benzothiophene selective estrogen receptor modulator. *Chem Res Toxicol 19*, 779-787.

145. Barbier, O., Albert, C., Martineau, I., Vallee, M., High, K., Labrie, F., Hum, D.W., Labrie, C., and Belanger, A. (2001) Glucuronidation of the Nonsteroidal Antiestrogen EM-652 (SCH 57068), by Human and Monkey Steroid Conjugating UDP-Glucuronosyltransferase Enzymes. *Molecular Pharmacology 59*, 636-645.

146. Sanceau, J.-Y., Larouche, D., Caron, B., Belanger, P., Coquet, A., Belanger, A., Labile, F., and Gauthier, S. (2007) Sythesis and deuterium labelling of the pure selective estrogen receptor modulator (SERM) acolbifene glucuronides. *Journal of Labelled Compounds and Radiopharmaceuticals 50*, 197-206.

147. Jordan, V.C. and O'Malley, B.W. (2007) Selective Estrogen-Receptor Modulators and Antihormonal Resistance in Breast Cancer. *Journal of Clinical Oncology 25*, 5815-5824.

148. Rutqvist, L.E., Johansson, H., Signomklao, T., Johansson, U., Fornander, T., and Wilking, N. (1995) Adjuvant Tamoxifen Therapy for Early Stage Breast Cancer and Second Primary Malignancies. *J. Natl. Cancer Inst. 87*, 645-651.

149. Bergman, L., Beelen, M., Gallee, M., Hollema, H., Benraadt, J., and van Leeuwen, F. (2000) Risk and prognosis of endometrial cancer after tamoxifen for breast cancer. Comprehensive Cancer Centres' ALERT Group. Assessment of Liver and Endometrial cancer Risk following Tamoxifen. *Lancet 356*, 881-887.

150. Greaves, P., Goonetilleke, R., Nunn, G., Topham, J., and Orton, T. (1993) Two-year carcinogenicity study of tamoxifen in Alderley Park Wistar-derived rats. *Cancer Research 53*, 3919-3924.

151. White, I. (1999) The tamoxifen dilemma. *Carcinogenesis 20*, 1153-1160.

152. Musgrove, E.A. and Sutherland, R.L. (2009) Biological determinants of endocrine resistance in breast cancer. *Nat. Rev. Cancer 9*, 631-643.

153. Zhou, C., Zhong, Q., Rhodes, L., Townley, I., Bratton, M., Zhang, Q., Martin, E., Elliott, S., Collins-Burow, B., Burow, M., and Wang, G. (2012) Proteomic analysis of acquired tamoxifen resistance in MCF-7 cells reveals expression signatures associated with enhanced migration. *Breast Cancer Research 14*, R45.

154. Hiscox, S., Baruah, B., Smith, C., Bellerby, R., Goddard, L., Jordan, N., Poghosyan, Z., Nicholson, R., Barrett-Lee, P., and Gee, J. (2012) Overexpression of CD44 accompanies acquired tamoxifen resistance in MCF7 cells and augments their sensitivity to the stromal factors, heregulin and hyaluronan. *BMC Cancer 12*, 458.

155. Lufkin, E.G., Whitaker, M.D., Nickelsen, T., Argueta, R., Caplan, R.H., Knickerbocker, R.K., and Riggs, L.B. (1998) Treatment of established postmenopausal osteoporosis with raloxifene: a randomized trial. *Journal of Bone and Mineral Research 13*, 1747-1754.

156. Lippman, M., Cummings, S., Disch, D., Mershon, J., Dowsett, S., Cauley, J., and Martino, S. (2006) Effect of Raloxifene on the Incidence of Invasive Breast Cancer in Postmenopausal Women with Osteoporosis Categorized by Breast Cancer Risk. *Clinical Cancer Research 12*, 5242-5247.

157. Martino, S., Cauley, J., Barrett-Connor, E., Powles, T., Mershon, J., Disch, D., Secrest, R., and Cummings, S. (2004) Continuing Outcomes Relevant to Evista: Breast Cancer Incidence in Postmenopausal Osteoporotic Women in a Randomized Trial of Raloxifene *JNCI 96*, 1751-1761.

158. Delmas, P., Ensrud, K., Adachi, J., Harper, K., Sarkar, S., Gennari, C., Reginster, J., Pols, H., Recker, R., Harris, S., Wu, W., Genant, H., Black, D., and Eastell, R. (2002) Efficacy of raloxifene on vertebral fracture risk reduction in postmenopausal women with osteoporosis: four-year results from a randomized clinical trial. *J Clin Endocrinol Metab 87*, 3609-3617.

159. Vogel, V. (2008) Managing the risk of invasive breast cancer in women at risk for breast cancer and osteoporosis: the role of raloxifene. *Clinical Interventions in Aging 3*, 601-609.

160. Davis, S., O'neill, S., Eden, J., Baber, R., Ekangaki, A., Stocks, J., and Thiebaud, D. (2004) Transition from estrogen therapy to raloxifene in postmenopausal women: effects on treatment satistaction and the endometrium-a pilot study. *Menopause 11*, 167-175.

161. Delmas, P.D., Bjarnason, N.H., Mitlak, B.H., Ravoux, A.-C., Shah, A.S., Huster, W.J., Draper, M., and Christiansen, C. (1997) Effects of raloxifene on bone mineral density, serum cholesterol concentrations, and uterine endometrium in postmenopausal women. *New England Journal of Medicine 337*, 1641-1647.

162. Pickar, J.H. (2009) The endometrium - from estrogens alone to TSECs. *Climacteric 12*, 463-477.

163. Lewiecki, E. (2007) Bazedoxifene and bazedoxifene combined with conjugated estrogens for the management of postmenopausal osteoporosis. *Expert Opinion on Investigational Drugs 16*, 1663-1672.

164. Cauley, J., A., Robbins, J., Chen, Z., Cummings, S.R., Jackson, R.D., LaCroix, A.Z., LeBoff, M., Lewis, C.E., McGowan, J., Neuner, J., Pettinger, M., Stefanick, M., Wactawski-Wende, J., and Watts, N.B. (2003) Effects of Estrogen Plus Progestin on Risk of Fracture and Bone Mineral Density. *Journal of the American Medical Association 290*, 1729-1738.

165. Komm, B.S. and Lyttle, C.R. (2001) Developing a SERM: stringent preclinical selection criteria leading to an acceptable candidate (WAY-140424) for clinical evaluation. *Annals New York Academy of Sciences 949*, 317-326.

166. Gennari, L., Merlotti, D., De Paola, V., Martini, G., and Nuti, R. (2008) Bazedoxifene for the prevention of postmenopausal osteoporosis. *Therapeutics and Clinical Risk Management 4*, 1229-1242.

167. Chang, K.C.N., Wang, Y., Bodine, P.V.N., Nagpal, S., and Komm, B.S. (2010) Gene expression profiling studies of three SERMs and their conjugated estrogen combinations in human breast cancer cells: Insights into the unique antagonistic effects of bazedoxifene on conjugated estrogens. *Journal of Steroid Biochemistry and Molecular Biology 118*, 117-124.

168. Frasor, J., Stossi, F., Danes, J.M., Komm, B.S., Lyttle, C.R., and Katzenellenbogen, B.S. (2004) Selective Estrogen Receptor Modulators: Discrimination of Agonistic versus Antagonistic Activities by Gene Expression Profiling in Breast Cancer Cells. *Cancer Research 64*, 1522-1533.

169. Berrodin, T.J., Chang, K.C.N., Komm, B.S., Freedman, L.P., and Nagpal, S. (2009) Differential BIochemical and Cellular Actions of Premarin Estrogens: Distinct Pharmacology of Bazedoxifene-Conjugated Estrogens Combination. *Molecular Endocrinology 23*, 74-85.

170. Kulak Jr, J., Ferriani, R.A., Komm, B.S., and Taylor, H.S. (2013) Tissue Selective Estrogen Complexes (TSECs) Differentially Modulate Markers of Proliferation and Differentiation in Endometrial Cells. *Reproductive Sciences 20*, 129-137.

171. Komm, B.S., Kharode, Y., and Bodine, P.V.N. (2003) Combining a SERM with conjugated estrogens (CE) to improve the SERM profile: not all SERMs may succeed. *Journal of Bone and Mineral Research 18*, S273.

172. Stovall, D., Utian, W., Gass, M., Qu, Y., Muram, D., Wong, M., and Plouffe, L.J. (2007) The effects of combined raloxifene and oral estrogen on vasomotor symptoms and endometrial safety. *Menopause 14*, 510-517.

173. Carranza-Lira, S., Gooch, A., Salvidar, N., and Osterwalder, M. (2007) Climacteric symptom control after the addition of low-dose esterified conjugated estrogens to raloxifene standard doses. *Int J Fertil Womens Med 52*, 93-96.

174. Pickar, J.H., Yeh, I.-T., Bachmann, G., and Speroff, L. (2009) Endometrial effects of a tissue selective estrogen complex containing bazedoxifene/conjugated estrogens as a menopausal therapy. *Fertility and Sterility 92*, 1018-1024.

175. Ethun, K.F., Wood, C.E., Register, T.C., Cline, J.M., Appt, S.E., and Clarkson, T.B. (2012) Effects of bazedoxifene acetate with and without conjugated equine estrogens on the breast of postmenopausal monkeys. *Menopause 19*, 1242-1252.

176. Van Duren, D., Ronkin, S., and Pickar, J.H. (2006) Bazedoxifene combined with conjugated estrogens: a novel alternative to traditional hormone therapies. *Fertility and Sterility 86*, S88-S89.

177. Hemachandra, L.P.M.P., Patel, H., Chandrasena, R.E.P., Choi, J., Wang, S., Wang, Y., Bolton, J.L., and Thatcher, G.R. (2013) Benzothiophene SERMs act as breast cancer chemopreventive agents by modulating estrogen oxidative metabolism in human mammary epithelial cells. *(in preparation)*

178. Kastrati, I., Edirisinghe, P.D., Hemachandra, L.P.M.P., Chandrasena, E.R., Choi, J., Wang, Y.-T., Bolton, J.L., and Thatcher, G.R.J. (2011) Raloxifene and Desmethylarzoxifene Block Estrogen-Induced Malignant Transformation of Human Breast Epithelial Cells. *PLoS ONE 6*, e27876.

179. Steiner, C., Peters, W.H., Gallagher, E.P., Magee, P., Rowland, I., and Pool-Zobel, B.L. (2007) Genistein protects human mammary epithelial cells from benzo(a)pyrene-7,8-dihydrodiol-9,10-epoxide and 4-hydroxy-2-nonenal genotoxicity by modulating the glutathione/glutathione S-transferase system. *Carcinogenesis 28*, 738-48.

180. Ingle, J., Ahmann, D., Green, S., Edmonson, J., Bisel, H., Kvols, L., Nichols WC, Creagan, E., Hahn, R., Rubin, J., and Frytak, S. (1981) Randomized clinical trial of diethylstilbestrol versus tamoxifen in postmenopausal women with advanced breast cancer. *New England Journal of Medicine 304*, 16-21.

181. Ingle, J.N. (2004) Sequencing of Endocrine Therapy in Postmenopausal Women with Advanced Breast Cancer. *Clinical Cancer Research 10*, 362s-367s.

182. Ingle, J. (2002) Estrogen as therapy for breast cancer. *Breast Cancer Res 4*, 133 - 136.

183. Song, R.X.D. and Santen, R.J. (2003) Apoptotic action of estrogen. *Apoptosis 8*, 55-60.

184. Molloy, M., White, B., Gherezghiher, T., Michalsen, B., Zhao, H., Thatcher, G., and Tonetti, D. (in preparation) Novel Benzothiophene Selective Estrogen Receptor Modulators for the Treatment of PKCα-Overexpressing Tamoxifen-Resistant Breast Cancer.

185. Assender, J., Gee, J., Lewis, I., Ellis, I., Robertson, J., and Nicholson, R. (2007) Protein kinase C isoform expression as a predictor of disease outcome on endocrine therapy in breast cancer. *Journal of Clinical Pathology 60*, 1216-1221.

186. Tonetti, D., Morrow, M., Kidwai, N., Gupta, A., and Badve, S. (2003) Elevated protein kinase C alpha expression may be predictive of tamoxifen treatment failure. *British Journal of Cancer 88*, 1400-1402.

187. Chisamore, M., Ahmed, Y., Bentrem, D., Jordan, V., and Tonetti, D. (2001) Novel Antitumor Effect of Estradiol in Athymic Mice Injected with a T47D Breast Cancer Cell Line Overexpressing Protein Kinase Calpha. *Clinical Cancer Research 7*, 3156-3165.

188. Dubal, D., Shughrue, P., Wilson, M., Merchenthaler, I., and Wise, P. (1999) Estradiol Modulates bcl-2 in Cerebral Ischemia: A Potential Role for Estrogen Receptors. *The Journal of Neuroscience 19*, 6385-6393.

189. Abdelhamid, R., Luo, J., VandeVrede, L., Kundu, I., Michalsen, B., Litosh, V.A., Schiefer, I.T., Gherezghiher, T., Yao, P., Qin, Z., and Thatcher, G.R. (2011) Benzothiophene Selective Estrogen Receptor Modulators Provide Neuroprotection by a Novel GPR30-Dependent Mechanism. *ACS Chemical Neuroscience 2*, 256-268.

190. Coker, L., Espeland, M., Rapp, S., Legault, C., Resnick, S., Hogan, P., Gaussoin, S., Dailey, M., and Shumaker, S. (2010) Postmenopausal hormone therapy and cognitive outcomes: the Women's Health Initiative Memory Study (WHIMS). *Journal of Steroid Biochemistry and Molecular Biology 118*, 304-310.

191. Simpkins, J., Richardson, T., Yi, K., Perez, E., and Covey, D. (2013) Neuroprotection with non-feminizing estrogen analogues: An overlooked possible therapeutic strategy. *Hormones and Behavior 63*, 278-283.

192. Velázquez-Zamora, D., Garcia-Segura, L., and González-Burgos, I. (2012) Effects of selective estrogen receptor modulators on allocentric working memory performance and on dendritic spines in medial prefrontal cortex pyramidal neurons of ovariectomized rats. *Hormones and Behavior 61*, 512-517.

193. Yaffe, K., Krueger, K., Cummings, S., Blackwell, T., Henderson, V., Sarkar, S., Ensrud, K., and Grady, D. (2005) Effect of Raloxifene on Prevention of Dementia and Cognitive Impairment in Older Women: The Multiple Outcomes of Raloxifene Evaluation (MORE) Randomized Trial. *Am. J. Psychiatry 162*, 683-690.

194. Goekoop, R., Duschek, E., Knol, D., Barkhof, F., Netelenbos, C., Scheltens, P., and Rombouts, S. (2005) Raloxifene exposure enhances brain activation during memory performance in healthy elderly males; its possible relevance to behavior. *Neuroimage 25*, 63-75.

195. Goekoop, R., Barkhof, F., Duschek, E., Netelenbos, C., Knol, D., Scheltens, P., and Rombouts, S. (2006) Raloxifene treatment enhances brain activation during recognition of familiar items: a pharmacological fMRI study in healthy elderly males. *Neuropsychopharmacology 31*, 1508-1518.

196. Jacobsen, D., Samson, M., Emmelot-Vonk, M., and Verhaar, H. (2010) Raloxifene improves verbal memory in late postmenopausal women: a randomized, double-blind, placebo-controlled trial. *Menopause 17*, 309-314.

197. Inagaki, T. and Etgen, A. (2013) Neuroprotective action of acute estrogens: Animal models of brain ischemia and clinical implications. *Steroids http://dx.doi.org/10.1016/j.steroids.2012.12.015*,

198. VandeVrede, L., Abdelhamid, R., Qin, Z., Choi, J., Piyankarage, S., Luo, J., Larson, J., Bennett, B., and Thatcher, G. (2013) A nitric oxide donor strategy for procognitive selective estrogen receptor modulators to overcome thrombosis and loss of eNOS function. *PNAS (submitted)*,

199. Gkaliagkousi, E. and Ferro, A. (2011) Nitric oxide signalling in the regulation of cardiovascular and platelet function. *Front Biosci 16*, 1873-1897.

200. Saitta, A., Altavilla, D., Cucinotta, D., Morabito, N., Frisina, N., Corrado, F., D'Anna, R., Lasco, A., Squadrito, G., Gaudio, A., Cancellieri, F., Arcoraci, V., and Squadrito, F. (2001) Randomized, double-blind, placebo-controlled study on effects of raloxifene and hormone replacement therapy on plasma no concentrations, endothelin-1 levels, and endothelium-dependent vasodilation in postmenopausal women. *Arteriosclerosis, Thrombosis, and Vascular Biology 21*, 1512-1519.

201. Simoncini, T., Genazzani, A., and Liao, J. (2002) Nongenomic mechanisms of endothelial nitric oxide synthase activation by the selective estrogen receptor modulator raloxifene. *Circulation 105*, 1368-1373.

202. Bachmann, G. and Komi, J. (2010) Ospemifene effectively treats vulvovaginal atrophy in postmenopausal women: results from a pivotal phase 3 study. *Menopause 17*, 480-486.

203. Burich, R., McCall, J., Mehta, N., Greenberg, B., Bell, K., Griffey, S., DeGregorio, M., and Wurz, G. (2012) Ospemifene and 4-Hydroxyospemifene Effectively Prevent and Treat Breast Cancer in the MTag.Tg Transgenic Mouse Model. *Menopause 19*, 96-103.

Appendix

400 MHz ^{1}H NMR of Compound 6b

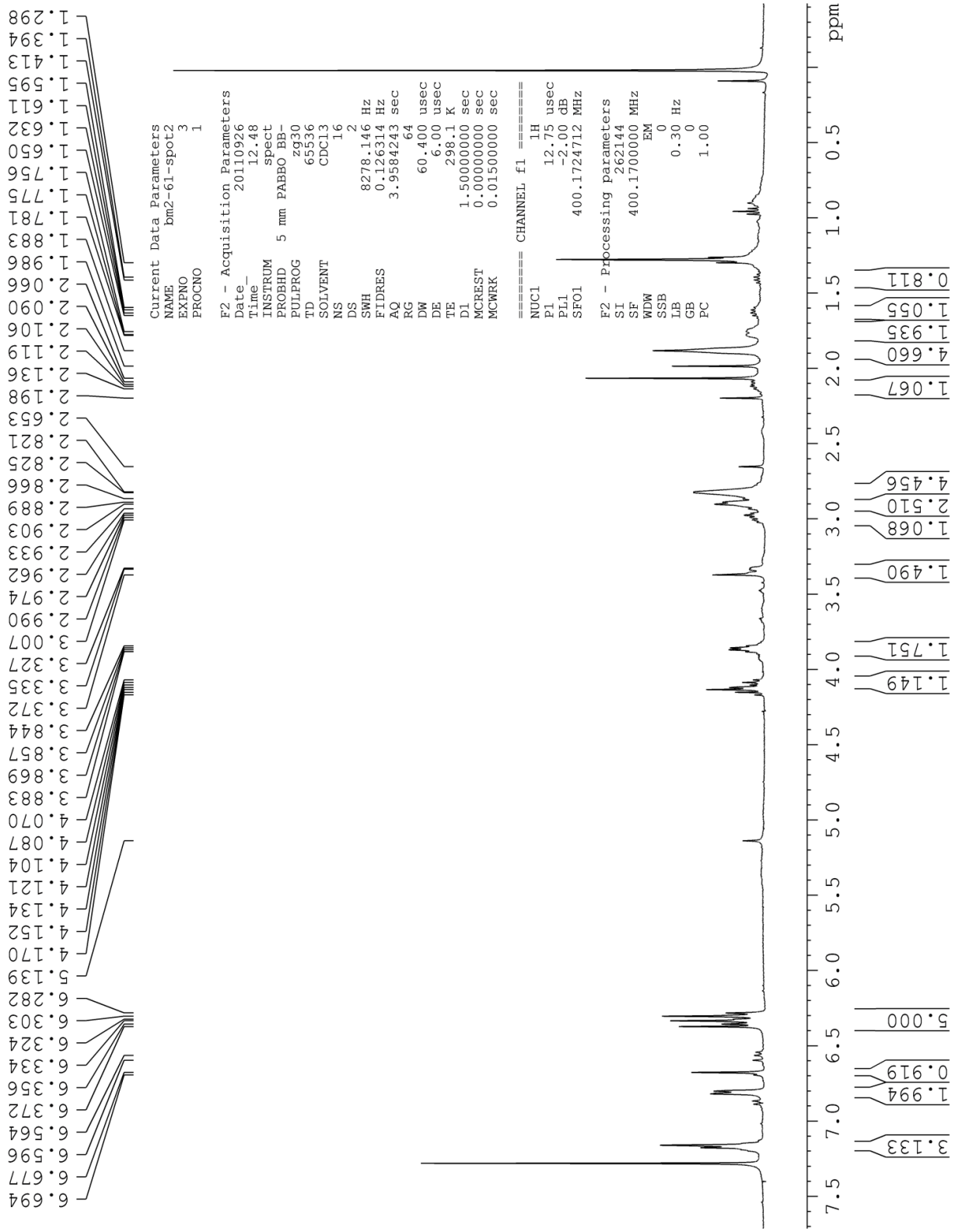

400 MHz ^{1}H NMR of Compound 18

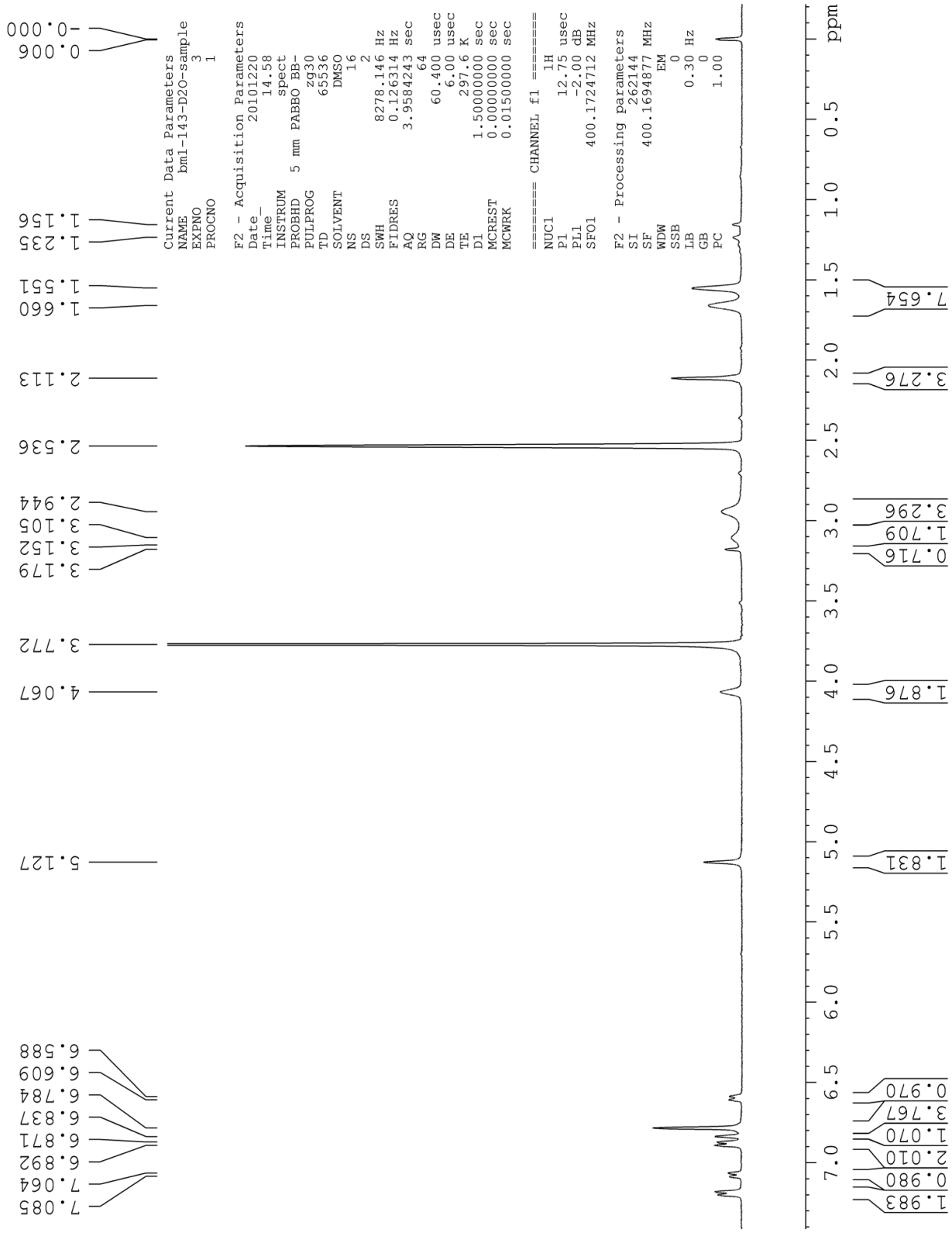

400 MHz ^{1}H NMR of Compound 19

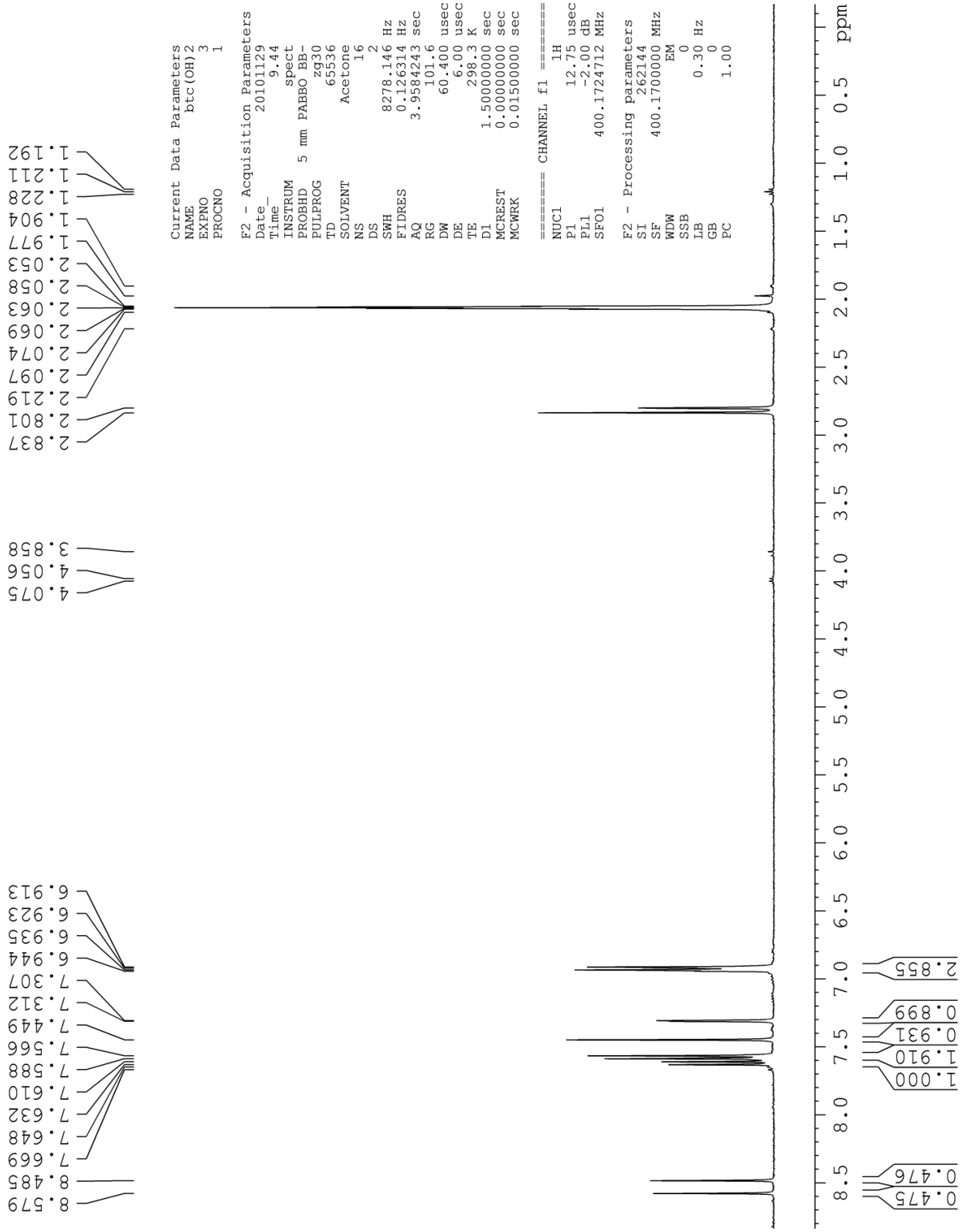

400 MHz ^{1}H NMR of Compound 21

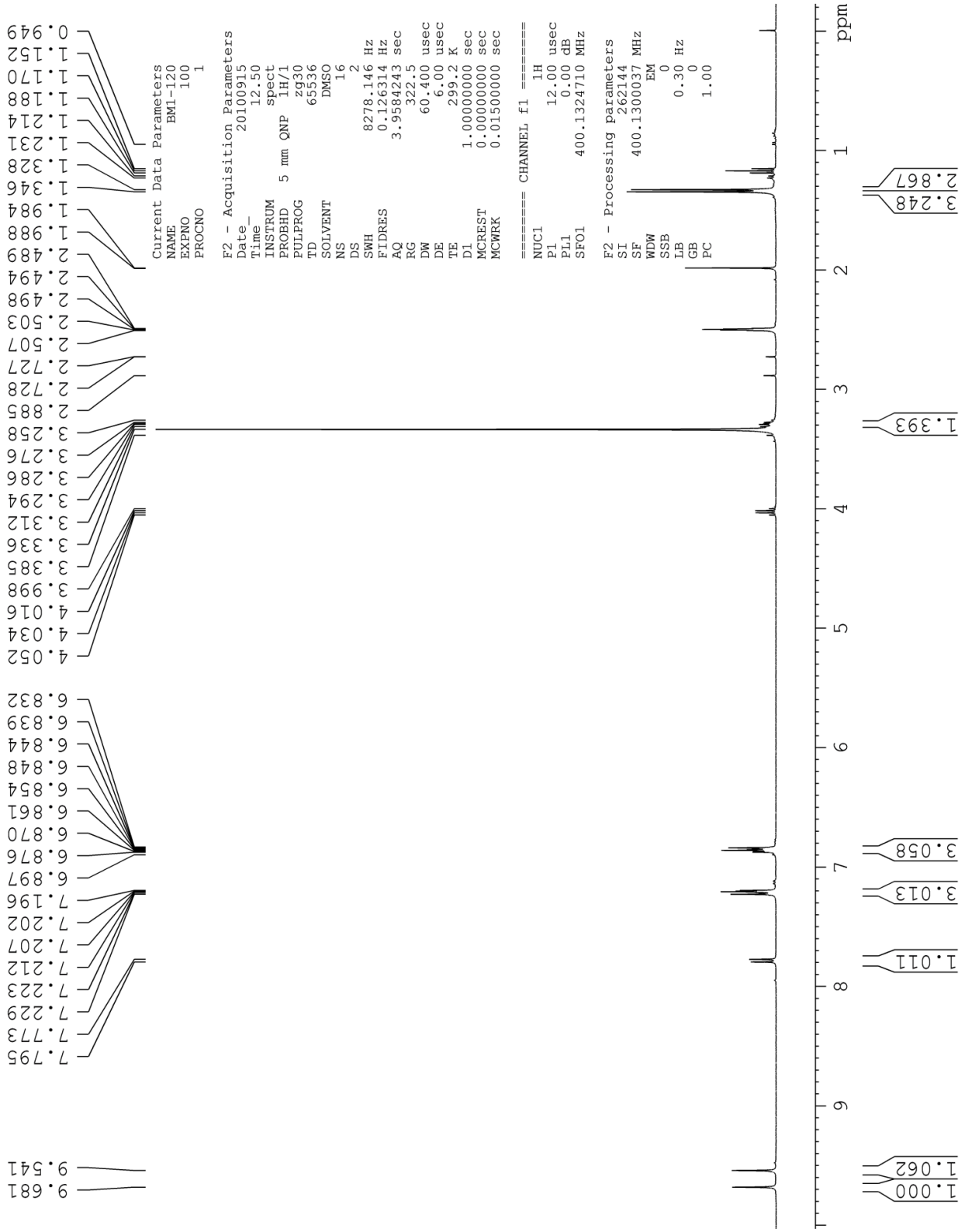

400 MHz ^{1}H NMR of Compound 23

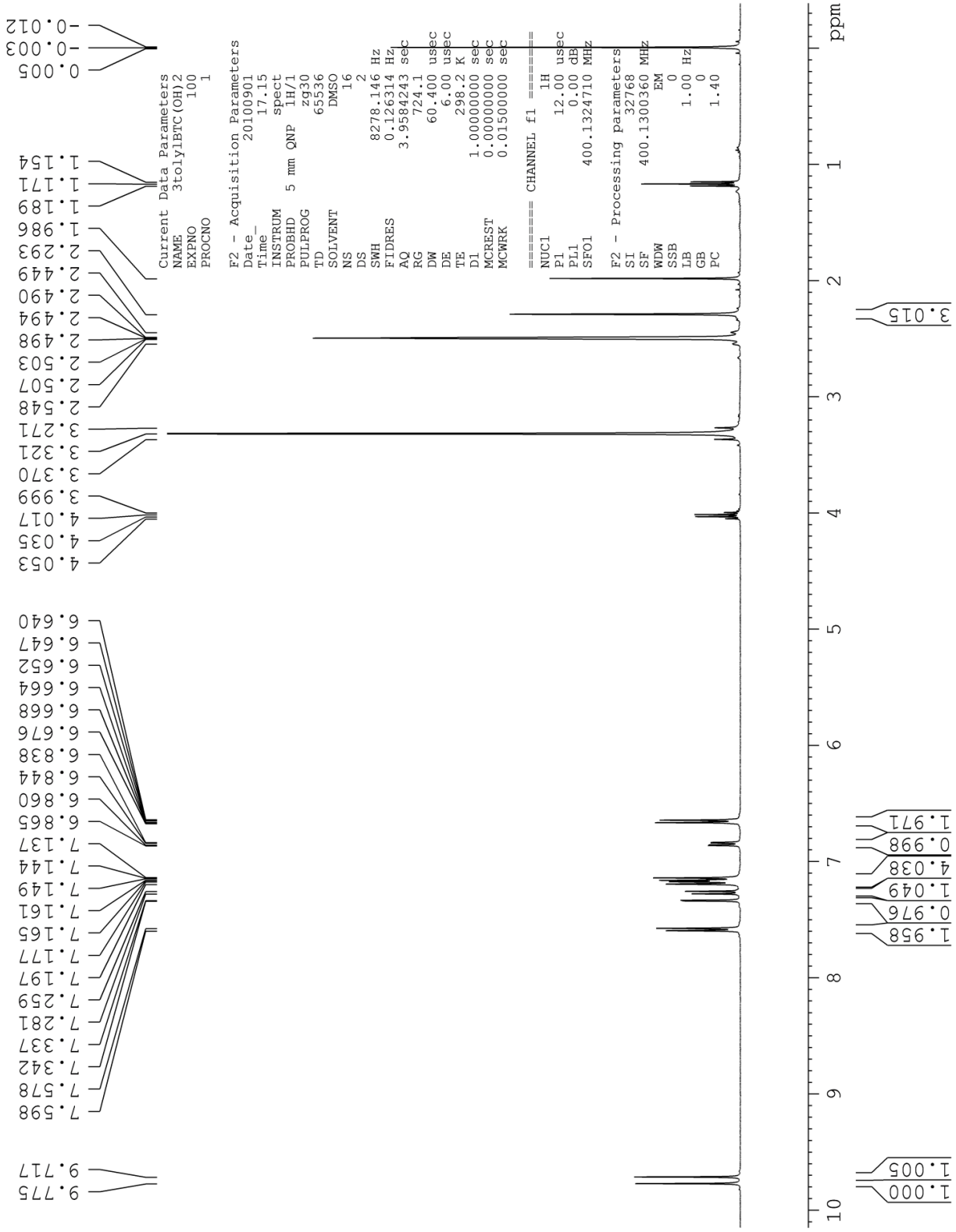

400 MHz ^{1}H NMR of Compound 25

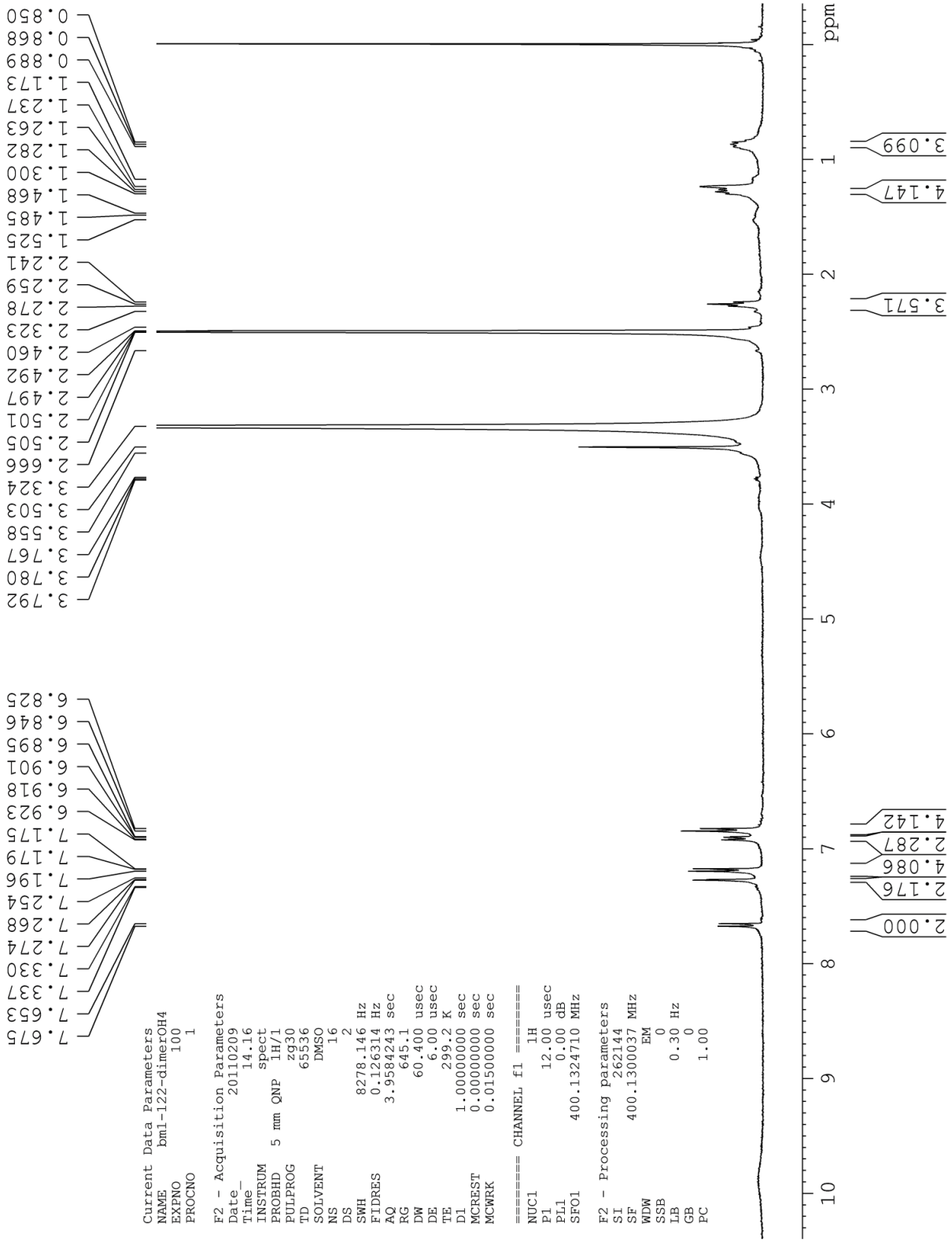

400 MHz ^{1}H NMR of Compound 32

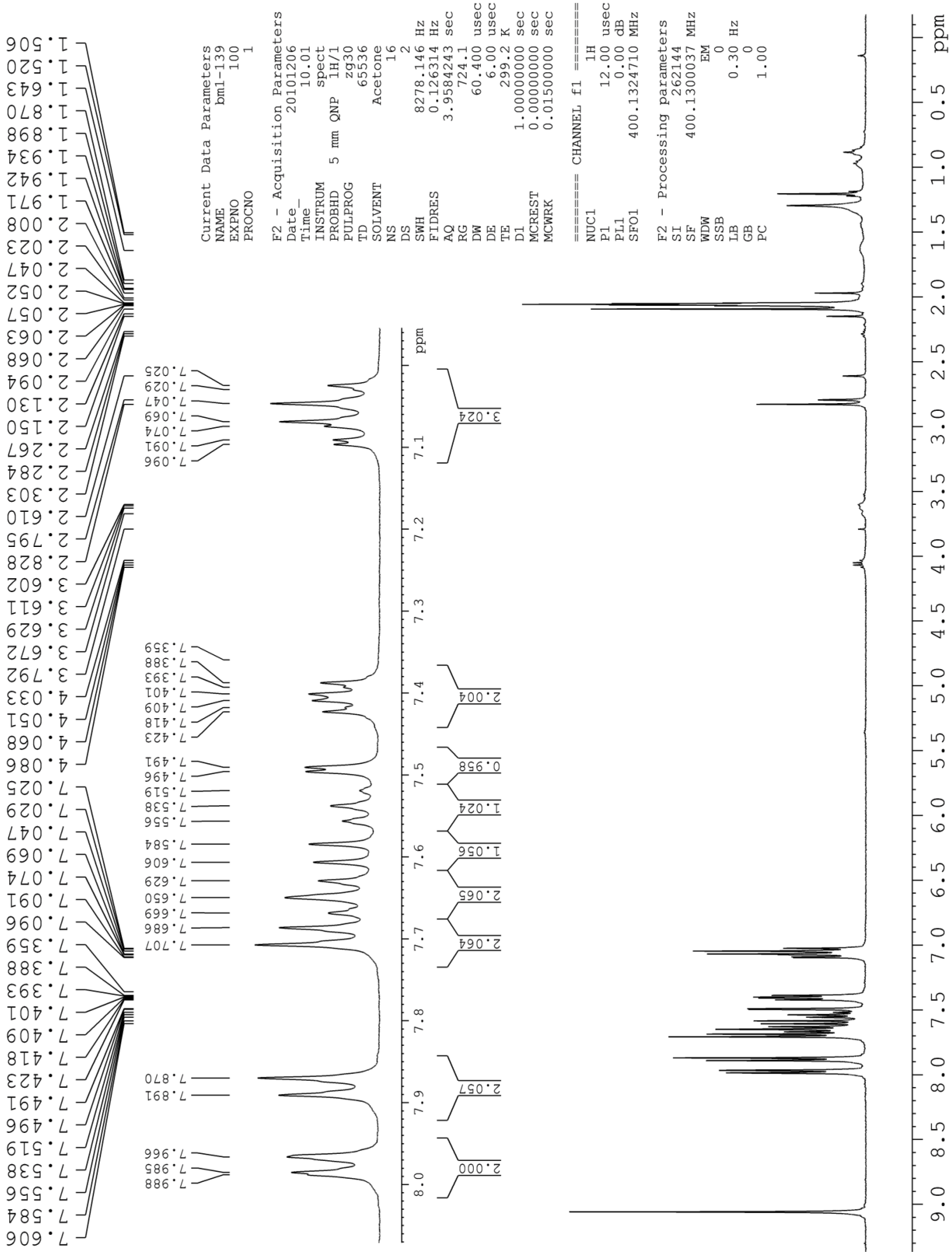

400 MHz ^{1}H NMR of Compound 37

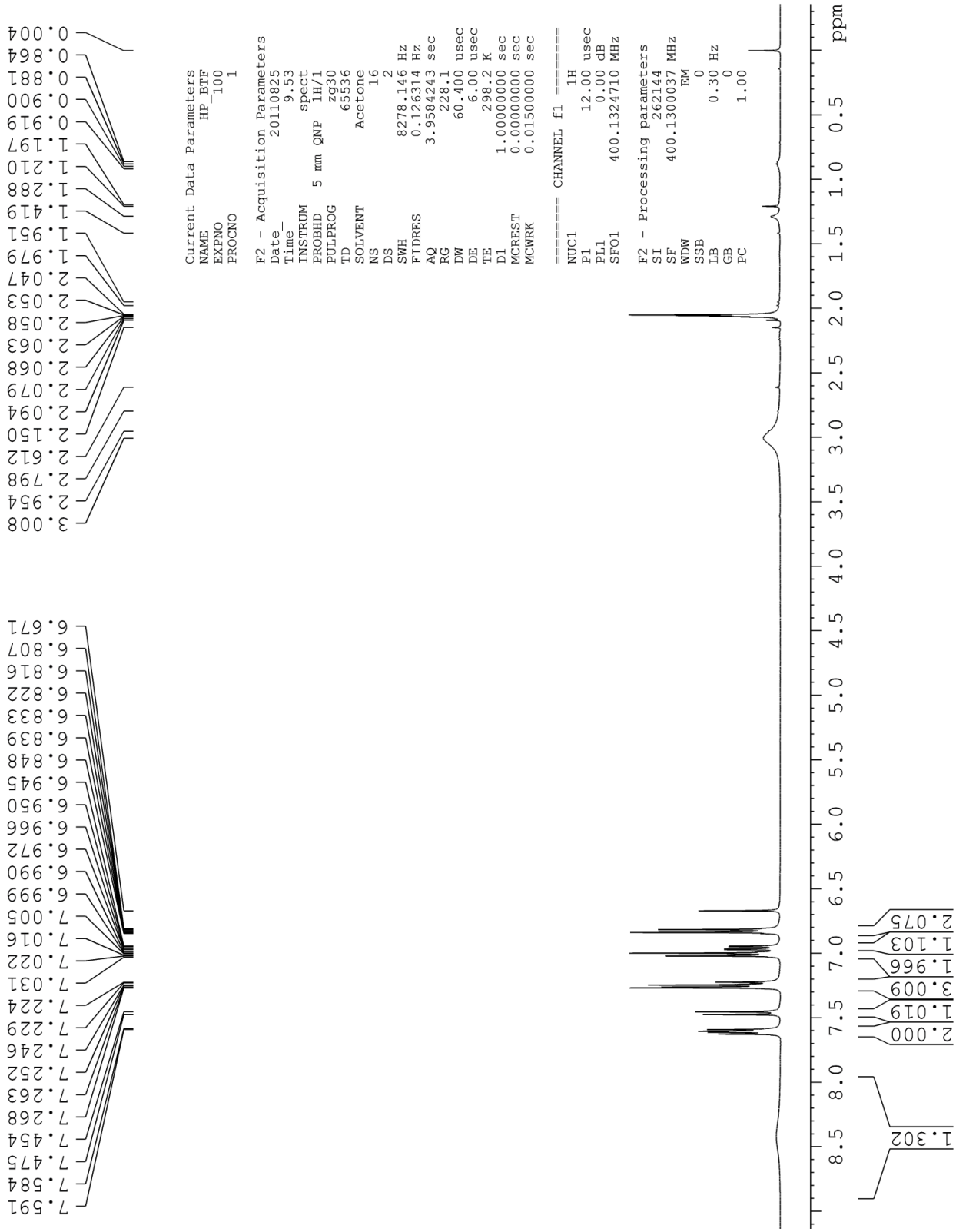

400 MHz ^{1}H NMR of Compound 41

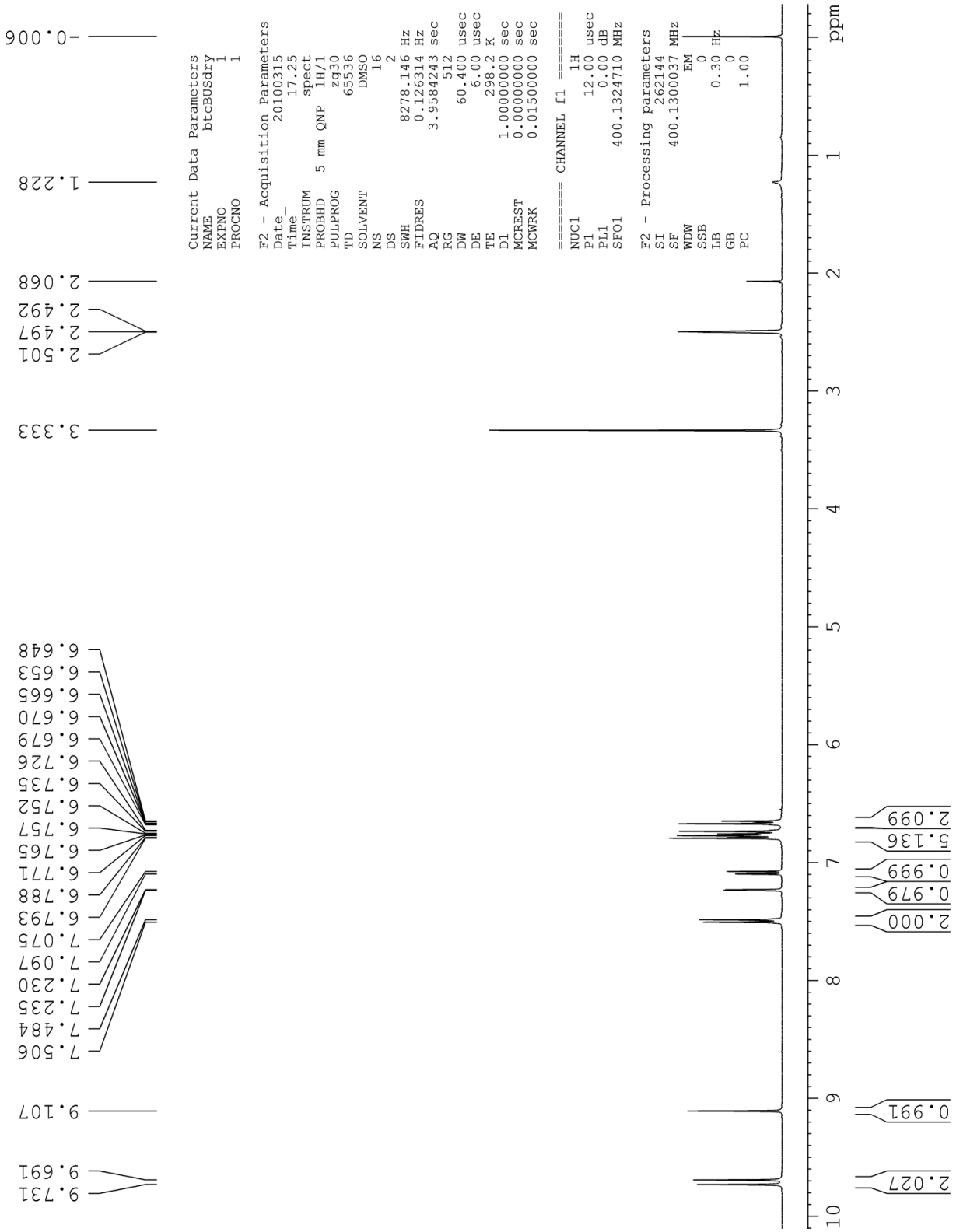

400 MHz ^{1}H NMR of Compound 44

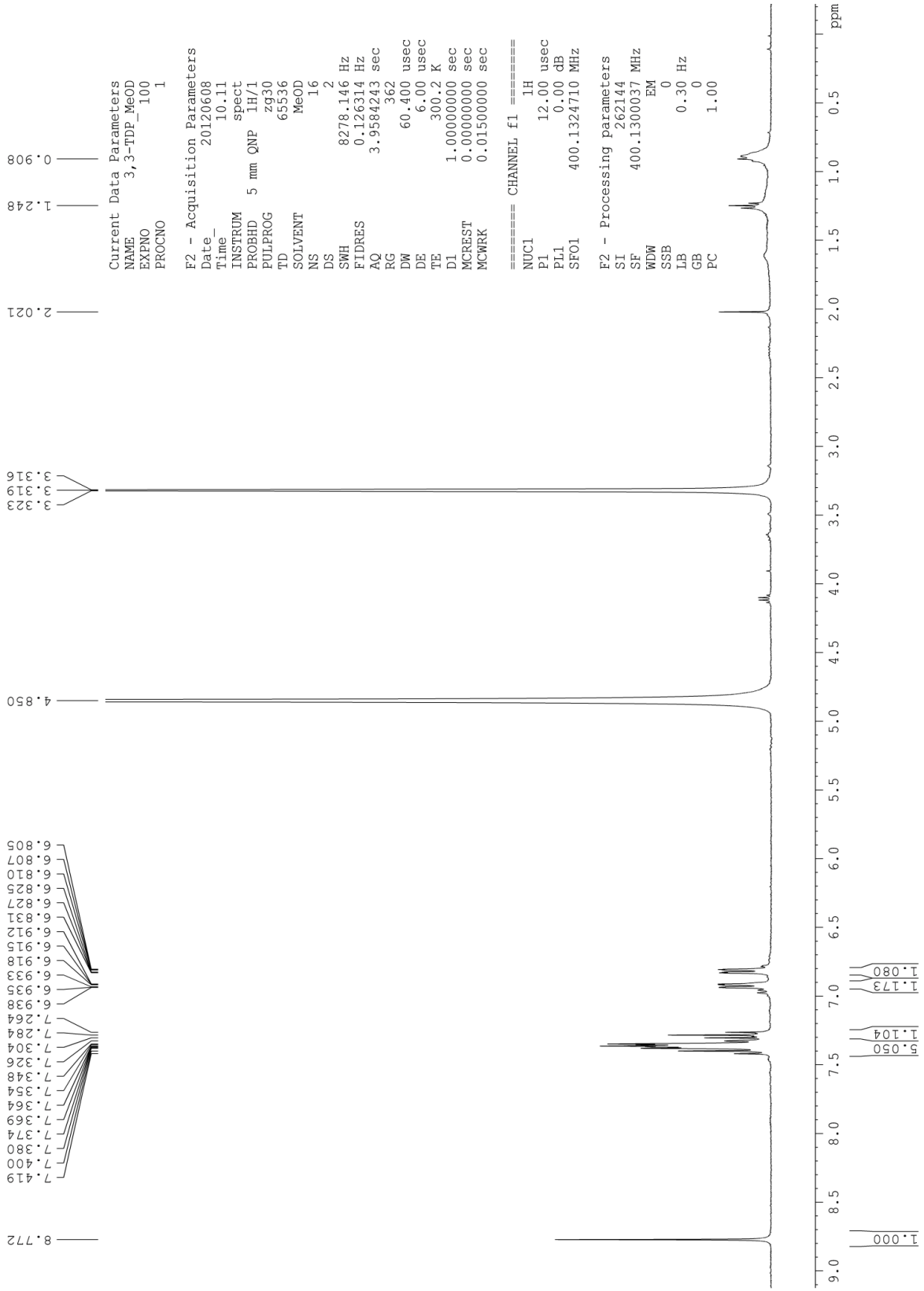

400 MHz ^{1}H NMR of Compound 46

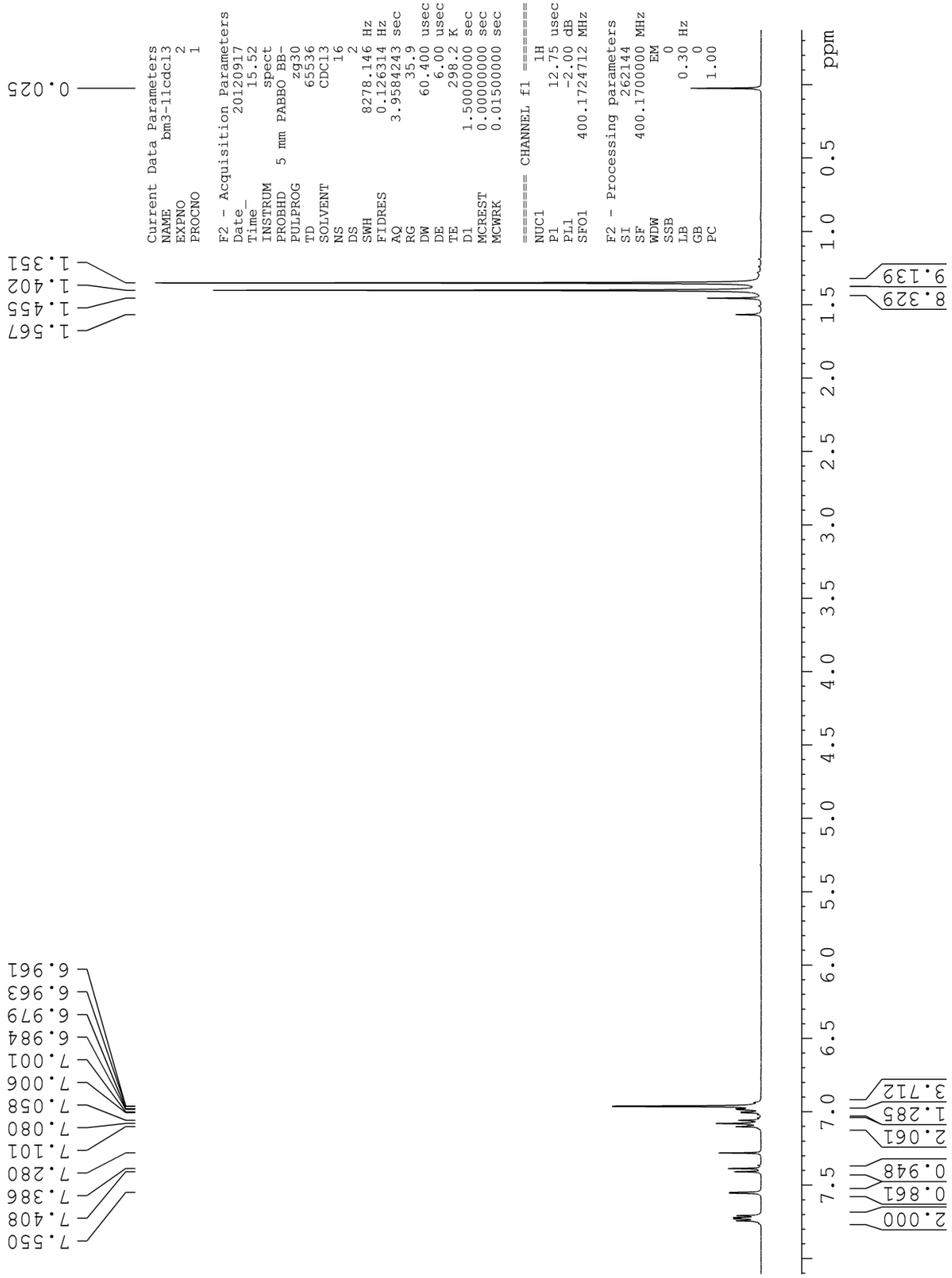

400 MHz ^{1}H NMR of Compound 47

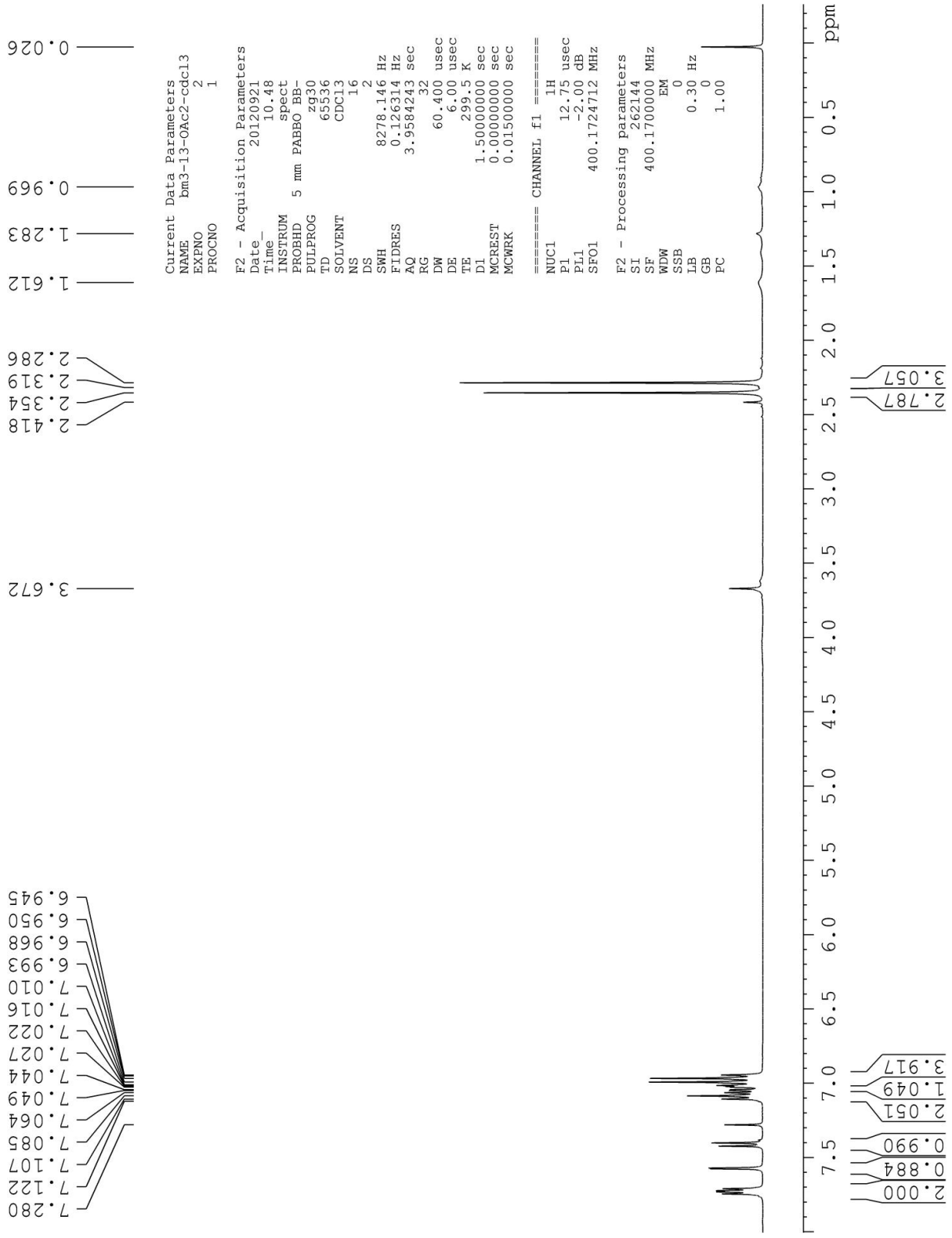

400 MHz ^{1}H NMR of Compound 48

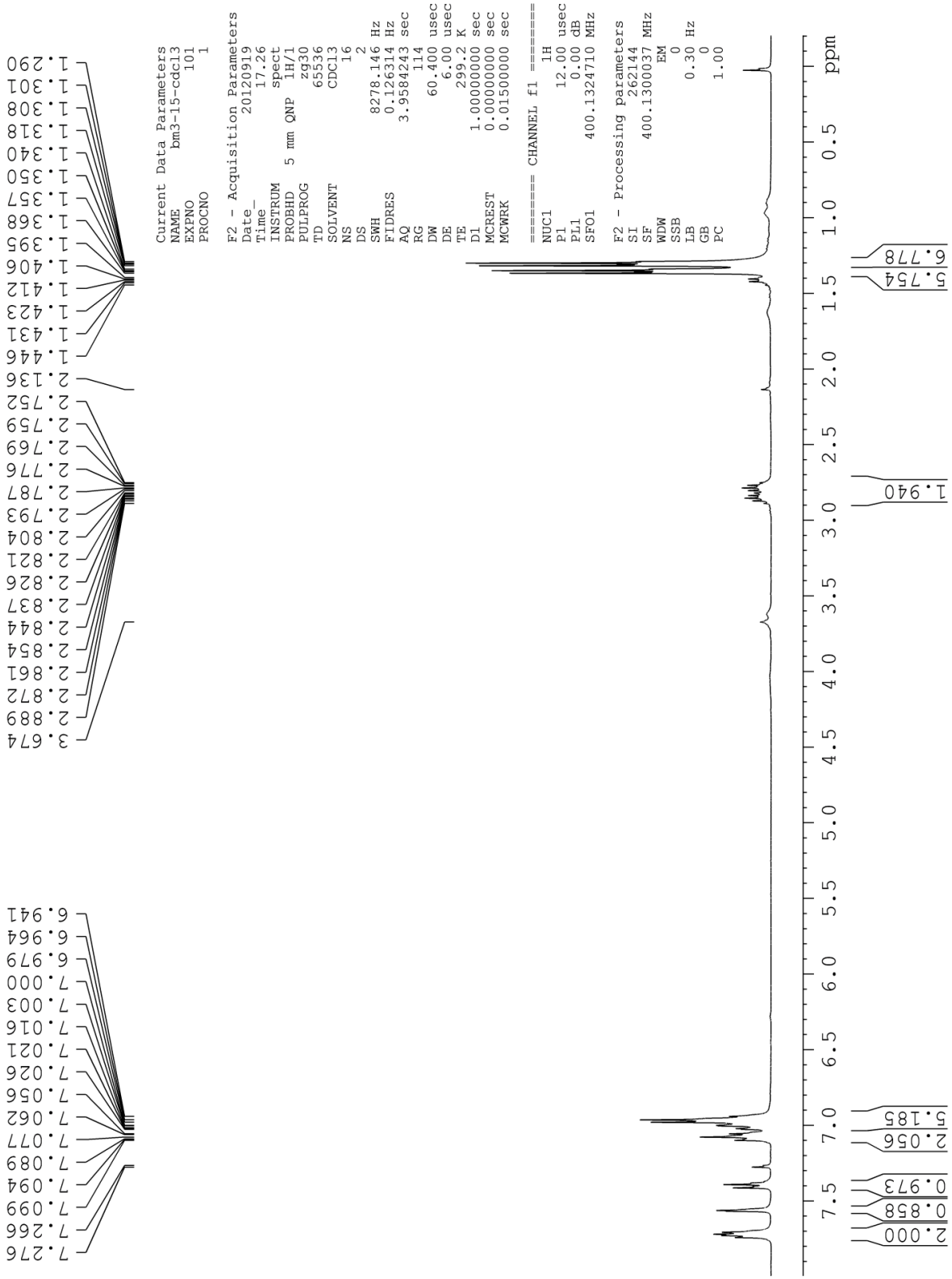

400 MHz ^{1}H NMR of Compound 49

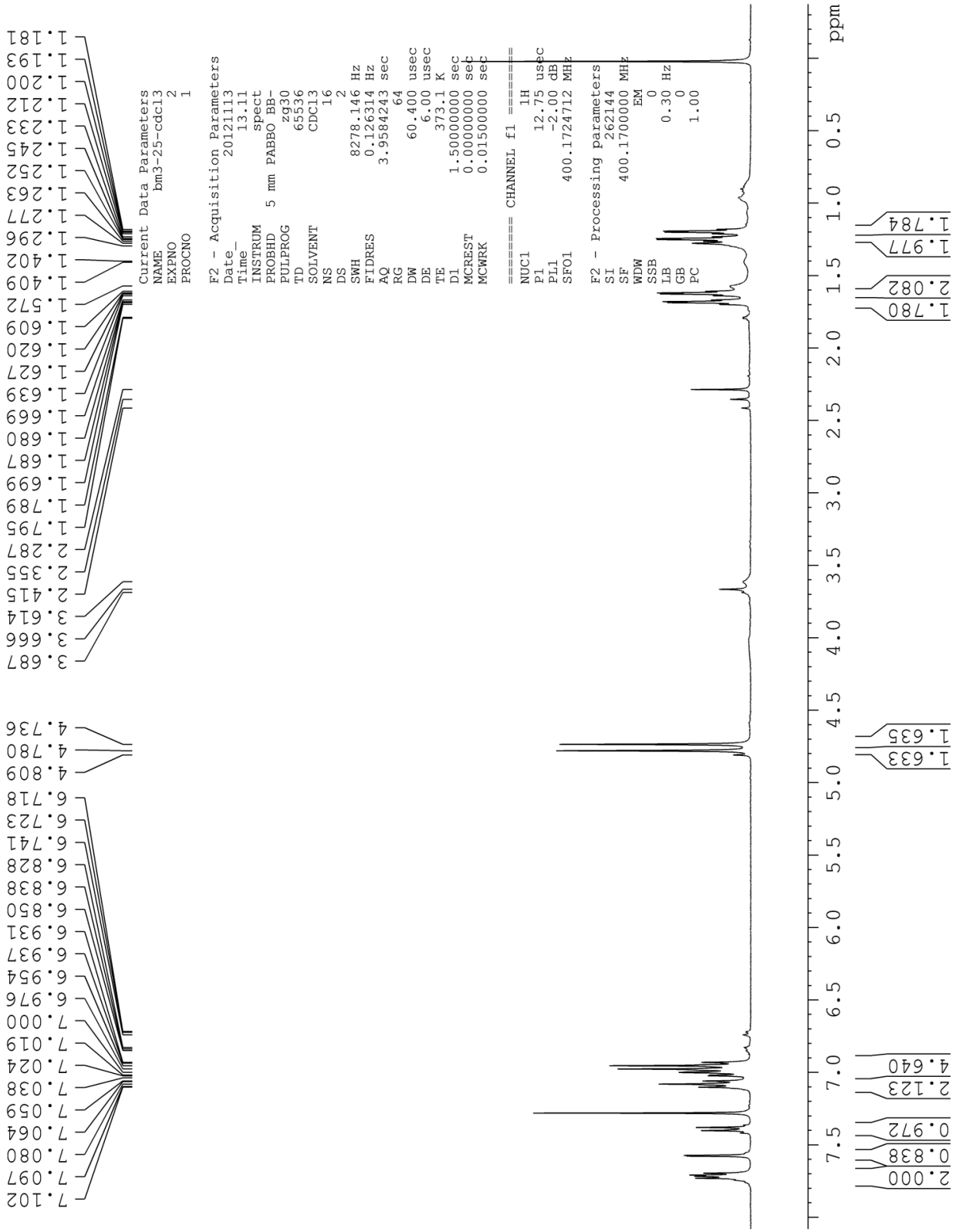

400 MHz ^{1}H NMR of Compound 51

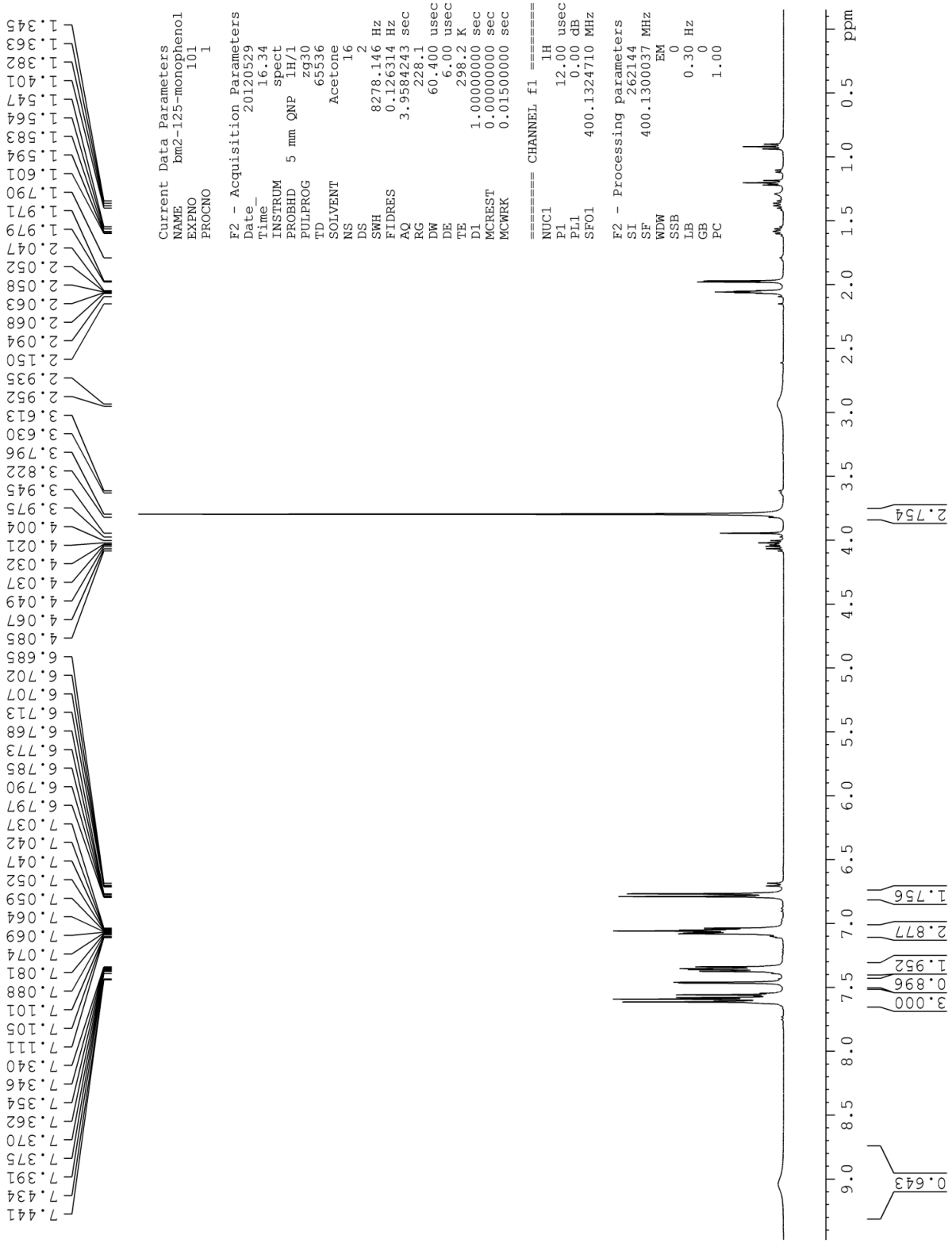

400 MHz ^{1}H NMR of Compound 52

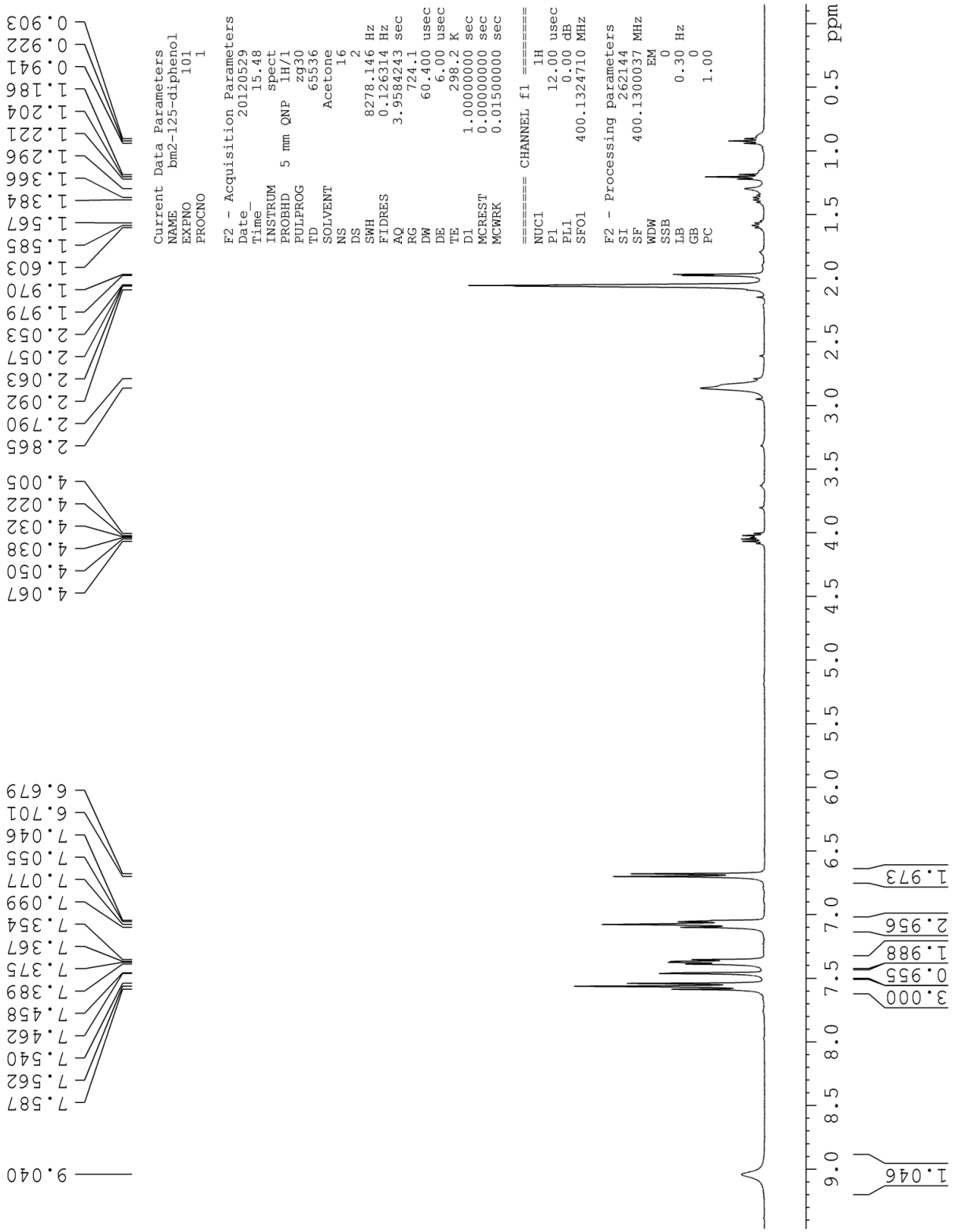

VITA

Bradley Thomas Michalsen

Education:

Ph.D., Medicinal Chemistry, University of Illinois at Chicago, Chicago, Illinois (2013)

B.A., Chemistry, Lake Forest College, Lake Forest, Illinois (2008)

Honors:

W.E. van Doren Scholar, University of Illinois at Chicago (2012)

Cum Laude graduate, Lake Forest College (2008)

Memberships:

American Chemical Society, Medicinal Chemistry Division

Teaching Experience:

Teaching Assistant, Department of Medicinal Chemistry and Pharmacognosy, University of Illinois at Chicago, Nuclear Magnetic Resonance Facility (2012-2013)

Teaching Assistant, Department Medicinal Chemistry and Pharmacognosy, University of Illinois at Chicago, Courses covered: Fundamentals of Drug Action I, Fundamentals of Drug Action II (2008-2010)

Research Experience:

Associate Scientist, Molecular Probes Group, Medicinal Chemistry Technologies, Global Pharmaceutical Research and Development, Abbvie (May, 2013-present)

Research Assistant, Department of Medicinal Chemistry and Pharmacognosy, University of Illinois at Chicago (2008-2013)

Research Assistant, Department of Chemistry, Lake Forest College (2007)

Publications:

"Novel Benzothiophene Selective Estrogen Receptor Modulators for the Treatment of PKCα-Overexpressing Tamoxifen-Resistant Breast Cancer." Malloy, Mary Ellen; White, Bethany Perez; Gherezghiher, Teshome B.;

Michalsen, Bradley; Zhao, Huiping; Thatcher, Gregory R. J.; Tonetti, Debra A. Clinical Cancer Research (in preparation).

"Benzothiophene SERMs act as breast cancer chemopreventive agents by modulating estrogen oxidative metabolism in human mammary epithelial cells." Hemachandra, L. P. M. P., Patel, H., Chandrasena, R. E. P., Choi, J., Wang, S., Wang, Y., Schism, R., **Michalsen, B. T**., Bolton, J. L., and Thatcher, G. R. J. Cancer Prevention Research (submitted, under review).

"Selective Estrogen Receptor Modulator (SERM) Lasofoxifene Forms Reactive Quinones Similar to Estradiol." **Michalsen, Bradley;** Gherezghiher, Teshome B.; Choi, Jaewoo; Chandrasena, R. Esala; Qin, Zhihui; Thatcher, Gregory R. J.; Bolton, Judy L. Chemical Research in Toxicology (2012), 25(7), 1472-83.

"The Naphthol Selective Estrogen Receptor Modulator (SERM), LY2066948, is Oxidized to an o-Quinone Analogous to the Naphthol Equine Estrogen, Equilenin." Gherezghiher, Teshome B.; **Michalsen, Bradley**; Chandrasena, R. Esala P.; Qin, Zhihui; Sohn, Johann; Thatcher, Gregory R. J.; Bolton, Judy L. Chemico-Biological Interactions (2012), 196(1-2), 1-10.

"Benzothiophene Selective Estrogen Receptor Modulators Provide Neuroprotection by a Novel GPR30-Dependent Mechanism." Abdelhamid, Ramy; Luo, Jia; Vande Vrede, Lawren; Kundu, Indraneel; **Michalsen, Bradley**; Litosh, Vladislav A.; Schiefer, Isaac T.; Gherezghiher, Teshome; Yao, Ping; Qin, Zhihui; Thatcher, Gregory R. J. ACS Chemical Neuroscience (2011), 2(5), 256-268.

"NO-SSRIs: Nitric Oxide Chimera Drugs Incorporating a Selective Serotonin Reuptake Inhibitor." Abdul-Hay, Samer; Schiefer, Isaac T.; Chandrasena, R. Esala P.; Li, Min; Abdelhamid, Ramy; Wang, Yue-Ting; Tavassoli, Ehsan; **Michalsen, Bradley**; Asghodom, Rezene T.; Luo, Jia; Thatcher, Gregory R. J. ACS Medicinal Chemistry Letters (2011), 2(9), 656-661.

"Synthesis of Novel Benzothiophene Selective Estrogen Receptor Modulators That Provide Neuroprotection by a Novel GPR30-Dependent Mechanism." V. A. Litosh, **B. T. Michalsen**, R. P. Gandhi, R. Abdelhamid, J. Luo, L. VandeVrede, I. Kundu, I. T. Schiefer, T. Gherezghiher, P. Yao, Z. Qin, and G. R. J. Thatcher. Abstract, **242nd ACS National Meeting***,* Denver, CO (2011), MEDI-085.

Presentations:

"Synthesis and Bioactivation of Selective Estrogen Receptor Modulators (SERMs) bazedoxifene and lasofoxifene" Oral presentation, University of Minnesota, 51st Annual MIKI meeting (2013)

“Synthesis and Bioactivation of Selective Estrogen Receptor Modulators (SERMs)” Dissertation defense, University of Illinois at Chicago, College of Pharmacy (2013)

“The Selective Estrogen Receptor Modulators (SERMs) Lasofoxifene and LY2066948 are Metabolized *o*-Quinones, Analogous to Estradiol and Equilenin.” Poster, University of Illinois at Chicago, Cancer Center Research Forum (2012)

“The Selective Estrogen Receptor Modulators (SERMs) Lasofoxifene and LY2066948 are Metabolized o-Quinones, Analogous to Estradiol and Equilenin.” Poster, University of Illinois at Chicago, College of Pharmacy Research Day (2012)

“Selective Estrogen Receptor Modulators (SERMs): Current Status and Future Prospects.” Public lecture, University of Illinois at Chicago, College of Pharmacy (2011)